


The responses of endothelium to insult: Does endothelial heterogeneity play a role in *in vitro* cell models?

by
Mashudu Mthethwa



*Dissertation presented for the degree of Doctor of Philosophy
(Medical Physiology) in the
Faculty of Medicine and Health Sciences at
Stellenbosch University*

Supervisor: Prof Hans Strijdom
Co-supervisor: Prof Anna-Mart Engelbrecht

December 2015

Declaration

By submitting this thesis/dissertation electronically, I declare that the entirety of the work contained therein is my own, original work, that I am the sole author thereof (save to the extent explicitly otherwise stated), that reproduction and publication thereof by Stellenbosch University will not infringe any third party rights and that I have not previously in its entirety or in part submitted it for obtaining any qualification.

December 2015

Copyright © 2015 Stellenbosch University

All rights reserved

Abstract

Endothelial injury and dysfunction precede the development of cardiovascular diseases. The endothelium may be regarded as the first line of defence against inflammation / obesity-induced vascular injury, therefore gaining more information on the mechanisms of injury and response to injury, as well as modulating endothelial function may be key in the prevention of cardiovascular diseases. Endothelial cells differ in structure and function, therefore endothelial heterogeneity may be relevant when investigating endothelial function and dysfunction. Understanding endothelial heterogeneity in response to pathophysiological stimuli may be of significance in the prevention of cardiovascular diseases. Oleanolic acid (OA), a plant-derived triterpenoid, has been shown to possess endothelium-protective properties; however, its role in reversing endothelial injury is poorly understood.

This study investigated endothelial heterogeneity between aortic endothelial cells (AECs) and cardiac microvascular endothelial cells (CMECs) at baseline and in response to an inflammatory insult via the cytokine, tumour necrosis factor- α (TNF- α). An *in vitro* model of endothelial injury was developed by treating AECs and CMECs with 20 ng/ml TNF- α for 24 hours. Endothelial heterogeneity was investigated by comparing intracellular nitric oxide (NO) and reactive oxygen species (ROS) production, protein expression and phosphorylation, and large-scale protein expression and regulation in AECs and CMECs. The experimental techniques included flow cytometry, western blots and proteomic analyses. An *ex vivo* model of endothelial injury was included to investigate vascular function in aortic rings from lean and high fat diet (HFD) rats. The role of OA in reversing TNF- α -induced injury and modulating vascular function in the *ex vivo* model was investigated.

Although baseline NO-levels were similar between AECs and CMECs, heterogeneity was observed with regards to the NO biosynthetic pathway in terms of increased eNOS expression in CMECs. Baseline ROS levels were heterogeneous between AECs and CMECs, interestingly CMECs possessed higher anti-oxidant capacity. An *in vitro* model of TNF- α -induced injury was confirmed by decreased NO-levels, increased ROS-levels and necrosis, up-regulation of apoptotic proteins and activation of inflammatory pathways in AECs and CMECs. Here, heterogeneity between AECs and CMECs was also observed: endothelial activation was mediated through different proteins in AECs (CD9 molecule, galectin) and

CMECs (ICAM-1 and IL-36 α). Apoptosis was mediated by caspase 3 in AECs and Bid in CMECs. AECs appeared to advance to a dysfunctional state shown by up-regulation of endothelin-converting enzyme and angiotensin II-converting enzyme, while CMECs maintained an activated state. OA reversed TNF- α -induced injury through restoring NO-production, decreasing ROS-production in both AECs and CMECs, and inhibiting necrosis in AECs. In the *ex vivo* model of injury, aortic rings from 16-week HFD rats showed a pro-contractile response to phenylephrine-induced contraction, a response that was reversed by OA.

In conclusion, we demonstrated novel findings with regards to endothelial heterogeneity between AECs and CMECs under baseline and TNF- α -treated conditions. Although reduced NO-bioavailability may be the hallmark of endothelial dysfunction, signalling pathways mediating endothelial injury may differ between cell types as was shown in this study. We demonstrated that OA possess protective properties in AECs and CMECS, an observation which was translated to the *ex vivo* model.

Opsomming

Endoteelbesering en –disfunksie gaan die ontwikkeling van kardiovaskulêre siektes vooraf. Die endoteel word as die eerste linie van verdediging teen inflammasie / vetsuggeïnduseerde vaskulêre skade beskou; dus is die ontginning van nuwe inligting betreffende die meganismes van en respons tot besering, asook die modulering van endoteelfunksie essensieël in die voorkoming van kardiovaskulêre siektes. Endoteelselle verskil t.o.v. struktuur en funksie, en dus is endoteel-heterogeniteit relevant tydens die ondersoek van endoteelfunksie en –disfunksie. 'n Beter begrip van endoteel-heterogeniteit in die respons tot patofisiologiese stimuli kan betekenisvol tot die voorkoming van kardiovaskulêre siektes bydra. Oleanoliese suur (OA), 'n triterpenoïed afkomstig van plante is voorheen bewys om endoteelbeskerende eienskappe te besit; die rol van OA in die omkering van endoteelbesering is egter minder bekend.

Hierdie studie het endoteel-heterogeniteit tussen aorta endoteelselle (AECs) en hart mikrovaskulêre endoteelselle (CMECs) by basislyn en in respons tot 'n inflammatoriese besering via die sitokien, tumor nekrose faktor-alfa (TNF- α), ondersoek. 'n *In vitro* model van endoteelbesering is ontwikkel deur AECs en CMECs met 20 ng/ml TNF- α vir 24 uur te behandel. Endoteel-heterogeniteit was ondersoek deur intrasellulêre stikstofoksied (NO) en reaktiewe suurstofspesies (ROS) produksie, proteïenuitdrukking en fosforilering, en grootskaalse proteïenuitdrukking en regulering in AECs en CMECs te vergelyk. Die eksperimentele tegnieke het ingesluit: vloeisitometrie, western blots en proteomika. 'n *Ex vivo* model van endoteelbesering was ook ingesluit deur die vaskulêre funksie in aortaringe van normale en hoë vet dieet-gevoerde (HFD) rotte te meet. Die rol van OA in die omkering van TNF- α -geïnduseerde besering en modulering van vaskulêre funksie was in hierdie model is ondersoek.

Alhoewel basislyn NO-vlakke vergelykbaar was in AECs en CMECs, is heterogeniteit wel aangetoon m.b.t. die NO biosintese pad met verhoogde eNOS uitdrukking in die CMECs. Basislyn ROS-vlakke was verskillend in AECs en CMECs en die CMECs het hoër anti-oksidadant kapasiteit getoon. 'n *In vitro* model van TNF- α -geïnduseerde besering is bevestig met die waarneming van verlaagde NO-vlakke, verhoogde ROS-vlakke en nekrose, opregulering van apoptotiese proteïene en aktivering van inflammatoriese paaie in AECs en CMECs. Hier was heterogeniteit ook opmerkbaar: endoteelaktivering was deur verskillende proteïene in AECs

(CD9 molekule, galektien) en CMECs (ICAM-1, IL-36 α) bemiddel. Apotose was deur kaspase 3 in AECs en Bid in CMECs bemiddel. Dit het geblyk dat AECs tot 'n staat van endoteeldisfunksie gevorder het met die opregulering van endotelien-omsettingsensiem en angiotensien II-omsettingsensiem, terwyl CMECs eerder 'n geaktiveerde staat gehandhaaf het. OA het TNF- α -geïnduseerde besering omgekeer deur NO-produksie te herstel, ROS-produksie te onderdruk in beide AECs en CMECs, en nekrose te inhibeer in AECs. In die *ex vivo* model van besering, het aortaringe van 16-week HFD rotte 'n pro-kontraktiele respons tot fenielefrien-geïnduseerde kontraksie getoon, wat deur OA omgekeer is.

Ten slotte, nuwe bevindinge is waargeneem m.b.t. endoteel-heterogeniteit tussen AECs en CMECs onder basislyn en TNF- α -behandelde omstandighede. Alhoewel verlaagde NO-biobeskikbaarheid die waarmerk van endoteeldisfunksie is, het hierdie studie getoon dat seintransduksiepaaie wat endoteelbesering medieer verskillend is tussen selteipes. Die studie het verder ook gedemonstreer dat OA beskermende eienskappe toon in AECs en CMECs, 'n waarneming wat ook in die *ex vivo* model aangetoon kon word.

Acknowledgements

I would like to acknowledge the following people:

To my supervisor, **Prof Hans Strijdom**: thank you for your invaluable contribution, guidance, insight and dedication throughout this study. Thank you for being an inspiring leader, and for always thriving for excellence in every project.

My co-supervisor, **Prof Anna-Mart Engelbrecht**, for her invaluable input and guidance.

My family (siblings and sister in law) for their continuous support throughout this project

My colleagues Amanda and Corli for their assistance and support throughout the project.

My husband for the words of encouragement whenever I felt like giving up and continuous support.

Everyone in the department for creating a warm and friendly environment, and for all the assistance.

I thank God for seeing me through all the challenges in the duration of this study.

List of Tables

Chapter 1

Table 1.1: Summary of endothelium-derived vasoactive factors	11
Table 1.2: Differences between arteries and veins	49
Table 1.3: Differences in the molecular markers expressed in arterial and venous endothelium.....	49
Table 1.4: Endothelio-protective agents and their mechanisms of action	58

Chapter 2

Table 2.1: Proteins measured by western blotting	77
Table 2.2: Western blot protocols	77
Table 2.3: Details of data acquisition	83
Table 2.4: Protein search parameters	84
Table 2.5: Composition of the HFD and control diets	87

Chapter 3

Table 3.1: List of up-regulated proteins in control, untreated AECs (vs. CMECs).....	149
Table 3.1 (continued): List of up-regulated proteins in control, untreated AECs (vs. CMECs)	150
Table 3.2: Biological processes associated with strongly represented proteins in control, untreated AECs (vs. CMECs).....	152
Table 3.3: Cellular components associated with strongly represented proteins in control, untreated AECs (vs control, untreated CMECs).....	153
Table 3.4: List of up-regulated proteins in control, untreated CMECs (vs AECs)	154
Table 3.4 (continued): List of up-regulated proteins in control, untreated CMECs (vs AECs)	155
Table 3.5: Biological processes associated with strongly represented proteins in control, untreated CMECs (vs control, untreated AECs).....	157
Table 3.6: Cellular components associated with strongly represented proteins in control, untreated CMECs (vs. control, untreated AECs).....	158
Table 3.7: List of up-regulated proteins in AECs + TNF (vs untreated AECs).....	160

Table 3.8: Biological processes associated with strongly represented proteins in AECs+TNF samples (vs control, untreated AECs)162

Table 3.9: List of up-regulated proteins in CMECs + TNF (vs control, untreated CMECs)164

Table 3.10: Biological processes associated with strongly represented proteins in CMECs+TNF (vs control, untreated CMECs)166

Table 3.11: List of up-regulated proteins in AECs + TNF (vs CMECs + TNF)169

Table 3.11 (continued): List of up-regulated proteins in AECs + TNF (vs CMECs + TNF)170

Table 3.11 (continued): List of up-regulated proteins in AECs + TNF (vs CMECs + TNF)171

Table 3.12: Biological processes associated with strongly represented proteins in AECs+TNF (vs CMECs + TNF)173

Table 3.13: Cellular components associated with strongly represented proteins in AECs+TNF (vs CMECs + TNF)174

Table 3.14: List of up-regulated proteins in CMECs + TNF (vs AECs + TNF)177

Table 3.14 (continued): List of up-regulated proteins in CMECs + TNF (vs AECs + TNF)178

Table 3.14 (continued): List of up-regulated proteins in CMECs + TNF (vs AECs + TNF)179

Table 3.15: Biological processes associated with strongly represented proteins in CMECs+TNF (vs AECs + TNF)181

Table 3.16: Cellular components associated with strongly represented proteins in CMECs+TNF (vs AECs + TNF)182

Chapter 4

Table 4.1: Heterogeneous protein expression and phosphorylation patterns under baseline conditions.....243

Table 4.2: Heterogeneous anti-oxidant protein up-regulation in response to TNF- α 253

List of figures

Chapter 1

Figure 1.1: Global non-communicable disease related deaths in the age group of under 70 in 2008	3
Figure 1.2: Cardiovascular diseases as the major cause of death in the Western Cape in the year 2000	4
Figure 1.3: Twenty major conditions associated with death in the Western Cape during the year 2000.	5
Figure 1.5: A depiction of the flow of electrons during catalysis of NO production.....	15
Figure 1.6: Phosphorylation sites and the kinases involved in eNOS.....	18
Figure 1.7: Different stages of endothelial activation	26
Figure 1.8: ED and progression to atherosclerosis in a nutshell	28
Figure 1.9: eNOS uncoupling	32
Figure 1.10: Progression of insulin resistance to type 2 diabetes parallels progression of ED to atherosclerosis.....	35
Figure 1.11: ADMA synthesis and NOS inhibition	43
Figure 1.12: Participation of ox-LDL in atherogenesis in different cells in the vascular system	45
Figure 1.13: Endothelial cell heterogeneity in arterial, venous and capillary endothelium ...	51
Figure 1.14: Paracrine communication between CMECs and cardiomyocytes.....	53

Chapter 2

Figure 2.1: Passaging of cells and storage in liquid nitrogen	67
Figure 2.2: A representative example of a forward-side scatter plot with a gate representing the cell population of interest	69
Figure 2.3: The experimental protocols for DAF-2/DA, DHR-123 incubation, and positive controls administrations	72
Figure 2.4: A representative histogram showing the autofluorescence, and DAF-2/DA fluorescence in control and positive control samples, measured in the FL1-H channel of the flow cytometer.....	72

Figure 2.5: The experimental protocol for DCF incubation and positive control.....	72
Figure 2.6: The experimental protocol for PI incubation	74
Figure 2.7: A representative histogram of a sample exposed to an injurious insult resulting in a high percentage necrotic cells as demonstrated by the high PI-uptake in the necrotic cell sub-population.....	74
Figure 2.8: Protocols to determine the TNF- α concentration-response effects for 24 or 48 hour treatment durations.....	80
Figure 2.9: Protocols for baseline studies with 40 μ M OA	80
Figure 2.10: OA pre-treatment protocol prior to injury induction by means of TNF- α administration for 24 hours.....	80
Figure 2.11: The tissue organ bath system.....	87
Figure 2.12: Schematic representation of the incisions made for the removal of the aorta..	89
Figure 2.13: The excised aorta placed on cold Krebs-Henseleit buffer and cleaned of excess fat and connective tissue	89
Figure 2.14: A 4 mm aortic ring mounted on two stainless steel hooks and lowered into the organ bath.....	90
Figure 2.15: A representative recording obtained from the LabChart pro software showing the standard isometric tension protocol	93
Figure 2.16: A representative recording obtained from the LabChart pro software showing the OA pre-treatment protocol	94

Chapter 3

Figure 3.1 A: A histogram representation of the mean DAF-2/DA fluorescence intensity generated by 100 μ M DEA/NO administration (positive control for DAF-2/DA).....	97
Figure 3.1 B: A histogram representation of the mean DHR-123 and DCF fluorescence intensity generated by 100 μ M authentic ONOO ⁻ and 100 μ M H ₂ O ₂ administration respectively (positive controls for DHR-123 and DCF)	97
Figure 3.2: Baseline mean DAF-2/DA fluorescence in AECs and CMECs.....	98
Figure 3.3 A: Baseline mean DHR-123 fluorescence in AECs and CMECs	99
Figure 3.3 B: Baseline mean DCF fluorescence in AECs and CMECs	99
Figure 3.4 A: AECs: DAF-2/DA TNF- α concentration-response findings after 24 hours treatment.....	101

Figure 3.4 B: AECs: DAF-2/DA TNF- α concentration-response findings after 48 hours treatment.....101

Figure 3.4 C: CMECs: DAF-2/DA TNF- α concentration-response findings after 24 hours treatment.....102

Figure 3.4 D: CMECs: DAF-2/DA TNF- α concentration-response findings after 48 hours treatment.....102

Figure 3.5 A: Direct comparison of % changes in DAF-2/DA fluorescence between AECs and CMECs treated with TNF- α for 24 hours.....104

Figure 3.5 B: Direct comparison of % changes in DAF-2/DA fluorescence between AECs and CMECs treated with TNF- α for 48 hours.....104

Figure 3.6 A: AECs: DHR-123 TNF- α concentration-response findings after 24 hours treatment.....106

Figure 3.6 B: AECs: DHR-123 TNF- α concentration-response findings after 48 hours treatment.....106

Figure 3.6 C: CMECs: DHR-123 TNF- α concentration-response findings after 24 hours treatment.....107

Figure 3.6 D: CMECs: DHR-123 TNF- α concentration-response findings after 48 hours treatment.....107

Figure 3.7 A: Direct comparison of % changes in DHR-123 fluorescence between AECs and CMECs treated with TNF- α for 24 hours.....109

Figure 3.7 B: Direct comparison of % changes in DHR-123 fluorescence between AECs and CMECs treated with TNF- α for 48 hours.....109

Figure 3.8 A: AECs: DCF TNF- α concentration-response findings after 24 hours treatment.111

Figure 3.8 B: AECs: DCF TNF- α concentration-response findings after 48 hours treatment111

Figure 3.8 C: CMECs: DCF TNF- α concentration-response findings after 24 hours treatment112

Figure 3.8 D: CMECs: DCF TNF- α concentration-response findings after 48 hours treatment112

Figure 3.9 A: Direct comparison of % changes in DCF fluorescence between AECs and CMECs treated with TNF- α for 24 hours.....114

Figure 3.9 B: Direct comparison of % changes in DCF fluorescence between AECs and CMECs treated with TNF- α for 48 hours.....114

Figure 3.10 A: AECs: TNF- α concentration-response findings after 24 hours treatment showing % propidium iodide-stained cells116

Figure 3.10 B: AECs: TNF- α concentration-response findings after 48 hours treatment showing % propidium iodide-stained cells116

Figure 3.10 C: CMECs: TNF- α concentration-response findings after 24 hours treatment showing % propidium iodide-stained cells117

Figure 3.10 D: CMECs: TNF- α concentration-response findings after 48 hours treatment showing % propidium iodide-stained cells.117

Figure 3.11 A: Direct comparison of changes in the % propidium iodide-stained cells between AECs and CMECs treated with TNF- α for 24 hours.....119

Figure 3.11 B: Direct comparison of changes in the % propidium iodide-stained cells between AECs and CMECs treated with TNF- α for 48 hours.....119

Figure 3.12 A & B: (A) Total eNOS expression and (B) phosphorylated eNOS (Ser 1177) in AECs and CMECs with or without TNF- α treatment (20 ng/ml; 24 hours).....121

Figure 3.12 C: Phospho / total eNOS ratios in AECs and CMECs with or without TNF- α treatment (20 ng/ml; 24 hours).....121

Figure 3.13 C: Phospho / total PKB/Akt ratios in AECs and CMECs with or without TNF- α (20 ng/ml; 24 hours)123

Figure 3.14: Heat shock 90 expression in AECs and CMECs with or without TNF- α (20 ng/ml; 24 hours).124

Figure 3.15: IKB-alpha expression in AECs and CMECs with or without TNF- α (20 ng/ml; 24 hours).....125

Figure 3.16: Nitrotyrosine expression in AECs and CMECs with or without TNF- α (20 ng/ml; 24 hours)126

Figure 3.17 A: AECs: DAF-2/DA fluorescence data with 10 and 40 μ M OA treatment for 1 hour.....128

Figure 3.17 B: CMECs: DAF-2/DA fluorescence data with 10 and 40 μ M OA treatment for 1 hour.....128

Figure 3.18 A: AECs: DCF fluorescence data with 40 μ M OA treatment for 1 hour.....130

Figure 3.18 B: CMECs: DCF fluorescence data with 40 μ M OA treatment for 1 hour130

Figure 3.19 A: AECs: % propidium iodide-stained cells treated with 40 μ M OA (1 hour).....132

Figure 3.19 B: CMECs: % propidium iodide-stained cells treated with 40 μ M OA (1 hour)..132

Figure 3.20 A: AECs: DAF-2/DA fluorescence data in AECs treated with 40 μ M OA (24 hours)
.....134

Figure 3.20 B: CMECs: DAF-2/DA fluorescence data in CMECs treated with 40 μ M OA (24 hours).....134

Figure 3.21 A: AECs: DCF fluorescence data in AECs treated with 40 μ M OA (24 hours).....136

Figure 3.21 B: CMECs: DCF fluorescence data in CMECs treated with 40 μ M OA (24 hours)
.....136

Figure 3.22 A: AECs: % propidium iodide-stained cells treated with 40 μ M OA (24 hours) .138

Figure 3.22 B: CMECs: % propidium iodide-stained cells treated with 40 μ M OA (24 hours)
.....138

Figure 3.23 A: AECs: DAF-2/DA fluorescence data in OA, TNF- α and OA pre-treatment groups.140

Figure 3.23 B: CMECs: DAF-2/DA fluorescence data in OA, TNF- α and OA pre-treatment groups140

Figure 3.24 A: AECs: DCF fluorescence data in OA, TNF- α and OA pre-treatment groups...142

Figure 3.24 B: CMECs: DCF fluorescence data in OA, TNF- α and OA pre-treatment groups.
.....142

Figure 3.25 A: AECs: % propidium iodide-stained cells in OA, TNF- α and OA pre-treatment groups144

Figure 3.25 B: CMECs: % propidium iodide-stained cells in OA, TNF- α and OA pre-treatment groups144

Figure 3.26 A: Venn diagram showing the total protein expression distribution in control, untreated AECs and CMECs.145

Figure 3.26 B: Venn diagram showing the total protein expression distribution in TNF- α treated AECs and CMECs.145

Figure 3.27 A: Graph showing the differentially regulated protein abundance (measured as normalised total spectra) of Aldehyde dehydrogenase, dimeric NADP-preferring in three control, untreated AEC samples (AEC1, AEC2, AEC3) compared to three control, untreated CMEC samples (CMEC1, CMEC2, CMEC3).....151

Figure 3.27 B: Graph showing the differentially regulated protein abundance (measured as normalised total spectra) of Aldehyde dehydrogenase L1 in three control, untreated AEC samples (AEC1, AEC2, AEC3) compared to three control, untreated CMEC samples (CMEC1, CMEC2, CMEC3).	151
Figure 3.28 A: Graph showing the differentially regulated protein abundance (measured as normalised total spectra) of Tight junction protein-1 in three control, untreated CMEC samples (CMEC1, CMEC2, CMEC3) compared to three control, untreated AEC samples (AEC1, AEC2, AEC3).	156
Figure 3.28 B: Graph showing the differentially regulated protein abundance (measured as normalised total spectra) of BCL-2 related protein A1B in three control, untreated CMEC samples (CMEC1, CMEC2, CMEC3) compared to three control, untreated AEC samples (AEC1, AEC2, AEC3).	156
Figure 3.29 A: Graph showing the differentially regulated protein abundance (measured as normalised total spectra) of Superoxide dismutase [Mn] mitochondrial in three TNF- α treated AEC samples (AEC+TNF1, AEC+TNF2, AEC+TNF3) compared to three control, untreated AEC samples (AEC1, AEC2, AEC3).	161
Figure 3.29 B: Graph showing the differentially regulated protein abundance (measured as normalised total spectra) of NF-KB p49/p100 in three TNF- α treated AEC samples (AEC+TNF1, AEC+TNF2, AEC+TNF3) compared to three control, untreated AEC samples (AEC1, AEC2, AEC3).	161
Figure 3.30 A: Graph showing the differentially regulated protein abundance (measured as normalised total spectra) of Plasminogen activator inhibitor-1 (PAI-1) in three TNF- α treated CMEC samples (CMEC+TNF1, CMEC+TNF2, CMEC+TNF3) compared to three control, untreated CMEC samples (CMEC1, CMEC2, CMEC3).	165
Figure 3.30 B: Graph showing the differentially regulated protein abundance (measured as normalised total spectra) of NF-KB p49/p100 in three TNF- α treated CMEC samples (CMEC+TNF1, CMEC+TNF2, CMEC+TNF3) compared to three control, untreated CMEC samples (CMEC1, CMEC2, CMEC3).	165
Figure 3.31 A: Graph showing the differentially regulated protein abundance (measured as normalised total spectra) of Endothelin-converting enzyme 1 in three TNF- α treated AEC samples (AEC+TNF1, AEC+TNF2, AEC+TNF3) compared to three TNF- α -treated CMEC samples (CMEC+TNF1, CMEC+TNF2, CMEC+TNF3).	172

Figure 3.31 B: Graph showing the differentially regulated protein abundance (measured as normalised total spectra) of Aldehyde dehydrogenase L1 in three TNF- α treated AEC samples (AEC+TNF1, AEC+TNF2, AEC+TNF3) compared to three TNF- α -treated CMEC samples (CMEC+TNF1, CMEC+TNF2, CMEC+TNF3)	172
Figure 3.32 A: Graph showing the differentially regulated protein abundance (measured as normalised total spectra) of Platelet endothelial cell adhesion molecule in three TNF- α treated CMEC samples (CMEC+TNF1, CMEC+TNF2, CMEC+TNF3) compared to three TNF- α -treated AEC samples (AEC+TNF1, AEC+TNF2, AEC+TNF3).	180
Figure 3.32 B: Graph showing the differentially regulated protein abundance (measured as normalised total spectra) of Plexin D1 in three TNF- α treated CMEC samples (CMEC+TNF1, CMEC+TNF2, CMEC+TNF3) compared to three TNF- α -treated AEC samples (AEC+TNF1, AEC+TNF2, AEC+TNF3).....	180
Figure 3.33: Total body weights of lean and HFD rats after 16 weeks.....	184
Figure 3.34: Total body weights of lean and HFD rats after 24 weeks.....	184
Figure 3.35: Intra-peritoneal fat mass in lean and HFD rats after 16 weeks	185
Figure 3.36: Intra-peritoneal fat mass in lean and HFD rats after 24 weeks	185
Figure 3.37: Phenylephrine-induced aortic ring contraction in lean and HFD groups.....	187
Figure 3.38: Acetylcholine-induced aortic ring relaxation in lean and HFD groups (16 weeks)	187
Figure 3.39: Phenylephrine-induced contraction in aortic rings from lean animals (16 weeks) exposed to OA administration	189
Figure 3.40: Acetylcholine-induced relaxation in aortic rings from lean animals (16 weeks) exposed to OA administration.	189
Figure 3.41: Phenylephrine-induced contraction in aortic rings from HFD animals (16 weeks) exposed to OA administration	191
Figure 3.42: Acetylcholine-induced relaxation in aortic rings from HFD animals (16 weeks) exposed to OA administration.....	191
Figure 3.43: Phenylephrine-induced contraction in aortic rings from lean animals (24 weeks) exposed to OA administration.	193
Figure 3.44: Acetylcholine-induced relaxation in aortic rings from lean animals (24 weeks) exposed to OA administration.....	193

Figure 3.45: Phenylephrine-induced contraction in aortic rings from HFD animals (24 weeks) exposed to OA administration.....195

Figure 3.46: Acetylcholine-induced relaxation in aortic rings from HFD animals (24 weeks) exposed to OA administration195

Figure 3.47: Direct, cumulative administration of OA after phenylephrine pre-contraction to assess possible pro-relaxation effects in aortic rings from lean and HFD rats.....196

Chapter 4

Figure 4.1: Proposed mechanism of TNF- α induced cell necrosis.....215

Figure 4.2: The TNF- α signalling pathway229

Figure 4.3: Summary of the effects of TNF- α on NO production, ROS production and necrosis in AECs and CMECs.245

Figure 4.4: Proposed TNF- α signalling in the AECs based on the integration of flow cytometry, western blot and proteomic data247

Figure 4.5: Proposed TNF- α signalling in the CMECs based on the integration of flow cytometry, western blot and proteomic data.249

Figure 4.6: The loss of balance in vasoconstrictor and vasodilator factor synthesis in TNF- α treated AECs compared to TNF- α CMECs.....251

Figure 4.7: TNF- α signalling in AECs compared to CMECs.....255

Figure 4.8: TNF- α signalling in CMECs compared to AECs.....255

List of abbreviations

ACE	angiotensin converting enzyme
Ach	acetylcholine
ADMA	asymmetric dimethyl arginine
AECs	aortic endothelial cells
AGEs	advanced glycation end-products
AMPK	AMP-activated protein kinase
ASS	argininosuccinate synthase
ATP	adenosine triphosphate
BH ³	trihydrobiopterin radical
BH ₄	tetrahydrobiopterin
Bid	BH3 interacting domain death agonist
BMI	body mass index
CaMKII	calcium / calmodulin-dependent protein kinase II
cAMP	cyclic adenosine monophosphate
cGKI	cGMP-dependent protein kinase I
cGMP	cyclic guanosine monophosphate
CMECs	cardiac microvascular endothelial cells
COX	cyclooxygenase
CRP	c-reactive protein
DAF-2/DA	diaminofluorescein diacetate
DAF-2T	diaminofluorescein-triazol
DAVID	the Database for Annotation, Visualization and Integrated Discovery
DCF	2',7'-dichlorofluorescein
DDAH	dimethylaminohydrolases
DEA/NO	diethylammonium
DHR-123	Dihydrorhodamine-123
DiL-ac-LDL	1,1-dioctadecyl-3,3,3',3'-tetramethylindocarbocyanine perchlorate-acylated-low density lipoprotein
DMSO	dimethyl sulfoxide
ECE	endothelin converting enzyme

ED	endothelial dysfunction
EDHF	endothelial derived hyperpolarizing factor
EDRF	endothelium-derived relaxation factor
EETs	epoxyeicosatrienoic acids
EGM	endothelial growth medium
eNOS	endothelial nitric oxide synthase
ESL	endothelial surface layer
ET-1	endothelin-1
ETE	endothelin converting enzyme
FAD	flavin adenine dinucleotide
FADD	fas-associated death domain
FASP	filter aided sample preparation
FBS	fetal bovine serum
FMN	flavin mononucleotide
GO	gene ontology
GTP	guanosine triphosphate
H ₂ O ₂	hydrogen peroxide
hEGF	human epidermal growth factor
HFD	high fat diet
HOMA-IR	homeostatic model assessment of insulin resistance
HSP 90	heat shock protein 90
HUVECs	human umbilical vein endothelial cells
ICAM-1	intercellular adhesion molecule 1.
I κ B-alpha	i-kappa-B-alpha
IHD	ischaemic heart disease
IL-1	Interleukin-1
IL-36 α	interleukin-36 alpha
IL-6	Interleukin-6
iNOS	inducible nitric oxide synthase
LDL	low density lipoprotein
LOX-1	lectin-like ox-LDL receptor 1

LPS	lipopolysaccharide
MCP-1	monocyte chemoattractant protein 1
MLCP	myosin light chain phosphatase
MMTS	methyl methanethiosulphonate
MnSOD	manganese superoxide dismutase
mRNA	messenger ribonucleic acid
NaCl	sodium chloride
NADPH	nicotinamide adenine dinucleotide phosphate
NaVO ₃	sodium orthovanadate
NFκB	nuclear factor kappa-B
nNOS	neuronal nitric oxide synthase
NO	nitric oxide
NOS	nitric oxide synthase
O ₂ ⁻	superoxide anion
ONOO ⁻	peroxynitrite
ox-LDL	oxidised low density lipoprotein
PARP-1	Poly [ADP-ribose] polymerase 1
PBS	phosphate buffered saline
PDE2A	phosphodiesterase 2A
PDEs	phosphodiesterases
PE	phenylephrine
PECAM-1	platelet endothelial cell adhesion molecule 1
PGI ₂	prostacyclin
PI	propidium iodide
PKA	protein kinase A
PKB / Akt	protein kinase B
PKC	protein kinase C
PMRT	protein arginine N-methyltransferase
R ³ -IGF-1	human insulin-like growth factor
RAGE	receptor for AGEs
RIP	receptor interacting protein

RNA	ribonucleic acid
ROS	reactive oxygen species
SDS	sodium dodecylsulfate
Ser	serine
sGC	soluble guanylyl cyclase
SOD	superoxide dismutase
SODD	silencer of death domain
TCEP	triscarboxyethyl phosphine
TEAB	triethyl ammonium bicarbonate
TFA	trifluoroacetic acid
Thr	threonine
TIC	total ion current
TNFR1	tumour necrosis factor receptor 1
TNFR2	tumour necrosis factor receptor 2
TNF- α	tumor necrosis factor-alpha
TRADD	TNF receptor-associated death domain
TRAF	TNF receptor-associated factor
TXA ₂	thromboxane A2
Tyr	tyrosine
VCAM-1	vascular cell adhesion molecule 1
VE-cadherin	vascular endothelial-cadherin
VEGF	vascular endothelial growth factor
VLDL	very low density lipoprotein
VSMCs	vascular smooth muscle cells
VVOs	vesiculo-vacuolar organelles
vWF	von Willebrand factor
WHO	world health organisation
WPBs	weibel-palade bodies

Units of measurements

° C	degree celcius
%	percentage
ng	nanogram
ml	millilitre
µl	microliter
kDa	kilodalton
rpm	revolutions per minute
µg	microgram
mm	millimetre
nM	nanomolar
mM	millimolar
M	molar
g	gram
µm	micrometre
kJ	kilojoule

Table of Contents

Declaration.....	i
Abstract.....	ii
Opsomming.....	iv
Acknowledgements.....	vi
List of Tables	vii
List of figures.....	ix
List of abbreviations.....	xvii
Chapter 1: Literature review	1
1.1 Introduction	1
1.2 The endothelium.....	6
1.2.1 Anatomy and structure of the endothelium.....	7
1.3 Endothelial physiology and function	10
1.3.1 Endothelium-derived factors	12
1.3.1.1 Nitric oxide (NO)	12
1.3.1.1.1 Nitric oxide synthase (NOS)	12
1.3.1.1.2 Endothelial nitric oxide synthase (eNOS)	16
1.3.1.1.3 eNOS activation	16
1.3.1.1.4 Effects of NO	19
1.3.1.2 Endothelium hyperpolarising factor (EDHF)	20
1.3.1.3 Prostanoids	21
1.3.1.4 Endothelin-1.....	22
1.3.1.5 Angiotensin II	23
1.4 Pathophysiological changes in the endothelium.....	24
1.4.1 Endothelial activation	24
1.4.2 Endothelial dysfunction (ED)	27

1.4.2.1	Reduced NO production	29
1.4.2.3	Oxidative / Nitrosative stress.....	29
1.4.2.3	eNOS uncoupling	31
1.4.2.4	Protein nitration.....	33
1.4.3	Atherosclerosis.....	33
1.5	Risk factors associated with pathophysiological changes of the endothelium.....	34
1.5.1	Diabetes / Insulin resistance.....	34
1.5.2	Hyperlipidaemia /Hypercholesterolaemia.....	36
1.5.3	Smoking.....	36
1.5.4	Aging	37
1.5.5	Inflammation and oxidative stress	38
1.6	Harmful stimuli associated with pathophysiological changes.....	40
1.6.1	Tumour necrosis factor-alpha (TNF- α)	40
1.6.2	Asymmetric dimethyl arginine (ADMA).....	41
1.6.3	Oxidised low density lipoprotein (ox-LDL).....	44
1.7	Endothelial heterogeneity	46
1.7.1	Venous, arterial and capillary endothelium	48
1.7.1.1	Venous and arterial endothelium.....	48
1.7.1.2	Capillary endothelium.....	50
1.7.2	Cardiac microvascular endothelial cells (CMECs) and aortic endothelial cells (AECs).	52
1.8	Studying obesity as a risk factor of endothelial dysfunction.....	55
1.9	Anti-endothelial dysfunction therapy.....	57
1.9.1	Oleanolic acid (OA)	59
1.10	Rationale and motivation	61
1.11	Hypotheses	62

1.12 Research aims	63
1.12.1 <i>In vitro</i> studies.....	63
1.12.2 <i>Ex vivo</i> studies.....	64
Chapter 2: Materials and Methods.....	65
2.1 Cell culture studies (<i>in vitro</i> studies).....	65
2.1.1 Cardiac microvascular endothelial cells (CMECs) and aortic endothelial cells (AECs)	65
2.1.2 Flow cytometric analyses.....	68
2.1.2.1 NO measurements	70
2.1.2.2 ROS measurements.....	71
2.1.2.3 Cell viability measurements.....	73
2.1.3 Western blot analyses.....	75
2.1.4 Experimental Protocols: Endothelial injury and oleanolic acid studies.....	78
2.1.4.1 Induction of endothelial injury with TNF- α	78
2.1.4.2 Oleanolic acid studies	78
2.1.4.3 OA pre-treatment studies.....	79
2.2 Proteomic Analyses.....	81
2.2.1 Protein extraction	81
2.2.2 Filter aided sample preparation (FASP)	81
2.2.3 LC MS/MS analysis	82
2.2.4 Data analysis	84
2.2.4.1 Protein Identification	84
2.2.4.2 Label free protein quantitation and differential regulation	85
2.2.4.3 Functional annotation analyses of proteins	85
2.3 Rat aortic ring isometric tension studies (<i>ex vivo</i> studies)	86
2.3.1 Aortic ring model	86

2.3.2 Animals.....	86
2.3.3 Isolation of the aortic rings	88
2.3.4 Isometric tension measurement protocol	91
2.3.5 Assessment of the effects of <i>ex vivo</i> OA administration on aortic ring contraction and relaxation	92
2.3.5.1 Pre-treatment protocol.....	92
2.3.5.2 Protocol assessing OA's direct pro-relaxation effects	92
2.4 Statistical analyses	95
Chapter 3: Results	96
3.1 Cell culture studies (<i>in vitro</i> models):	96
3.1.1 Validation of fluorescence probe-specificity (DAF-2/DA, DHR-123 and DCF).....	96
3.1.2 Baseline studies	98
3.1.2.1 Baseline NO levels in AECs and CMECs.....	98
3.1.2.2 Baseline ROS levels in AECs and CMECs	99
3.1.3 Endothelial injury induction: NO-production, ROS production and cell viability.100	
3.1.3.1 Concentration-response investigations.....	100
3.1.3.1.1 NO measurements with DAF-2/DA.....	100
3.1.3.1.2 ROS Measurements with DHR-123 and DCF.....	105
3.1.3.1.3 Necrosis measurements with PI	115
3.1.4 Endothelial injury induction: Western blot analyses of signalling proteins	120
3.1.4.1 Total and phosphorylated eNOS (Ser 1177)	120
3.1.4.2 Total and phosphorylated PKB/Akt (Ser 473).....	122
3.1.4.3 Heat shock protein 90 (HSP 90) expression.....	124
3.1.4.4 IKB alpha expression	125
3.1.4.5 Nitrotyrosine expression.....	126
3.1.5 Oleanolic acid (OA) studies	127

3.1.5.1 1 hour treatment studies	127
3.1.5.2 24 hour treatment studies	133
3.1.6 OA (40 μ M) pre-treatment studies	139
3.1.6.1 DAF-2/DA (NO production) fluorescence measurements with OA pre-treatment	139
3.1.5.2 DCF (H ₂ O ₂ production) fluorescence measurements with OA pre-treatment	141
3.2 Proteomics studies	145
3.2.1 Control, untreated AECs and CMECs	146
3.2.1.1 Comparative differential protein regulation and functional annotation analysis: Strongly represented proteins in control, untreated AECs (compared to CMECs)	146
3.2.1.2 Comparative differential protein regulation and functional annotation analysis: Strongly represented proteins in control, untreated CMECs (compared to AECs)	147
3.2.2 TNF- α treated AECs and CMECs	159
3.2.2.1 Differential protein regulation and functional annotation analysis: Strongly represented proteins in TNF- α treated AECs (compared to control, untreated AECs)	159
3.2.2.2 Differential protein regulation and functional annotation analysis: Strongly represented proteins in TNF- α treated CMECs (compared to control, untreated CMECs)	163
3.2.2.3 Differential protein regulation and functional annotation analysis: Strongly represented proteins in TNF- α treated AECs compared to TNF- α treated CMECs ...	167
3.3 Rat aortic ring isometric tension studies (<i>ex vivo</i> studies)	183
3.3.1 Biometric data	183
3.3.2 Baseline isometric tension studies in aortic rings from Lean and HFD (16 weeks)	186

3.3.3 Effects of <i>ex vivo</i> oleanolic acid (OA) administration on aortic ring contraction and relaxation from lean and HFD rats (16 weeks)	188
3.3.3.1 OA administration (aortic rings from lean rats).....	188
3.3.3.2 OA administration (aortic rings from HFD rats).....	190
3.3.4 Effects of <i>ex vivo</i> oleanolic acid (OA) administration on aortic ring contraction and relaxation from lean and HFD rats (24 weeks)	192
3.3.4.1 OA administration (aortic rings from lean rats).....	192
3.3.4.2 OA administration (aortic rings from HFD rats).....	194
3.3.5 Effects of direct OA administration on rat aortic rings (24 weeks)	196
Chapter 4: Discussion	197
4.1 Cell culture studies (<i>in vitro</i> models)	197
4.1.1 Summary of findings	197
4.1.1.1 Baseline findings	197
4.1.1.2 Endothelial injury induction findings.....	197
4.1.1.3 Western blot analyses of signalling proteins.....	199
4.1.1.4 Oleanolic acid studies	200
4.1.2 Discussion of cell culture (<i>in vitro</i> models) data.....	201
4.1.2.1 Baseline findings	202
4.1.2.2 Endothelial injury induction.....	206
4.1.2.3 Oleanolic acid studies	217
4.2 Proteomics	219
4.2.1 Endothelial cell proteomics	219
4.2.2 Large scale protein expression and regulation in control, untreated AECs and CMECs	219
4.2.2.1 Strongly represented proteins in untreated control AECs compared to CMECs	220

4.2.2.2 Strongly represented proteins in untreated control CMECs compared to AECs	223
4.2.3 Large scale protein expression and regulation in TNF- α treated AECs and CMECs	226
4.2.3.1 Strongly represented proteins in TNF- α treated AECs (compared to control, untreated AECs)	226
4.2.3.2 Strongly represented proteins in TNF- α treated CMECs (compared to control, untreated CMECs).....	230
4.2.3.3 Differential protein regulation and functional annotation analysis: Strongly represented proteins in TNF- α treated AECs compared to TNF- α treated CMECs. ...	233
4.2.3.4 Differential protein regulation and functional annotation analysis: Strongly represented proteins in TNF- α treated CMECs compared to TNF- α treated AECs. ...	235
4.3 Rat isometric tension studies (ex vivo studies).....	237
4.3.1 Summary of findings	237
4.3.2 Discussion of data	238
4.3.2.1 Isometric tension studies in aortic rings from lean and HFD rats (16 week diet)	238
4.3.2.2 Effects of <i>ex vivo</i> oleoic acid (OA) pre-administration on aortic ring contraction and relaxation from lean and HFD rats (16 and 24 week diet).....	239
4.3.2.3 Effects of direct OA administration on aortic rings (24 week diet).....	241
4.4 Integration of findings.....	242
4.4.1 Baseline endothelial heterogeneity in AECs and CMECs.....	242
4.4.2 Heterogeneity in AEC and CMEC model of endothelial injury	244
4.4.2.1 TNF- α signalling in AECs (compared to control, untreated AECs).....	246
4.4.2.2 TNF- α signalling in CMECs (compared to control, untreated CMECs).....	248
4.4.2.3 NO production and eNOS signalling in TNF- α treated AECs vs. TNF- α treated CMECs.	250

4.4.2.4 ROS production in TNF- α treated AECs vs. TNF- α treated CMECs	252
4.4.2.5 Cell viability in TNF- α treated AECs vs. TNF- α treated CMECs	254
4.4.2.6 TNF- α signalling in AECs vs. CMECs	254
4.4.2.7 Modulation of endothelial injury by OA	256
4.4.3. Aortic ring experiments	257
Chapter 5: Conclusions	259
Limitations of the current study:	265
Outputs emanating directly or indirectly from the current study.....	266
References	257

Chapter 1

1.1 Introduction

Globally, under the non-communicable disease category, cardiovascular diseases are reported to be the leading cause of death according to the World Health Organisation (WHO 2011b; http://www.who.int/cardiovascular_diseases/publications/atlas_cvd/en/). Furthermore, according to the WHO, cardiovascular diseases accounted for 30 % (approximately 17 million deaths) of total global deaths in 2008 (Figure 1.1) (WHO 2011a: http://www.who.int/nmh/publications/ncd_report2010/en/). From these statistics about 7.3 million deaths were attributable to coronary artery disease (WHO 2011b). By the year 2030, cardiovascular disease associated deaths are expected to rise to a staggering 23.3 million (Mathers & Loncar 2006). In South Africa, cardiovascular diseases accounted for about 195 deaths per day between 1995 and 2004 (Steyn 2007). Cardiovascular disease related deaths are envisaged to increase by 41 % between 2000 and 2030 in the working age group (ages 35-64 years) in South Africa (Steyn 2007). In the Western Cape, cardiovascular diseases were reported to be the leading cause of death where about 1 in 4 people died from cardiovascular diseases in the year 2000 (Figure 1.2 & 1.3) (Bradshaw *et al* 2000).

Cardiovascular disease describes a group of pathophysiological conditions affecting the blood vessels such as atherosclerosis and coronary artery disease, as well as affecting the heart such as myocardial ischaemia or ischaemic heart disease (IHD) (WHO 2011b). Atherosclerosis is described as the hardening of the arteries due to cholesterol and fatty acid build up which may lead to a blockage in the coronary artery (Mehta *et al* 2006). Myocardial Ischaemia or IHD describes a condition by which blood supply to the heart is diminished due to a blockage in the blood vessel, leading to oxygen deprivation and infarction of heart cells (cardiomyocytes) (Shimokawa & Yasuda 2008). Obesity, diabetes, tobacco use, hypertension and hyperlipidaemia / dyslipidaemia are documented as the top risk factors associated with development of cardiovascular diseases (Deaton *et al* 2011).

The endothelium, the cell layer lining the blood vessels, holds key to the development of atherosclerosis and eventually IHD (Michiels 2003). Introduction of risk factors such as those mentioned above, lead to pathophysiological changes of the endothelium that result in endothelial activation and dysfunction (Hunt & Jurd 1998, Hadi *et al* 2005). The endothelium shifts from a vascular homeostasis maintaining cell layer to an atherosclerotic disease-mediating cell layer (Esper *et al* 2006). Endothelial activation and dysfunction represent the initial reversible steps towards the development of atherosclerosis (Deanfield *et al* 2007). Hence understanding endothelial physiology especially with regards to vascular bed specificity, including vascular bed specific endothelial cell characteristics and functions, is imperative in the prevention and management of atherosclerosis.

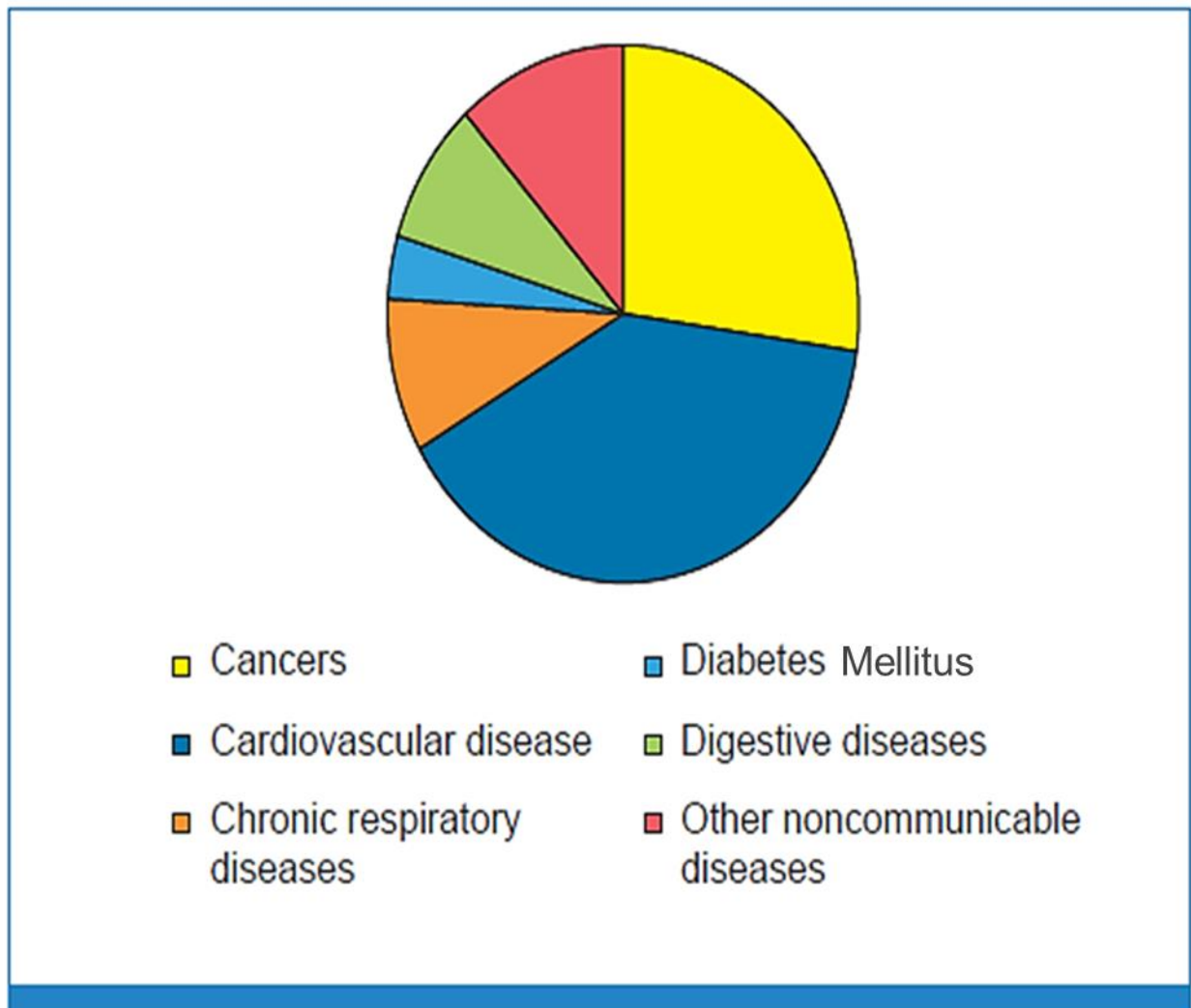


Figure 1.1: Global non-communicable disease related deaths in the age group of under 70 in 2008. Cardiovascular diseases accounted for a large proportion of non-communicable disease related deaths (WHO 2011a).

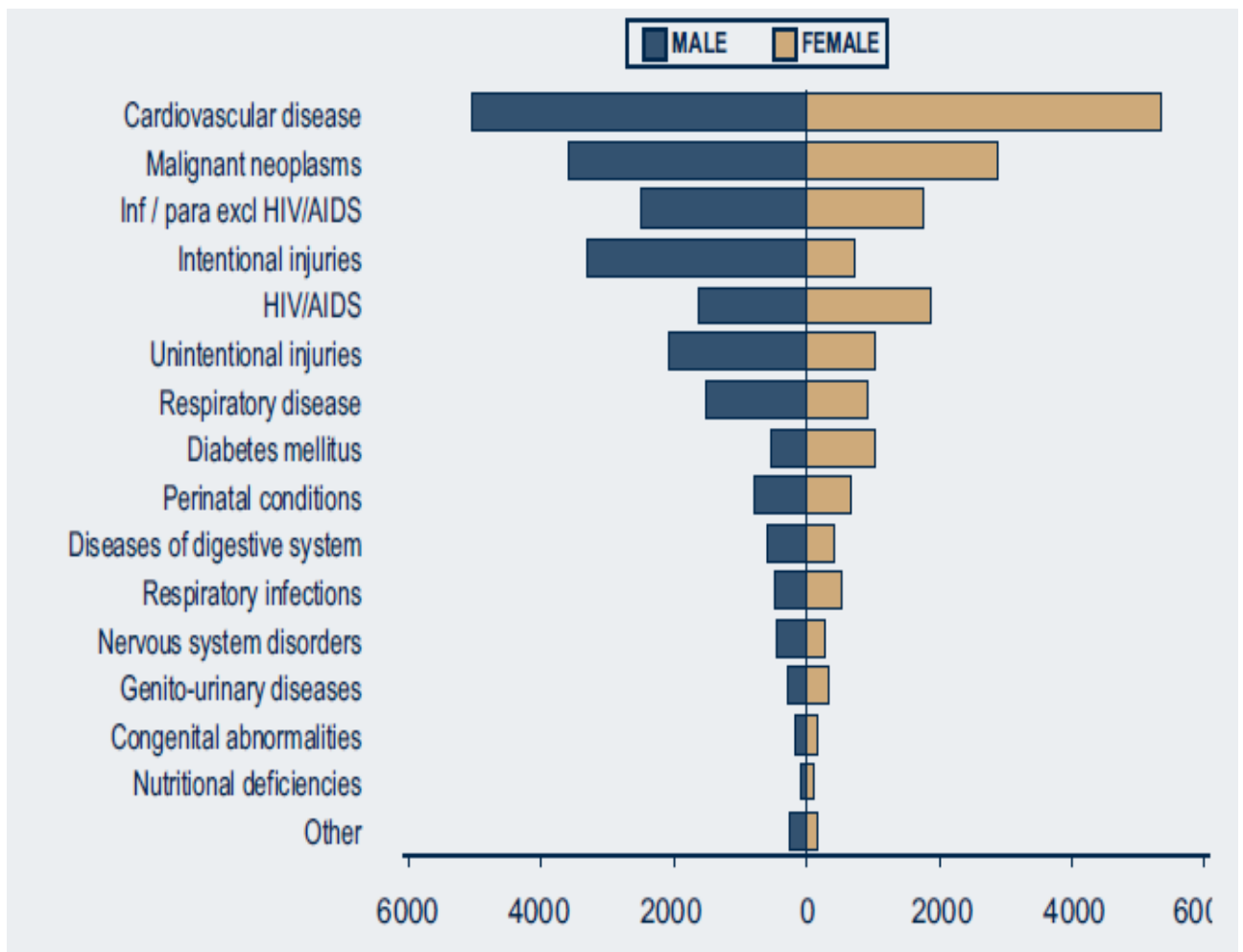


Figure 1.2: Cardiovascular diseases as the major cause of death in the Western Cape in the year 2000 (Bradshaw *et al* 2000).

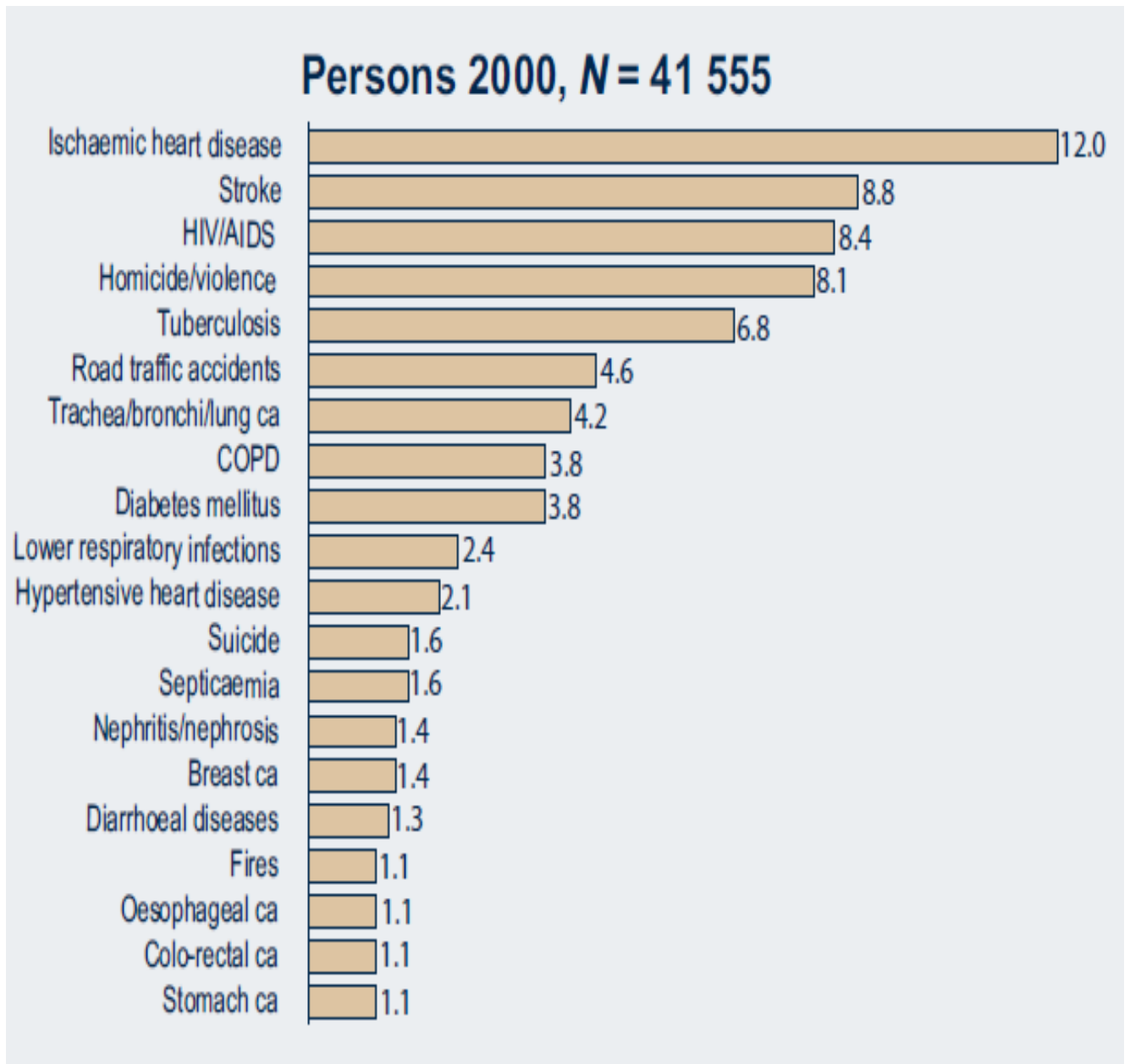


Figure 1.3: Twenty major conditions associated with death in the Western Cape during the year 2000. Ischaemic heart disease accounted for 12 % of all deaths (Bradshaw *et al* 2000).

1.2 The endothelium

In the nineteenth century, Rudolph Virchow observed a cell layer inside a capillary vessel and referred to it as a simple membrane with flattened nuclei (Laubichler *et al* 2007). The word endothelium was invented by a Swiss anatomist Wilhelm His in 1865 (Laubichler *et al* 2007). According to His, the endothelium lined the body cavities such as blood vessels, lymphatics and other mesothelial-lined spaces (Aird 2007a). The description of the word endothelium was later refined to an inner cell lining of the blood vessels and lymphatics (Laubichler *et al* 2007, Aird 2007a).

Wilhelm His differentiated the endothelium from the epithelium, stating that subsequent to their development, endothelial cells assume their characteristic flattened shape, becoming quiescent and not significantly contributing to growth processes in the body (Laubichler *et al* 2007). For many years after its discovery, the endothelium was deemed an inactive, partially permeable barrier which merely served to protect the underlying tissues from their external environment (Mas 2009). However, over the years, this cell layer evoked a lot of interest in research, thus leading to ground breaking discoveries of its function on the vascular system in health and disease (Michiels 2003). With some authors now referring to it as the *cellular orchestra maestro* (Nachman 2012, Eliseyeva 2013), it has now been established that the endothelium is by no means an inactive organ.

The endothelium is now perceived as a receptor effector organ which is able to input and process different types of chemical or mechanical stimuli, and elicits a response by producing factors appropriate for each stimulus (Esper *et al* 2006). In this way, the endothelium is able to accomplish some of its major roles such as to maintain vascular homeostasis, regulate vascular tone and vascular inflammation during physiological conditions (Eliseyeva 2013). Regulating vascular homeostasis entails keeping a constant balance between a vasodilatory state and a vasoconstrictory state (Esper *et al* 2006). During a vasodilatory state, factors such as nitric oxide (NO), endothelium derived hyperpolarising factor (EDHF) and prostacyclin (PGI₂) are released by endothelial cells. All these factors are commonly associated with anti-oxidant, anti-inflammatory and anti-thrombotic activity (Mudau *et al* 2012). Conversely, a vasoconstrictory state is accompanied by the endothelial release of factors such as endothelin-1 (ET-1), angiotensin-II and thromboxane A₂ (TXA₂), all

of which are associated with pro-oxidant, pro-inflammatory, and pro-thrombotic activity (Mudau *et al* 2012). Via the release of these vasoactive factors, the endothelium regulates vasomotor tone in response to increased blood flow or shear stress in addition to maintaining the structural integrity of the blood vessel (Mas 2009). A diversion in this delicate balance favours development of endothelial dysfunction (ED) which is a predecessor of various life threatening cardiovascular diseases such as atherosclerosis and ischaemic heart disease (Strijdom & Lochner 2009). Hence the endothelium could be considered a gatekeeper of the vascular system during physiological conditions.

1.2.1 Anatomy and structure of the endothelium

The endothelium is a single cell layer comprised of about ten trillion cells serving as a semi permeable barrier between blood and underlying tissues in the entire vascular system (Ait-Oufella *et al* 2010). The endothelium contributes about 1-1.5 kg of overall body weight and can be spread out to cover an enormous surface area of about 4000-7000 m² (Ait-Oufella 2010, Galley & Webster 2004). Endothelial cells are typically thin and flat, with their length ranging from 25 to 50 µm, width from 10 to 15 µm and up to 5 µm in thickness (Thorin & Shreeve 1998, Limaye & Vadas 2006).

Within the same species or individual segments of the blood vessels, endothelial cells may differ in structure, function, and antigen expression thus giving rise to the phenomenon of endothelial heterogeneity (Thorin & Shreeve 1998, Aird 2007a). Endothelial heterogeneity is influenced by the location, size and function of the host blood vessel (Thorin & Shreeve 1998). For example, endothelial cells in high endothelial venules are plump or cuboidal unlike the typically flat characteristic observed in other endothelial cells across the vascular tree (Girard & Springer 1995). Capillary and vein derived endothelial cells are ± 0.1 µm in thickness and round in shape, whereas aortic endothelial cells are about 1 µm thick and spindle shaped (Aird 2007a, Mas 2009).

The plasma membranes of endothelial cells are endowed with various specific receptors, and proteins that facilitate signal transduction, maintenance of homeostasis, inflammation and permeability regulation, thus preserving a non-thrombogenic surface (Simionescu *et al*

2002). Weibel-palade bodies (WPBs) are plasmalemmal vesicles exclusively found in endothelial cells, which store a procoagulant, von Willebrand factor (vWF) and proinflammatory protein, P-selectin; hence playing a role in vascular injury response (Mas 2009). However, these vesicles are not equally distributed across the vascular tree, and they are not expressed in all endothelial cells (Thorin & Shreeve 1998, Aird 2007a). WPBs have been found to occur in high numbers in vessels that are in close proximity to the heart and are low in some microvessels (Thorin & Shreeve 1998). Capillary-derived endothelial cells have more WPBs than arteriolar-derived endothelial cells (Thorin & Shreeve 1998). The density of caveolae has also been found to differ in endothelial cells in different sites of the vascular system (Aird 2012). Caveolae are flask shaped invaginations of the cellular membrane which mediate signal transduction and movement of substances through the endothelium (transcytosis) (Aird 2012, Mas 2009). Capillary-derived endothelial cells are profusely supplied with caveolae, amounting to a density of up to 10 000 per cell, than endothelial cells from other sites such as arteries, arterioles, veins and venules (Aird 2012). However, this also differs according to the location in the vascular tree. For instance, capillary endothelium in the blood-brain barrier has significantly lower density of caveolae than myocardial capillary endothelium (Simionescu *et al* 2002).

Endothelial cell to cell attachment is mediated by three types of intercellular junctions, namely, adherens junctions, tight junctions and gap junctions (Mas 2009). Adherens junctions are made up of transmembrane proteins, vascular endothelial cadherin (VE-cadherin), whereas tight junctions are made up of transmembrane proteins, occludin and claudin-5 (Mas 2009). These structures are not merely intercellular connecting junctions, but are also involved in the regulation of cell growth and apoptosis (Dejana 2004). Tight junctions regulate paracellular transport of solutes and ions, as well as cell polarity (Dejana 2004, Aird 2007a). Gap junctions are composed of channels referred to as connexons, which are made up of six transmembrane proteins, connecting the cytoplasm of adjacent cells. Gap junctions can either link two neighbouring endothelial cells with each other (homocellular junctions), or link endothelial cells to adjacent smooth muscle cells (heterocellular junctions) (Mas 2009).

A layer lining the endothelium is found at the luminal surface of the vascular system (Pries *et al* 2000). This layer is referred to as the glycocalyx and has a membrane bound gel-like

composition of macromolecules such as proteins, glycolipids, glycoproteins and proteoglycans (Pries *et al* 2000; VanTeefflen *et al* 2007). The glycocalyx is coated by a much thicker layer of fixed plasma which can prohibit red blood cells and other larger molecular solutes from permeating the endothelium (Pries *et al* 2000). These two layers are collectively referred to as the endothelial surface layer (ESL) (Reitsma *et al* 2007). Besides controlling what penetrates the endothelium, this layer also regulates shear stress sensing, leukocyte adhesion and signalling (Reitsma *et al* 2007). Several studies have shown that this layer is altered in pathophysiological conditions such as diabetes, ischaemia / reperfusion and atherosclerosis (Reitsma *et al* 2007). Although endothelial cells have mitochondria, they preferentially derive their energy or adenosine triphosphate (ATP) from anaerobic glycolysis, and hence the major role of mitochondria in endothelial cells may be signalling, such as to modulate reactive oxygen species (ROS) production (Kluge *et al* 2013). Endothelial heterogeneity has been shown to influence the quantity of mitochondria across the vascular tree (Kluge *et al* 2013). For example, endothelial cells from the blood-brain barrier express larger numbers of mitochondria than capillaries of other vascular locations (Oldendorf *et al* 1977).

1.3 Endothelial physiology and function

Under normal circumstances, the endothelium strives to maintain vascular homeostasis, which includes the regulation of vascular tone, vascular inflammation, leukocyte trafficking and blood coagulation (Strijdom & Lochner 2009). Functionally, the endothelium may exhibit regional specialization such that vasomotor tone is primarily regulated in the arteries and arterioles, leukocyte trafficking in venules whereas selective solute exchange is primarily regulated in the capillaries (Aird 2007a, Mas 2009). However, regardless of the vascular location, the release of endothelium-derived factors is crucial for endothelial cells to carry out most of their physiological functions (Table 1.1).

Table 1.1: Summary of endothelium-derived vasoactive factors (Mudau *et al* 2012).

Endothelium-derived factors	Physiological effects	Enzymatic source and mechanism of action
1. Nitric Oxide (NO)	<ul style="list-style-type: none"> • Potent vasodilator • Inhibits inflammation, VSMC proliferation and migration, platelet aggregation and adhesion, and leukocyte adhesion. • Regulates myocardial contractility. • Regulates cardiac metabolism. • Cardioprotective during ischaemia-reperfusion injury. 	<ul style="list-style-type: none"> • It is synthesised by the enzymes: eNOS, nNOS and iNOS, with eNOS being the major source of NO during physiological conditions in the endothelium. • Diffuses from endothelial cells to underlying VSMCs where it binds to an enzyme, soluble guanylyl cyclase, leading to a cascade of events that ultimately result in vascular relaxation.
2. Prostacyclin (PGI₂)	<ul style="list-style-type: none"> • Vasodilatory agent. • Inhibits platelet aggregation. 	<ul style="list-style-type: none"> • Derived from arachidonic acid by enzyme cyclooxygenase-2 (COX-2).
3. Endothelium-derived hyperpolarising factor (EDHF)	<ul style="list-style-type: none"> • Exerts vasodilatory effects particularly in small arteries of diameter of $\leq 300 \mu\text{m}$. 	<ul style="list-style-type: none"> • Its identity is still under suspicion with proposed candidates such as potassium ions and, hydrogen peroxide. • Causes relaxation of VSMCs by means of membrane hyperpolarisation.
4. Endothelin-1 (ET-1)	<ul style="list-style-type: none"> • A potent vasoconstrictor. 	<ul style="list-style-type: none"> • Synthesised by endothelin-converting enzyme. • Exerts its effects via two receptors: ET_A expressed on endothelial cells and ET_B on VSMCs. ET_A receptors promote vasoconstriction, whereas ET_B receptors promote NO production and ultimately reduction in ET-1 production.
5. Thromboxane A₂ (TXA₂)	<ul style="list-style-type: none"> • A potent vasoconstrictor. 	<ul style="list-style-type: none"> • Derived from arachidonic acid by enzyme COX-1.
6. Angiotensin II	<ul style="list-style-type: none"> • A potent vasoconstrictor. 	<ul style="list-style-type: none"> • Synthesised by angiotensin converting enzyme. • Elicits its effects via two receptors: AT₁ which promotes vasoconstriction and cell proliferation, and AT₂ which antagonises the effects of AT₁.

1.3.1 Endothelium-derived factors

1.3.1.1 Nitric oxide (NO)

NO is a diatomic gas and a free radical which up until the 1980s was considered to be nothing more than a toxic atmospheric pollutant (Strijdom *et al* 2009). Its discovery as the endothelium-derived relaxing factor (EDRF) (Ignaro *et al* 1987, Hutschingson *et al* 1987), led to vast amounts of research and hence publications, revealing its dynamic role in the cardiovascular system. NO is endogenously produced by a family of enzymes, referred to as nitric oxide synthases (NOS) from an amino acid L-arginine (Andrew & Mayer 1999) . NO is endowed with biochemical properties that favour signalling thus leading to a wide array of physiological reactions (Strijdom *et al* 2009). For example, NO being a gas and a free radical, allows for easy diffusion between cells and interaction with various molecules in the body (Strijdom *et al* 2009). Furthermore, NO is extremely soluble in hydrophobic milieus (Rochette *et al* 2013).

1.3.1.1.1 Nitric oxide synthase (NOS)

NOS is an enzyme with a molecular mass which varies from 131 to 161 kDa and catalyses the conversion of L- arginine to NO and L-citrulline as a by-product (Bruckdofer 2005). This enzyme exists in three isoforms dubbed, neuronal NOS (nNOS) first isolated in neuronal tissues, inducible NOS (iNOS) first isolated in the macrophages and endothelial NOS (eNOS) first isolated in endothelial cells (Daff 2010). eNOS and nNOS are constitutively expressed and are calcium dependent whereas, iNOS is expressed upon a pro-inflammatory stimuli such as an increase in circulating inflammatory cytokines due to injury / insult, and is calcium independent (Fostermann & Sessa 2011). Upon induction, iNOS can produce large amounts of NO, in fact a 1000-fold more than eNOS and nNOS (Strijdom *et al* 2009). As NO has high affinity for superoxide anion (O_2^-) (Strijdom & Lochner 2009), excess NO immediately reacts with O_2^- producing a highly reactive nitrogen species known as peroxynitrite ($ONOO^-$) (Strijdom *et al* 2009). Amongst other roles, nNOS-derived NO in the central nervous system has been reported to modulate central blood pressure (Togashi *et al* 1992, Fostermann and Sessa 2011). The eNOS isoform is considered to be the major source

of physiological (baseline) NO production in the cardiovascular system (Fostermann & Munzel 2006).

NOS enzymes are synthesized in monomeric forms (Fostermann & Munzel 2006). However, for optimal enzyme activity, dimerization of the two monomers is required forming a homodimer (Figure 1.4) (Rochette *et al* 2013). Co-factors such as tetrahydrobiopterin (BH₄), nicotinamide adenine dinucleotide phosphate (NADPH), calmodulin and substrates oxygen and L-arginine are essential for catalytic activity of the enzyme (Fostermann & Munzel 2006). All NOS isoforms are expressed with an N-terminal oxygenase domain that binds a haem prosthetic group, BH₄, oxygen and L-arginine, and a C-terminal reductase domain which binds NADPH, flavin mononucleotide (FMN) and flavin adenine dinucleotide (FAD) (Balligand 2002). The dimeric structure of NOS is arranged in such a manner that the reductase domain of one dimer coordinates with the oxygenase domain of the other dimer (Rochette *et al* 2013). Homodimers comprise of a zinc thiolate cluster at the dimer frontier, which arises from a zinc ion that is arranged in a tetrahedral conformation to pairs of cysteine residues [Cys-(X)₄-Cys motif], from each monomer (Fostermann & Munzel 2006, Raman *et al* 1998). This structure facilitates the binding of L-arginine and BH₄ (Raman *et al* 1998). BH₄ may serve as an electron donor for oxygen reduction during synthesis of NO (Fostermann & Munzel 2006).

NO synthesis involves the flow of electrons from NADPH through the flavins (FMN and FAD) to the haem (Stuehr *et al* 2001). Binding of calmodulin increases the movement of electrons to the haem (Stuehr *et al* 2001). For calcium dependent eNOS and iNOS, a rise in intracellular calcium levels is necessary for calmodulin to bind to the enzyme (Fostermann & Sessa 2011). However, in iNOS, calmodulin readily binds to the enzyme at low levels of intracellular calcium (Fostermann and Sessa 2011). Upon reaching the haem, the electrons reduce and activate oxygen as well as oxidising L-arginine (Daff 2010, Fostermann & Sessa 2011). L-arginine is metabolised in two steps, it is initially hydroxylated into N^ω-hydroxy-L-arginine, which is further oxidized into L-citrulline and NO (Stuehr *et al* 2001, Daff 2010) (Figure 1.5).

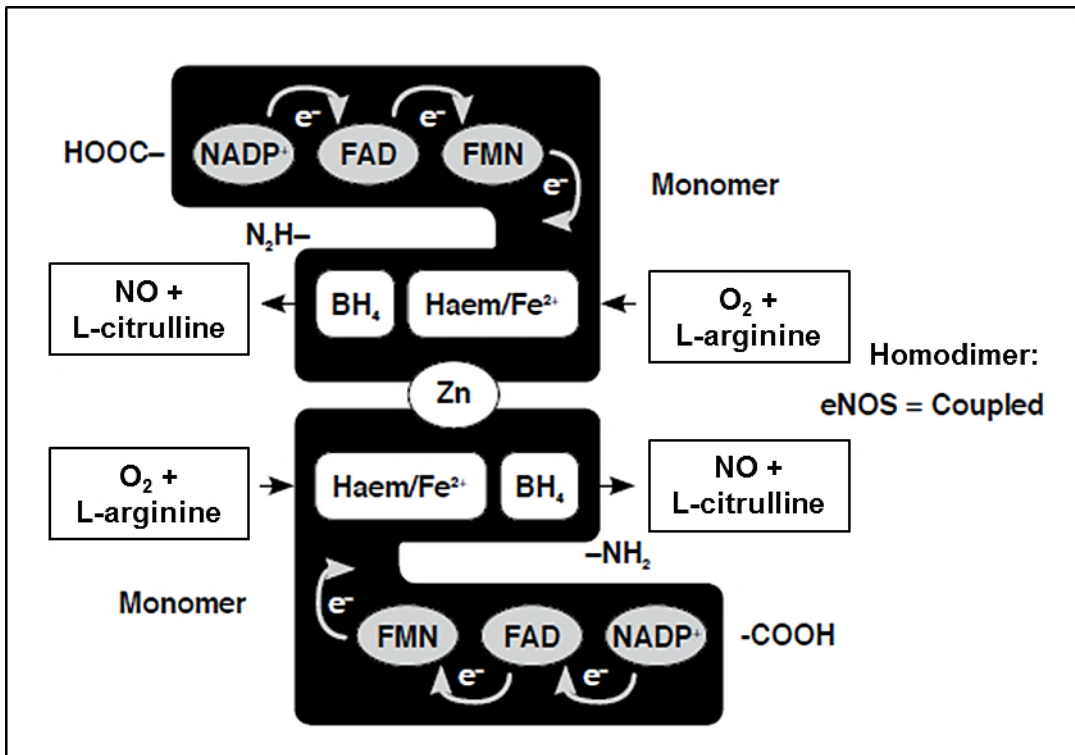


Figure 1.4: A diagram showing the structure of the eNOS homodimer (Mudau *et al* 2012).

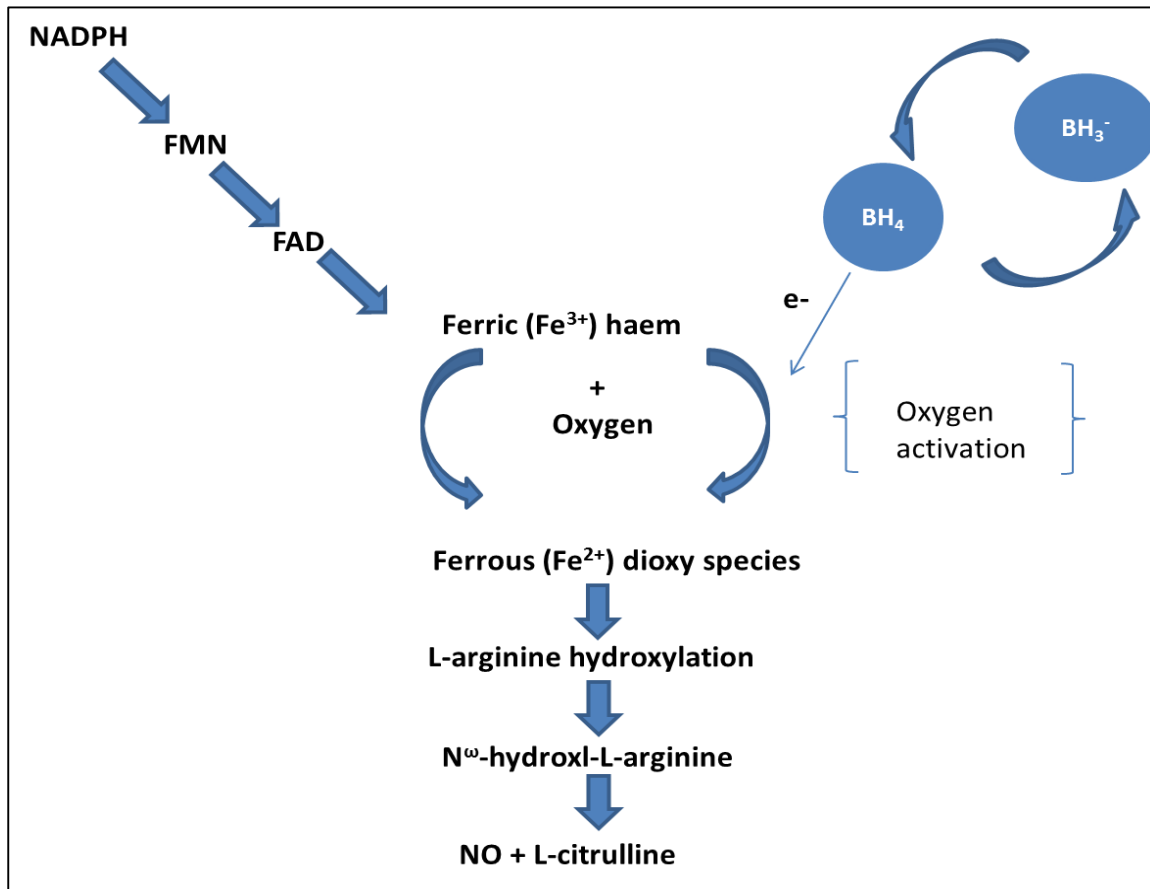


Figure 1.5: A depiction of the flow of electrons during catalysis of NO production. Electrons flow from the reductase domain through the flavins to the haem where oxygen is activated. BH_4 may donate one electron, itself being reduced to BH_3^- . Ascorbic acid may recycle BH_3^- to BH_4 . Activation of oxygen leads to L-arginine hydroxylation and formation of NO.

1.3.1.1.2 Endothelial nitric oxide synthase (eNOS)

eNOS as the name suggests, was initially discovered in endothelial cells, but is also expressed in, among others, cardiac myocytes, platelets, some neuronal tissue in the brain and tubular epithelial cells in the kidneys (Forstermann *et al* 1998). When inactive, eNOS is confined to caveolae where it interacts with a caveolae-derived scaffolding protein known as caveolin-1 (Feron *et al* 1998). The eNOS-caveolin-1 association significantly diminishes the activity of eNOS (Feron *et al* 1998). In fact, caveolin-1 deficient mice have been shown to have increased endothelium dependent vasodilation (Frank *et al* 2003). Binding of calmodulin to eNOS in response to an intracellular rise in calcium, displaces eNOS from caveolin-1 into the cytoplasm thus leading to enzyme activity (Frank *et al* 2003). Hence, caveolin-1 may serve-as a modulator of eNOS activity during physiological conditions (Frank *et al* 2003).

1.3.1.1.3 eNOS activation

eNOS activity is regulated by a multitude of factors such as localization to caveolae, post-translational alteration such as phosphorylation or association with certain regulatory proteins such as heat shock protein 90 (HSP 90) (Takahashi & Mendelsohn 2003a). Various agonists such as shear stress, acetylcholine, bradykinin, insulin, oestrogen, vascular endothelial growth factor (VEGF) can stimulate eNOS activity via a variety of signalling pathways (Figure 1.6) (Kolluru *et al* 2010, Fostermann & Sessa 2011). Shear stress can activate eNOS in a calcium-independent fashion via phosphorylation of the enzyme (Fisslthaler *et al* 2000). Phosphorylation of eNOS can occur at different sites such as Serine (Ser) residues, Tyrosine (Tyr) residues and Threonine (Thr) residues by various kinases (Kolluru *et al* 2010). Sites such as Ser 1177/1179, Ser 617/615, and Ser 633/635 facilitate eNOS activity whereas sites such as Ser 116 and Thr 495 have an inhibitory effect (Figure 1.6) (Kolluru *et al* 2010). Phosphorylation at site Ser 1177, for example, in response to shear stress, enhances the flow of electrons to the haem, and the affinity of calcium / calmodulin for eNOS thereby activating the enzyme (Fleming & Busse 2003). Kinases involved in eNOS phosphorylation include protein kinase B (PKB / Akt), calcium / calmodulin-dependent protein kinase II (CaMKII), AMP-activated protein kinase (AMPK), Protein kinase A (PKA), and

protein kinase C (PKC) (Figure 1.6) (Fleming 2010). Recruitment of kinases for eNOS phosphorylation may differ in accordance with the respective agonists (Fleming & Busse 2003). For example, shear stress, oestrogen, vascular endothelial growth factor (VEGF) and insulin activate eNOS via phosphorylation of Ser 1177 by PKB / Akt, AMPK or PKA (Fisslthaler *et al* 2000, Balligand 2002, Kolluru *et al* 2010). On the other hand, the agonist bradykinin employs CaMKII to phosphorylate eNOS at Ser 1177 (Kolluru *et al* 2010).

HSP 90 is a molecular chaperone that is involved in folding, stabilization and refolding of other proteins (Papapetropoulos *et al* 2005). In eNOS, HSP 90 takes part in the placing of the haem to the developing enzyme, as well as activating the enzyme (Fleming 2010). Certain agonists such as shear stress, insulin, VEGF enhance the binding of HSP 90 to eNOS leading to eNOS activation and hence an increase in NO production (Takahashi & Mendelsohn 2003a). HSP 90 can either increase the binding of calmodulin to eNOS or stimulate PKB / Akt to phosphorylate eNOS thus leading to enzyme activity (Dudzinski & Michel 2007). The latter has been reported to result in formation of eNOS-HSP 90-PKB / Akt complex with a subsequent yield in NO production (Takahashi & Mendelsohn 2003b).

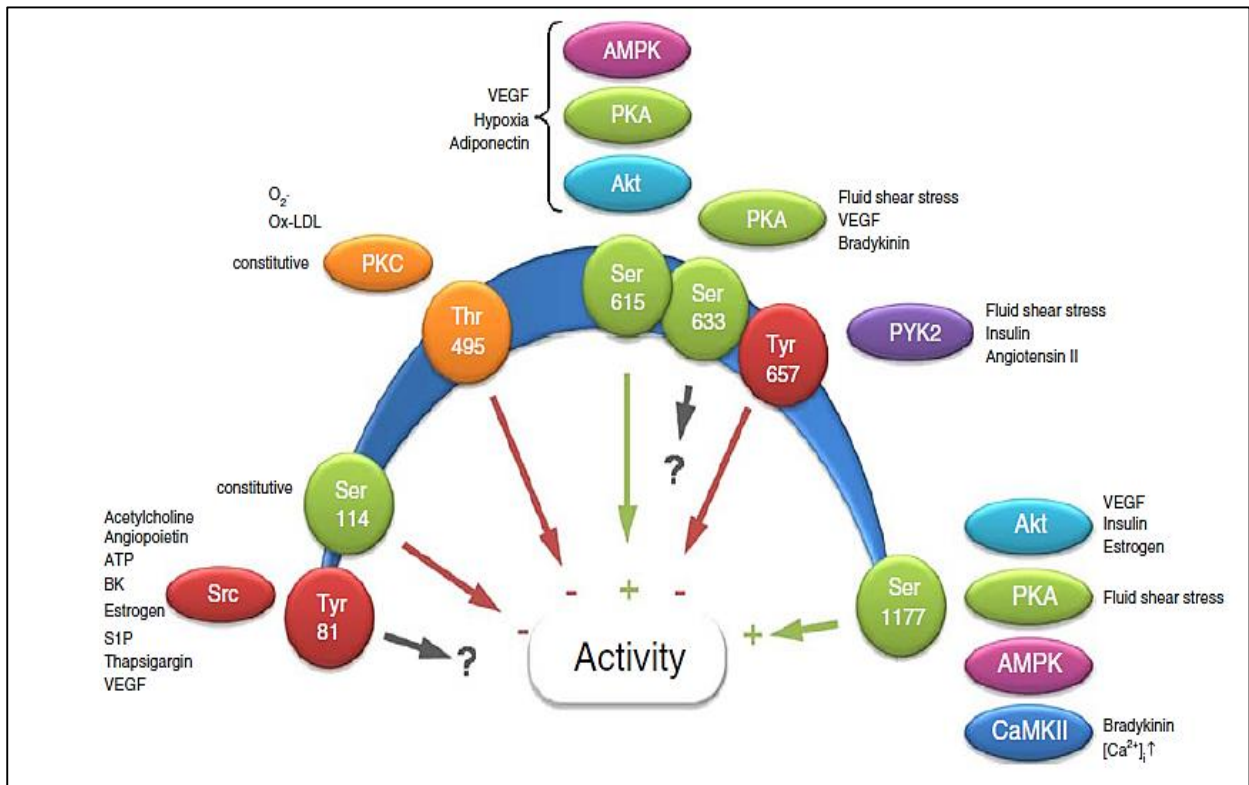


Figure 1.6: Phosphorylation sites and the kinases involved, in eNOS. eNOS activity is regulated at different phosphorylation sites in response to various agonists (Fleming 2010).

1.3.1.1.4 Effects of NO

Physiological effects of NO are widespread, and hence the existence of the three isoforms of NOS in their specialized areas, producing NO in response to specific stimuli in each target organ (Bruckdorfer 2005). Amongst its diverse physiological signalling actions, the first recognised role of NO was vasodilation, though the identification of the EDRF as NO and the pathway through which vasodilation occurs was elucidated at a later stage (Rastaldo *et al* 2007). Acetylcholine (ACh), an endogenous neurotransmitter, was reported to induce vasodilation in the presence of the endothelium and vasoconstriction in the absence of the endothelium (Furchgott & Zawadzki 1980). It was later established that ACh is an agonist that stimulates the endothelium to release of NO (initially recognised as the EDRF) leading to relaxation of vascular smooth muscle and hence vasodilation (Ignarro *et al* 1987).

In smooth muscle containing blood vessels such as the arteries, NO acts in a paracrine manner, immediately diffusing into the underlying vascular smooth muscle cells (VSMCs) where it targets a protein called soluble guanylyl cyclase (sGC) (Bruckdofer 2005). NO binds to the haem of sGC, activating it to catalyse the conversion of guanosine triphosphate (GTP) to cyclic guanosine monophosphate (cGMP) (Bruckdofer 2005). cGMP activates a cGMP-dependent protein kinase I (cGKI) which acts downstream to activate specific proteins that alters the smooth muscle contraction pathways (Pfeifer *et al* 1998). For example, by lowering intracellular calcium levels or increasing activity of myosin light chain phosphatase (MLCP), which is a phosphatase that dephosphorylates the myosin light chain, thus decreasing contraction, leading to relaxation of the VSMCs (Pfeifer *et al* 1998, Bruckdofer 2005). The smooth muscle cell levels of cGMP are regulated by a group of proteins known as phosphodiesterases (PDEs) (Soderling *et al* 2000). PDEs, especially PDE5, degrade cGMP and are hence involved in vascular tone regulation (Soderling *et al* 2000).

Similarly, NO accomplishes its anti-platelet aggregation role by diffusing from the endothelium into the platelets (Bruckdofer 2005). However, platelets have also been reported to produce their own NO (Gkaliagkousi *et al* 2007). In the platelets, NO binds to the haem of sGC leading to the production of cGMP, and hence activation of cGK1 (Smolenski 2012). Platelet cGK1 phosphorylates specific downstream proteins that lead to a

decrease in intracellular calcium levels, and deterrence of granule secretion and platelet aggregation (Moro *et al* 1996).

Aside from regulating vascular tone, NO possesses anti-inflammatory and anti-atherogenic properties (Strijdom *et al* 2009). NO has been reported to regulate the Nuclear factor kappa-B (NF- κ B) / I κ B-alpha complex, thereby regulating inflammation (Peng *et al* 2005). NF- κ B is a transcriptional factor that is involved in the inflammatory response by recruiting certain pro-inflammatory proteins (Kempe *et al* 2005). In the absence of a stimulus, I κ B-alpha regulates NF- κ B activity, by binding to NF- κ B and keeping it inactive (Matthwes *et al* 1996). Prolonged degradation of I κ B, such as during chronic inflammatory conditions (Viatour *et al* 2005) leads to over activity of NF- κ B which can result in vascular dysfunction (Kassan *et al* 2013). Studies with NO donors have shown that NO increases I κ B messenger RNA expression and hinder NF- κ B activity (Peng *et al* 1995, Spiecker *et al* 1998). In addition, NO donors have been found to reduce cytokine-stimulated expression of adhesion molecules, such as vascular cell adhesion molecule-1 (VCAM-1) and intercellular adhesion molecule (ICAM-1) which are markers of endothelial activation and inflammation (Khan *et al* 1996, De Caterina *et al* 1995)

1.3.1.2 Endothelium hyperpolarising factor (EDHF)

Vascular relaxation has been shown to persist even after blocking NO synthesis or other vasodilatory factors in some blood vessels, especially in the small arteries (Nakashima *et al* 1993, Cowan & Cohen 1991). This has since been attributed to the hyperpolarisation of the vascular smooth muscle cells (VSMCs), a mechanism that has been found to induce relaxation independent of an increase in cyclic nucleotides such cGMP (Cohen & Vanhoutte 1995). The factor responsible for this hyperpolarising mechanism has been termed EDHF (Edwards *et al* 1998), however, its identity still remains elusive (Coats *et al* 2001).

EDHF causes hyperpolarisation of the VSMCs by opening the potassium channels, resulting in vasodilation (Ohashi *et al* 2012). Numerous substances such as potassium ions, hydrogen peroxide (H₂O₂) and epoxyeicosatrienoic acids (EETs) (a product of arachidonic acid metabolism), have been suggested as the candidates for EDHF (Edwards *et al* 1998, Matoba

et al 2002, Coats *et al* 2001); however none of them has been formally identified as EDHF (Stankevicius *et al* 2003). EDHF has been found to be of high significance in particularly small vessels, with its pro-vasodilatory properties being inversely proportional to the diameter of the vessels (Shimokawa *et al* 1996).

1.3.1.3 Prostanoids

Prostanoids, such as PGI₂ and TXA₂, are synthesised from arachidonic acid, via a reaction catalysed by the enzymes cyclooxygenases (COX) 1 and 2 (COX-1 for TXA₂ and COX-2 for PGI₂ synthesis) (Moncada *et al* 1977). PGI₂ and TXA₂ are major pro-inflammatory mediators, and hence the development of COX inhibitors for treatment against pain and inflammation (Zivkovic *et al* 2013). In the vascular system, PGI₂ is endothelium-derived and plays a major role in vasodilation and platelet anti-aggregation (Moncada *et al* 1977) whereas TXA₂ is mostly derived from activated platelets and facilitates vasoconstriction and platelet aggregation (Kobayashi *et al* 2004).

In view of the opposing roles played by these two prostanoids in the vascular system, it is critical that a biosynthetic balance is maintained (Minuz *et al* 1990). Cheng *et al* (2002) found that mice with genetic deletion of PGI₂ receptors exhibit platelet hyperactivity and vascular proliferation upon vascular injury; however, these effects were not seen in mice devoid of both PGI₂ and TXA₂ receptors. Furthermore, a TXA₂ antagonist was able to reverse the enhanced platelet activation in response to vascular injury. TXA₂ has been found to be augmented in children with congenital heart disease and pulmonary vascular disorders (Adatia *et al* 1993).

Selective COX-2 inhibition decreases PGI₂ synthesis, which may result in a PGI₂ / TXA₂ biosynthetic imbalance in favour of TXA₂ and has been associated with thrombotic events and myocardial infarction (Murkhejee *et al* 2001). Furthermore, Zivkovic *et al* (2013) reported poor cardiac function and coronary flow with COX-2 selective inhibition in rat hearts, a response that was exacerbated by blocking NO synthesis. PGI₂ causes vasodilation and inhibition of platelet aggregation via activating adenylyl cyclase to catalyse formation of cyclic adenosine monophosphate (cAMP). cAMP activates PKA to phosphorylate

downstream proteins, resulting in VSMCs relaxation and platelet aggregation (Smolenski 2012, Sprague *et al* 2008).

1.3.1.4 Endothelin-1

Endothelin-1 (ET-1) is a potent endothelium-derived vasoconstrictor, produced continuously in small amounts during physiological conditions and participating in vascular tone regulation (Pollock *et al* 1995). Factors that modulate the biosynthesis of ET-1 include shear stress which has been reported to decrease ET-1 synthesis (Malek & Izumo 1992), a change in pH in the renal endothelium (Wesson *et al* 1998), hypoxia (Rakugi *et al* 1990), and exercise which has been shown to stimulate myocardial ET-1 synthesis (Maeda *et al* 1998). ET-1 expression is also increased by various cardiovascular risk factors such as diabetes mellitus (Schneider *et al* 2002), obesity (Weil *et al* 2011), and aging (Donato *et al* 2009). Enhanced expression of ET-1 is associated with cell proliferation and adhesion, thrombosis, inflammation (Yang *et al* 2004, Bohm & Pernow 2007) and atherosclerosis (Barton *et al* 1998).

ET-1 exerts its effects via two G-coupled protein receptors, namely ET_A receptors expressed in VSMCs and ET_B receptors expressed in endothelial cells and VSMCs (Pollock *et al* 1995). During physiological conditions, activation of ET_A receptors lead to vasoconstriction by prompting calcium release from intracellular stores, whereas activation of ET_B receptors prompt the endothelial release of NO leading to vasodilation (Pollock *et al* 1995). Hence ET_B receptors may counteract the vasoconstrictive effects of ET-1 via the NO pathway during physiological conditions (Liu *et al* 2003). This is suggestive that, during conditions of decreased NO bioavailability such as in ED, the vasoconstrictor effects of ET-1 are enhanced. On the other hand, enhanced expression of ET-1 has been reported to decrease eNOS expression and hence NO production via a PKC mediated mechanism (Sud & Black 2009).

1.3.1.5 Angiotensin II

Angiotensin II forms part of the renin-angiotensin system and is among the most potent endothelial derived vasoconstrictors, playing a major role in modulating blood pressure (Mehta & Griendling 2007). The enzyme renin cleaves angiotensinogen to angiotensin I which is further processed to angiotensin II by the angiotensin converting enzyme (ACE) (Mehta & Griendling 2007). Receptors associated with angiotensin II functions are AT₁ and AT₂ (Schmieder *et al* 2007). AT₁ receptors are associated with most of angiotensin II functions such as vasoconstriction, cell proliferation and inflammation, whereas AT₂ receptors appear to oppose the proliferative effect of AT₁ receptors (Schmieder *et al* 2007).

1.4 Pathophysiological changes in the endothelium

1.4.1 Endothelial activation

Although endothelial cells are constantly monitoring their external environment and regulating homeostasis metabolically, they are considered to be quiescent, resembling a non-thrombogenic smooth surface during physiological conditions (Hunt & Jurd 1998, Dryden *et al* 2012). Endothelial activation involves structural changes in the endothelium, which is, induced by inflammation, is characterised by endothelial expression of adhesion molecules such as ICAM-1, VCAM-1, and E-selectin (Hunt & Jurd 1998). Inducers of endothelial activation include pro-inflammatory cytokines such as tumour necrosis factor- α (TNF- α), interleukin-1 (IL-1) and interleukin-6 (IL-6) (Bach *et al* 1997, Liao 2013).

Endothelial activation occurs in two phases, namely, Type I endothelial cell activation and Type II endothelial cell activation (Figure 1.7) (Zhang *et al* 2010). Type I endothelial cell activation is a reversible step that appears directly after exposure to the stimulus and does not involve an increase in protein synthesis or gene transcription (Hunt & Jurd 1998). During this phase, endothelial retraction occurs, which may result in haemorrhage, oedema and increased permeability (Zhang *et al* 2010). The adhesion molecule, P-selectin, is expressed, accompanied by the release of vWF (Hunt & Jurd 1998). Type II endothelial activation is a late reaction and involves an increase in synthesis of proteins and transcription of genes involved in adhesion such as ICAM-1, VCAM-1, E-selectin, and those involved in cytokine, chemokine and tissue factor formation (Hunt & Jurd 1998, Zhang *et al* 2010). The structural changes associated with the Type II endothelial activation phase include endothelial cell protrusion into the vascular lumen, endothelial cell enlargement, enhanced vascular permeability and enhancement of biosynthetic organelles such as Golgi apparatus, endoplasmic reticulum and ribosomes (Zhang *et al* 2010).

When kept under control, endothelial activation may be reversible and the cells may revert to their quiescent phenotype, however, uncontrolled progression can lead to endothelial apoptosis (Bach *et al* 1997). Endothelial activation should not be confused with endothelial injury as the two are not the same, they may however overlap (Blann 2000). During endothelial activation, endothelial cells undergo structural modifications with inducible new functions, without loss of integrity (Zhang *et al* 2010). This may however progress to

endothelial injury and consequently, dysfunction in states of chronic activation (Zhang *et al* 2010). NO has been shown to play a role in modulation of endothelial activation (Liao 2013). De Caterina *et al* (1995) reported decreased cytokine induced expression of ICAM-1, VCAM-1, and E-selectin with NO donors. Increased production of ROS associated with inflammation during endothelial activation may lead to decreased NO bioavailability which may lead to ED (Liao 2013). Decreased NO bioavailability will result in endothelial activation progressing uncontrolled which will lead to endothelial cell injury and death, thus worsening the condition of ED (Liao 2013, Zhang *et al* 2010).

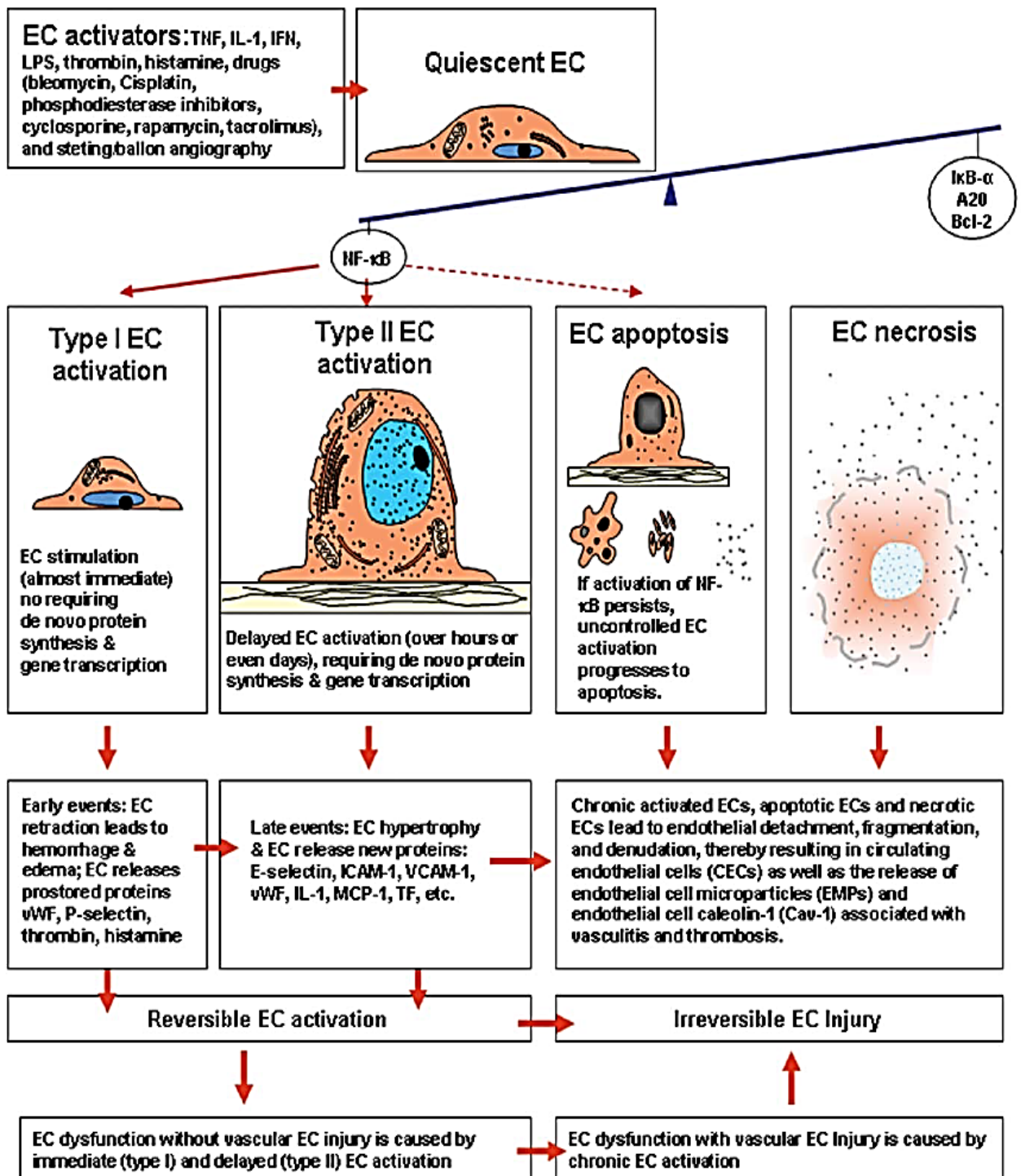


Figure 1.7: Different stages of endothelial activation (Zhang *et al* 2010).

1.4.2 Endothelial dysfunction (ED)

NO takes centre stage in endothelial function and hence ED is described as the reduced bioavailability of NO which may be partly mediated by increased oxidative stress (Strijdom & Lochner 2009, Rubanyi & Vanhoutte 1986, Galan *et al* 2014). ED is characterised by loss of a homeostatic balance between a vasodilatory and a vasoconstrictory state in favour of the latter (Strijdom & Lochner 2009). The endothelium assumes a pathophysiological role, releasing vasoconstricting, pro-oxidant, pro-coagulant, proinflammatory and prothrombotic factors (Esper *et al* 2006). The significance of ED as a subject of research lies in that it precedes the development of atherosclerosis and it is reversible (Figure 1.8), therefore prevention of ED can prevent cardiovascular diseases (Mudau *et al* 2012). The pathophysiological impact of ED extends beyond the cardiovascular system (Malyszko 2010); it is of major importance in kidney function (Malyszko 2010), erectile function and brain function (Schwartz & Kloner 2011). However, for the purpose of this study, cardiovascular function will be the main focus.

Pathological conditions commonly associated with ED include diabetes mellitus / insulin resistance, obesity, metabolic syndrome, aging, smoking, inflammation and oxidative stress (Hadi *et al* 2005). Although oxidative stress itself can be an inducing factor for ED, it also appears to be the common underlying cellular mechanism of ED associated with the pathological conditions mentioned above (Mudau *et al* 2012). In addition to reduced NO bioavailability and oxidative stress, other cellular mechanisms involved in ED include eNOS uncoupling and protein nitration which will be discussed below. More recently, endoplasmic reticulum stress was documented as another risk factor for development of ED, a process which is mediated via oxidative stress (Galan *et al* 2014). The endoplasmic reticulum is responsible for protein translation, folding and trafficking in a cell (Galan *et al* 2014). Endoplasmic reticulum stress can be brought on by factors such as hyperglycaemia, oxidative stress, hypoxia, high levels of calcium and certain chemicals (Kim *et al* 2008).

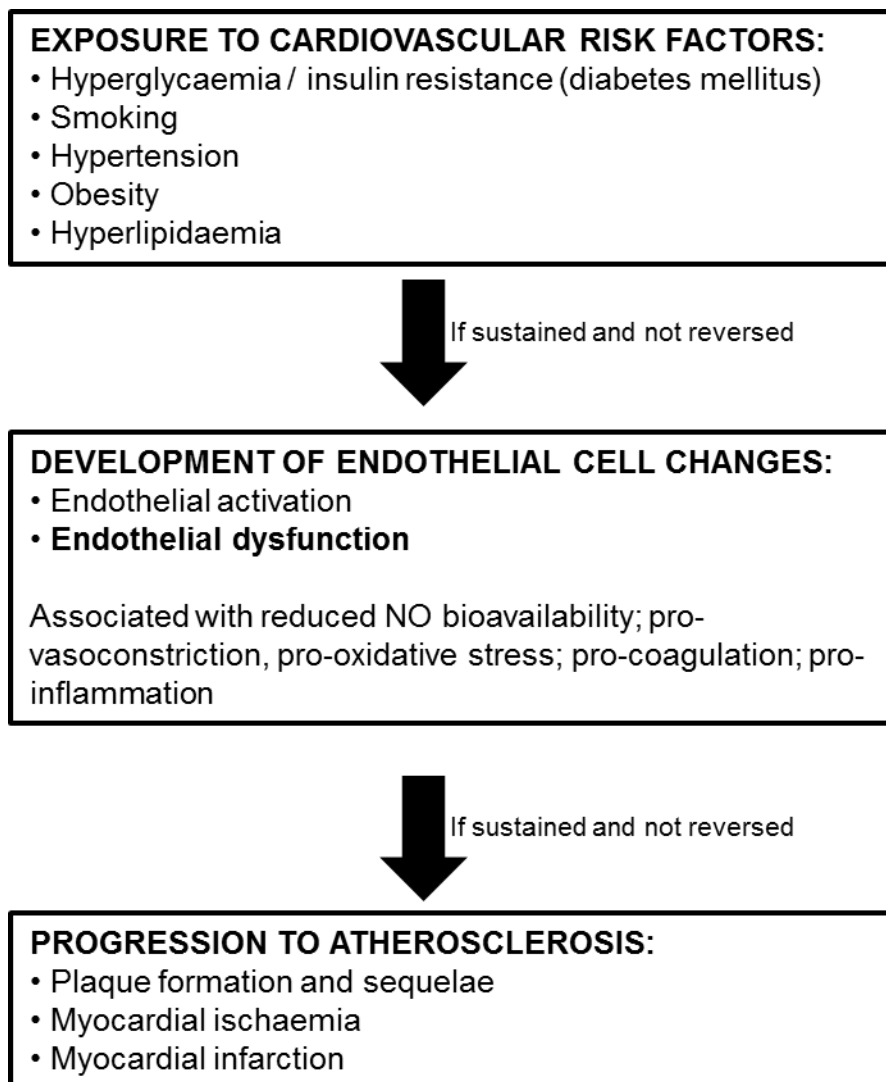


Figure 1.8: ED and progression to atherosclerosis in a nutshell (Mudau *et al* 2012).

1.4.2.1 Reduced NO production

Reduced vascular NO bioavailability may be attributable to factors such as decreased expression and activity of eNOS, or enhanced NO degradation due to increased O_2^- levels during conditions of oxidative stress (Cai & Harrison 2000). eNOS activity may be decreased by lack of eNOS cofactors and substrates such as BH_4 and L-arginine (Yan *et al* 2012), increased interaction of eNOS-caveolin-1 protein (Davignon & Ganz 2004, Geraldes & King 2010), reduced activity of upstream phosphorylators such as PKB / Akt at site Ser 1177 or increased PKC mediated phosphorylation of the inhibitory site Thr 495 (Fleming 2010). During pathophysiological conditions such as oxidative stress, eNOS has been shown to produce ROS at the expense of NO, hence further contributing to oxidative stress and ED (Fostermann & Munzel 2006).

Recently a new mechanism that may lead to decreased NO production has been reported (Pleger *et al* 2008, Sen *et al* 2014). An elongation factor-hand type calcium binding protein called S100A1 has been shown to be expressed in endothelial cells and its deficiency can result in ED (Pleger *et al* 2008, Sen *et al* 2014). Pleger *et al* (2008) studied thoracic aortas derived from S100A1 knockout mice, and reported decreased Ach-induced relaxation as compared to wild type mice, whereas transfection of endothelial cells with S100A1 significantly increased Ach-stimulated NO production. Furthermore this study validated the expression of the protein in different endothelial cell types such as rat cardiac endothelial cells, mouse aortic endothelial cells and human coronary artery endothelial cells. Sen *et al* (2014) reported decreased eNOS activity and hence loss of NO in cytokine mediated decrease of S100A1. S100A1 is an inositol triphosphate receptor agonist and thus stimulate the release of intracellular calcium (Most *et al* 2013). Since eNOS is a calcium dependent enzyme, S100A1 mediated decrease of NO production may be explained by decreased eNOS enzyme activity (Most *et al* 2013).

1.4.2.3 Oxidative / Nitrosative stress

Oxidative stress is described as the augmented production of ROS such as O_2^- , $ONOO^-$ and H_2O_2 , coupled with a decrease in antioxidant activity by superoxide dismutase (SOD) and glutathione peroxidase (Fenster *et al* 2003). These mechanisms ultimately lead to a scenario

whereby ROS overwhelms the defensive mechanisms of antioxidants (Cai & Harrison 2000, Esper *et al* 2006). Cardiovascular oxidative stress is associated with conditions such as heart failure (Landmesser *et al* 2002a), atherosclerosis, hyperlipidaemia, diabetes, hypertension, and smoking (Fenster *et al* 2003). Implications of oxidative stress on vascular function include impaired vasomotor function, oxidation of lipids, VSMC growth, increased expression of adhesion molecules, apoptosis, activation of matrix metalloproteinases and hence vascular remodelling (Harrison *et al* 2003, Griendling *et al* 2000).

Cardiovascular sources of ROS include NADPH oxidase, xanthine oxidase, and uncoupled eNOS (Cai & Harrison 2000). Mitochondria may also contribute to oxidative stress through the electron transport chain (Mittal *et al* 2014). Recently, changes in mitochondrial dynamics such as fission and fusion have been implicated in oxidative stress (Kluge *et al* 2013). Mitochondrial fission is a physiological process whereby the mitochondrion divides to form new individual smaller mitochondria in an attempt to dispose of damaged mitochondria (Youle & Van Der Blik 2012). Enhanced fission has been shown to cause ED via oxidative stress in diabetic patients and in cultured human aortic endothelial cells (AECs) exposed to high glucose (Shenouda *et al* 2011). Makino *et al* (2010) reported similar observations in type-1 diabetic mouse derived coronary endothelial cells.

Landmesser *et al* (2002a) reported a 200 % increase in xanthine oxidase which was associated with oxidative stress and impaired vasodilation in patients with chronic heart failure. Arterial vasodilation was improved with administration of xanthine oxidase inhibitors in smokers (Guthikonda *et al* 2004). However, NADPH oxidase is reported to be the major source of ROS in the vascular system (Griendling *et al* 2000, Guzik *et al* 2000, Landmesser *et al* 2002b). Physiologically, cardiovascular NADPH oxidase is constitutively expressed and produces low amounts of O_2^- at a relatively slow rate (Griendling *et al* 2000). Angiotensin II has been shown to play a role in NADPH oxidase activation in endothelial cells and VSMCs (Griendling *et al* 1994, Li & Shah 2003), which has been linked to increased oxidative stress, decreased endothelium dependent vasodilation and uncoupled eNOS in mice (Dikalov *et al* 2010). NADPH oxidase is composed of membrane bound subunits p22phox, gp91phox and cytosol residing subunits such as p47phox and p67phox in endothelial cells (Jones *et al* 1996, Bayraktutan *et al* 1998). These subunits are used as markers of increased NADPH oxidase expression and activity by many researchers. p22phox

expression has been shown to be increased with oxidative stress in human coronary arteries (Azumi *et al* 1999), in human umbilical vein endothelial cells (HUVECs) together with gp91phox (Gorlach *et al* 2000) and in rat aortas during angiotensin II mediated hypertension (Fukui *et al* 1997). On the other hand p47phox has been associated with enhanced oxidative stress in angiotensin II induced hypertension in mice, and in mouse AECs (Landmesser *et al* 2002b). Guzik *et al* (2002) showed increased expression of p22phox, p47phox and p67phox in arteries and veins of diabetic patients. One of the major implications of increased O_2^- in the cardiovascular system is that it reacts with NO to form another potent oxidant, ONOO⁻ (Reiter *et al* 2000, Yokoyama 2004). O_2^- has been shown to react much faster with NO than it does with the enzyme responsible for its clearance, namely SOD (rate constant = 6.7×10^9 m/s with NO as compared with SOD, rate constant = 2.0×10^9 m/s) (Huang 2003). ONOO⁻ has been reported to result in protein nitration, DNA damage, lipid oxidation and destabilising the structure of eNOS (Mihm *et al* 2000, Kuzkaya *et al* 2003).

1.4.2.3 eNOS uncoupling

eNOS uncoupling is described as the deviation of eNOS from its critical physiological role of producing NO to a pathophysiological role of producing O_2^- (Fostermann & Munzel 2006). A lack of substrate L-arginine or essential cofactors such as BH₄ results in eNOS uncoupling (Yang *et al* 2009). As eNOS functions optimally in producing NO as dimer, failure of the enzyme to dimerise has been linked to eNOS uncoupling, as eNOS monomers catalyse the formation O_2^- in place of NO (Fostermann & Munzel 2006). Although eNOS expression might be expected to decrease with the development of cardiovascular risk factors, it may also unexpectedly increase with exposure to some risk factors (Li H *et al* 2002). This has been attributed to H₂O₂ which has been shown to enhance eNOS expression at transcriptional and post-transcriptional level in human and bovine AECs (Drummond *et al* 2000). Even so, enhanced ROS production and decreased NO are observed in the presence of cardiovascular risk factors (Fostermann & Munzel 2006). ONOO⁻ has been reported to induce eNOS uncoupling by oxidising the cofactor BH₄ or oxidising the Zn ion from the zinc thiolate cluster, thus destabilising the dimeric structure of eNOS (Figure 1.9) (Zou *et al* 2002). BH₄ as a supplement has been shown to restore eNOS function (Yang *et al* 2009).

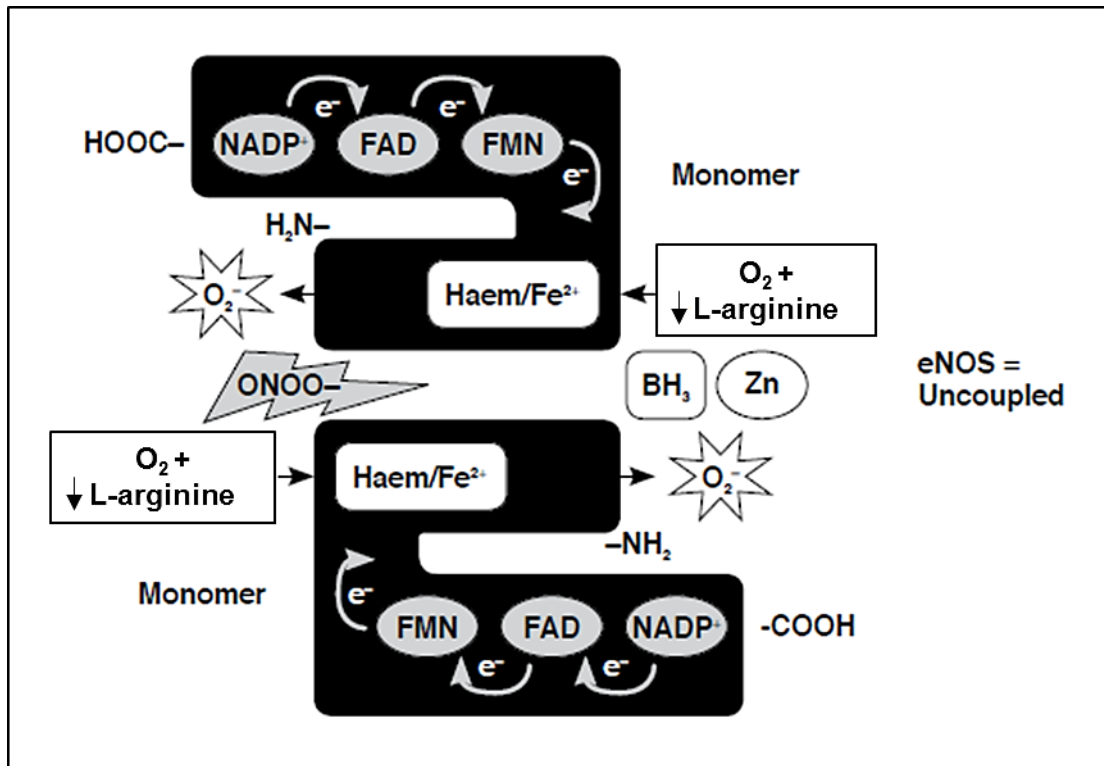


Figure 1.9: eNOS uncoupling. ONOO $^-$ oxidises BH $_4^-$ and releases the zinc ion from the zinc thiolate cluster, destabilising the dimer and leading to eNOS uncoupling (Mudau *et al* 2012).

1.4.2.4 Protein nitration

In addition to inducing eNOS uncoupling, ONOO⁻ is known to cause nitration of proteins at the tyrosine residues forming nitrotyrosine (Beckman 1996). Prostacyclin synthase has also been shown to be a target of nitration by ONOO⁻, thus leading to decreased production of prostacyclin (Nie *et al* 2006). Nitrotyrosine has been used as a marker of oxidative protein damage in a variety of pathological conditions (Beckman 1996). Elevated nitrotyrosine has been found in conditions such as coronary artery disease (Shishehbor *et al* 2003), myocardial inflammation (Neil *et al* 1997), hyperlipidaemia (Onody *et al* 2003), and TNF- α mediated ED in type 2 diabetes (Gao *et al* 2007). Pretreatment with nitrotyrosine has been shown to impair Ach-dependent vasodilation and induce DNA damage in thoracic aortic rings harvested from healthy rats (Mihm *et al* 2000).

1.4.3 Atherosclerosis

Initiation of the atherosclerotic process begins with inflammation, which progresses throughout the disease (Libby *et al* 2002). In fact, atherosclerosis has been described as an inflammatory disease *per se* (Libby *et al* 2002, Ross 1999). Deposition of lipids into the arterial wall, as well as co-occurrence of other cardiovascular risk factors initiates endothelial activation, thus leading to an inflammatory response (Mannarino & Pirro 2008). Endothelial activation culminates in the adhesion of monocytes and subsequent infiltration into the intimal space, due to enhanced expression of adhesion molecules and chemokines such as monocyte chemoattractant protein-1 (MCP-1) (Gu *et al* 1998). In the intima, monocytes are transformed into macrophages that express receptors enabling them to engulf lipids and lipoproteins such as oxidised low density lipoprotein (ox-LDL) and hence transforming into so-called foam cells (Libby *et al* 2002). Activated macrophages and recruitment of more leukocytes into the intima lead to production of cytokines such as IL-1 and TNF- α which further amplifies the inflammatory response (Ross 1999). VSMC proliferation and migration are enhanced, accompanied by increased extracellular matrix, all contributing to the progression of inflammation to atherosclerosis (Ross 1999). This cascade of events represents the initiation and progression of the atherosclerotic lesion.

Furthermore, advanced stages of atherosclerosis have been associated with VSMC apoptosis (Bennett 1999).

1.5 Risk factors associated with pathophysiological changes of the endothelium

1.5.1 Diabetes / Insulin resistance

Insulin resistance can be defined as the reduced ability of the cells to utilize insulin leading to glucose uptake failure and hence hyperglycaemia which may ultimately lead to diabetes mellitus (Kim *et al* 2006). Insulin resistance may occur hand and in hand with conditions such as diabetes, obesity and dyslipidaemia, all which are risk factors of ED (Kim *et al* 2006). Both type 1 and type 2 diabetes are strong predictors of cardiovascular disease (Grundy *et al* 1999). Progression of insulin resistance to diabetes mellitus has been reported to occur concurrently with the progression of ED to atherosclerosis (Figure 1.10) (Hsue *et al* 2004). Oxidative stress has been shown to be the primary mediator of ED in diabetes as evidenced by increased NADPH expression and eNOS uncoupling (Guzik *et al* 2002).

Hyperglycaemia has been shown to enhance PKC activation via oxidative stress. PKC phosphorylates eNOS at its inhibitory site Thr 495 leading to diminished eNOS activity (Geraldes & King 2010). Furthermore PKC activation also increases ET-1 production leading to enhanced contractility (Park *et al* 2000), increases adhesion molecule expression and cytokine release leading to an inflammatory response (Booth *et al* 2002). Consequences of the latter include increased extracellular matrix production, cellular proliferation and vascular permeability (Koya & king 1998). Hyperglycaemia and oxidative stress result in increased glycation of proteins and lipids leading to the formation of advanced glycation end-products (AGEs) (Goldin *et al* 2006). AGEs are known to reduce NOS activity and increase ET-1 production (Xu *et al* 2003, Quehenberger *et al* 2000). Binding of AGEs to receptors for AGEs (RAGE) has been shown to enhance activity of the pro-inflammatory NF- κ B, adhesion molecules such as VCAM-1, ICAM-1 and E-selectin, and cytokines such as TNF- α , all of which lead to the amplification of the inflammatory response (Goldin *et al* 2006).

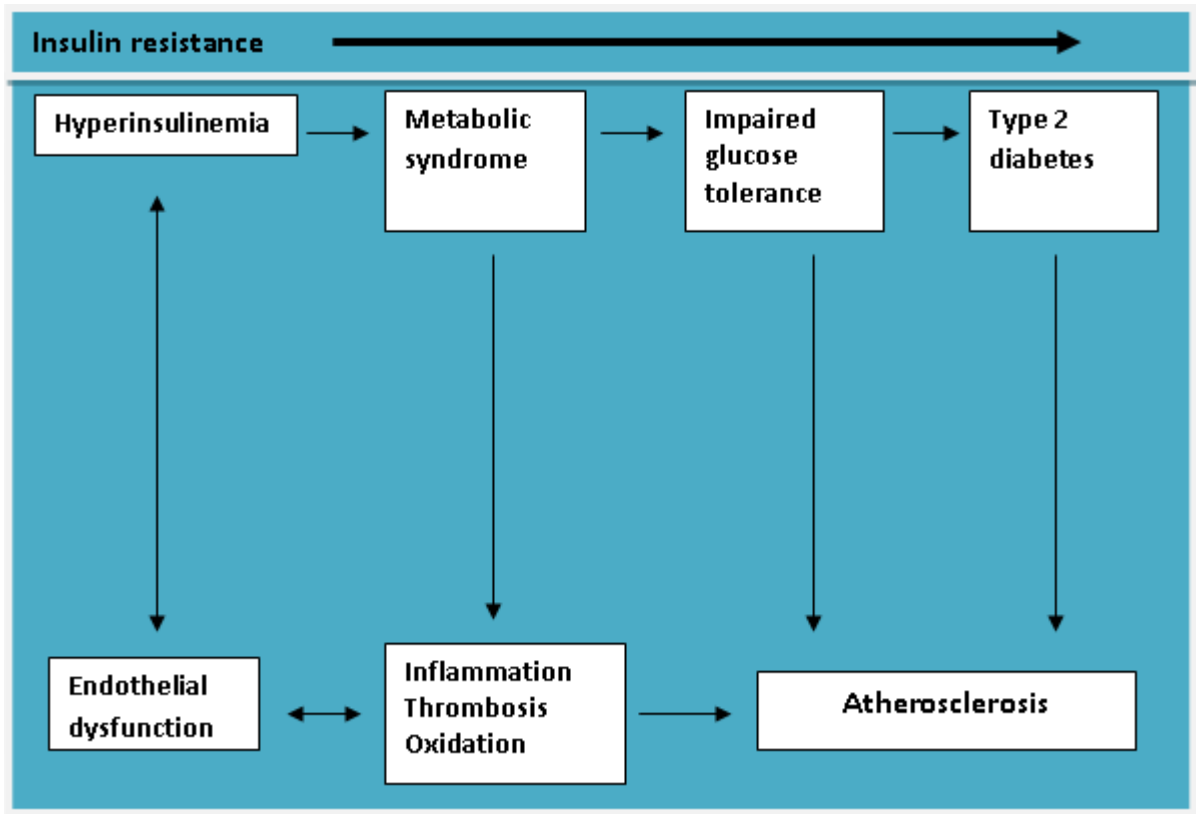


Figure 1.10: Progression of insulin resistance to type 2 diabetes parallels progression of ED to atherosclerosis (Hsue *et al* 2004).

1.5.2 Hyperlipidaemia /Hypercholesterolaemia

A state of hyperlipidaemia is characterised by increased circulating triglycerides, LDL and very low density lipoprotein (VLDL) (Park 2009). Hyperlipidaemia has been associated with atherogenesis via increased oxidative stress (Yang *et al* 2008) and increased plasma levels of asymmetric dimethyl arginine (ADMA) (Böger *et al* 1998). ADMA may act as an eNOS inhibitor as it competes with L-arginine for a binding site on eNOS, leading to production of O_2^- instead of NO (Böger *et al* 1998). Cooke *et al* (1999) showed improved endothelial function in rabbits with hypercholesterolaemia following infusion of L-arginine. LDL is vulnerable to oxidation by ROS leading to the formation of ox-LDL, which plays a major role in atherogenesis, as it is engulfed by macrophages resulting in foam cell formation (Morawietz 2007). Through binding to the lectin-like ox-LDL receptor -1 (LOX-1), ox-LDL impairs endothelial function by decreasing NO (Cominacini *et al* 2001) and increasing ET-1 production (Boulanger *et al* 1992), amplifying endothelial activation, and causing apoptosis of endothelial cells and VSMCs. Furthermore, hypercholesterolaemia has been reported to decrease eNOS activity by enhancing caveolin-1 expression and its inhibitory association with eNOS, thus decreasing NO production (Feron *et al* 1999). Dyslipidaemia and insulin resistance may occur in obesity which is an independent risk factor of cardiovascular disease. Excess white adipose tissue is associated with the release of free fatty acids and inflammatory cytokines such as TNF- α and IL-6, which blunt the functions of insulin and induce endothelial activation (Caballero 2003, Hotamisligil *et al* 1995).

1.5.3 Smoking

Cigarette smoking has been reported to pose a risk for the development of cardiovascular disease (Burke & Fitzgerald 2003). Endothelium functional changes associated with cigarette smoking are said to be reversible upon smoking cessation (Benowitz 2003). Passive smoking has also been implicated in inducing endothelial damage (Benowitz 2003). Oxidative stress has been linked to cigarette smoking-induced endothelial damage (Raj *et al* 2001). Cigarette smoke is a rich source of oxidants, and not only does it directly deposit free radicals into the circulation, but it also facilitates the endogenous production of oxidants (Burke & Fitzgerald 2003). Cigarette smoking has been associated with an enhanced inflammatory response

which is improved by administration of antioxidants such as vitamin C, suggesting that oxidative stress is a major role player in cigarette smoking induced endothelial activation (Kalra *et al* 1994, Webber *et al* 1996, Lehr *et al* 1994). Furthermore, smokers were reported to have higher levels of nitrotyrosine as compared to non-smokers, which is indicative of increased ONOO⁻ production (Pignatelli *et al* 2001). Esen *et al* (2004) showed decreased flow mediated dilation and enhanced wall thickness in brachial arteries of smokers, whereas Raji *et al* (2001) reported decreased Ach-dependent relaxation in cigarette smoke exposed aortic rings, which could be prevented by SOD. This is suggestive of reduced NO bioavailability, which may be due to O₂⁻ scavenging in smokers. Presence of increased ox-LDL, ONOO⁻, and nitrotyrosine has been confirmed in smokers (Yagamuchi *et al* 2005, Heizter *et al* 1996).

1.5.4 Aging

Aging is associated with development and progression of cardiovascular diseases (Herrera *et al* 2010). Furthermore, conditions such as diabetes mellitus, inflammation, hypertension and hypercholesterolaemia have been observed with aging, further worsening the cardiovascular morbidity (Herrera *et al* 2010). Production of ROS is increased with aging, and hence plays a major role in development of cardiovascular disease (Seals *et al* 2011). Endothelium dependent relaxation is also decreased with aging (Matz *et al* 2000), a response which is often observed in larger vessels such as the aorta (Brandes *et al* 2005, Seals *et al* 2011). Though NO may be reduced with aging, some studies have reported increased expression and activation of eNOS, whereas others have shown downregulated eNOS mRNA expression (Van Der Loo *et al* 2000, Seals *et al* 2011). These disparities may be reflective of vascular bed differences. On the other hand iNOS is said to increase with aging, which may be attributed to the presence of inflammatory cytokines in aged vessels (Herrera *et al* 2010). Indeed, iNOS is associated with the generation of large amounts of NO, which in combination with O₂⁻ results in the formation of ONOO⁻ (Yamaoka *et al* 2002, Lancel *et al* 2004, Xia *et al* 2010).

The activity of the enzyme arginase I has been shown to increase with aging (Katusic 2007). Arginase I or II is responsible for the conversion of L-arginine to urea and ornithine, hence it

may compete with eNOS for the substrate L-arginine leading to eNOS uncoupling (Berkowitz *et al* 2003). Blocking arginase I activity was reported to improve NO production (White *et al* 2006, Berkowitz *et al* 2003). Antioxidant capacity decreases with aging in the endothelium, which may be attributed to tyrosine nitration of SODs, as shown by Van Der Loo *et al* (2000) in aged rat aortas where increased ONOO⁻ resulted in nitration of manganese SOD (MnSOD).

1.5.5 Inflammation and oxidative stress

Although inflammation and oxidative stress are independent risk factors associated with pathophysiological changes of the endothelium, they also appear to mediate the development of endothelial damage induced by cardiovascular risk factors, hence playing central roles in cellular mechanisms of ED induction (Mudau *et al* 2012). An intimate relationship appears to exist between inflammation and oxidative stress. Oxidative stress initiates a cascade of events that leads to endothelial activation and inflammation, whereas inflammatory cytokines and cells aggravate oxidative stress (Harrison 2012). In fact, ROS are considered to be a major factor in the progression of inflammation (Mittal *et al* 2014). Mitochondrial ROS have been implicated in induction of pro-inflammatory cytokines such as IL-1, IL-6 and TNF- α (Bulua *et al* 2011). During physiological conditions, vascular inflammation is well regulated by factors such as NO, however during pathophysiological conditions, inflammation progresses uncontrolled (De Caterina *et al* 1995). On the other hand, oxidation of LDL by ROS is one the major steps in initiation and progression of an atherosclerotic lesion, a process which further amplifies inflammation and ROS generation (Berliner *et al* 1995). Hence atherosclerosis has been deemed an inflammatory disease (Libby *et al* 2002).

Pro-inflammatory cytokines such as TNF- α and IL-6 play a major role in inducing vascular inflammation and oxidative stress (Barnes & Karin 1997). The major signalling pathway involved in inflammation is the I κ B- α / NF- κ B pathway (Barnes & Karin 1997). The inhibitory interaction between I κ B- α and NF- κ B regulates and inhibits NF- κ B activity until an introduction of certain stimuli (Barnes & Karin 1997). Upon a stimulus, NF- κ B translocates to the nucleus, where it assumes the role of regulating the transcription of inflammatory genes (Viridis & Schiffrin 2003). NF- κ B activation is stimulated by factors such

as inflammatory cytokines (TNF- α , IL-1, or IL-6), AGEs, ox-LDL and angiotensin II (Brasier 2010) and ROS (Barnes & Karin 1997). Active NF- κ B in turn facilitates transcription and expression of genes for adhesion molecules, chemokines and cytokines (Barnes & Karin 1997). This will lead to enhanced endothelial activation and production of more cytokines including TNF- α which recruits inflammatory cells (leukocytes) to the site (Barnes & Karin 1997). Inflammatory cells are in turn associated with ROS generation. The pro-inflammatory cytokine TNF- α has been shown to induce NADPH oxidase activity and O₂⁻ generation in human dermal microvascular endothelial cells (Li J-M *et al* 2005).

NF- κ B may also play a role in induction of iNOS (Barnes & Karin 1997), in response to inflammatory cytokines during inflammatory conditions (MacNaul & Hutchinson 1993). Large amounts of NO produced by iNOS may play a role in endothelial damage during inflammation via ONOO⁻ formation and consequent nitrosative stress (Beckman 1996). Clinically, increased circulating inflammatory markers such as C-reactive protein (CRP) are strongly associated the development of cardiovascular disease (Viridis & Schiffrin 2003). CRP has been shown to stimulate the release of IL-6 and TNF- α from monocytes, and the endothelial cell expression of VCAM-1, ICAM-1 and MCP-1 (Pasceri *et al* 2001). CRP may contribute to ED by decreasing eNOS expression and activity as was shown in human AECs, a response which was accompanied by an increase in monocyte adhesion (Venugopal *et al* 2002).

1.6 Harmful stimuli associated with pathophysiological changes

1.6.1 Tumour necrosis factor-alpha (TNF- α)

TNF- α is an inflammatory cytokine that is released by a variety of cells such as macrophages, endothelial cells, adipocytes, fibroblasts, neuronal cells, lymphoid tissue and cardiomyocytes (Wajant *et al* 2003, Hotamisligil *et al* 1995, Meldrum 1998). TNF- α exerts its functions via two receptors, namely tumour necrosis factor receptor 1 and 2 (TNFR1 and TNFR2) (Wajant *et al* 2003). TNFR1 is constitutively expressed and is associated with caspase-mediated apoptosis of injured or stressed cells (Wajant *et al* 2003). Through binding to the receptor, TNF- α activates NF- κ B via facilitating the phosphorylation of its inhibitor I κ B-alpha, leading to the dissociation of I κ B-alpha from the NF- κ B, and consequent NF- κ B translocation to the nucleus (Sakurai *et al* 2003). TNF- α may also induce an inflammatory response via the sphingomyelinase pathway leading to production of PKC, which in turn induces the expression of cell adhesion molecules on endothelial cells (Schutze *et al* 1994).

The importance of TNF- α in the development of cardiovascular diseases such as myocardial infarction, chronic heart failure, atherosclerosis and myocarditis has previously been established (Meldrum 1998). Increased TNF- α has been observed in cardiovascular risk factors such as hyperlipidaemia, diabetes and aging (Zhang H *et al* 2009). In the endothelium, TNF- α has been shown to decrease eNOS expression in human umbilical vein endothelial cells (Lai *et al* 2003), and human AECs (MacNaul & Hutchinson 1993). The decrease in eNOS expression was accompanied by an increase in iNOS in human AECs (MacNaul & Hutchinson 1993). The increased iNOS expression may be via TNF- α mediated NF κ B activation. It has been suggested that TNF- α may reduce eNOS expression through rapid eNOS mRNA degradation, as shown in human umbilical vein endothelial cells where TNF- α shortened the eNOS mRNA half-life from 48 to 3 hours (Yoshizumi *et al* 1993). Indeed, TNF- α has been associated with diminished NO dependent vasodilation in coronary arteries (Gao *et al* 2007, Picchi *et al* 2006, Ahmad *et al* 2002). Recycling of the NO synthesis by-product L-citrulline back to L-arginine is another factor that regulates NO synthesis and is mediated by the enzyme argininosuccinate synthase (ASS). TNF- α has been reported to downregulate ASS mRNA and protein expression in aortic endothelial cells (Goodwin *et al* 2007).

TNF- α has also been implicated in the impairment of the EDHF mediated vasodilation in human omental arteries and porcine coronary arteries (Gillham *et al* 2008, Kessler *et al* 1999). EETs are amongst the proposed candidates of EDHF and are derived from arachidonic acid through the action of cytochrome P450 oxygenase (Coats *et al* 2001). TNF- α has been shown to diminish cytochrome P450 protein expression in porcine aortic endothelial cells (Kessler *et al* 1999).

In addition to decreasing eNOS expression, TNF- α may lead to ED via ROS induction (Chen *et al* 2008). Conditions such as diabetes have been linked with TNF- α mediated generation of ROS via increased NADPH oxidase (Gao *et al* 2007, Picchi *et al* 2006). Furthermore, AGEs-mediated activation of NF- κ B in diabetes leads to increased production of TNF- α which in turn increases ROS (Gao *et al* 2007). TNF- α has been linked with increased NADPH expression in rat coronary microvascular endothelial cells and human dermal microvascular endothelial cells (Li J-M *et al* 2005). Other sources of TNF- α -mediated ROS production include mitochondria through the electron transport chain and xanthine oxidase (Chen *et al* 2008). In myocardial ischaemia / reperfusion, TNF- α has been reported to induce O_2^- via activation of xanthine oxidase leading to ED (Zhang *et al* 2006). In the myocardium, TNF- α has been linked with contractile dysfunction and cardiomyocyte apoptosis (Meldrum 1998).

1.6.2 Asymmetric dimethyl arginine (ADMA)

ADMA has emerged as a harmful stimulus associated with the development of cardiovascular disease (Ito *et al* 1999). Increased levels of ADMA are associated with various cardiovascular risk factors such as diabetes mellitus, hypercholesterolaemia, hypertension and cigarette smoking (Cooke 2004). ADMA uncouples eNOS by acting as an L-arginine competitor for a binding site in eNOS, thus leading to O_2^- generation (Böger *et al* 1998). Böger *et al* (2000) showed that ADMA can be synthesised in endothelial cells and it is associated with increased ROS production and expression of adhesion molecules. Levels of ADMA may be regulated by the balance between the ADMA synthetic enzyme, protein arginine N-methyltransferase (PRMT), and the ADMA degrading enzyme dimethylaminohydrolase (DDAH) (Cooke 2004). ADMA synthesis involves protein methylation of arginine residues by the action of PRMTs (Figure 1.11) (Böger *et al* 2000).

TNF- α and ox-LDL have been found to increase ADMA levels and decrease activity of DDAH (Ito *et al* 1999). Hypercholesterolaemia was also shown to be associated with diminished DDAH activity in rabbits (Ito *et al* 1999).

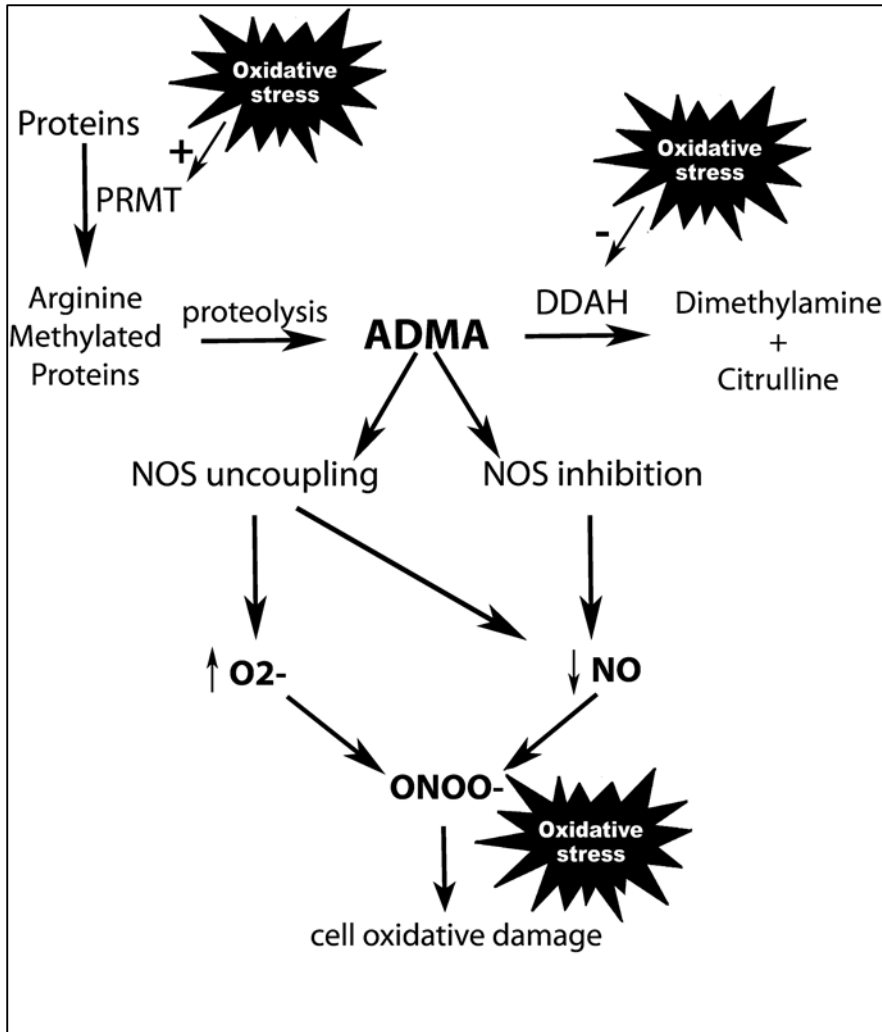


Figure 1.11: ADMA synthesis and NOS inhibition. Conditions such as oxidative stress may lead to enhanced ADMA synthesis by PRMTs. ADMA competitively inhibits NOS, leading to NOS uncoupling and consequent ROS production. ADMA is degraded to dimethylamine and citrulline by the enzyme DDAH (Carraro *et al* 2013).

1.6.3 Oxidised low density lipoprotein (ox-LDL)

Ox-LDL has been shown to be a good marker of coronary artery disease and has been positively correlated with cardiovascular risk factors such as type 2 diabetes, obesity, hypercholesterolaemia and aging (Holvoet *et al* 2001). Ox-LDL has been implicated in major atherogenesis processes such as endothelial activation and dysfunction, formation of foam cells, and proliferation and migration of VSMCs (Pirillo *et al* 2013). Introduction of ox-LDL to human coronary endothelial cells led to the expression of VCAM-1, ICAM1, E selectin and P selectin via the receptor LOX-1, thus initiating an endothelial inflammatory process (Li D *et al* 2002). LOX-1 expression is low under physiological conditions, but is up-regulated by ox-LDL, inflammatory cytokines (TNF- α , IL-1), ROS, angiotensin II, ET-1 (Pirillo *et al* 2013), and are expressed in endothelial cells (Sawamura *et al* 1997), macrophages and VSMCs (Figure 1.12) (Draude *et al* 1999, Kataoka *et al* 2001).

Interestingly, Blair *et al* (1999) showed that ox-LDL led to displacement of caveolin-1 and eNOS from caveolae to the internal membrane compartment, which compromised eNOS activity in porcine pulmonary artery endothelial cells. On the other hand, Liao *et al* (1995) reported decreased eNOS mRNA expression with ox-LDL treatment in human saphenous vein endothelial cells. Furthermore, ox-LDL has been shown to enhance arginase II activity in human AECs, which like arginase I, competes with eNOS for L-arginine, thus uncoupling eNOS (Ryoo *et al* 2006). Evidently ox-LDL initiates the process of endothelial activation and dysfunction. ET-1 has been shown to facilitate endothelial cell uptake of ox-LDL (Morawietz *et al* 2001). Li *et al* (2003) showed that ox-LDL via LOX-1 leads to the expression of the ACE gene. Furthermore, ox-LDL may result in apoptosis of endothelial cells via activation of caspases and downregulation of anti-apoptotic proteins (Chen *et al* 2004).

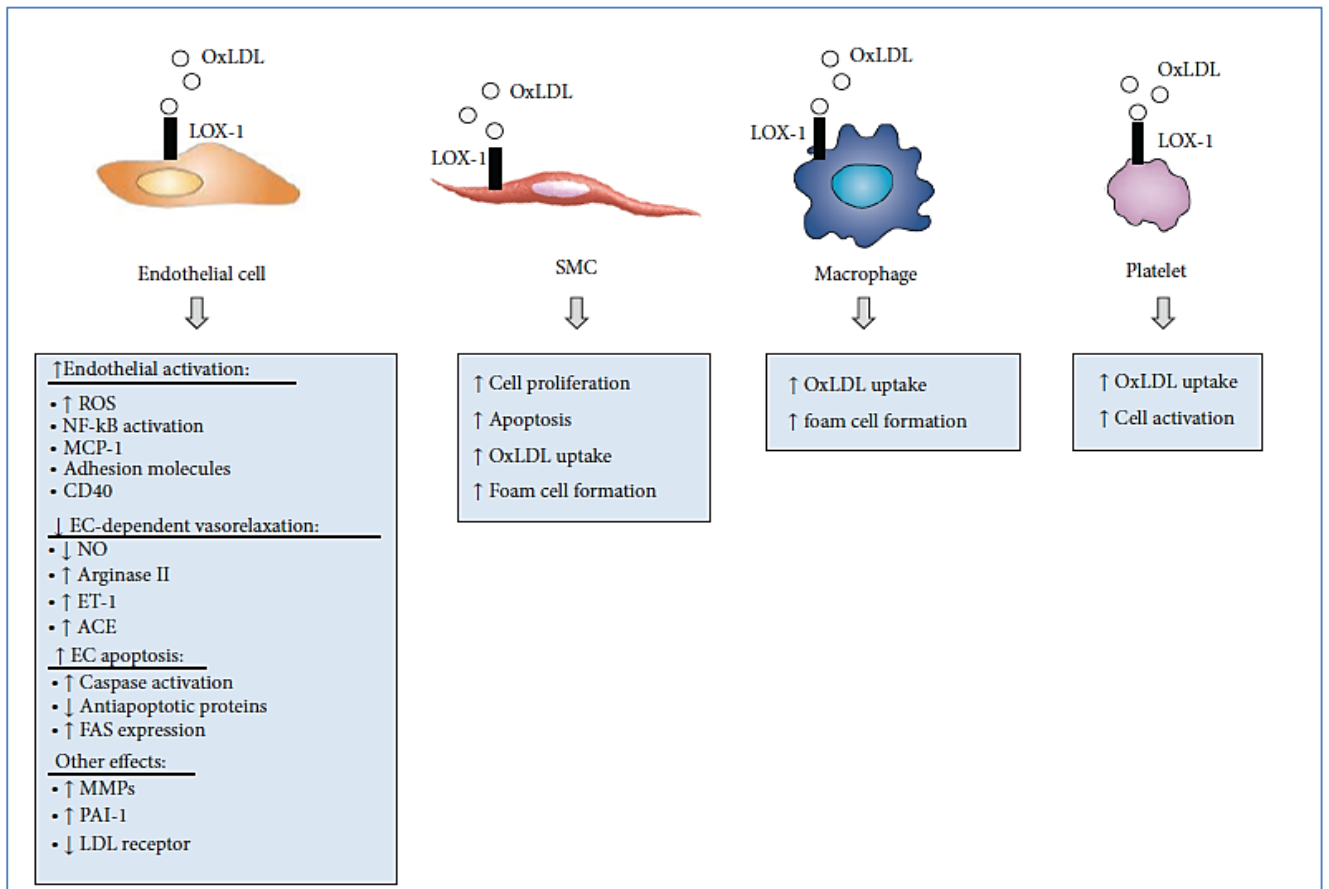


Figure 1.12: Participation of ox-LDL in atherogenesis in different cells in the vascular system. Binding of ox-LDL TO LOX-1 receptors in endothelial cells leads to endothelial activation, decreased vasorelaxation, and enhanced apoptosis. In VSMCs, ox-LDL via LOX-1 leads enhanced proliferation, apoptosis and foam cell formation. ox-LDL prompts foam cell formation in macrophages and platelet activation in platelets (Pirillo *et al* 2013).

1.7 Endothelial heterogeneity

In 1966, Florey (1966) stated that: “*now it is recognised that there are many kind of endothelial cells which differ from one another substantially in structure, and to some extent in function*”. As mentioned previously, endothelial cells from different organs, or within the same organ, in the same species may differ in structure, function and antigenic properties (Thorin & Shreeve 1998). Endothelial heterogeneity can be viewed as the adaptive trait of the endothelium to cater to the various needs of the underlying tissues (Aird 2007a). For example, throughout the vascular tree, the endothelium demonstrates a *remarkable division of labour* as Aird (2006) puts it; such that the endothelium contained in smooth muscle containing vessels (arterial endothelium) is primarily dedicated at regulating vasomotor tone, postcapillary venule endothelium at mediating leukocyte trafficking and capillary endothelium at regulating solute exchange or modulating organ specific barrier needs such as in the blood brain barrier (Aird 2006). Other endothelial cell subtypes primarily regulate organ-specific homeostasis and function. For example endocardial endothelium together with the myocardial capillary endothelium in the heart regulate cardiomyocyte growth and function in a paracrine manner (Brustaert 2003).

The extracellular environment and epigenetics may play a major role in determining mechanisms of endothelial cell heterogeneity (Aird 2006). The environmental influences include biomechanical forces such as shear stress, and biochemical signals such as hormones, growth factors, cytokines, chemokines, pH, and constituents of the extracellular matrix (Aird 2006). For example, arterial endothelial cells are situated in territories of elevated shear stress due to increased blood flow, as opposed to capillary and venous endothelial cells that experience low levels of shear stress (Davies 2007). However, within the arterial system, flow patterns may differ, with some areas experiencing an undisturbed laminar flow with higher shear stress, whereas other areas are exposed to a disturbed laminar flow with lower shear stress (Davies 2007). Hence, arterial endothelial cells in these two distinct regions are acclimatised to different extracellular environments, a factor which may play a role in phenotypic heterogeneity (Passerini *et al* 2005). Capillary-derived endothelial cells in the heart receive paracrine factors from cardiomyocytes and are subjected to forces of myocardial contractions whereas endothelial cells of the blood brain barrier receive paracrine factors from the astroglia cells (Aird 2007a). Hence, endothelial cell

site specific properties may be lost when endothelial cells are removed from their microenvironment and cultured in *in vitro* conditions. Cell shape, protein expression, barrier function, cell growth, apoptosis and leukocyte adhesion modifications may all represent phenotypic responses to extracellular environmental factors (Aird 2006).

Epigenetically-induced endothelial cell heterogeneity may be mediated by deoxyribonucleic acid (DNA) methylation, histone modification, and chromatin remodelling (Fish *et al* 2005). It has been established that arteries are more prone to developing atherosclerosis than veins. Deng *et al* (2006) reported increased expression of proliferative, adhesive and apoptotic genes in response to treatment with ox-LDL, TNF- α and IL-1 in coronary arterial endothelial cells compared to saphenous vein endothelial cells in culture. The fact that these differences were maintained in culture may be representative of the role played by epigenetics in endothelial heterogeneity (Aird 2007a). In another study, freshly isolated endothelial cells derived from post-capillary high endothelial venules in lymphoid tissue of tonsils was compared with the same cells that had been in culture for at least two days (Laccore *et al* 2004). The cultured cells had lost some of their site specific properties following two days of culture as compared to their freshly isolated counterparts, however, some properties were maintained (Laccore *et al* 2004). This is suggestive of the two-way role played by both microenvironment and epigenetics in these cells.

Endothelial heterogeneity has also been observed with regards to the release of endothelium-derived vasoactive factors (Thorin & Shreeve 1998). Arterial endothelial cells exhibit greater eNOS expression than venous endothelial cells (Andries *et al* 1998). In live rats, infusion of a NOS inhibitor elicited varied responses in different vascular beds, with vascular resistance strongly increasing in skeletal muscle and increasing to a lesser extent in the cerebellum (Greenblatt *et al* 1993). Endothelial cells have been reported to release variable amounts of ET-1 in different vascular beds regardless of the vessel size (Thorin & Shreeve 1998). Large porcine artery derived endothelial cells were shown to release more ET-1 than small coronary artery derived-endothelial cells (Ohbayashi *et al* 1994). Rabbit cerebral arteries produced more ET-1 than the aorta (Thorin & Shreeve 1998), while human cerebral endothelium was shown to produce less ET-1 than the superficial temporal vessel derived-endothelial cells (Thorin *et al* 1997). In sheep, pulmonary endothelium produced more PGI₂ than endocardial or AECs (Thorin & Shreeve 1998). On the other hand, hypoxia-

induced PGI₂ production was observed in endocardial and pulmonary endothelial cells and not in AECs (Mebazza *et al* 1995).

1.7.1 Venous, arterial and capillary endothelium

1.7.1.1 Venous and arterial endothelium

Arteries and veins are both conduit blood vessels and possess continuous non-fenestrated endothelium (Aird 2007b). However, arteries and veins show some variation in structure and function (Table 1.2 and Figure 1.13) (Aird 2007b, Dela Paz & D'Amore 2009). Arterial and venous endothelial cells have both been shown to express distinct genetic markers from the onset of vessel development, which are independent of their respective microenvironment influences. (Table 1.3) (Wang *et al* 1998). Arterial endothelial cells are orientated in the direction of blood flow in the regions of undisturbed laminar flow and possess properly developed tight junctions, a feature representative of their low permeability (Aird 2007b). On the other hand, venous endothelial cells are not aligned with the direction of blood flow and have less tight endothelial junctions, with post capillary venules having scantily developed endothelial tight junctions (Aird 2007b). Arterial endothelial cells are long and narrow, whereas venous endothelial cells are short and wide, with the high endothelial venules showing a plumper phenotype (Dela Paz & D'Amore 2009). Venous endothelial cells (venules in particular) are endowed with cytoplasmic bound vesicles, referred to as vesiculo-vacuolar organelles (VVOs), which may be representative of their permeability and leukocyte trafficking role (Aird 2007a).

During inflammatory conditions, leukocyte trafficking and permeability primarily takes place in the postcapillary venules (Aird 2007a, Dela Paz & D'Amore 2009). The process of leukocyte trafficking involves cell adhesion molecules such as E-selectin and P-selectin (Aird 2007a). E-selectin is expressed during endothelial activation, largely in the postcapillary venules (Aird 2007a). P-selectin is also predominantly found in the postcapillary venules (Aird 2007a).

Table 1.2: Differences between arteries and veins (Aird 2007b, Dela Paz & D'Amore 2009).

Arteries	Veins
Thick walls, pulsate	Thin walls, do not pulsate
Tighter endothelial cell junctions	Loose endothelial cell junctions
Carries oxygenated blood	Carries deoxygenated blood
Some regions i.e. branching points and curvatures are exposed to disturbed laminar flow, making them susceptible to inflammation, coagulation and atherosclerosis	High inflammatory response capacity
More prone to atherosclerosis	Rarely affected
Conduit function	Conduit function
Have no valves	Have valves
Shear stress level at 10-40 dyne/cm ²	Shear stress levels at 1-5 dyne/cm ²

Table 1.3: Differences in the molecular markers expressed in arterial and venous endothelium (Aird 2007b, Dela Paz & D'Amore 2009)

Arterial endothelium	Venous endothelium
<ul style="list-style-type: none"> ✓ ephrinB2 ✓ Delta-like 4 (DII4) ✓ Activin-receptor-like kinase 1 (Alk1) ✓ Endothelial PAS domain protein 1 (EPAS1) ✓ Hey1 and Hey2 ✓ Neuropilin 1 (NRP1) ✓ Decidual protein induced by progesterone (Depp) ✓ VEGF ✓ Notch 1, 4, and 5 ✓ Jagged 1 and 2 ✓ Connexin 40 	<ul style="list-style-type: none"> ✓ EphB4 ✓ Neuropilin2 (NRP2) ✓ COUP-TFII ✓ Lefty-1 and Lefty-2 ✓ Tie2 ✓ Flt4 ✓ Endomucin

1.7.1.2 Capillary endothelium

Capillaries are mainly involved in solute and fluid exchange between blood and the underlying tissue and hence capillary endothelium is specifically acclimatised to its underlying tissue environment, thus playing a role in maintaining of the underlying tissue homeostasis (Aird 2007b). In accordance with the requirements of the underlying tissues, capillary endothelium may be continuous and fenestrated, or continuous and non-fenestrated, or discontinuous (Simionescu *et al* 2002). Continuous non-fenestrated endothelium resides in the vessels of the brain, heart, skin and lungs whereas continuous fenestrated endothelium is inherent in territories that are more involved with filtration or secretion such as vessels of the exocrine and endocrine glands, glomeruli, gastric and intestinal mucosa (Simionescu *et al* 2002, Aird 2007a). Discontinuous endothelium is characterized by larger fenestrations with no diaphragm and a scantily formed basement membrane and can be located in territories such as the vessels of the liver sinusoids (Aird 2007a). Territories with reduced permeability such as the blood brain barrier are characterized by a continuous non-fenestrated endothelium with a reduced number of caveolae and increased tight junctions (Figure 1.13) (Aird 2012).

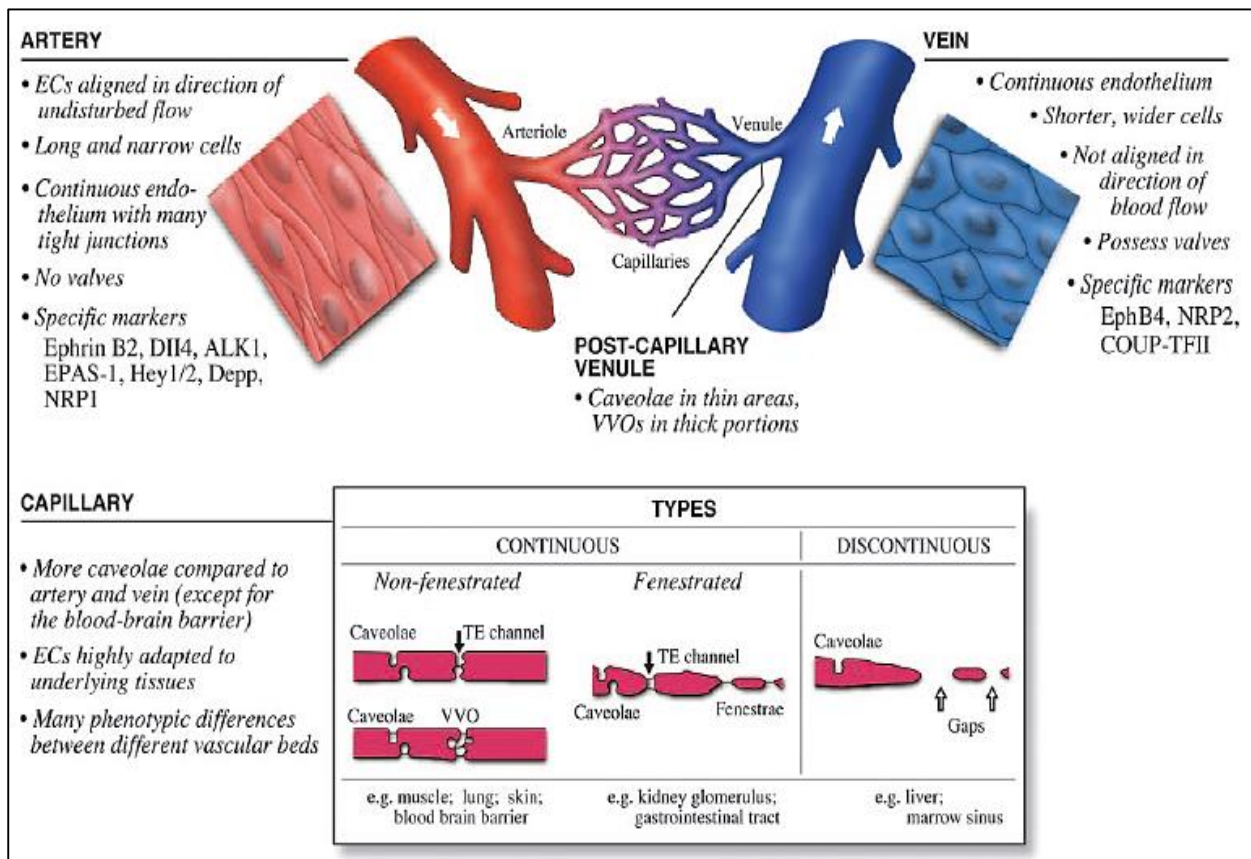


Figure 1.13: Endothelial cell heterogeneity in arterial, venous and capillary endothelium (Aird 2007b).

1.7.2 Cardiac microvascular endothelial cells (CMECs) and aortic endothelial cells (AECs).

CMECs and endocardial endothelial cells collectively form the cardiac endothelium (Strijdom & Lochner 2009), and it has been shown that the two cardiac endothelial cell types share many common features (Brutsaert *et al* 1998). Hendrickx *et al* (2004) compared gene expression in endocardial endothelial cells and AECs in culture, and reported heterogeneous expression of certain genes in these cell lines, which was further validated *in vivo*. Genes that were preferentially expressed in AECs included decorin which is associated with angiogenesis, connexin 26 which is a gap junction protein, VCAM-1 which is an adhesion molecule and vasopressin V1a receptor which regulates cell contraction and proliferation (Hendrickx *et al* 2004). CMECs, the focus of the current study, are in close association with cardiomyocytes and are hence primarily dedicated at regulating cardiomyocyte homeostasis and function (Brutsaert 2003). CMECs are of significance as they constitute approximately 33 % of the total cells in the ventricular wall, and are exposed to a larger fraction of the myocardial muscle cells (Nishida *et al* 1993, Shah & MacCarthy 2000). Furthermore, it has been proposed that for each cardiomyocyte there is one capillary and each cardiomyocyte is surrounded by at least 3 CMECs (Brutsaert 2003, Hsieh *et al* 2006). Capillaries do not contain smooth muscle tissue and hence CMECs do not participate in vasodilation (Strijdom & Lochner 2009). However, CMECs-derived bioactive factors such as NO, ET-1 and PGI₂ diffuse into the underlying cardiomyocytes in a paracrine manner, thus influencing cardiomyocyte growth, contraction and rhythmicity (Figure 1.14) (Strijdom & Lochner 2009). Furthermore, CMECs also receive paracrine factors such NO, angiotensin-1 and VEGF-A (Strijdom & Lochner 2009) (Figure 1.14).

CMEC-derived ET-1 stimulates NO and PGI₂ release via activation of ET_A receptors in an autocrine fashion, while inducing myocardial contraction in a paracrine manner via ET_B receptor activation on cardiomyocyte (Hsieh *et al* 2006). Within the cardiac endothelium, endothelial cell heterogeneity has been observed with endocardial endothelium showing more gap junctions and deeper intercellular clefts than the CMEC (Aird 2007b). The endocardial endothelium exhibits a high expression of eNOS which is more located in the golgi body than CMECs (Andries *et al* 1998). vWF is also more abundant in the endocardial endothelium compared to CMECs (Aird 2007b).

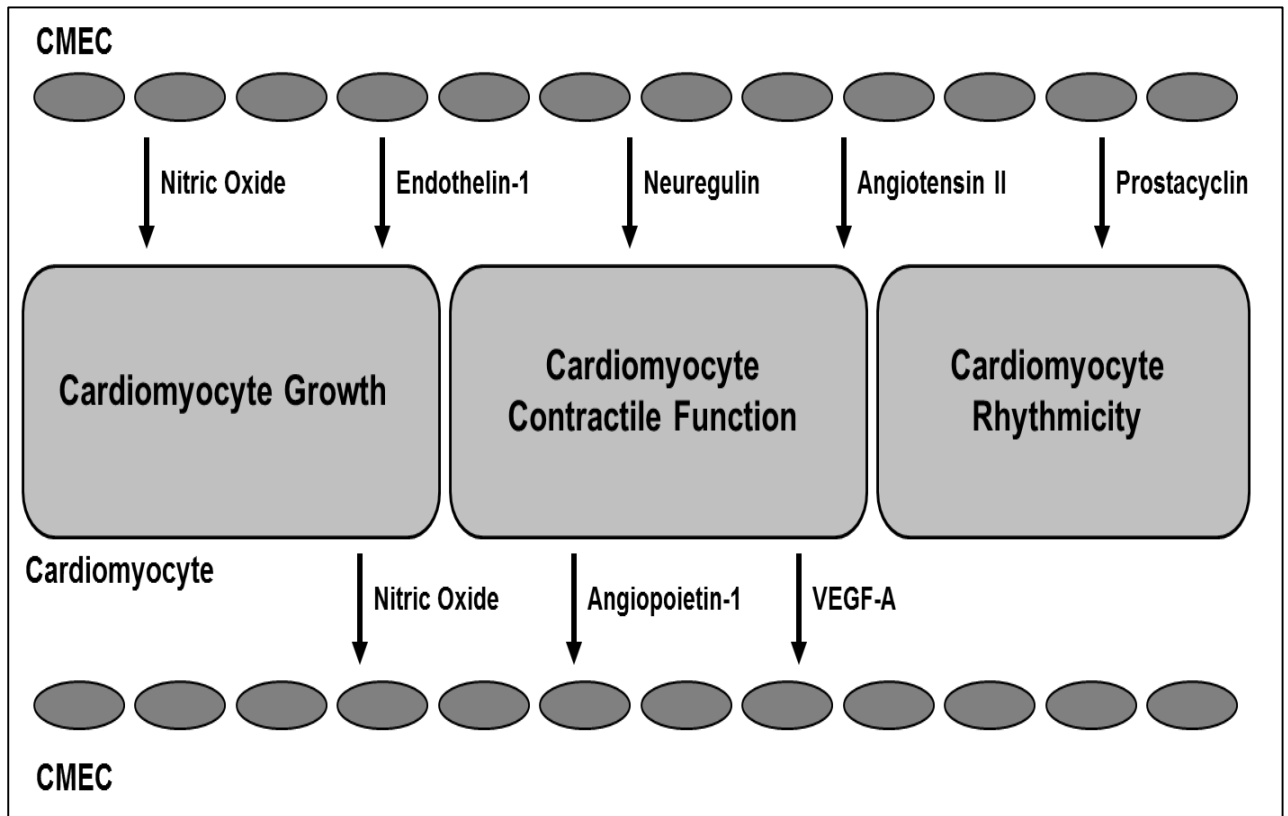


Figure 1.14: Paracrine communication between CMECs and cardiomyocytes. Paracrine factors released from CMECs regulate cardiomyocyte growth, contractile function and rhythmicity, similarly factors released from the cardiomyocytes regulate CMEC growth, function and activity (Strijdom & Lochner 2009).

Unlike CMECs, AECs are not in close proximity to cardiomyocytes and are more involved in regulation of systemic circulation (Dela Paz & D'Amore 2009). In the vascular wall, AECs lie adjacent to VSMCs and are hence primarily dedicated at maintaining vascular homeostasis (Strijdom & Lochner 2009). Owing to their location in the main muscular artery of the body, AECs are constantly exposed to high degrees of shear stress (Davies 2007). However arterial cells are more prone to developing ED (Davies 2007), especially those that lines the branching points or curvatures of the arteries (Aird 2006). As was reported by Deng *et al* (2006), coronary arterial endothelial cells showed genetic propensity to developing ED. In human AECs, Li *et al* (2004) showed C-reactive protein (CRP)-mediated enhanced expression of LOX-1, leading to increased AEC-monocyte adhesion and ox-LDL uptake. Through gene expression profiling studies, Brooks *et al* (2002) compared mRNA expression in cultured human AECs when exposed to high shear steady laminar flow or low non-steady, non-unidirectional disturbed flow. They reported increased expression of pro-atherosclerotic genes in AECs exposed to low non-steady disturbed flow, including genes for adhesion molecules, chemokines and pro-inflammatory cytokines, which were downregulated upon exposure to high shear steady laminar flow. Furthermore, conditions of disturbed flow were associated with downregulation of genes encoding for antioxidants such as SOD1 and 2. The authors further showed that treatment with TNF- α increased monocyte adhesion on AECs exposed to disturbed flow as compared to AECs exposed to static conditions.

Clearly AECs and CMECs are situated in and acclimatised to two different microenvironments which will have an influence on the heterogeneity between the two endothelial cell types. CMECs receive paracrine factors from cardiomyocytes and are subjected to contractions of the myocardium *in vivo* (Brutsaet 2003). On the other hand, AECs most likely receive paracrine factors from VSMCs and are subjected to factors such as enhanced shear stress *in vivo* (Strijdom & Lochner 2009), all of which will play a role in endothelial heterogeneity. However, whether endothelial heterogeneity between these two distinct cell lines is also present *in vitro* or in cell culture conditions is poorly investigated, and to the best of our knowledge, no evidence exists in the literature of studies that have investigated this question.

1.8 Studying obesity as a risk factor of endothelial dysfunction

By 2005, approximately 1.3 billion people globally were reported to be overweight (Goedecke *et al* 2006). At that time in South Africa, over 29 % men and 56 % women were overweight or obese (Goedecke *et al* 2006). Obesity poses a major risk for the development of cardiovascular disease (Hubert *et al* 1983). Obesity often arises from a high caloric diet combined with a sedentary lifestyle and low basal metabolism (Goedecke *et al* 2006). In humans, obesity is characterised by a body mass index (BMI) of 30 kg/m² and higher, and is associated with conditions such as dyslipidaemia, insulin resistance, type 2 diabetes, and metabolic syndrome (Perticone *et al* 2001). As discussed in the previous sections, these factors impact negatively on the endothelium, initiating endothelial activation and dysfunction, which if untreated, progresses to atherosclerosis.

In view of the obesity burden, diet-induced obese rat models have been employed to study a variety of conditions such as insulin resistance, obesity and type 2 diabetes mellitus (Reuter 2007). The development of laboratory-based, animal models of obesity is a useful tool in studying the *in vivo*, *ex vivo* and *in vitro* implications of obesity. Our own laboratory has developed models of diet-induced obesity in Wistar rats, namely a high sucrose diet with added sugar and condensed milk, and a diet containing high fat (prepared with holsum cooking fat) combined with high sucrose and condensed milk (Salie *et al* 2014). Following a 16 week feeding programme, these animals exhibited significant increases in body weight, intra-peritoneal fat, blood glucose and insulin levels, and hence insulin resistance as determined by the homeostatic model assessment of insulin resistance index (HOMA-IR index) (Huisamen *et al* 2013). Obesity and insulin resistance has previously been shown to induce endothelial dysfunction (Kim *et al* 2006). The high fat diet is further associated with development of hypertension (Huisamen *et al* 2013).

Previous studies have shown that animals receiving a high fat diet developed endothelial dysfunction. In a study on mice fed with a high fat diet, diabetes-induced endothelial dysfunction was observed, which was characterised by impaired endothelium dependent vasodilation, increased nitrotyrosine formation (indicative of increased ONOO⁻ production), and decreased expression of eNOS dimers suggesting eNOS uncoupling (Molnar *et al* 2005).

In the current study, a high fat model developed in our laboratory was employed to study the effects of obesity on endothelial-dependent aortic function.

1.9 Anti-endothelial dysfunction therapy

ED may be modulated by a variety of interventions, including diet, exercise, pharmacological drugs, and the use of medicinal plant extracts. Pharmacological drugs such as statins and fibrates have been shown to possess eNOS stimulating properties (in addition to their traditional role of lowering cholesterol), hence improving NO dependent vasodilation (Davignon & Ganz 2004). The statin family includes drugs such as pravastatin, atorvastatin, simvastatin and fluvastatin. In addition to increasing eNOS activity, statins have also been shown to increase eNOS expression via stabilising its mRNA (Beckman and Creager 2006). Statins have a stimulatory effect on PKB / Akt which in turn activates eNOS (Davignon & Ganz 2004). Furthermore, statins may inhibit endothelial cell cytokines, chemokines, and adhesion molecules via modulation of NF- κ B activity (Beckman and Creager 2006). Fibrates such as fenofibrate have been shown to induce eNOS activation and NO production via AMPK-induced phosphorylation at site Ser 1177 in human umbilical vein endothelial cells (Murakami *et al* 2006). Using a similar cell line, Liu *et al* (2011) showed that fenofibrate was able to restore BH₄ levels which were initially reduced by the endotoxin lipopolysaccharide, hence fenofibrate may restore eNOS function and diminish eNOS uncoupling. In older individuals fenofibrate improved endothelial function and resulted in the reduction of plasma levels of ox-LDL (Walker *et al* 2012).

In addition to the statins and fibrates, a variety of other pharmacological agents have been shown to improve endothelial function. For a summary of other endothelio-protective agents and drugs, see Table 1.4. In addition to the development and use of traditional pharmacological drugs, there is a growing number of studies investigating the potential clinical application of non-traditional, plant-derived compounds. The putative antioxidant, anti-inflammatory and cardioprotective properties of many plant extracts have gained much interest as many societies globally have been using such extracts for healing purposes for centuries (Usharani *et al* 2013). Oleanolic acid is one such plant extract that has been derived from the leaves of the African Waterberry tree in the north eastern parts of South Africa.

Table 1.4: Endothelio-protective agents and their mechanisms of action (Versari *et al* 2008, Balakumar *et al* 2009).

Endothelio-protective agents	Mechanisms
Nebivolol (β_1 -blocker)	Stimulation of NOS function, Antioxidant mechanisms (decreases ROS generation).
Carvedilol (β/α_1 -blocker)	Antioxidant mechanisms (decreases ROS generation).
Calcium channel blockers	Inhibition of calcium channels, reduces blood pressure.
ACE inhibitors Angiotensin receptor blocker	Antioxidant, anti-inflammatory mechanisms.
Glitazones (insulin sensitizing agents)	Inhibition of ADMA.
Demethylasterriquinone	Activates PKB / Akt.
8-Br-cAMP	Activates PKA.
Daidzein 17- β -estradiol	Inhibition of caveolin-1-eNOS interaction.

1.9.1 Oleanolic acid (OA)

OA is a plant derived triterpenoid that has been shown to exert a variety of beneficial effects and is isolated from plant species such as *Syzigium Cordatum* (African Waterberry tree) and *Olea europaea* (Liu *et al* 1995, Mapanga *et al* 2009, Pollier & Goosens 2012). This plant extract has been shown to have anti-cancer, anti-inflammatory, anti-diabetic, hepato-protective, anti-hyperlipidaemic, and anti-oxidant properties (Liu *et al* 1995, Teodoro *et al* 2008). Recently OA has also been shown to exert beneficial effects on the cardiovascular system (Senthil *et al* 2007, Mapanga *et al* 2012, Rodriguez-Rodriguez *et al* 2008). One study showed that *ex vivo* administration of OA resulted in NO-dependent relaxation in aortic rings derived from rat superior and small mesenteric arteries (Rodriguez-Rodriguez *et al* 2008). Furthermore, OA enhanced phosphorylation of PKB / Akt at site Ser 473 and eNOS at site Ser 1177 in human umbilical vein endothelial cells (Rodriguez-Rodriguez *et al* 2008). OA has been found to protect against hyperglycaemia-mediated oxidative stress and apoptosis following myocardial ischaemia / reperfusion injury (Mapanga *et al* 2012). According to Senthil *et al* (2007), pre-treatment of rats with OA elicited protection against isoproterenol-induced myocardial ischaemia. In VSMCs, OA was reported to induce production of PGI₂ via upregulation of COX-2 (Martinez-Gonzalez *et al* 2008). OA improved vasodilation in aortic rings derived from spontaneously hypertensive rats and increased eNOS expression (Rodriguez-Rodriguez *et al* 2007).

Inflammation plays a major role in mediating development of cardiovascular diseases, and OA has been shown to exert anti-inflammatory effects. In human umbilical vein endothelial cells, OA elicited protection against lipopolysaccharide (LPS)-induced expression of adhesion molecules, and enhanced permeability and transendothelial migration of leukocytes (Lee *et al* 2013). Furthermore, OA inhibited LPS-induced production of TNF- α and NF κ B activation (Lee *et al* 2013). In rats fed a high cholesterol-diet, OA was able to lower serum levels of total cholesterol and triglycerides (Liu *et al* 2007).

Evidently OA appears to have stimulatory effects on NO production and anti-inflammatory effects and may thus be beneficial to endothelial function. However chronic use and high doses may have detrimental effects (Xu *et al* 2013). Concentrations of 500 μ mol / kg and higher were associated with hepatocyte necrosis and apoptosis, and liver dysfunction in

mice (Xu *et al* 2013). Further studies are necessary to elucidate the cellular mechanisms of OA with regards to endothelial injury and vascular bed cell specificity.

1.10 Rationale and motivation

As South Africa is a developing nation, morbidity and mortality due to cardiovascular disease are rapidly increasing, claiming lives of individuals in both the older and younger generations, and thus also beginning to affect the economically active population. The development of atherosclerosis, and by extension IHD, is highly dependent on endothelial function. Therefore, studies that aim to explore the function of the endothelium and mechanisms underlying its responses to physiological and pathophysiological stimuli are imperative. There is a plethora of studies on endothelial function and dysfunction, however, the concept of endothelial heterogeneity is rarely addressed, particularly in the *in vitro* setting. The proposed study therefore aims to bridge this apparent gap in the literature. Furthermore, we propose to investigate the above in endothelial cells derived from two distinct locations in the vascular tree, namely from the myocardial capillary network (CMECs) and from the aorta (AECs) respectively. CMECs are situated in close proximity to cardiomyocytes and are thus primarily involved with the regulation of myocardial function, whereas AECs are associated with the traditional role of regulating vascular homeostasis. In spite of these important *in vivo* differences, CMECs and AECs are rarely investigated with a view to compare their responses to harmful stimuli, particularly to evaluate whether the *in vivo* functional differences are retained or abolished when exposed to the *in vitro* culture environment.

The burden of obesity has risen greatly in South Africa, and its relationship with metabolic syndrome, type 2 diabetes and cardiovascular disease has been documented. Excess fat is associated with the release of factors that impact negatively on the endothelium leading to endothelial activation and dysfunction. The occurrence of conditions such as type 2 diabetes with obesity further worsens the cardiovascular morbidity. Hence an *ex vivo* model of studying endothelial function in aortic segments derived from normal weight and obese rats was developed and established for this study. We aimed to explore whether aortic segments from obese rats exhibited ED, and whether administration of OA could improve endothelial function.

1.11 Hypotheses

- A. In view of the location and functional differences between CMECs and AECs, and previous studies on differences in genetic propensity to atherosclerosis in different vascular beds, we hypothesise that AECs and CMECs will exhibit a heterogeneous phenotype under baseline conditions, and in response to endothelial insult as assessed by the measurement of NO production, cell viability and underlying cellular mechanisms. We furthermore hypothesize that OA will increase NO production via the activation of eNOS.
- B. In view of the negative impacts of obesity on the cardiovascular system, and the endothelium in particular, we hypothesize that the aortic rings derived from obese (high fat diet) rats will exhibit ED when compared to aortic rings from lean, age-matched rats. We further hypothesise that OA will improve *ex vivo* endothelial function, as studied by isometric tension measurements of aortic ring segments.

1.12 Research aims

1.12.1 *In vitro* studies

The first part of this study aimed to investigate and compare the cellular responses of endothelial cells derived from two distinct locations in the vascular tree, to both baseline conditions and to pathophysiological stimuli usually associated with cardiovascular risk factors. Data obtained from this part of the study were used to determine whether the two cell lines (CMECs and AECs) responded similarly, or differently to the stimuli.

A. This was achieved as follows:

- Establishment of optimal culture conditions for the two cell lines, namely CMECs and AECs.
- Evaluation and comparison of baseline functional parameters in CMECs and AECs with regard to cell viability (apoptosis and necrosis), NO production and ROS production.
- Induction and evaluation of endothelial cell injury by exposure to harmful stimuli. The stimulus TNF- α is designed to create an inflammatory microenvironment. Evaluation of endothelial cell injury was achieved by the measurement of cellular responses to TNF- α . Endpoints included necrosis, NO production, peroxynitrite production, ROS production and the expression and/or activation of various signalling proteins related to the NO, ROS and pathways.

B. The second part of this section aimed to investigate how the two cell lines (under baseline, control and TNF- α stimulated conditions) responded to the administration of the putatively beneficial compound, namely, a plant extract derived triterpenoid: OA. The effects of OA were evaluated by its administration prior to TNF- α treatment (OA pre-treatment). Similar endpoints as listed under (A) above were measured. Data obtained were analysed to determine whether the two cell lines responded similarly or differently to the administration OA.

C. In an attempt to explore large-scale protein expression and differential regulation patterns in AECs and CMECs in the presence or absence of TNF- α , proteomics studies were undertaken.

1.12.2 *Ex vivo* studies

A. In this section, we aimed to measure the endothelium-dependent vasomotor responses of aortic rings derived from obese and lean, age-matched control rats to a phenylephrine and acetylcholine challenge.

B. Furthermore, in order to establish whether the effects of the putatively beneficial compound, OA, in the *in vitro* setting translate into the *ex vivo* setting, the endothelium-dependent function of aortas from high fat-diet induced obese and lean, age-matched control rats was investigated via isometric tension organ bath studies.

Chapter 2

Materials and methods

2.1 Cell culture studies (*in vitro* studies)

2.1.1 Cardiac microvascular endothelial cells (CMECs) and aortic endothelial cells (AECs)

Both adult rat CMECs and AECs were purchased from VEC technologies (Rensselaer, New York, USA). The endothelial cell isolation protocols used by the suppliers have been previously described (Nishida *et al* 1993, Piper *et al* 1990). The cells arrived in fibronectin-coated 75 cm² tissue culture flasks and were grown to confluency in an endothelial growth medium (EGM) (Clonetics EGM-2MV; Lonza, Walkerville, MD). At confluency, cells were evenly distributed across the surface, reached maximum growth and entered the G0 phase of the cell cycle at which point no further mitotic activity occurred. Endothelial cell purity was confirmed by the cell uptake of an endothelial cell specific fluorescent probe 1,1-dioctadecyl-3,3,3',3'-tetramethylindocarbocyanine perchlorate-acylated-low density lipoprotein (Dil-Ac-LDL) (Biomed Technologies, Stroughton, MA). Microscopic examination of cells further showed a characteristic cobble stone appearance, a unique trait of endothelial cells in culture, further validating endothelial cell purity. For optimal endothelial cell growth and survival, the EGM was supplemented with 10 % foetal bovine serum (FBS) (Highveld Biological, RSA). The suppliers furthermore included a kit containing endothelial growth factors, namely vascular endothelial growth factor (VEGF), human epidermal growth factor (hEGF), human fibroblastic growth factor (hFGF), human insulin-like growth factor (R³-IGF-1), as well as the antibiotics gentamicin and amphotericin B. Other supplements that were supplied in the EGM kit included ascorbic acid, hydrocortisone and an addition of heparin for AECs. The cells were grown at a temperature of 37° C, under atmospheric conditions of 21 % oxygen, 5 % carbon dioxide, and 40-60 % humidity in a standard tissue culture incubator (NuAire, Plymouth, USA).

Upon reaching confluency, cells were removed from the 75 cm² flasks by addition of trypsin (500 BAEE units trypsin / 180 µg EDTA.4Na/ml in Dulbecco's PBS; Life Technologies, Carlsbad, Carlifonia, USA). Trypsin digests the fibronectin bonds thus releasing cells from the

surface of the flasks. Isolated cells obtained from each 75 cm² flask were centrifuged at 1000 rpm for 4 minutes, resuspended in EGM and re-seeded in five 25 cm² tissue culture flasks. When grown to confluency, the flasks were trypsinized as described above, and passaged in a 1:2 ratio, thus giving rise to ten 25 cm² flasks which were designated passage 1 (P1). Half of P1 was passaged to P2 while the isolated cells from each of the remaining flasks were resuspended in a so-called freezing medium, transferred into cryovials and stored in liquid nitrogen for later use. The freezing medium was composed of 90 % FBS, 5 % EGM and 5 % dimethyl sulfoxide (DMSO) (Sigma-Aldrich, Saint Louis, MO, SA). This was repeated until P3 was reached and frozen away for later use (Figure 2.1).

For experimental purposes, endothelial cells from P1, P2 or P3 were plated on 35 mm petri dishes. Petri dishes were coated with gelatine-containing attachment factor (Life Technologies, Carlsbad, California, USA), and cells grown to confluency. Upon reaching confluency, cells underwent trypsinization, and were plated in a 1:2 ratio until a sufficient number of plates were reached for experiments. Experiments were conducted from the cells of the 4th to 6th generations, as these generations provided enough sample size and cells while still at their optimum viability and function.

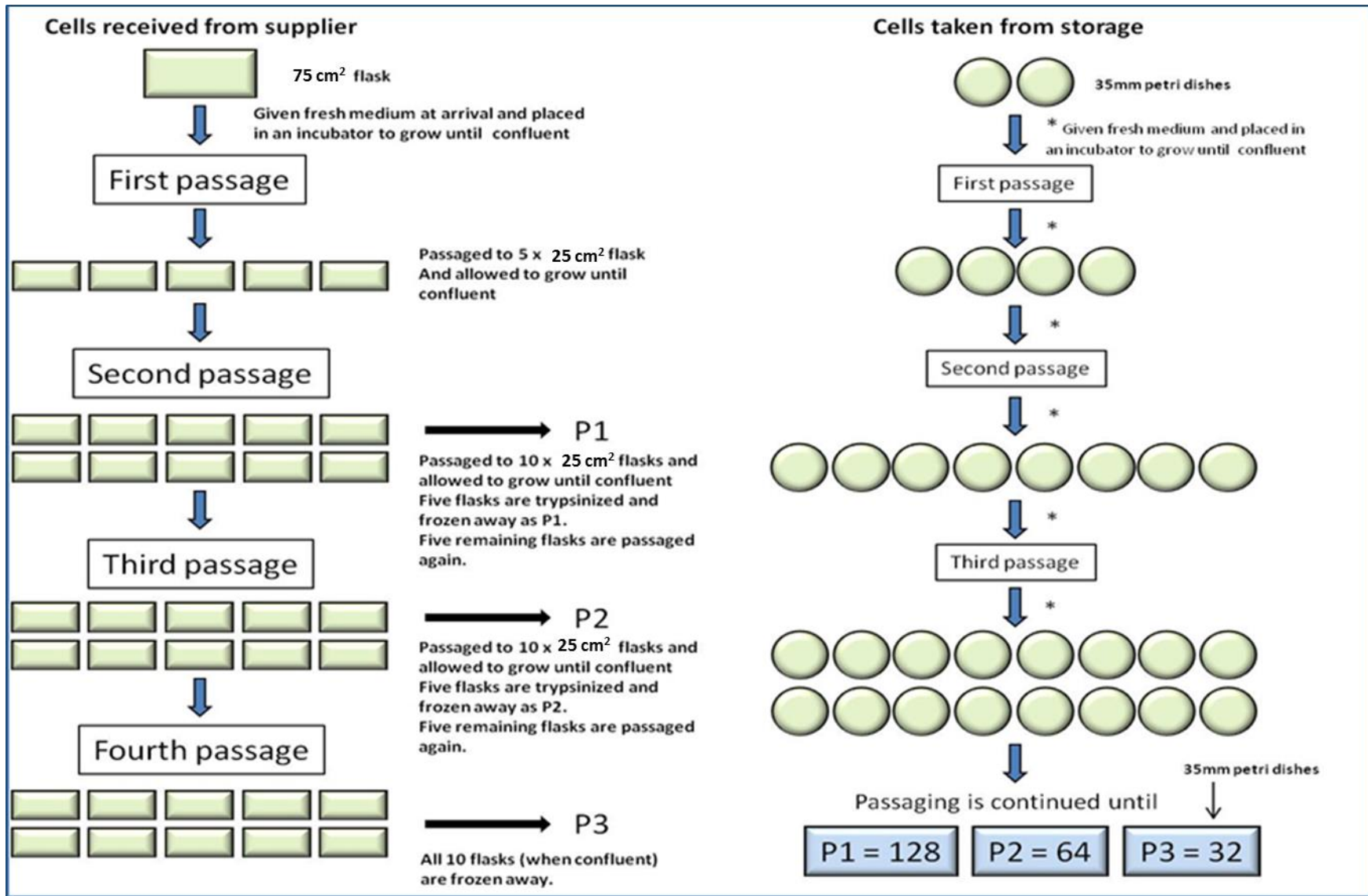


Figure 2.1: Passaging of cells and storage in liquid nitrogen (Adapted from Genis A, PhD thesis 2014).

2.1.2 Flow cytometric analyses

Cellular characteristics measured by flow cytometry include cell size, cell granularity and fluorescence intensity. In this study, flow cytometric analyses were performed on a flow cytometer (Becton-Dickinson FACSCalibur, Franklin Lakes, NJ) located in the Stellenbosch University-BD flow cytometry unit, Faculty of Medicine and Health Sciences. Analyses were mainly focussed on the measurement of NO and ROS production, and evaluating the development of cell injury (necrosis) by employing appropriate fluorescent probes. Data acquisition was performed by Cellquest Pro[®] software (Version 5.2.1) (Becton-Dickson and Co, San Jose, CA), and final analysis by Windows Multiple Document Interface for flow cytometry (WinMDI; version 2.9, Joseph Trotter, 1993-2000). All flow cytometric protocols have been established and previously described by Strijdom *et al* (2004 and 2006). A total of 5000-10000 events were acquired for each sample. Inter-sample uniformity was maintained throughout the acquisition of samples, by the process of gating cell populations of the control samples according to their forward scatter (cell size) and their side scatter (cell granularity) (Figure 2.2). The gating of a sample population served to exclude cellular debris and non-cellular particles that could contaminate the samples, thus ensuring acquisition (and ultimately analysis) of the cell populations of interest. The same gate was maintained for all control and experimental samples during acquisition and analysis of a given experimental group. Post-acquisition analysis was performed by recording the mean fluorescence intensity of each experimental sample as determined from histograms, and calculated as a percentage of control (control adjusted to 100 %). For the cell viability studies, the percentage necrotic cells were recorded and expressed as percentage of control (control adjusted to 100 %). For all flow cytometry analyses, experiments were repeated at least twice, and number of samples (N) ranged from 4 – 15.

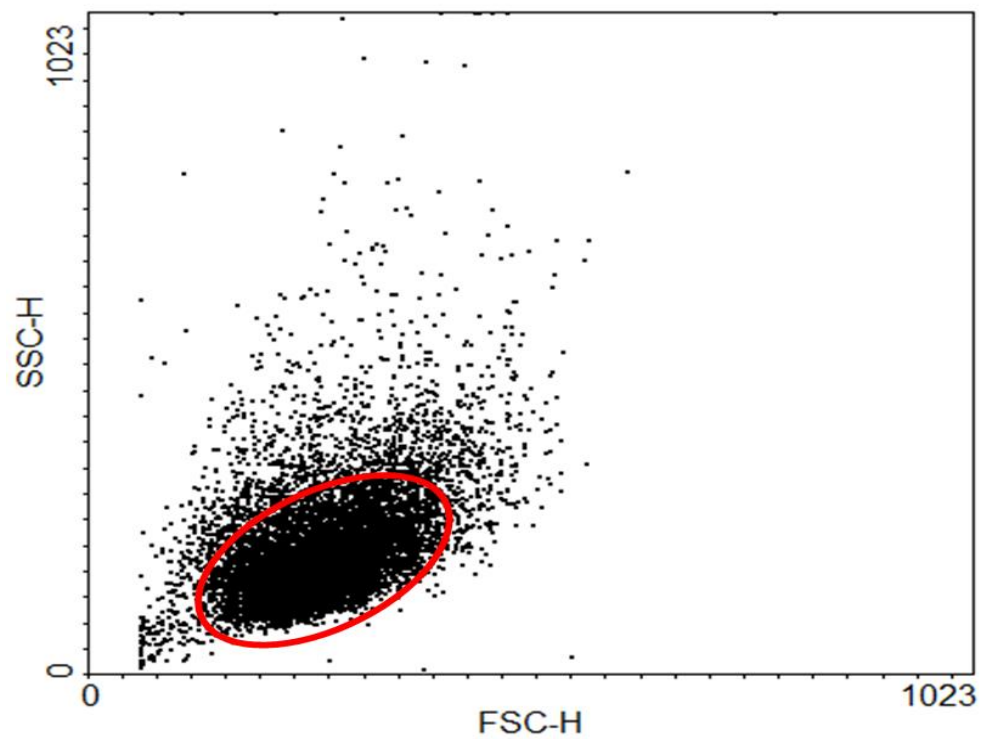


Figure 2.2: A representative example of a forward-side scatter plot with a gate (in red) representing the cell population of interest. (SSC-H: side scatter, FSC-H: forward scatter).

2.1.2.1 NO measurements

Intracellular NO levels were measured by flow cytometric analysis of the NO-specific fluorescent probe, diaminofluorescein diacetate (DAF-2/DA) (Calbiochem, San Diego, CA, USA). The DAF-2/DA protocol has previously been developed in our laboratory (Strijdom *et al.*, 2004 and 2006). When DAF-2/DA reacts with NO, the probe is oxidised to diaminofluorescein-triazol (DAF-2T) which emits a green fluorescence analysed in FL1-H channel.

DAF-2/DA protocol (Figure 2.3): Whilst in culture, cells were treated with 10 μ M DAF-2/DA dissolved in PBS and incubated for 3 hours at 37°C. After 3 hours, cells were removed from culture by trypsinization and resuspended in probe-free PBS for flow cytometry. For all experiments, absolute control samples (fluorescent probe-free) which was probe-free and a DAF-2/DA probe-containing samples were included to determine the auto-fluorescence or natural fluorescence of fluorescent probe-free cells and the DAF-2/DA fluorescence respectively. A significant increase in DAF-2/DA fluorescence as determined by comparing the absolute control and the DAF-2/DA-containing control sample confirmed sufficient DAF-/DA uptake by the cells, indicative of detectable baseline NO-levels in the cells. In order to validate the specificity of the DAF-2/DA probe, positive control samples treated with a NO donor, diethylammonium salt (DEA/NO) (Life Technologies, Carlsbad, California, USA) were also routinely included. Cells were treated with 100 μ M DEA/NO 1 hour after DAF-2/DA administration and incubated for a further 2 hours (Figure 2.3). A representative histogram depicting the mean DAF-2/DA fluorescence intensity in absolute control (autofluorescence), DAF-2/DA-containing control, and DEA/NO-treated positive control samples respectively is shown in Figure 2.4.

2.1.2.2 ROS measurements

Dihydrorhodamine-123 (DHR-123) and 2',7'-dichlorofluorescein (DCF) (Sigma-Aldrich, Saint Louis, MO, USA) fluorescent probes were employed to measure intracellular peroxynitrite (ONOO⁻) and H₂O₂ levels respectively.

DHR-123 protocol (Figure 2.3): Cells were treated with 2 μM DHR-123 dissolved in PBS and incubated for 3 hours at 37°C. After 3 hours, the cells were removed from culture, resuspended in probe-free PBS and analysed flow cytometrically in the FL3-H channel. Absolute control (probe-free) samples were included, as described previously for the DAF-2/DA experiments. Samples treated with authentic peroxynitrite (Millipore, Billerica, MA, USA) were included as positive controls to validate the specificity of the DHR-123 probe. Authentic peroxynitrite (100 μM) was added 1 hour after DHR-123 administration and incubated for a further 2 hours at 37°C.

DCF protocol (Figure 2.5): Cells were treated with 10 μM DCF dissolved in PBS and incubated for 1 hour at 37°C. Following the incubation period, cells were removed from culture, and resuspended in probe free PBS for analysis in the FL-2H channel. As with the DAF-2/DA and DHR-123 experiments, absolute control samples were included to distinguish between the autofluorescence of the cells and DCF uptake by the cells. To validate the H₂O₂-specificity of the DCF probe, H₂O₂ (Sigma-Aldrich, Saint Louis, MO, USA) was used as positive control. Briefly, 100 μM H₂O₂ was administered to the cells 30 minutes after DCF administration and incubated for a further 30 minutes at 37 °C.

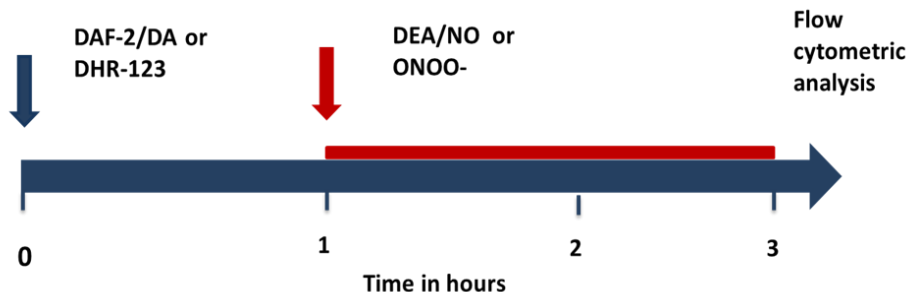


Figure 2.3: The experimental protocols for DAF-2/DA, DHR-123 incubation, and positive controls administrations (DEA/NO for DAF-2/DA and authentic peroxynitrite for DHR-123).

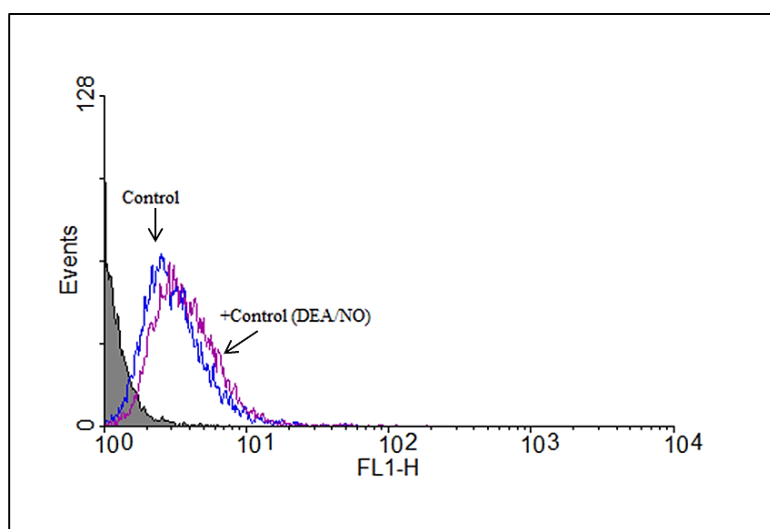


Figure 2.4: A representative histogram showing the autofluorescence (grey), and DAF-2/DA fluorescence in control (blue) and positive control (purple) samples, measured in the FL1-H channel of the flow cytometer. A shift in fluorescence to the right, as demonstrated by the autofluorescence vs. control, and control vs. positive control, indicates increasing intracellular levels of NO.

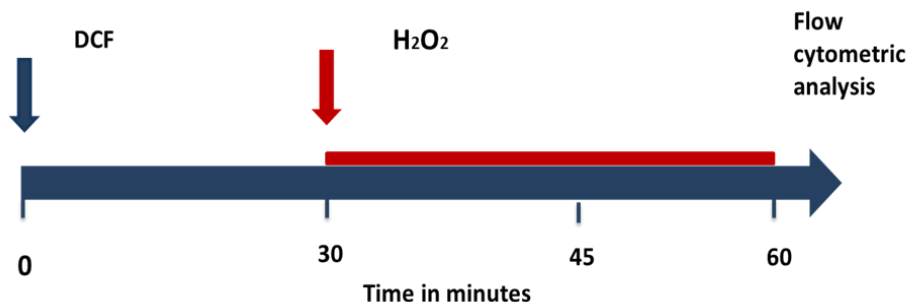


Figure 2.5: The experimental protocol for DCF incubation and positive control (H₂O₂).

2.1.2.3 Cell viability measurements

The propidium Iodide (PI) fluorescent probe (Sigma-Aldrich, Saint Louis, MO, USA) was employed to measure necrosis (Krysko *et al* 2008). When the cell is viable and its membrane integrity is intact, PI is unable to penetrate the cell. However, when the cell is damaged and membrane integrity is compromised, the PI probe is able to enter the cell and move into the nucleus where it stains nuclear nucleic acids resulting in the emission of a red fluorescence. Cells were removed from culture by trypsinization and resuspended in 1 ml PBS, followed by the addition of 5 μ M PI. Cells were subsequently incubated at room temperature in the dark for 15 minutes followed by flow cytometric analysis (Figure 2.6). For analysis, PI fluorescence was measured in the FL-2H channel as shown in Figure 2.7.



Figure 2.6: The experimental protocol for PI incubation. Cells were trypsinized prior to addition of the PI probe, followed by 15 minutes incubation in the dark at room temperature.

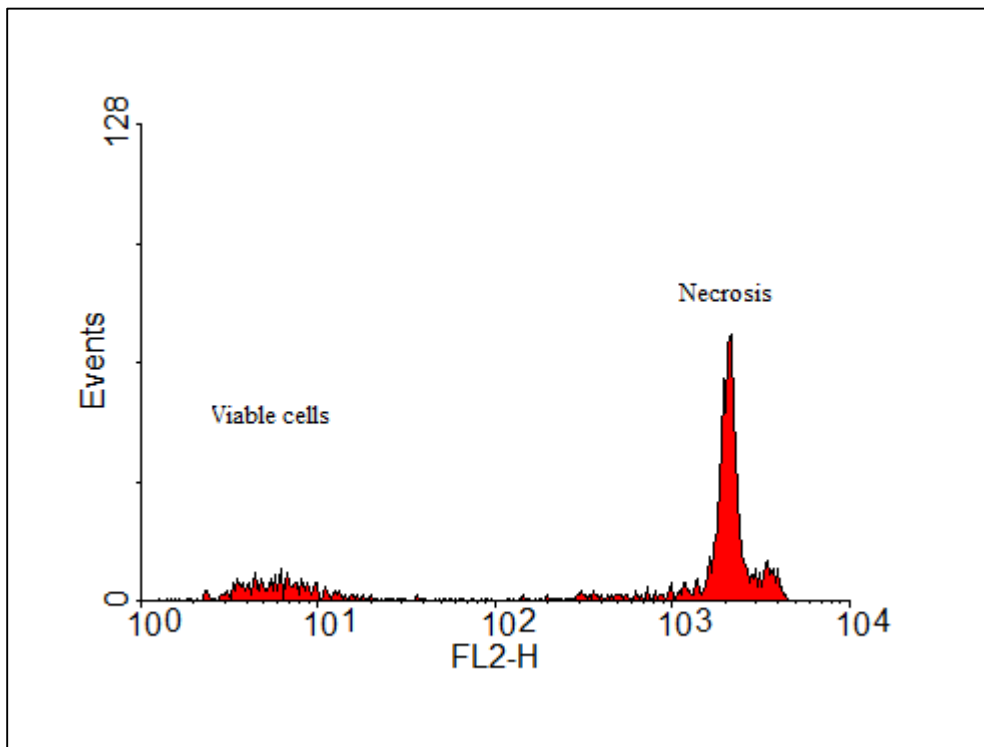


Figure 2.7: A representative histogram of a sample exposed to an injurious insult resulting in a high percentage necrotic cells as demonstrated by the high PI-uptake in the necrotic cell sub-population (peak on the right).

2.1.3 Western blot analyses

In order to further investigate possible evidence of endothelial heterogeneity between AECs and CMECs (untreated control and TNF- α -treated), western blot analyses were employed to determine the expression and / or phosphorylation of the following proteins: eNOS, PKB / Akt, heat shock protein 90 (HSP 90), I κ B- α ; and expression of the marker of protein nitration, nitrotyrosine. The process of extracting protein from the cells entailed removing cells from culture by trypsinisation followed by a cell lysis protocol. Trypsinised and isolated CMECs and AECs were centrifuged at 1000 rpm for 4 minutes until cell pellets were obtained. Ten petri dishes were pooled together for each experimental sample, in order to obtain a sufficient protein yield. Zirconium oxide beads (0.15 mm in size) were placed on the cell pellet and ~ 700 - 800 μ l of lysis buffer was added. The lysis buffer consisted of 20 mM Tris, 1 mM EGTA, 150 mM NaCl, 1 mM β -glycerophosphate, 1 mM sodium orthovanadate (NaVO₃), 2.5 mM tetra-sodium diphosphate, 1 mM PMSF, 0.1 % sodium dodecylsulfate (SDS), 10 μ g/ml aprotinin, 10 μ g/ml leupeptin, 50 nM NaF and 1 % triton-X100. The zirconium oxide beads and lysis buffer containing cell pellets were subjected to homogenisation in a Bullet Blender™ (Next Advance, Inc., NY, USA) followed by centrifugation at 10 000 rpm for 10 minutes.

The supernatant was analysed for protein content by means of the Bradford protein assay (Bradford 1976). Next, the calculated protein content was used to prepare the sample lysates, which were composed of the Laemmli buffer (4 % SDS, 20 % glycerol, 10 % 2-mercaptoethanol, 0.004 % bromopheno blue and 0.125 M Tris HCl), lysis buffer and the supernatant, ensuring a 50 μ g/10 μ l protein content for each sample. Cell lysate proteins were then loaded on a SDS-polyacrylamide gel and transferred onto a PVDF membrane (Immobilon™-P, from Millipore). Non-specific binding was eliminated by blocking with 5 % fat-free milk which was dissolved in Tris-buffered saline, 0.1 % tween-20 (Merck Millipore, Billerica, US).

Membranes were probed with the following specific rabbit polyclonal primary antibodies: anti-eNOS, anti-phospho eNOS (Ser 1177), anti-PKB / Akt, anti-phospho PKB (Ser 473), anti-heat shock protein 90, anti-I κ B- α (Cell Signaling Technologies, Beverly, MA, USA), and anti-nitrotyrosine (Santa Cruz Biotechnologies, Santa Cruz, CA, USA) (Table 2.1 and 2.2). This was

followed by exposing the membranes to a horseradish peroxidase-linked anti-rabbit IgG secondary antibody (AEC Amersham, Buckinghamshire, UK). Detection of protein bands was achieved by use of enhanced chemiluminescence (ECL™) (AEC Amersham, Buckinghamshire, UK). Densitometry (UN-SCAN-IT, Silk Scientific, Orem, UT, USA) was performed to analyse all western blot data. The sample size for all western blot experiments ranged from N = 3 – 4 per group. Western blot data were expressed as a ratio of AEC untreated control (adjusted to 1).

Table 2.1: Proteins measured by western blotting

Protein	Role
eNOS: <ul style="list-style-type: none"> Total eNOS Phosphorylated eNOS at Ser 1177 	Primary source of nitric oxide in endothelial cells.
PKB / Akt: <ul style="list-style-type: none"> Total PKB / Akt Phosphorylated PKB/Akt at Ser 473 	Upstream activator of eNOS by means of phosphorylation.
Heat shock protein 90 (HSP 90)	Chaperone protein that mediates eNOS phosphorylation by PKB / Akt
Nitrotyrosine	A marker of harmful protein nitration by peroxytrite.
IκB-alpha	Decreased expression of IκB-alpha was used as a marker of increased NFκB activity.

Table 2.2: Western blot protocols

Antibody	Size KDa	% Gel	Primary antibody dilution	Secondary antibody dilution	Exposure time (min)
eNOS	140	7.5	1:1000 in TBS/Tween	1:4000 in 5 % milk	10-20
phospho eNOS	140	7.5	1:1000 in TBS/Tween	1:4000 in 5 % milk	10-20
PKB	63	10	1:1000 in TBS/Tween	1:4000 in TBS/Tween	5-10
phospho PKB	63	10	1:1000 in TBS/Tween	1:4000 in 2.5 % milk	5-10
HSP 90	90	10	1:1000 in TBS/Tween	1:4000 in 5 % milk	3-5
Nitrotyrosine	90	10	1:500 in TBS/Tween	1:4000 in TBS/Tween	±1
IκB-alpha	35	12	1:1000 in TBS/Tween	1:4000 in TBS/Tween	±1
β-tubulin	55		1:1000 in TBS/Tween	1:4000 in 2.5 % milk	15

2.1.4 Experimental Protocols: Endothelial injury and oleanolic acid studies

2.1.4.1 Induction of endothelial injury with TNF- α

To induce endothelial cell injury, cells were exposed to treatment with the pro-inflammatory cytokine TNF- α . First, concentration-response experiments were conducted to determine the optimal concentration and incubation period for injury induction. The TNF- α concentrations were chosen from previous studies in the literature. Confluent AECs and CMECs were treated with 3 different concentrations of TNF- α and incubated at 37°C for 24 or 48 hours as follows (Figure 2.8):

AECs: 0.5, 5 and 20 ng/ml TNF- α (24 or 48 hours).

CMECs: 0.5, 5 and 20 ng/ml TNF- α (24 or 28 hours).

Following the incubation periods, cells were washed with PBS and treated with DAF-2/DA for NO measurements, or DHR-123 and DCF for ROS measurements or PI for necrosis measurements, as described earlier. Based on the results, the 20 ng/ml TNF- α for 24 hours treatment protocol was chosen for injury induction.

2.1.4.2 Oleanolic acid studies

OA (Sigma-Aldrich, Saint Louis, MO, USA) was dissolved in DMSO, and volume-matching vehicle control samples were included in all experiments (0.06 % DMSO for 10 μ M OA and 0.24 % DMSO for 40 μ M OA samples). To establish the optimum concentration of OA, concentration-response experiments were conducted, using two different concentrations. Confluent AECs and CMECs were treated with 10 or 40 μ M OA and incubated at 37°C for 1 hour. After 1 hour, cells were washed with PBS and treated with DAF-2/DA probe, followed by flow cytometric analyses of the DAF-2/DA fluorescence. Based on the results of the 1 hour concentration-response studies, 40 μ M OA was chosen for further experiments in view of the potent NO-increasing properties observed at this concentration.

Baseline studies were subsequently conducted with 40 μ M OA on both AECs and CMECs to investigate the effects of OA with regards to NO production, ROS production and cellular necrosis. Briefly, confluent AECs and CMECs were treated with 40 μ M OA and incubated at

37 °C for 1 hour or 24 hours (Figure 2.9). After the incubation periods, the following parameters were measured based on the protocols described earlier:

- NO production,
- ROS production (DCF fluorescence) or
- Necrosis

2.1.4.3 OA pre-treatment studies

Due to its ability to increase NO production, we further investigated putative beneficial effects of OA on TNF- α -induced endothelial cell injury. The aim of this part of the study was to determine whether OA pre-treatment was able to reduce or prevent the injurious effects of TNF- α on the endothelial cells. This was achieved by administration of OA to the cells prior injury induction with TNF- α . The OA pre-treatment protocol was identical for both AECs and CMECs:

Cells were pre-treated with 40 μ M OA 1 hour prior to the administration of 20 ng / ml TNF- α for a further 24 hours at 37°C. OA remained present for the full duration (25 hours in total) (Figure 2.10).

Following the 25 hour period, cells were washed with PBS and treated with:

- DAF- 2/DA for NO measurements, or
- DCF for ROS measurements, or
- PI for necrosis measurements, as described above.

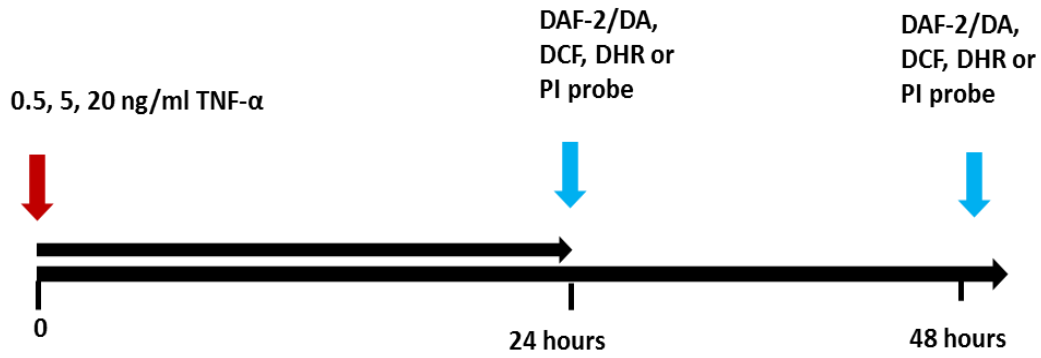


Figure 2.8: Protocols to determine the TNF- α concentration-response effects for 24 or 48 hour treatment durations.

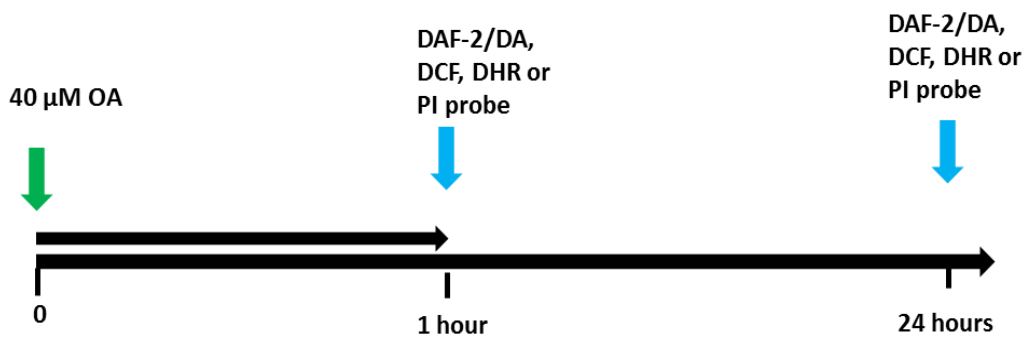


Figure 2.9: Protocols for baseline studies with 40 μ M OA.

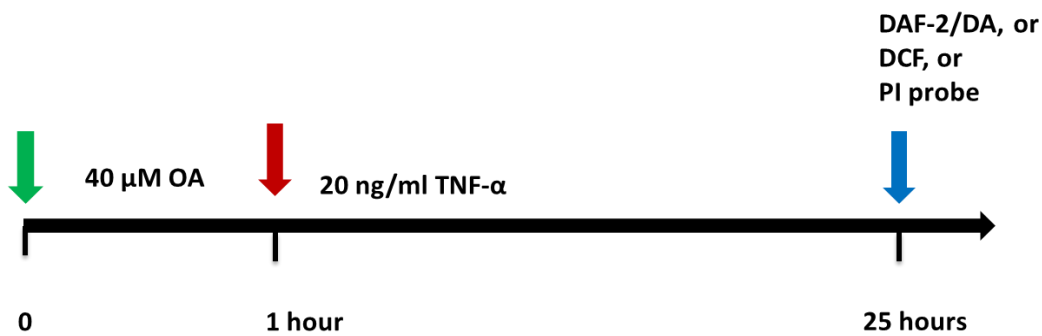


Figure 2.10: OA pre-treatment protocol prior to injury induction by means of TNF- α administration for 24 hours.

2.2 Proteomic Analyses

Analysing biological samples by proteomics provide a quantitative, comprehensive insight into large-scale protein expression and differential regulation patterns in samples exposed to experimental interventions vs. untreated controls. In this study, proteomic analyses were performed on both AECs and CMECs under untreated control and TNF- α treated conditions.

2.2.1 Protein extraction

Protein extraction from the various AEC and CMEC samples was performed in an identical fashion as described above for the western blot analyses (section 2.1.3), except that the lysis buffer was slightly modified by excluding triton and using 1 % SDS instead of 0.1 %. The experimental groups were as follows: AEC untreated control (N = 3), AEC TNF- α treated (N = 3), CMECs untreated control (N = 3) and CMECs TNF- α treated (N = 3). A final protein yield of 50 μ g/ 10 μ l was obtained for each sample. The experimental and protein extraction procedures were performed in our laboratory. All subsequent procedures described below were performed at the Centre for Proteomics and Genomics Research in Cape Town (CPGR; Dr Zac McDonald).

2.2.2 Filter aided sample preparation (FASP)

All reagents were analytical grade or equivalent. 200 μ g of total protein from each lysate was placed in a 1.5 ml LoBind Eppendorf tube and reduced with 0.1 volume 50 mM triscarboxyethyl phosphine (TCEP; Fluka) for 1 hour at 60 $^{\circ}$ C. After protein reduction, the SDS concentration was diluted to 0.5 % with 8 M urea (Sigma) 100 mM triethyl ammonium bicarbonate (TEAB; Sigma) buffer. Reduced protein was placed on a 30 kDA MWCO centrifugal filter (Amicon ultra; Millipore). The centrifugal filter ensures the reduction of the liquid volume thereby concentrating the proteins. Samples were concentrated down to 30 μ l by centrifugation at 13000 g. The retentate was alkylated by the addition of 100 μ l 15 mM methyl methanethiosulphonate (MMTS; Sigma) in 8 M urea 100 mM TEAB buffer for 15 minutes at 20 $^{\circ}$ C. Buffer was exchanged by adding 350 μ l 8 M urea 100 mM TEAB buffer to the alkylated sample and reducing the volume to 30 μ l by centrifugation at 13000 g. Buffer

exchange was repeated three times to ensure excess SDS was washed out. Urea concentration was reduced by two washes with 100 μ l 100 mM TEAB, each time reducing the retentate volume to 30 μ l by centrifugation at 13000 g. Proteins were digested by adding trypsin (Promega) in 100 mM TEAB to a final protein: trypsin ratio of 50:1, and then incubated for 18 hours at 37 °C. Peptides were collected in a new collection tube by 13000 g centrifugation, followed by two MilliQ H₂O filter washes. Samples were dried and re-suspended in 0.1 % trifluoroacetic acid (TFA; Sigma).

2.2.3 LC MS/MS analysis

Nano-RP LC MS/MS analysis was conducted with a Q-Exactive quadrupole-Orbitrap mass spectrometer (Thermo Fisher Scientific, USA) coupled with a Dionex ultimate 3000 nano-HPLC system (Thermo Fisher Scientific, USA). The sample volume injected was 4 μ l. The mobile phases consisted of solvent A (0.1 % formic acid in water) and solvent B (90 % ACN, 10 % water, and 0.1 % formic acid). Tryptic peptides (see above FASP protocol) from each sample were dried under vacuum and re-solubilized in sample loading buffer (95 % water, 5 % Acetonitrile, 0.05 % TFA). An estimated 3 μ g of total peptide was loaded on a C18 trap column (100 μ m \times 20 mm \times 5 μ m). Chromatographic separation was performed with an Acclaim[®] PepMap100 C18 column (75 μ m \times 250 mm \times 3 μ m) (Thermo Fisher Scientific, USA). The gradient was delivered at 250 nl/min and consisted of a linear gradient of mobile phase B initiating from solvent B, 6–30 % over 90 min. The mass spectrometer was operated in positive ion mode with a capillary temperature of 250 °C. The applied electrospray voltage was 1.95 kV. In one cycle the top 10 most abundant peptides were chosen for MS / MS fragmentation with a dynamic exclusion of 30s. Details of data acquisition are shown in Table 2.3.

Table 2.3: Details of data acquisition

Full Scan	
Resolution	70,000 (@ m/z 200)
AGC target value	3e6
Scan range	350-2000 m/z
Maximal injection time (ms)	100
Data-dependent MS/MS	
Resolution	17,500 (@ m/z 200)
AGC target value	1e5
Maximal injection time (ms)	50
Isolation window width (Da)	3
NCE (%)	27
Data-dependent Settings	
Underfill ratio (%)	1 %
Charge exclusion	Charge states 1,6-8,>8
Peptide match	preferred
Exclusion isotopes	on
Dynamic exclusion (s)	30

2.2.4 Data analysis

2.2.4.1 Protein Identification

Database interrogation was performed with the MASCOT algorithm (Matrix Science, London, U.K.; version 2.3) and X! Tandem (version CYCLONE™) using a taxonomic filtered “Rattus” only uniprotKB sourced database (<http://www.uniprot.org/>). Search parameters are detailed in Table 2.4. All identified peptides had an ion score above the Mascot peptide identity threshold and global false discovery rate was controlled to below 1.5 %. A protein was considered identified if at least two such unique peptide matches were apparent for the protein.

Table 2.4: Protein search parameters

Type of search	MS/MS Ion Search
Enzyme	Trypsin
Fixed modifications	Methylthio (C)
Variable modifications	Deamidated (NQ), Oxidation (M)
Mass values	Monoisotopic
Peptide mass tolerance	± 20 ppm
Fragment mass tolerance	± 20 mmu
Max missed cleavages	2
Instrument type	ESI-TRAP

2.2.4.2 Label free protein quantitation and differential regulation

Label free proteomic profiling was accomplished using either Scaffold software for MS / MS proteomics (Proteome Software, USA) or SIEVE 2.0 (Thermo Scientific, USA). Scaffold calculates the Spectrum Count quantitative value by normalizing spectral counts across an experiment. This is achieved by taking the sum of all the Total Spectrum Counts for each MS sample. These sums are then scaled so that they are all the same, after which Scaffold applies the scaling factor for each sample to each protein group and outputs a normalized quantitative value. SIEVE aligns chromatograms from different experimental conditions and then determines features in the data (m/z and retention time pairs) that differ across chromatograms. Significance was calculated within Scaffold or SIEVE using a standard T-test and results were filtered for a minimum of two peptides identified and quantified per protein with frames having a p -value of less than 0.05. Based on three biological replicates per condition a normalized fold change and a normalized p -value was calculated for each protein. Proteins were considered regulated if their fold change was greater than or equal to 1.5 and their corresponding p -value was less than or equal to 0.05. All protein quantification was normalized to total ion current (TIC).

2.2.4.3 Functional annotation analyses of proteins

Functional annotation analyses of the identified proteins in the various samples were performed by submitting protein lists to the functional annotation tool of DAVID (The Database for Annotation, Visualization and Integrated Discovery) Bioinformatics Resources 6.7 (Huang *et al* 2009). The DAVID functional annotation tool allocates functionally related proteins from the submitted lists to specific Gene Ontology (GO) terms, and in this study, we were interested in the significantly represented GO terms determined by biological process. Biological processes with p -values < 0.05 and larger fold-enrichments (≥ 1.5) were of particular interest when interpreting the functional annotation data.

2.3 Rat aortic ring isometric tension studies (*ex vivo* studies)

2.3.1 Aortic ring model

Endothelium-dependent vascular function was studied in thoracic aortic ring segments from high fat diet (HFD)-induced obese and age-matched lean, control male Wistar rats. In addition to investigating the effects of the high fat diet on aortic function, we also explored the short-term effects of *ex vivo* administered OA on the aortic rings. The isometric tension system consisted of a tissue-organ bath (AD Instruments, Bella Vista, New South Wales, Australia), connected to a 0 – 25 g force transducer (Figure 2.11). The organ bath system has a stainless steel stationery hook, whereas the transducer has a stainless steel hook attached to the transducer by a free flowing string, for tension adjustment. The aortic rings were mounted onto the two hooks as described in more detail below. Data were acquired via a PowerLab™ data acquisition amplifier (AD Instruments), and analysed with LabChart™ Pro 7 (version 7.3.1) data capturing software (AD Instruments).

2.3.2 Animals

For the animal studies, ethics clearance was obtained from the Research Ethics Committee for Animal Care and Use, Stellenbosch University (Ethics number: SU-ACUM11-00002). The animals were supplied by and housed in the Animal Research Facility (Faculty of Medicine and Health Sciences, Stellenbosch University), and they were given food and water *ad libitum*. Animals were housed according to the revised guidelines of the South African National Standard for the care and use of Animals for Scientific Purposes (South African Bureau of Standards, SANS 10386, 2008). Male Wistar rats (weighing ~ 250 g) were randomly divided in two groups, namely, the lean, control group (fed normal rat chow) and the HFD group (fed rat chow with added condensed milk and Holsum™ cooking fat). Rats remained on the feeding program for 16 or 24 weeks after which they were sacrificed and experiments commenced. The composition of the diets is shown in Table 2.5.

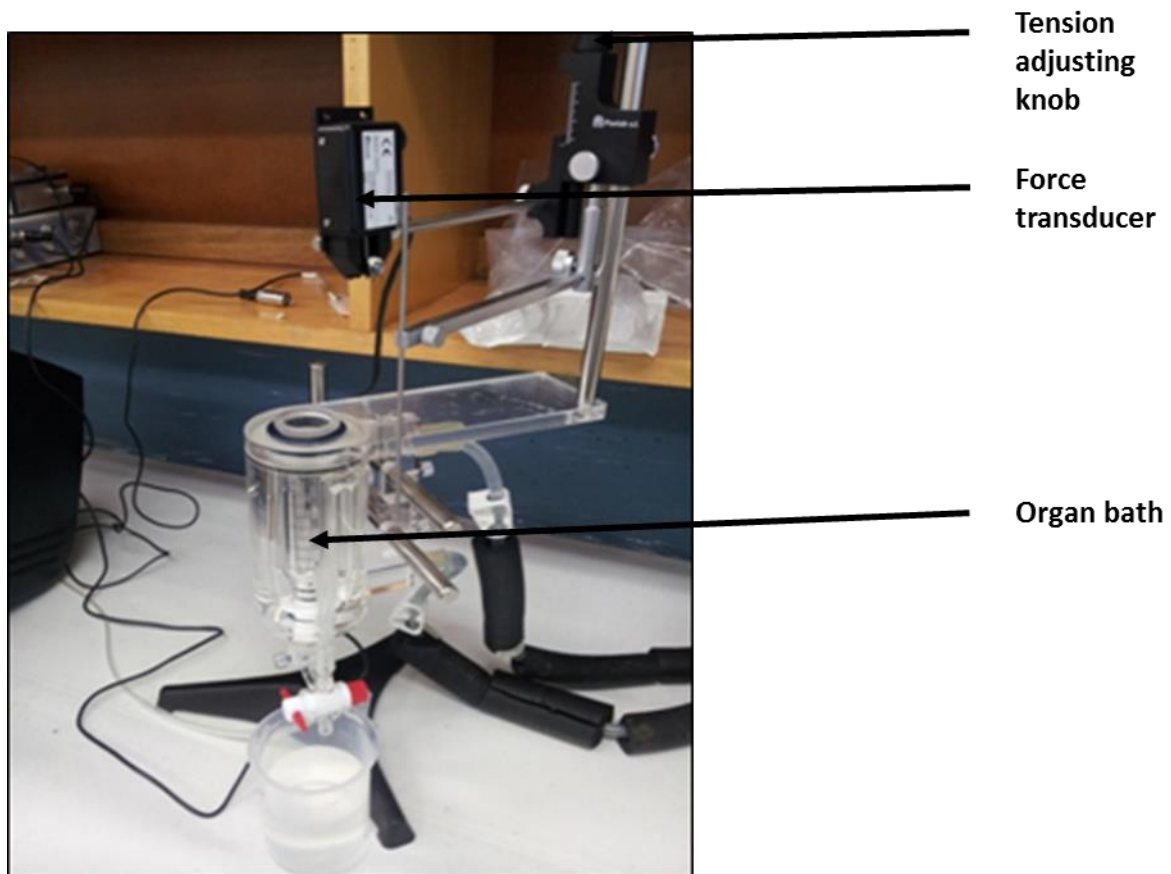


Figure 2.11: The tissue organ bath system (Adapted from Loubser DJ, MSc thesis 2014).

Table 2.5: Composition of the HFD and control diets.

	Lean, Control	HFD
Energy (kj / 100 g)	1 272	1 354
Total fat (g / 100 g)	4.8	11.5
Saturated fat (g / 100 g)	0.9	7.6
Cholesterol (mg / 100 g)	2.2	13
% protein	17.1	8.3
% carbohydrate	34.6	42
Sucrose (g / 100 g)	5.3	20.4

2.3.3 Isolation of the aortic rings

Rats were anaesthetised through intraperitoneal injection of 160 mg/kg pentobarbital. Upon loss of consciousness, rats were dissected by making an incision on the ventral side just below the thoracic region, moving from the left to the right lateral side (Figure 2.12). The diaphragm was subsequently cut open, thus revealing the thoracic cavity. The rib cage was cut at the lateral sides in a cranial direction (Figure 2.12), leaving the thoracic organs exposed. The heart and other thoracic organs (lungs, trachea and oesophagus) were all removed, thus exposing the aorta. The thoracic aorta was excised by dissecting at the lower region of the aorta just above the diaphragm and superiorly at a region just distal to the aortic arch. The aorta was subsequently placed in a cold Krebs-Henseleit (KH) buffer made up of 119.0 mM NaCl, 25.0 mM NaHCO₃, 4.75 mM KCl, 1.2 mM KH₂PO₄, 0.6 mM MgSO₄·7H₂O, 0.6 mM Na₂SO₄, 1.25 mM CaCl₂·H₂O and 10.0 mM glucose in distilled water (Figure 2.13). The aorta was cleaned by removing the excess connective tissue and perivascular fat, and subsequently cut into ~ 4 mm rings, which were mounted on the tissue-organ bath system.

The aortic rings were mounted by carefully sliding them over the two hooks from the transducer and the organ bath, where after the mounted rings were lowered into the organ bath filled with 25 ml KH buffer (Figure 2.14). The organ bath was kept at 37°C and gassed with 95 % oxygen and 5 % carbon dioxide. The ring was stabilised at 1.5 g tension for 30 minutes with KH buffer being changed every 10 minutes. About 4 – 9 aortic rings per group (N = 4 – 9 per group) were used for all experiments.

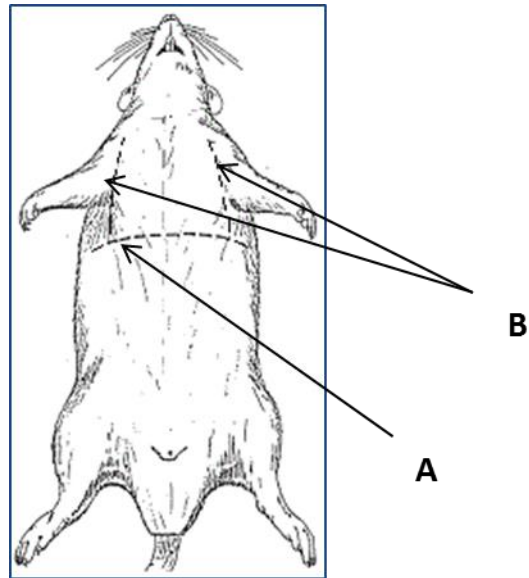


Figure 2.12: Schematic representation of the incisions made for the removal of the aorta (Adapted from Loubser DJ, MSc thesis 2014).



Figure 2.13: The excised aorta placed on cold Krebs-Henseleit buffer and cleaned of excess fat and connective tissue (Adapted from Loubser DJ, MSc thesis 2014).

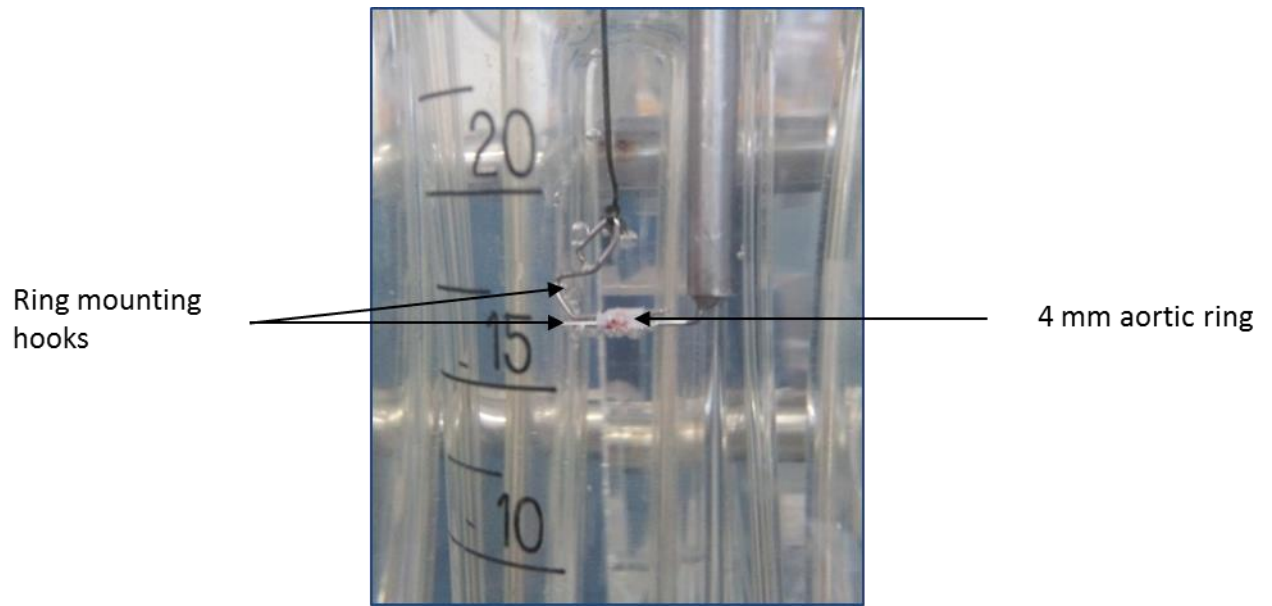


Figure 2.14: A 4 mm aortic ring mounted on two stainless steel hooks and lowered into the organ bath (Adapted from Loubser DJ, MSc thesis 2014).

2.3.4 Isometric tension measurement protocol

Following the 30 minutes stabilisation, the first contraction / relaxation measurements were performed to determine the endothelial functionality of the aortic ring. The first contraction was achieved by addition of a 100 nM phenylephrine (PE) bolus (Figure 2.15). PE is a selective α_1 -adrenergic receptor agonist which results in smooth muscle contraction. Following PE addition, the aortic ring was allowed to contract until the tension readings reached a plateau. A single administration of 10 μ M Ach followed, causing the aortic ring to undergo endothelium-dependent, NO-induced relaxation, with the relaxation readings allowed to reach their maximum values (Figure 2.15). Relaxation was expressed as the percentage of the maximum PE-induced contraction. Aortic rings achieving relaxation of $\geq 60\%$ were accepted as viable and included for the rest of the isometric tension experiment. Conversely, aortic rings not able to relax by more than 60 % of maximum PE-induced contraction were discarded and assumed to be injured by the excision and / or mounting procedure.

After the first contraction / relaxation, the KH buffer was rinsed out and replaced with fresh buffer. The aortic ring was subsequently stabilised for another 30 minutes at 1.5 g tension with buffer changes every 10 minutes. After the stabilisation period, the rings were subjected to a cumulative contraction and cumulative relaxation protocol. PE was administered in a cumulative fashion in order to obtain final concentrations of 100 nM, 300 nM, 500 nM, 800 nM and 1 μ M respectively after each addition (Figure 2.15). Once maximum contraction was reached after the final PE administration (total final concentration: 1 μ M), cumulative concentrations of Ach were administered in order to obtain final concentrations of 30 nM, 100 nM, 300 nM, 1 μ M and 10 μ M respectively after each addition (Figure 2.15), thus inducing relaxation.

2.3.5 Assessment of the effects of *ex vivo* OA administration on aortic ring contraction and relaxation

The effects of *ex vivo* OA administration on the contraction and relaxation of aortic rings were investigated via two different protocols:

2.3.5.1 Pre-treatment protocol

To investigate whether OA pre-treatment would affect aortic ring contraction and relaxation, a single administration of OA (40 μ M) was given after second 30 minutes stabilization period (baseline tension: 1.5 g), prior to PE-induced cumulative contractions. The OA was allowed to infuse for 15 minutes in the organ bath. The baseline tension remained stable at 1.5 g upon addition of OA and remained stable for the rest of the 15 minutes (Figure 2.16). After 15 minutes, the OA was not washed out, and cumulative PE-induced contraction followed by Ach-induced relaxation was subsequently performed as described earlier.

2.3.5.2 Protocol assessing OA's direct pro-relaxation effects

To investigate whether OA was able to induce direct pro-relaxation effects, OA was administered cumulatively following pre-contraction with PE. Following the second 30 minute stabilisation, cumulative PE-induced contraction was performed as per the previously described protocol, followed by cumulative additions of OA at 10 μ M, 10 μ M and 20 μ M (total final concentration: 40 μ M).

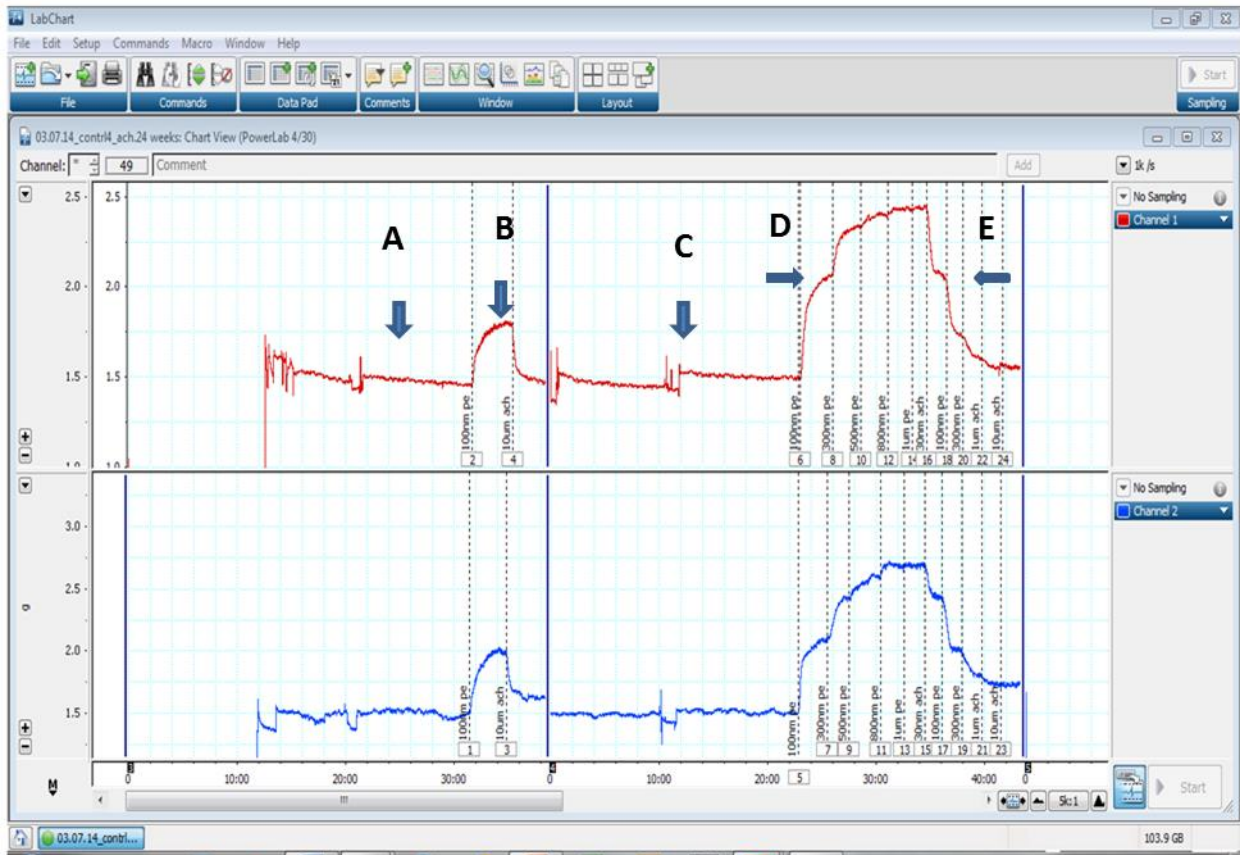


Figure 2.15: A representative recording obtained from the LabChart pro software showing the standard isometric tension protocol. A = first stabilization, B = pre-contraction with PE and relaxation with Ach to determine functionality of the ring, C = second stabilisation, D = cumulative contraction with PE, and E = cumulative relaxation with Ach.

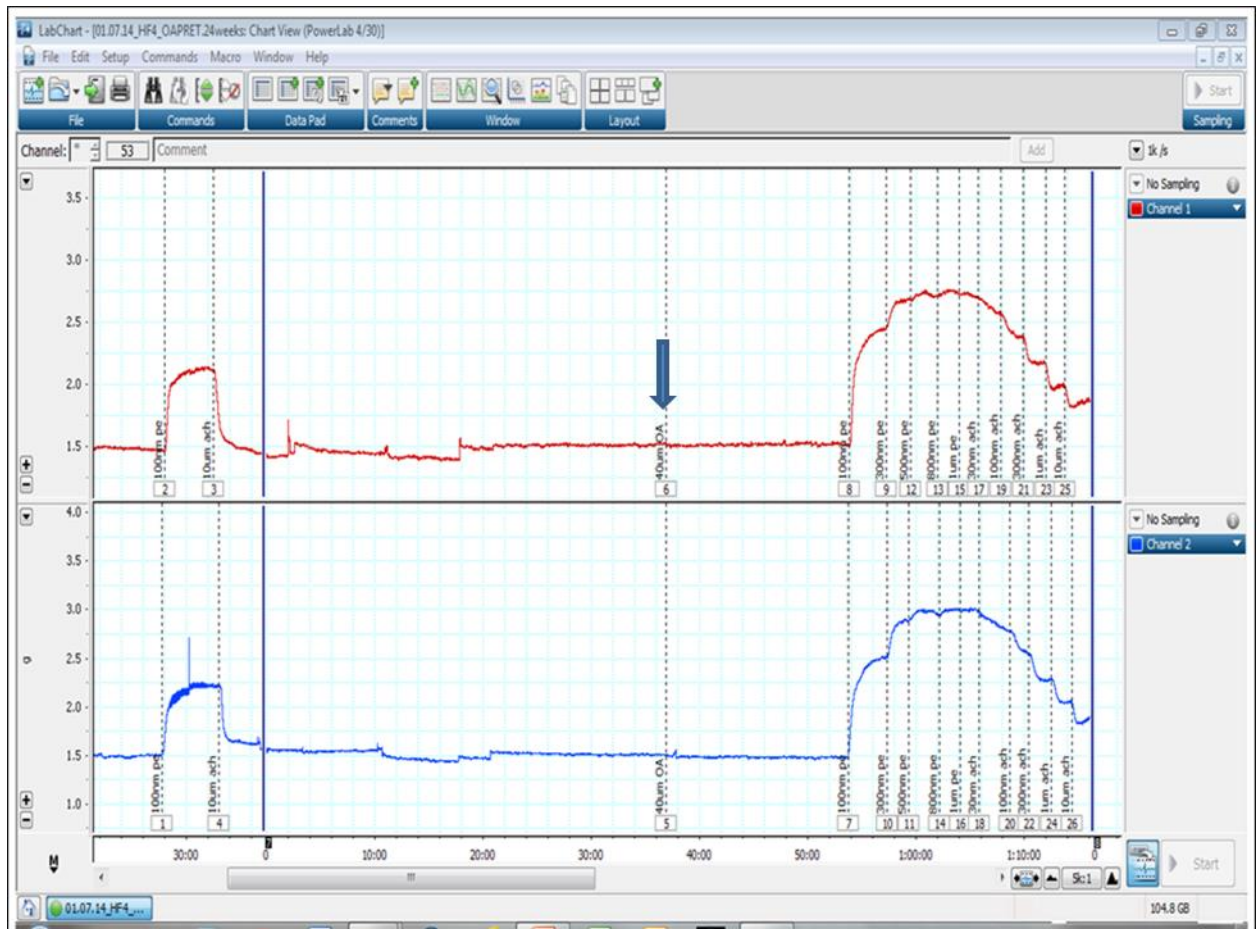


Figure 2.16: A representative recording obtained from the LabChart pro software showing the OA pre-treatment protocol. Pre-treatment with 40 μ M OA 15 minutes prior to cumulative contraction / relaxation shown by the arrow.

2.4 Statistical analyses

All data were analysed by Graph Pad Prism® version 5.01 software. Student's t-test, one-way ANOVA (with Bonferroni post-hoc test) or two-way ANOVA analyses were applied where appropriate. Data are expressed as mean \pm SEM and were considered statistically significant if displaying a p-value of < 0.05 .

Chapter 3

Results

3.1 Cell culture studies (*in vitro* models):

3.1.1 Validation of fluorescence probe-specificity (DAF-2/DA, DHR-123 and DCF)

In order to validate the NO-specificity of the DAF-2/DA fluorescent probe, the NO-donor, DEA/NO, was administered to CMECs as a positive control (see experimental protocol: Chapter 2, Section 2.1.2.1). Treatment of cells with 100 μ M DEA/NO significantly increased DAF-2/DA fluorescence (DEA/NO: 130.1 ± 3.4 %) vs. control (adjusted to 100%), $p < 0.05$, $N = 12$ (Figure 3.1 A).

The specificity of the ROS fluorescent probes, DHR-123 and DCF, was validated in CMECs with authentic peroxynitrite (ONOO^-) and H_2O_2 respectively (see experimental protocols: Chapter 2, Section 2.1.2.2). Treatment with 100 μ M authentic ONOO^- significantly increased DHR-123 fluorescence (182.9 ± 2.8 %, $p < 0.05$, $N = 4$) vs. 100 % control (Figure 3.1 B). Treatment with H_2O_2 (100 μ M) resulted in ~ 3 -fold increase in DCF fluorescence (383 ± 36.68 %) vs. 100 % Control, $p < 0.05$, $N = 4-8$ (Figure 3.1. B).

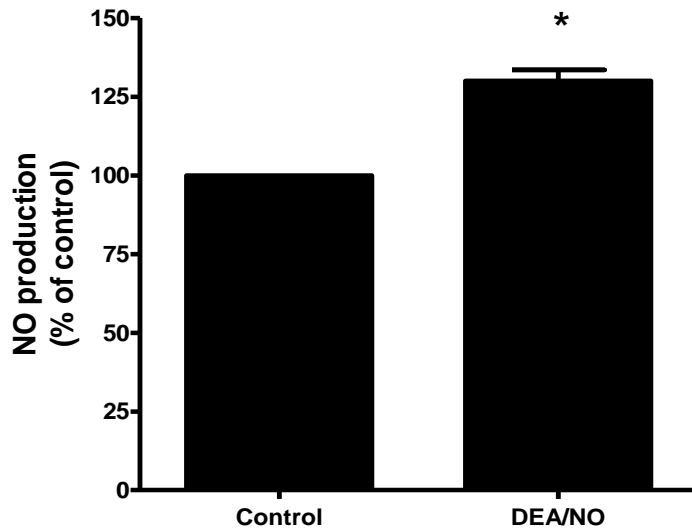


Figure 3.1 A: A histogram representation of the mean DAF-2/DA fluorescence intensity generated by 100 μ M DEA/NO administration (positive control for DAF-2/DA). * $p < 0.05$ vs control; control adjusted to 100 %.

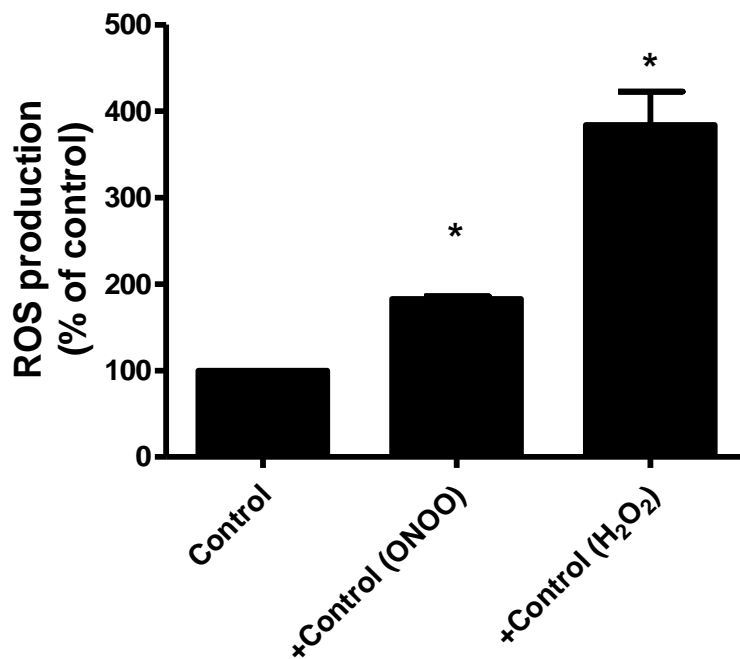


Figure 3.1 B: A histogram representation of the mean DHR-123 and DCF fluorescence intensity generated by 100 μ M authentic ONOO⁻ and 100 μ M H₂O₂ administration respectively (positive controls for DHR-123 and DCF). * $p < 0.05$ vs control; control adjusted to 100%.

3.1.2 Baseline studies

3.1.2.1 Baseline NO levels in AECs and CMECs

In order to compare NO levels in AECs and CMECs under control, baseline conditions, the mean DAF-2/DA fluorescence was measured and expressed as % of fluorescence observed in absolute control (DAF-2/DA-free samples), with absolute control fluorescence adjusted to 100 %. Results showed that the fluorescence intensity did not differ significantly between AECs and CMECs (N = 6) (Figure 3.2).

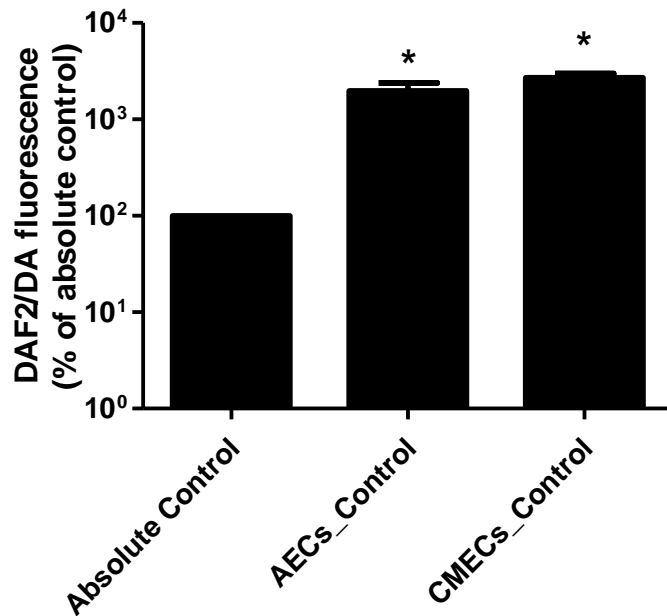


Figure 3.2: Baseline mean DAF-2/DA fluorescence in AECs and CMECs. * $p < 0.05$ vs. absolute control; absolute control adjusted to 100 %.

3.1.2.2 Baseline ROS levels in AECs and CMECs

Under control, baseline conditions, mean DHR-123 fluorescence (measuring ONOO⁻ levels) was significantly increased in CMECs (168.2 ± 8.4 %) compared to AECs (116.8 ± 10.8 %), $p < 0.05$, $N = 4$ (Figure 3.3 A). Conversely, mean DCF fluorescence (measuring H₂O₂ levels) was significantly increased in AECs (278.6 ± 12.7 %) compared to CMECs (196.5 ± 7.4 %) (Figure 3.3 B).

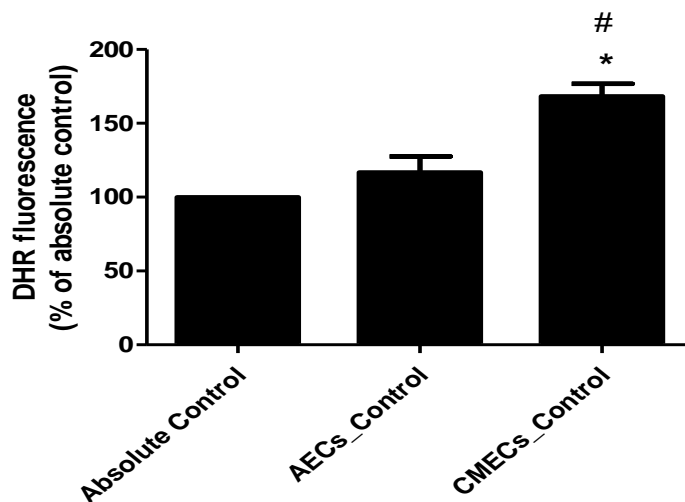


Figure 3.3 A: Baseline mean DHR-123 fluorescence in AECs and CMECs. * $p < 0.05$ vs. absolute control; absolute control adjusted to 100 %. # $p < 0.05$ vs. AECs control.

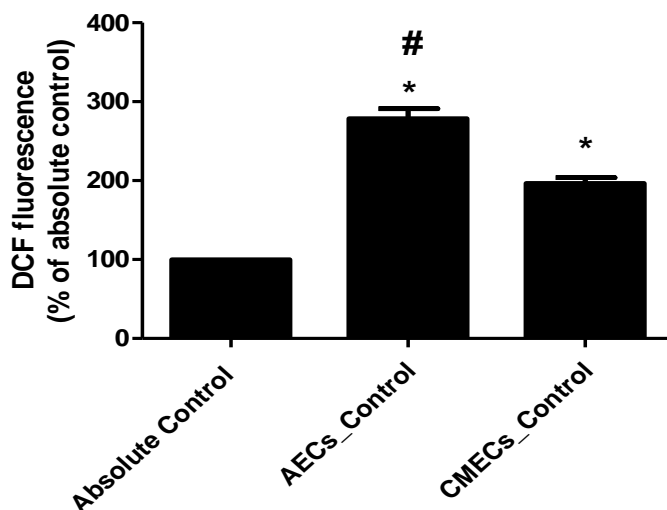


Figure 3.3 B: Baseline mean DCF fluorescence in AECs and CMECs. * $p < 0.05$ vs. absolute control; absolute control adjusted to 100 %. # $p < 0.05$ vs. CMECs control.

3.1.3 Endothelial injury induction: NO-production, ROS production and cell viability

3.1.3.1 Concentration-response investigations

Concentration-response investigations were conducted with the pro-inflammatory cytokine TNF- α at 0.5, 5 and 20 ng/ml (24 and 48 hours) in AECs and CMECs to determine the optimal concentration for endothelial injury induction.

3.1.3.1.1 NO measurements with DAF-2/DA

AECs: DAF-2/DA concentration-response investigations with TNF- α treatment

Mean DAF-2/DA fluorescence significantly decreased in AECs following treatment with TNF- α at all concentrations after 24 hours: 0.5 ng/ml TNF- α (73.20 ± 9.8 %), 5 ng/ml TNF- α (71.33 ± 2.98 %) and 20 ng/ml TNF- α (74.98 ± 7.1 %) vs. 100 % Control, $p < 0.05$, $N = 9-14$ (Figure 3.4 A). The margin of decrease in NO-production by TNF- α was even more pronounced at all concentrations after 48 hours: 0.5 ng/ml TNF- α (54.28 ± 9.0 %), 5 ng/ml TNF- α (52.81 ± 6.2 %) and 20 ng/ml (42.44 ± 8.9 %) vs. 100 % Control, $p < 0.05$, $N = 7-13$ (Figure 3.4 B).

CMECs: DAF-2/DA concentration-response investigations with TNF- α treatment

TNF- α treatment significantly decreased mean DAF-2/DA fluorescence after 24 hours at 5 ng/ml (79.34 ± 3.7 %) and 20 ng/ml (79.28 ± 3.7 %) vs. 100 % Control, $p < 0.05$, $N = 10-14$. However, 0.5 ng/ml had no significant effect on NO production after 24 hours (Figure 3.4 C). After 48 hours, TNF α significantly decreased mean DAF-2/DA fluorescence at all concentrations: 0.5 ng/ml TNF- α (66.39 ± 5.2 %), 5 ng/ml TNF- α (56.67 ± 3.6) and 20 ng/ml TNF- α (58.91 ± 2.8 %) vs. 100 % Control, $p < 0.05$, $N = 12-15$ (Figure 3.4 D).

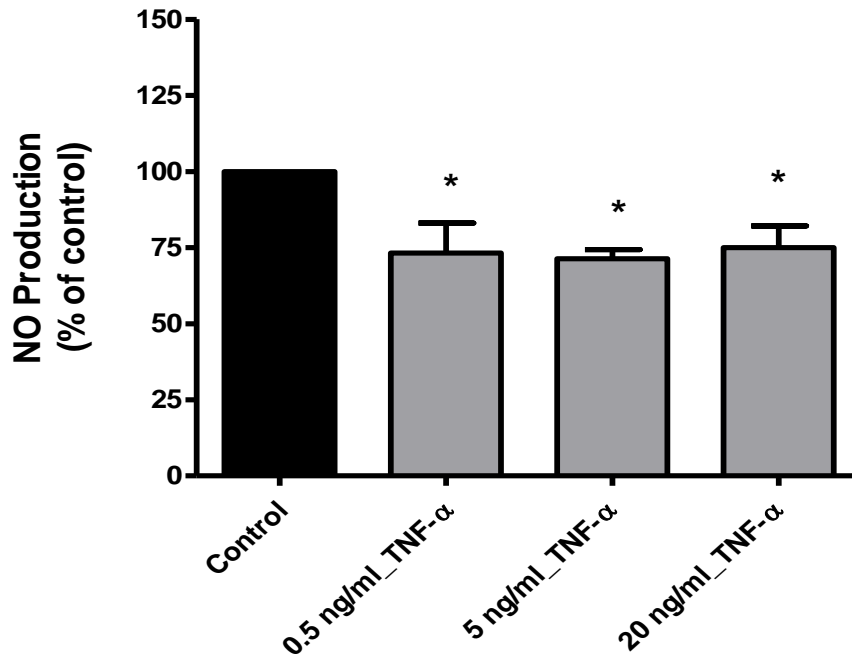


Figure 3.4 A: AECs: DAF-2/DA TNF-α concentration-response findings after 24 hours treatment. *p < 0.05 vs control; control adjusted to 100 %.

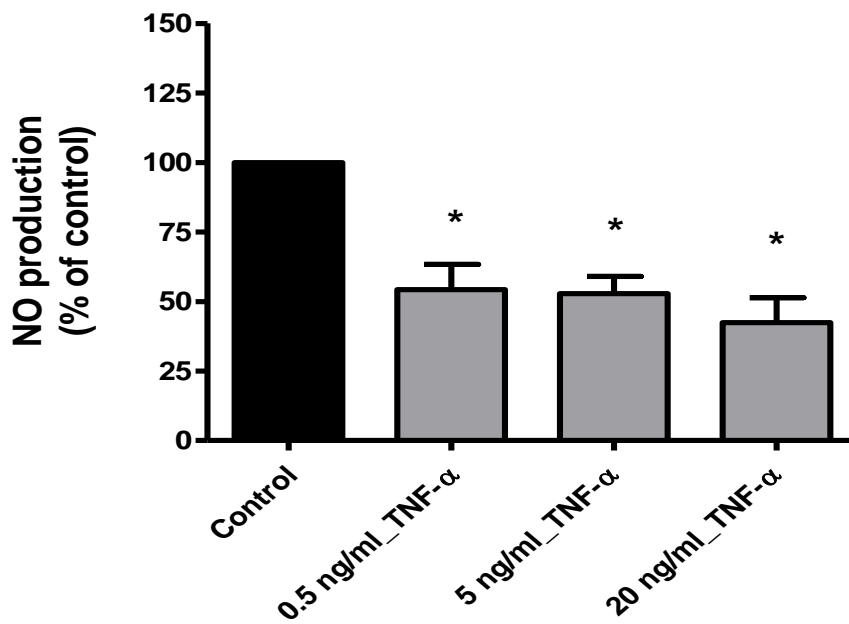


Figure 3.4 B: AECs: DAF-2/DA TNF-α concentration-response findings after 48 hours treatment. *p < 0.05 vs control; control adjusted to 100 %.

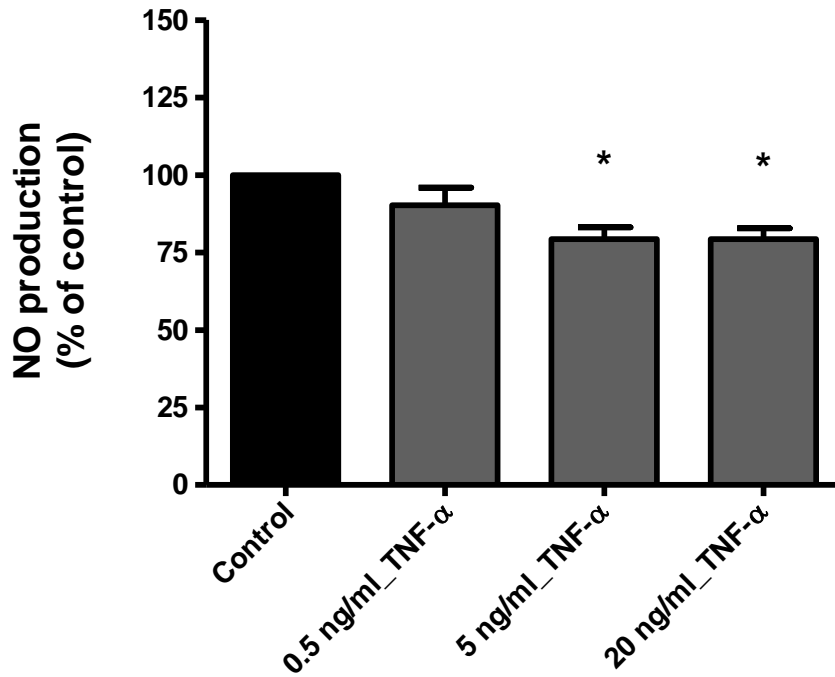


Figure 3.4 C: CMECs: DAF-2/DA TNF- α concentration-response findings after 24 hours treatment. *p < 0.05 vs control; control adjusted to 100 %.

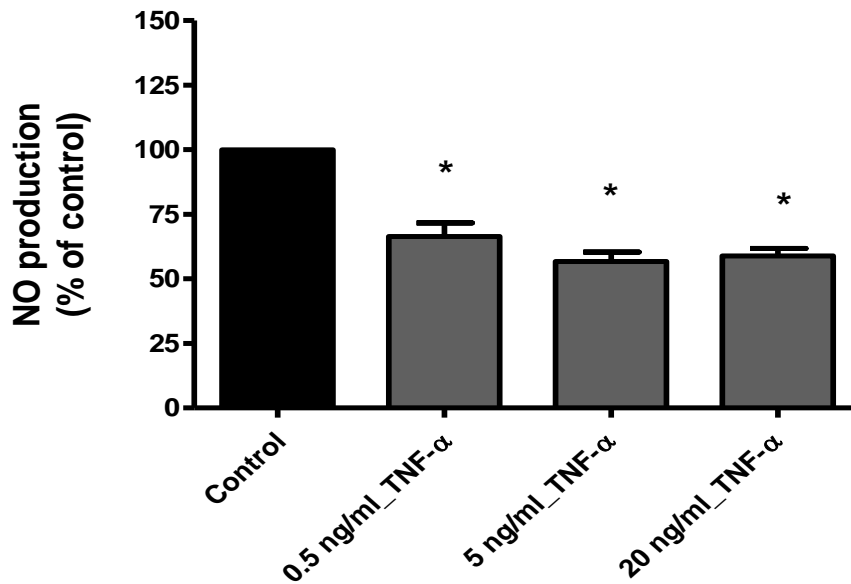


Figure 3.4 D: CMECs: DAF-2/DA TNF- α concentration-response findings after 48 hours treatment. *p < 0.05 vs. control; control adjusted to 100 %.

Direct comparisons between TNF- α treated AECs and CMECs: NO production

Next, the response in NO production to TNF- α treatment in the AECs and CMECs was directly compared. Following 24 hours, TNF- α treatment did not result in significant differences between AECs and CMECs at any of the TNF- α concentrations (Figure 3.5 A). However, after 48 hours, the mean DAF-2/DA fluorescence in AECs (20 ng/ml TNF- α) was significantly decreased when compared to CMECs at the same TNF- α concentration (AECs: 42.44 ± 8.9 % vs. CMECs: 58.91 ± 2.9 %, $p < 0.05$) (Figure 3.5 B).

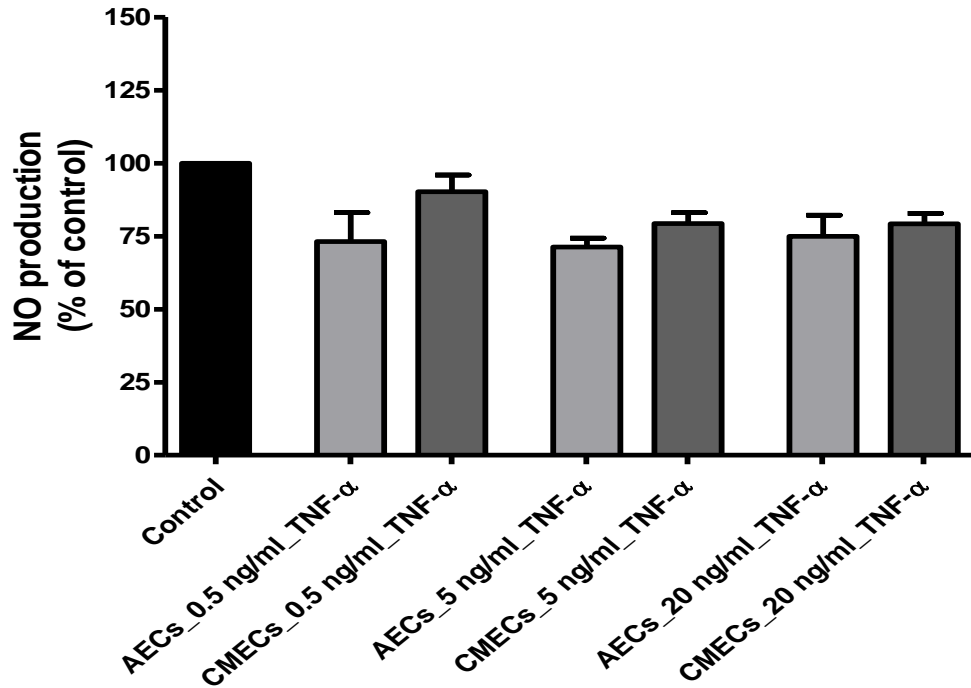


Figure 3.5 A: Direct comparison of % changes in DAF-2/DA fluorescence between AECs and CMECs treated with TNF-α for 24 hours.

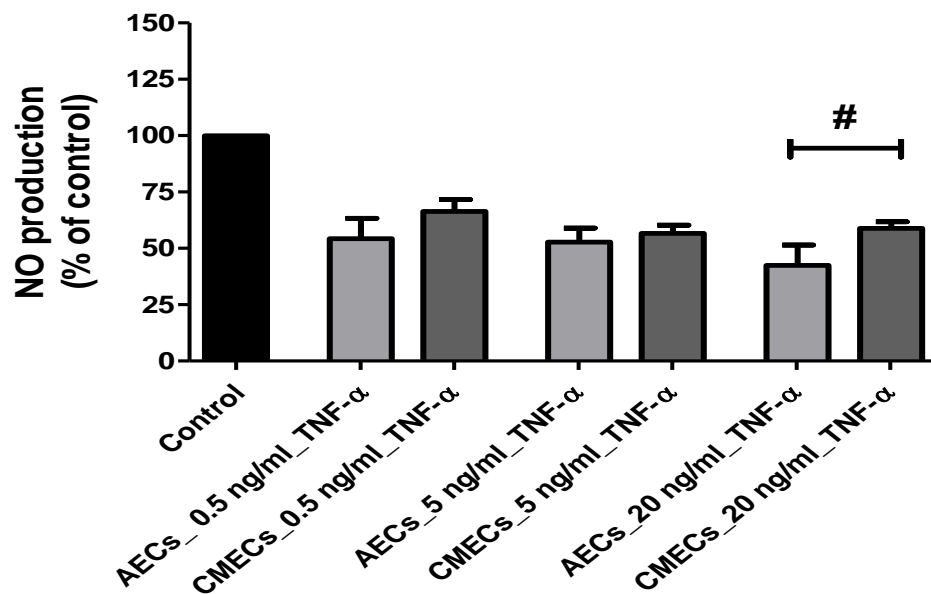


Figure 3.5 B: Direct comparison of % changes in DAF-2/DA fluorescence between AECs and CMECs treated with TNF-α for 48 hours. #p < 0.05: AECs vs. CMECs (TNF-α: 20 ng / ml).

3.1.3.1.2 ROS Measurements with DHR-123 and DCF

DHR-123 (ONOO⁻ production) concentration-response investigations with TNF- α treatment

AECs:

After 24 hours all concentrations of TNF- α significantly decreased mean DHR-123 fluorescence: 0.5 ng/ml (92.44 ± 2.1 %), 5 ng/ml (85.73 ± 1.4 %) and 20 ng/ml (85.41 ± 1.2 %) vs. 100 % Control, $p < 0.05$, $N = 7$ per group (Figure 3.6 A). Similar results were observed following the 48 hour treatment period: 0.5 ng/ml (94.57 ± 1.9 %), 5 ng/ml (91.20 ± 1.1 %) and 20 ng/ml (89.41 ± 1.5 %) vs. 100 % Control, $p < 0.05$, $N = 8$ per group (Figure 3.6 B).

CMECs:

Following 24 hours treatment, TNF- α significantly decreased mean DHR-123 fluorescence at all concentrations: 0.5 ng/ml (79.42 ± 1.5 %), 5 ng/ml (71.26 ± 1.4 %) and 20 ng/ml (65.95 ± 1.3 %) vs. 100 % Control, $p < 0.05$, $N = 7$ per group (Figure 3.6 C). Treatment with TNF- α for 48 hours also led to significant reductions in mean DHR-123 fluorescence at all concentrations: 0.5 ng/ml (86.14 ± 1.7 %), 5 ng/ml (81.46 ± 1.0 %) and 20 ng/ml (81.38 ± 2.4 %) vs. 100 % Control, $p < 0.05$, $N = 5$ per group (Figure 3.6 D).

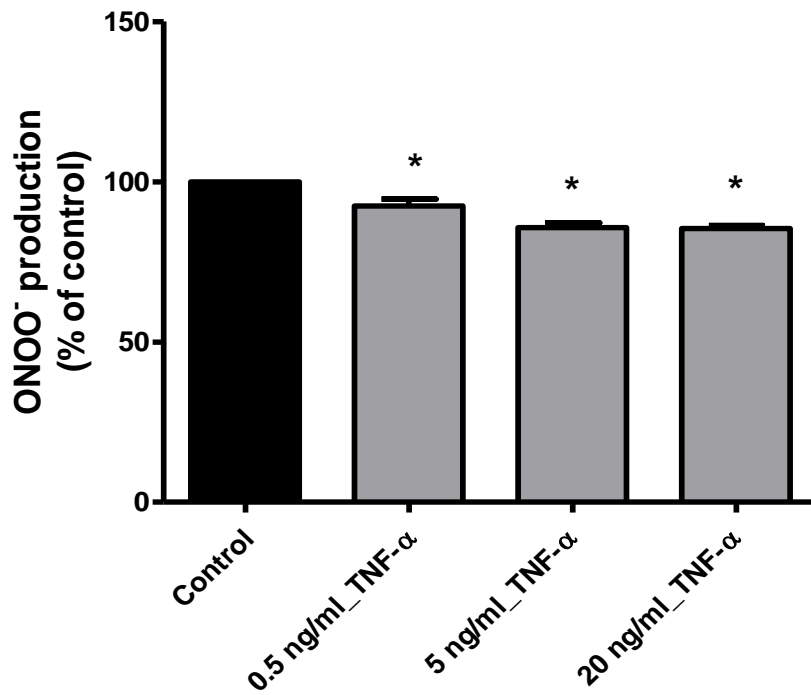


Figure 3.6 A: AECs: DHR-123 TNF-α concentration-response findings after 24 hours treatment. *p < 0.05 vs. control; control adjusted to 100 %.

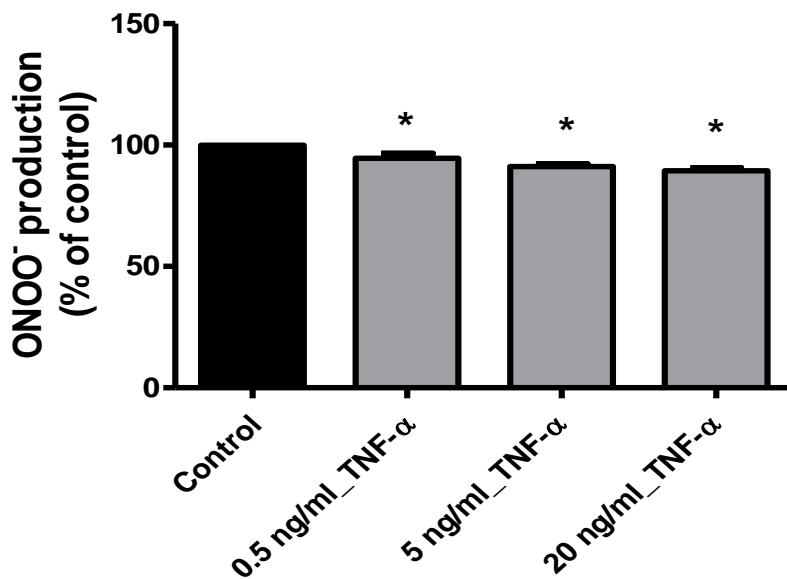


Figure 3.6 B: AECs: DHR-123 TNF-α concentration-response findings after 48 hours treatment. *p < 0.05 vs. control; control adjusted to 100 %.

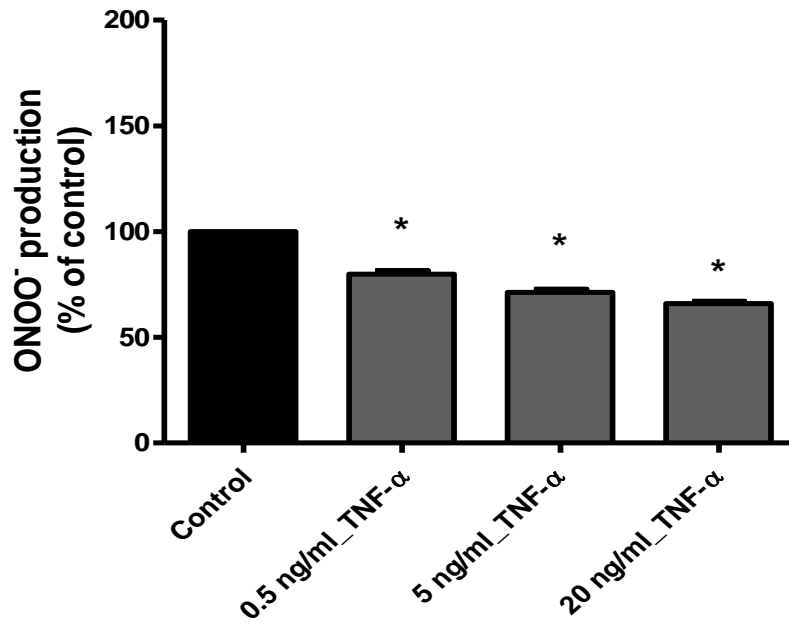


Figure 3.6 C: CMECs: DHR-123 TNF- α concentration-response findings after 24 hours treatment. *p < 0.05 vs. control; control adjusted to 100 %.

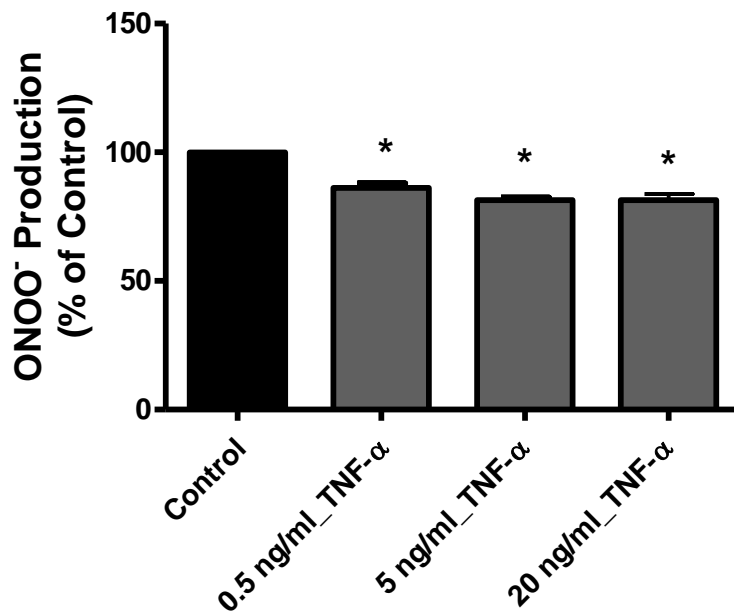


Figure 3.6 D: CMECs: DHR-123 TNF- α concentration-response findings after 48 hours treatment. *p < 0.05 vs. control; control adjusted to 100 %.

Direct comparisons between TNF- α treated AECs and CMECs: ONOO⁻ production

The mean DHR-123 fluorescence differed significantly between AECs and CMECs at both 24 and 48 hours TNF- α treatment periods. Overall, DHR-123 fluorescence intensity was consistently lower in CMECs when compared to AECs.

24 hours (Figure 3.7 A):

- 0.5 ng/ml TNF- α (AECs: 92.44 ± 2.1 % vs. CMECs: 79.92 ± 1.5 %, $p < 0.05$)
- 5 ng/ml TNF- α (AECs: 85.73 ± 1.4 % vs. CMECs: 71.26 ± 1.4 %, $p < 0.05$)
- 20 ng/ml TNF- α (AECs: 85.41 ± 1.2 % vs. CMECs: 65.95 ± 1.3 %, $p < 0.05$)

48 hours (Figure 3.7 B):

- 0.5 ng/ml TNF- α (AECs: 94.57 ± 1.9 % vs. CMECs: 86.14 ± 1.7 , $p < 0.05$)
- 5 ng/ml TNF- α (AECs: 91.20 ± 1.1 % vs. CMECs: 81.46 ± 1.0 %, $p < 0.05$)
- 20 ng/ml TNF- α (AECs: 89.41 ± 1.1 % vs. CMECs: 81.38 ± 2.4 %, $p < 0.05$)

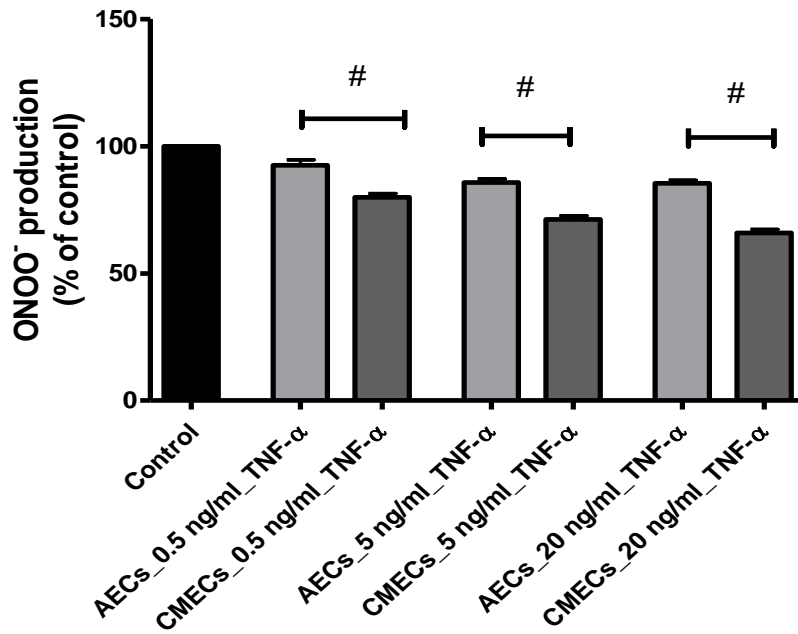


Figure 3.7 A: Direct comparison of % changes in DHR-123 fluorescence between AECs and CMECs treated with TNF-α for 24 hours. #p < 0.05: AECs vs. CMECs.

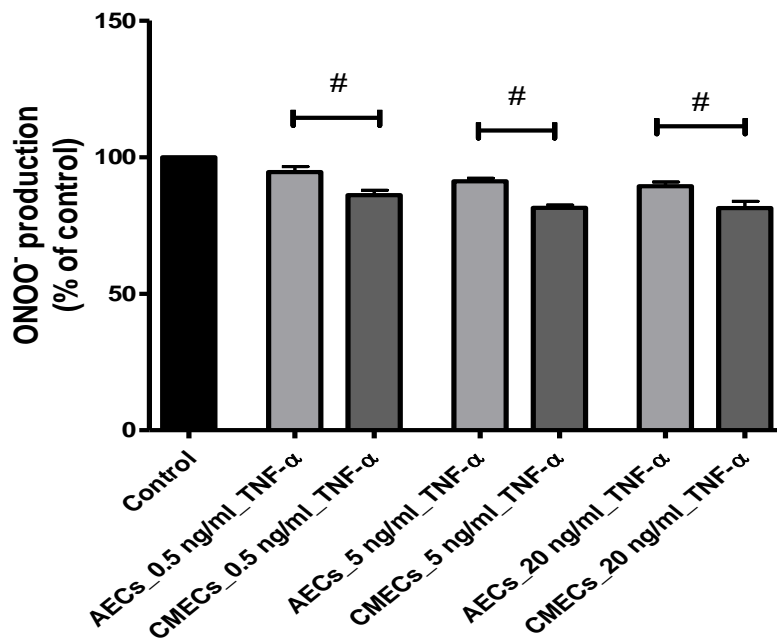


Figure 3.7 B: Direct comparison of % changes in DHR-123 fluorescence between AECs and CMECs treated with TNF-α for 48 hours. #p < 0.05: AECs vs. CMECs.

DCF (H₂O₂ production) concentration-response investigations with TNF- α treatment

AECs:

TNF- α , at all concentrations, significantly increased mean DCF fluorescence after 24 hours: 0.5 ng/ml (275.9 ± 14.98 %), 5 ng/ml (291.1 ± 21.19 %) and 20 ng/ml (279 ± 14.68) vs. 100 % Control, $p < 0.05$, N = 6 per group (Figure 3.8 A). However after 48 hours, 5 and 20 ng/ml TNF- α significantly decreased mean DCF fluorescence: 5 ng/ml (81.48 ± 7.8 %) and 20 ng/ml (77.20 ± 7.0 %) vs. 100 % Control, $p < 0.05$, N = 6 per group (Figure 3.8 B).

CMECs:

Treatment with 5 and 20 ng/ml TNF- α for 24 hours significantly increased mean DCF fluorescence: 5 ng/ml (113.9 ± 3.6 %) and 20 ng/ml (141.4 ± 4.5 %) vs. 100 % Control, $p < 0.05$, N = 6 per group (Figure 3.8 C). At 48 hours treatment, TNF- α exerted no significant effects on DCF fluorescence at any of the concentrations (Figure 3.8 D).

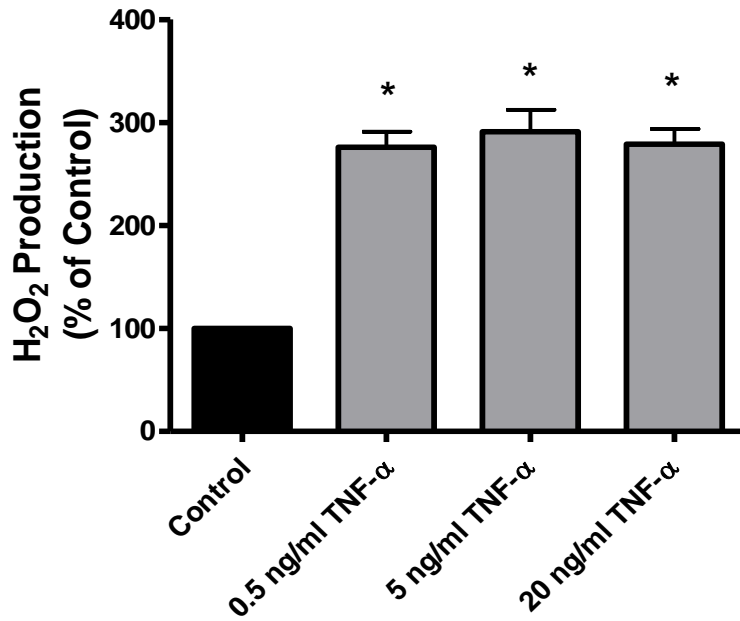


Figure 3.8 A: AECs: DCF TNF- α concentration-response findings after 24 hours treatment. *p < 0.05 vs. control; control adjusted to 100 %.

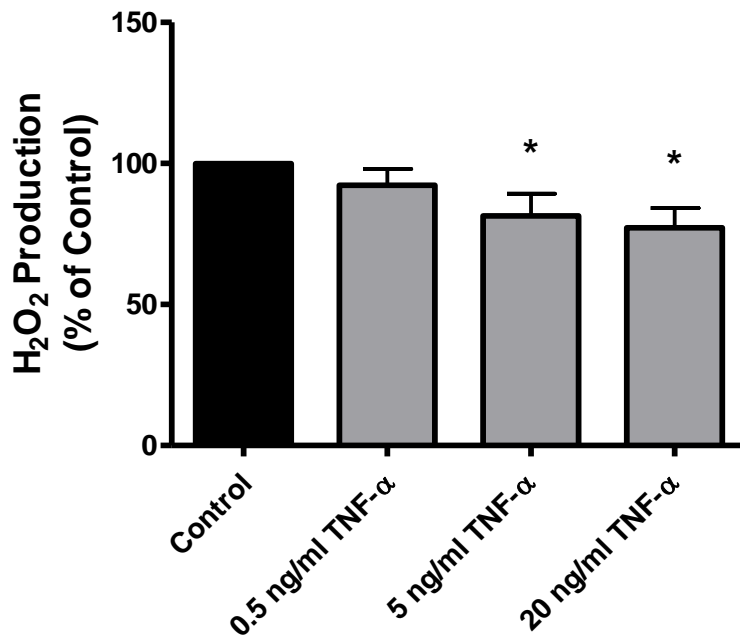


Figure 3.8 B: AECs: DCF TNF- α concentration-response findings after 48 hours treatment. *p < 0.05 vs. control; control adjusted to 100 %.

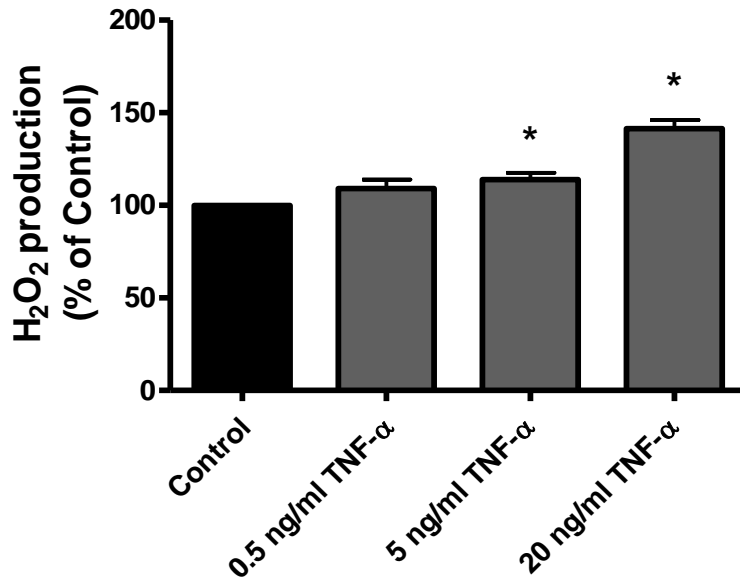


Figure 3.8 C: CMECs: DCF TNF-α concentration-response findings after 24 hours treatment. *p < 0.05 vs. control; control adjusted to 100 %.

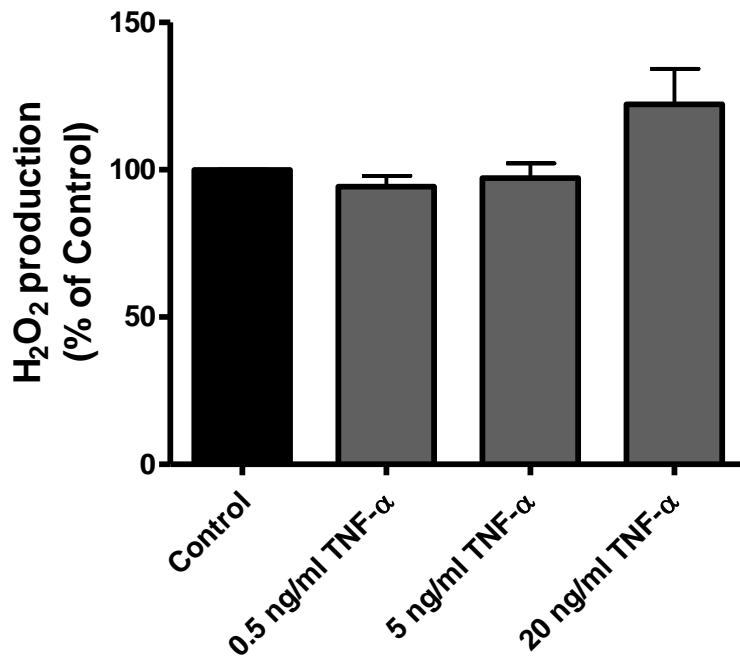


Figure 3.8 D: CMECs: DCF TNF-α concentration-response findings after 48 hours treatment.

Direct comparisons between TNF- α treated AECs and CMECs: H₂O₂ production

Mean DCF fluorescence intensity differed significantly between AECs and CMECs following 24 hour TNF- α treatments, with AECs generally responding to treatment with increased fluorescence measurements (Figure 3.9 A):

- 0.5 ng/ml (AECs: 275.9 ± 14.98 % vs. CMECs: 109 ± 4.9 %, $p < 0.05$)
- 5 ng/ml (AECs: 291 ± 21.19 % vs. CMECs: 113.9 ± 3.6 %, $p < 0.05$)
- 20 ng/ml (AECs: 279 ± 14.68 % vs. CMECs: 141 ± 4.5 %, $p < 0.05$)

Following 48 hours treatment, there were no significant differences in the DCF fluorescence readings between AECs and CMECs at 0.5 and 5 ng/ml TNF- α . However, at 20 ng/ml TNF- α , AECs displayed lower fluorescence compared to their concentration-matched CMEC counterparts (Figure 3.9 B):

- 0.5 ng/ml (AECs: 92.26 ± 5.7 % vs. CMECs: 94.33 ± 3.6 %, $p > 0.05$)
- 5 ng/ml (AECs: 81.48 ± 7.8 % vs. CMECs: 97.14 ± 5.0 %, $p > 0.05$)
- 20 ng/ml (AECs: 77.20 ± 7.0 % vs. CMECs: 122.2 ± 12.06 %, $p < 0.05$)

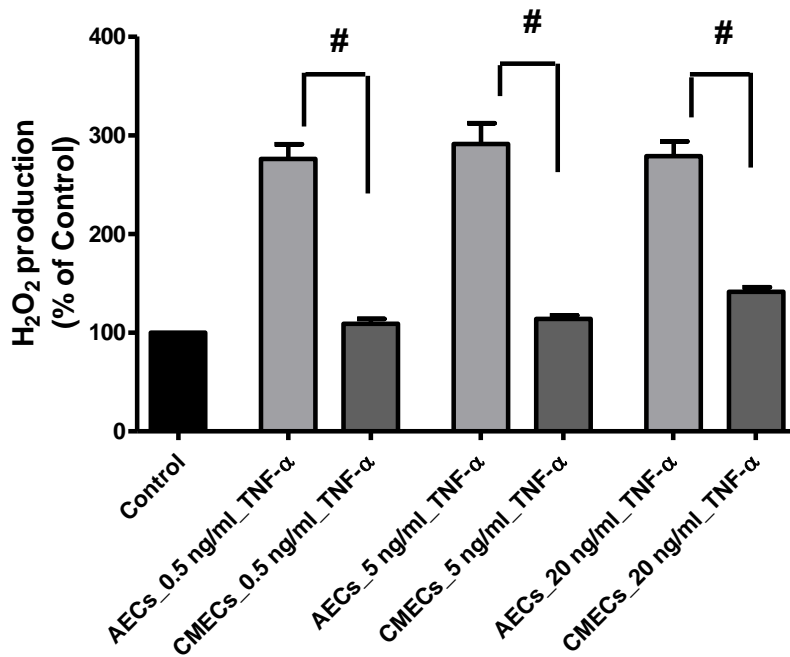


Figure 3.9 A: Direct comparison of % changes in DCF fluorescence between AECs and CMECs treated with TNF- α for 24 hours. #p < 0.05: AECs vs. CMECs.

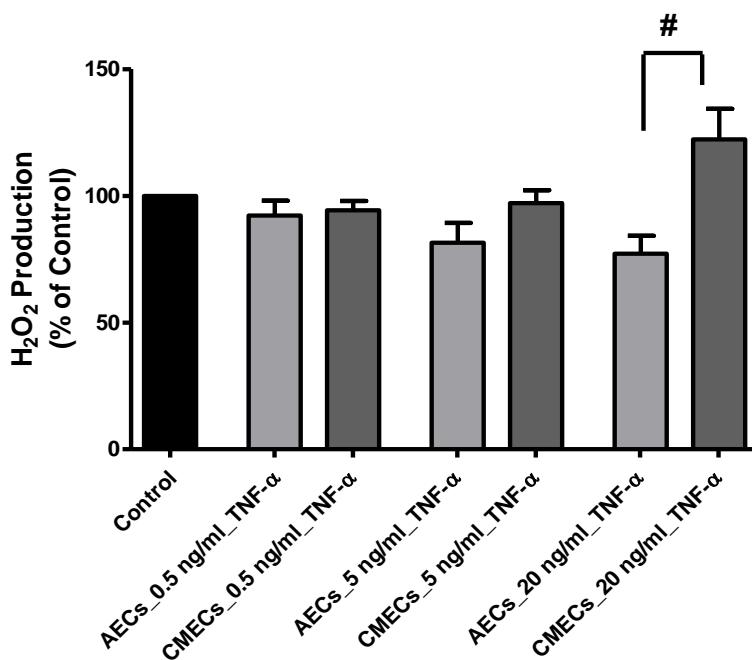


Figure 3.9 B: Direct comparison of % changes in DCF fluorescence between AECs and CMECs treated with TNF- α for 48 hours. #p < 0.05: AECs vs. CMECs.

3.1.3.1.3 Necrosis measurements with PI

Percentage cells that stained positively for PI were expressed as % of control, and control was adjusted to 100 %.

AECs:

Treatment with 5 and 20 ng/ml TNF- α for 24 hours significantly increased necrosis as measured by % cellular PI uptake: 5 ng/ml (156 ± 22.8 %) and 20 ng/ml (331.4 ± 91.1 %) vs. 100 % Control, $p < 0.05$, $N = 5-7$ per group (Figure 3.10 A). After 48 hours, TNF- α had no significant effect on necrosis in AECs at any of the concentrations (Figure 3.10 B).

CMECs:

TNF- α significantly increased necrosis as measured by % cellular PI uptake after 24 hours: 0.5 ng/ml (176.5 ± 34.7), 5 ng/ml (177.8 ± 15.6 %), 20 ng/ml (230.3 ± 26.9) vs. 100 % Control, $p < 0.05$, $N = 4-6$ per group (Figure 3.10 C). After 48 hours, 5 ng/ml TNF- α significantly decreased necrosis (70.6 ± 2.1 %) vs. 100 % Control (Figure 3.10 D). However, treatment with 20 ng/ml TNF- α significantly increased necrosis: (396.4 ± 61.6 % vs. 100 % Control, $p < 0.05$, $N = 4-6$ (Figure 3.10 D).

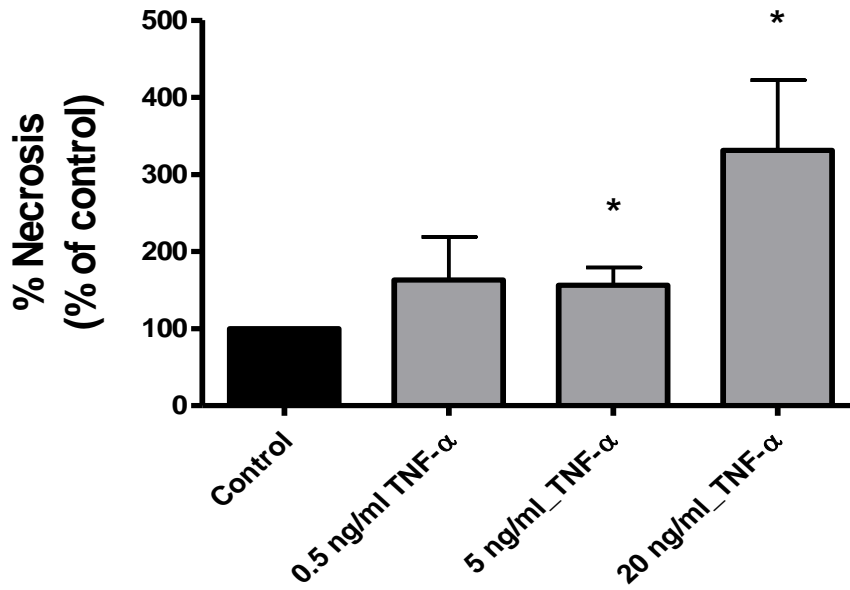


Figure 3.10 A: AECs: TNF- α concentration-response findings after 24 hours treatment showing % propidium iodide-stained cells. *p < 0.05 vs. control; control adjusted to 100 %.

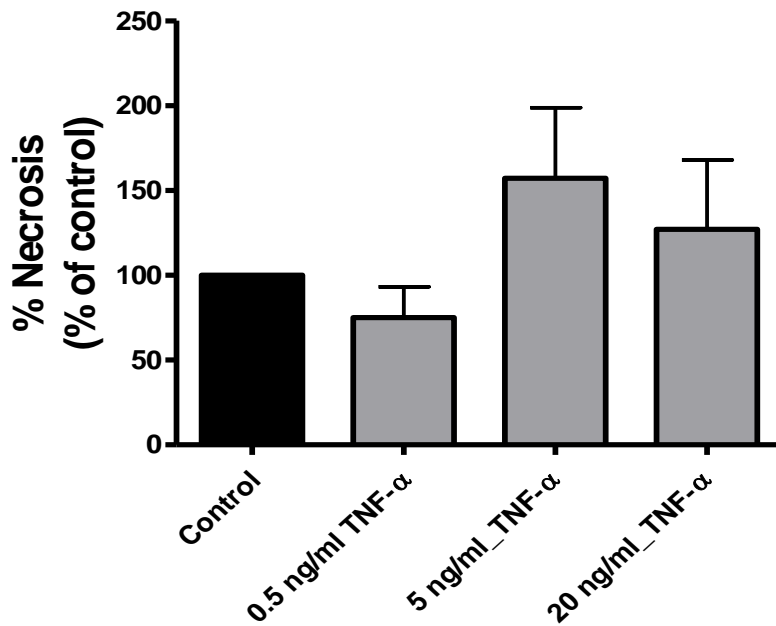


Figure 3.10 B: AECs: TNF- α concentration-response findings after 48 hours treatment showing % propidium iodide-stained cells.

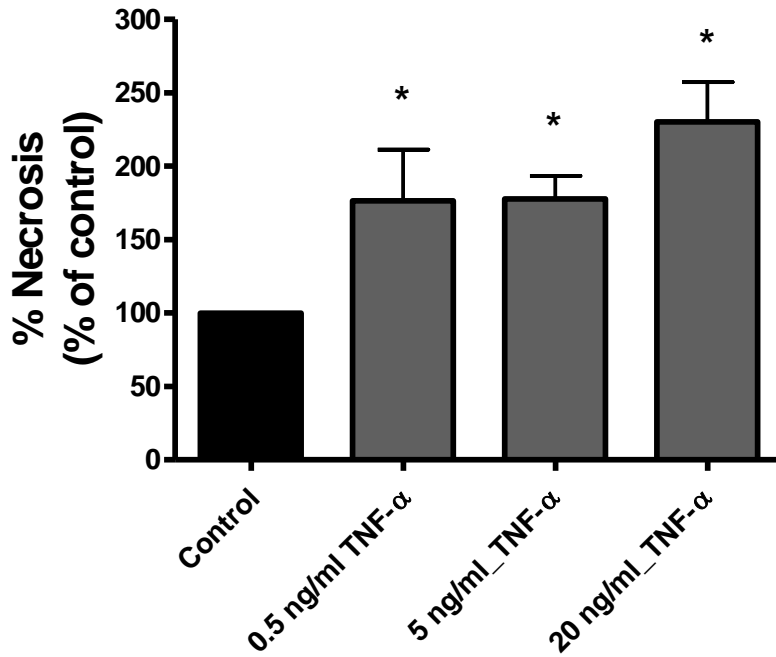


Figure 3.10 C: CMECs: TNF-α concentration-response findings after 24 hours treatment showing % propidium iodide-stained cells. *p < 0.05 vs. control; control adjusted to 100 %.

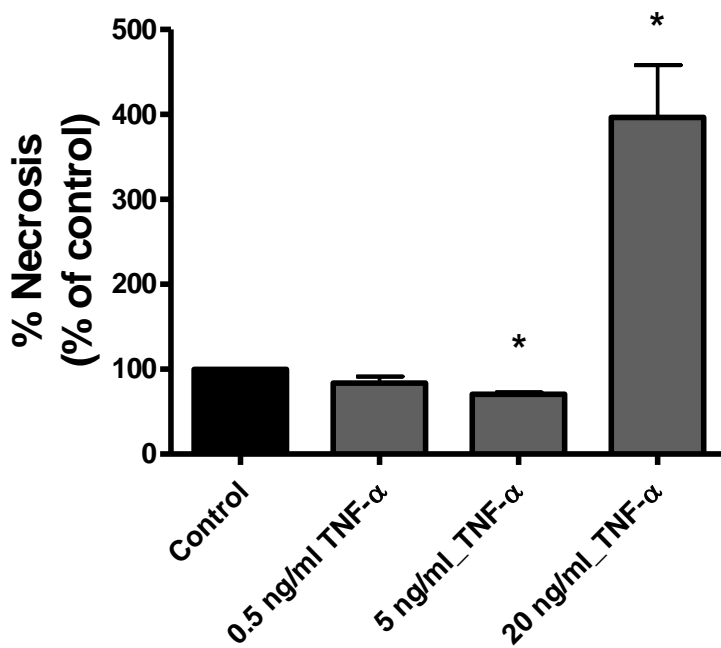


Figure 3.10 D: CMECs: TNF-α concentration-response findings after 48 hours treatment showing % propidium iodide-stained cells. *p < 0.05 vs. control; control adjusted to 100 %.

Direct comparisons between TNF- α treated AECs and CMECs: Necrosis

After 24 hours, TNF- α treated AECs and CMECs did not display any significant differences with regards to % propidium iodide-staining cells when compared directly with each other at identical TNF- α concentrations (Figure 3.11 A).

After 48 hours TNF- α treatment, no significant differences were observed between AECs and CMECs treated with 0.5 and 5 ng/ml TNF- α ; however, 20 ng/ml TNF- α treated CMECs showed a higher degree of % propidium iodide-staining cells compared to their AECs counterparts: AECs: 127.1 ± 40.8 % vs. CMECs: 396.4 ± 61.1 %, $p < 0.05$ (Figure 3.11 B):

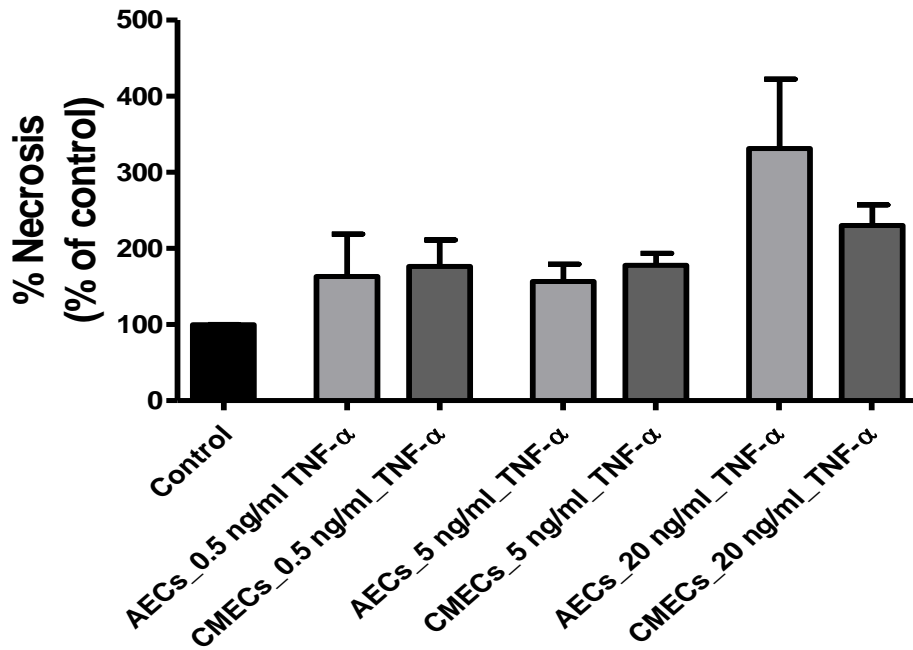


Figure 3.11 A: Direct comparison of changes in the % propidium iodide-stained cells between AECs and CMECs treated with TNF-α for 24 hours.

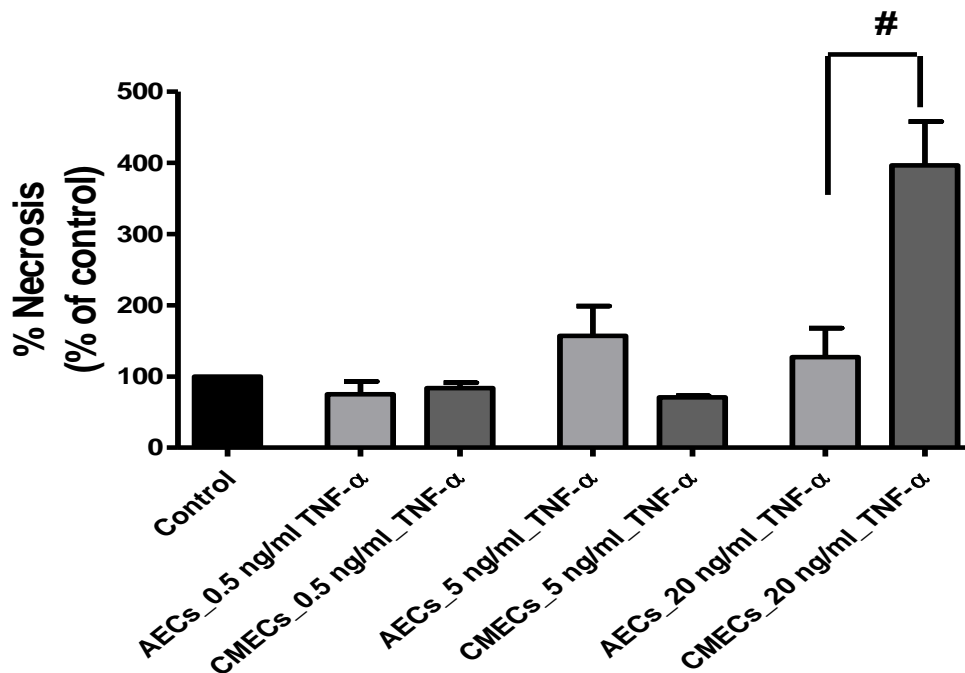


Figure 3.11 B: Direct comparison of changes in the % propidium iodide-stained cells between AECs and CMECs treated with TNF-α for 48 hours. #p < 0.05: AECs vs. CMECs.

Based on the concentration-response data, it was decided to continue with a TNF- α treatment regime of 20 ng/ml TNF- α for a period of 24 hours as the model of endothelial cell injury for all further investigations.

3.1.4 Endothelial injury induction: Western blot analyses of signalling proteins

All western blot data are expressed as a ratio of AEC untreated control, with AEC untreated control adjusted to 1. The housekeeping protein, β -tubulin, was used to control for equal protein loading.

3.1.4.1 Total and phosphorylated eNOS (Ser 1177)

There were no significant differences in the **total eNOS expression** between AECs and CMECs with or without TNF- α treatment (Figure 3.12 A).

There were no significant differences in **phosphorylated eNOS (Ser 1177) levels** between AECs and CMECs with or without TNF- α (Figure 3.12 B).

However, when **phosphorylated eNOS (Ser 1177) was expressed as a ratio of total eNOS expression**, the phospho / total ratios were significantly decreased in control, untreated CMECs and TNF- α -treated CMECs vs. their respective AEC counterparts (Figure 3.12 C):

- AEC-Control (1.0) vs. CMEC-Control (0.72 ± 0.05), $p < 0.05$, $N = 3$.
- AEC-TNF- α (0.98 ± 0.03) vs. CMEC-TNF- α (0.70 ± 0.12), $p < 0.05$, $N = 4$.

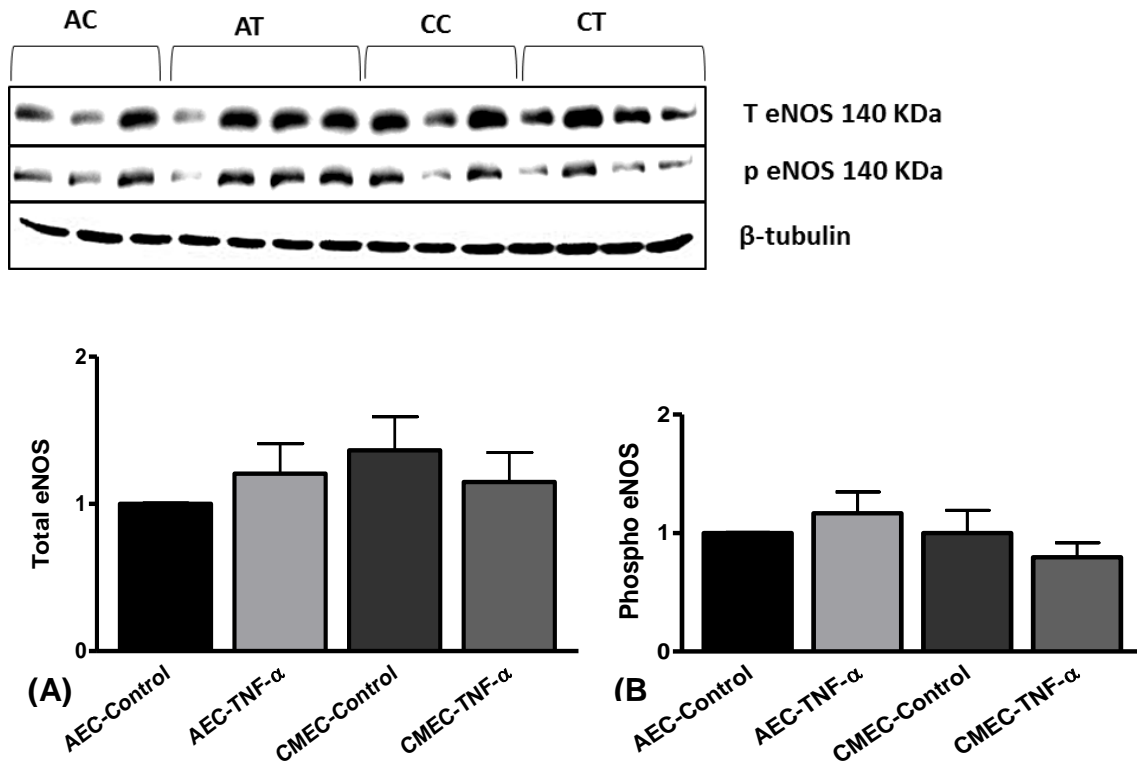


Figure 3.12 A & B: (A) Total eNOS expression and (B) phosphorylated eNOS (Ser 1177) in AECs and CMECs with or without TNF- α treatment (20 ng/ml; 24 hours). AC, AEC control; AT, AEC+TNF- α ; CC, CMEC control; CT, CMEC+TNF- α .

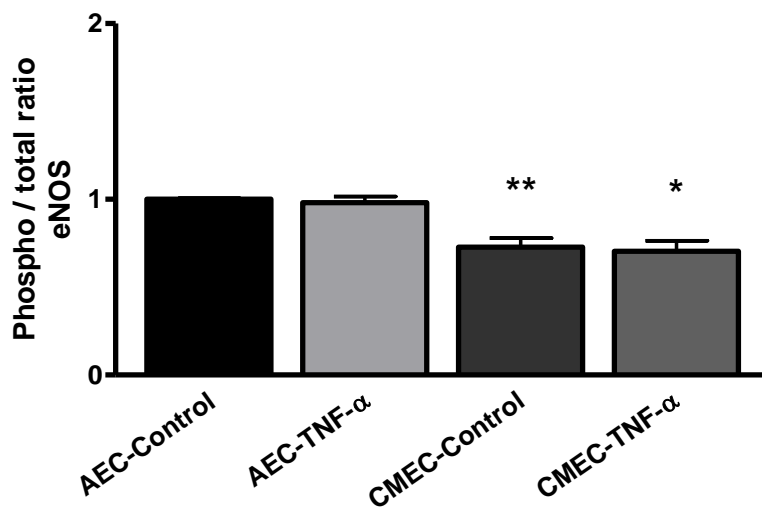


Figure 3.12 C: Phospho / total eNOS ratios in AECs and CMECs with or without TNF- α treatment (20 ng/ml; 24 hours). ** $p < 0.05$ vs. AEC-Control, * $p < 0.05$ vs. AEC-TNF- α .

3.1.4.2 Total and phosphorylated PKB/Akt (Ser 473)

Total PKB/Akt expression was significantly decreased in (i) TNF- α -treated AECs vs. control, untreated AECs, (ii) control, untreated CMECs vs. control, untreated AECs, and (iii) in TNF- α -treated AECs vs. TNF- α -treated CMECs (Figure 3.13 A):

- AEC-TNF- α (0.71 ± 0.01) vs. AEC-Control (1.0), $p < 0.05$, N = 3-4 per group.
- AEC-Control (1.0) vs. CMEC-Control (0.87 ± 0.04), $p < 0.05$, N = 3.
- AEC-TNF- α (0.71 ± 0.01) vs. CMEC-TNF- α (0.88 ± 0.03), $p < 0.05$, N = 4.

Phosphorylated PKB/Akt (Ser 473) was significantly increased in (i) control, untreated CMECs vs. control, untreated AECs, and (ii) in TNF- α -treated CMECs vs. TNF- α -treated AECs (Figure 3.13 B):

- AEC-Control (1.0) vs. CMEC-Control (1.41 ± 0.1), $p < 0.05$, N = 3.
- AEC-TNF- α (1.01 ± 0.11) vs. CMEC-TNF- α (1.57 ± 0.09), $p < 0.05$, N = 4.

PKB/Akt phospho / total ratios were significantly increased in control, untreated CMECs (1.61 ± 0.06) vs. control, untreated AECs (1.0), $p < 0.05$, N = 3 (Figure 3.13 C).

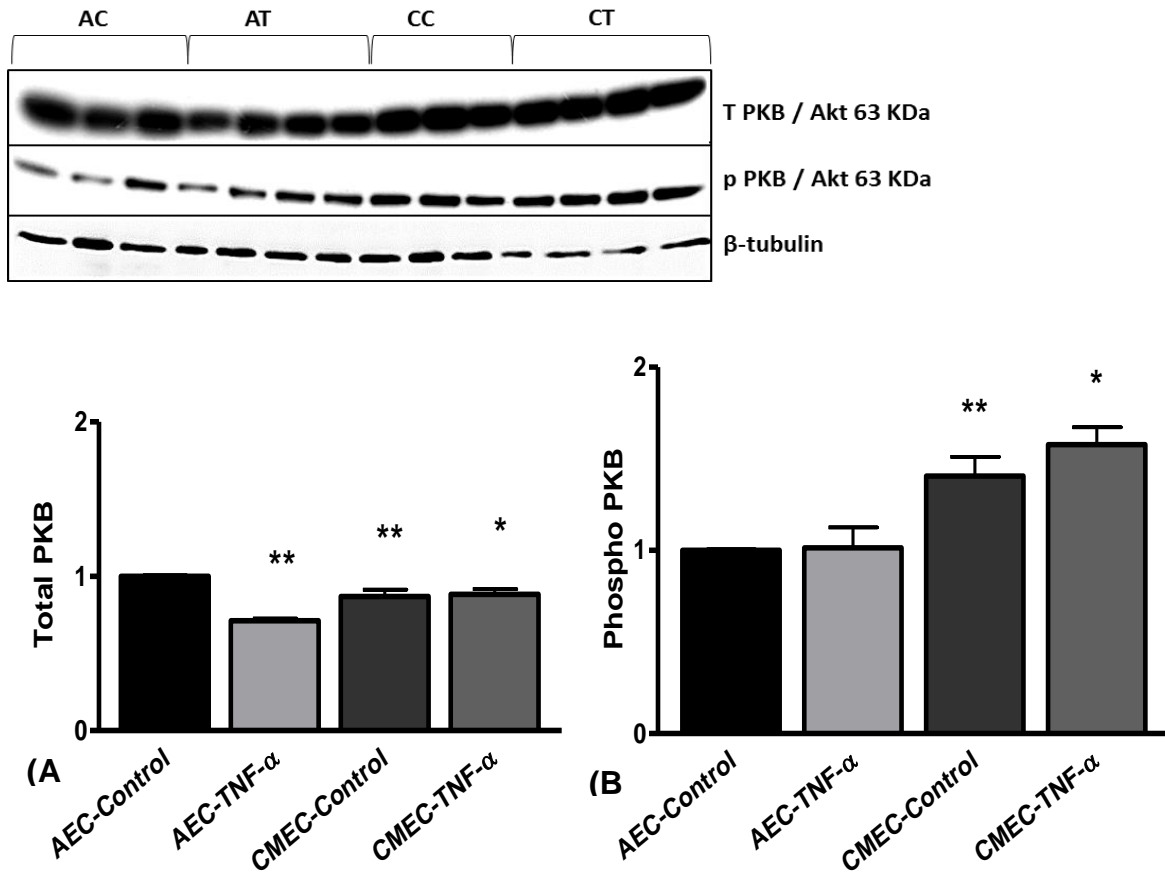


Figure 3.13 A & B: (A) Total PKB/Akt expression and (B) Phosphorylated PKB/Akt (Ser 473) in AECs and CMECs with or without TNF- α (20 ng/ml; 24 hours). **p < 0.05 vs. AEC-Control, *p < 0.05 vs. AEC-TNF- α . AC, AEC control; AT, AEC+TNF- α ; CC, CMEC control; CT, CMEC+TNF- α .

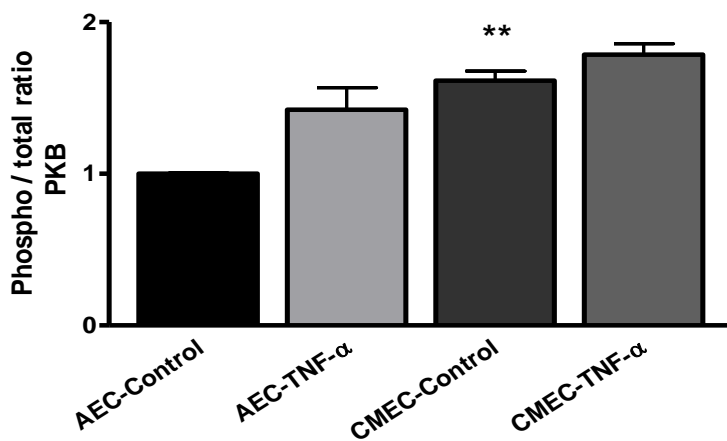


Figure 3.13 C: Phospho / total PKB/Akt ratios in AECs and CMECs with or without TNF- α (20 ng/ml; 24 hours). **p < 0.05 vs. AEC-Control.

3.1.4.3 Heat shock protein 90 (HSP 90) expression

HSP 90 expression was significantly decreased in TNF- α -treated AECs (0.37 ± 0.10) and control, untreated CMECs (0.28 ± 0.01) compared to control, untreated AECs (1.0), $p < 0.05$, $N = 3-4$ per group (Figure 3.14).

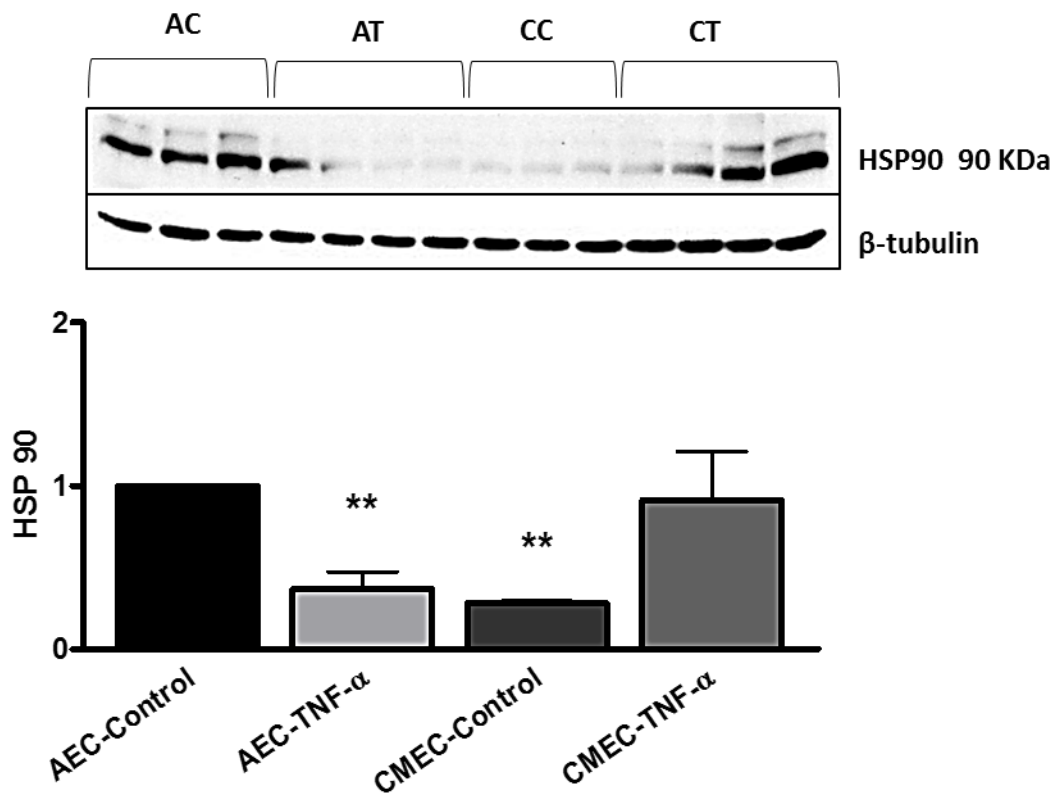


Figure 3.14: Heat shock 90 expression in AECs and CMECs with or without TNF- α (20 ng/ml; 24 hours). ** $p < 0.05$ vs. AEC-Control. AC, AEC control; AT, AEC+TNF- α ; CC, CMEC control; CT, CMEC+TNF- α .

3.1.4.4 IKB alpha expression

IKB alpha expression was significantly increased in control, untreated CMECs (1.23 ± 0.07) vs. control, untreated AECs (1.0), $p < 0.05$, $N = 3$, and significantly decreased in TNF- α -treated CMECs (0.78 ± 0.02) vs. control, untreated CMECs (1.23 ± 0.07), $p < 0.05$, $N = 3-4$ per group (Figure 3.15).

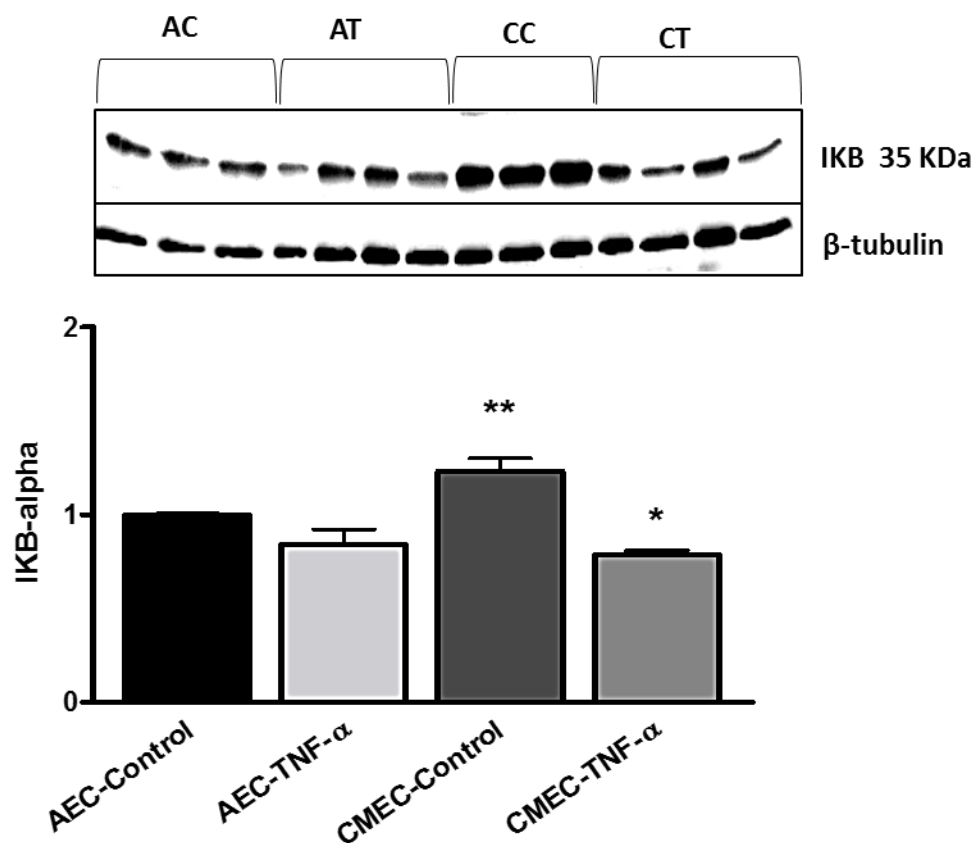


Figure 3.15: IKB-alpha expression in AECs and CMECs with or without TNF- α (20 ng/ml; 24 hours). *** $p < 0.05$ vs. AEC-Control, * $p < 0.05$ vs. CMEC-Control. AC, AEC control; AT, AEC+TNF- α ; CC, CMEC control; CT, CMEC+TNF- α .

3.1.4.5 Nitrotyrosine expression

Nitrotyrosine expression was significantly increased in control, untreated CMECs (1.30 ± 0.02) vs. control, untreated AECs (1.0), $p < 0.05$, $N = 3$ (Figure 3.16).

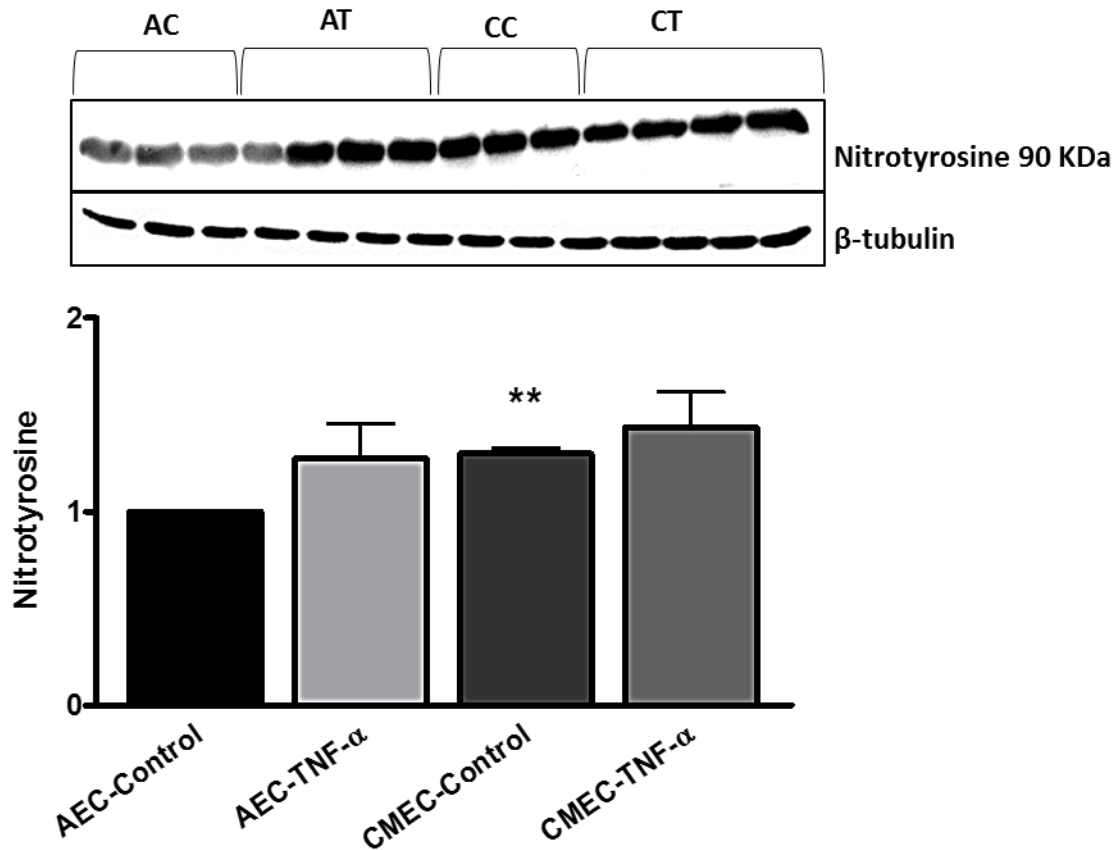


Figure 3.16: Nitrotyrosine expression in AECs and CMECs with or without TNF- α (20 ng/ml; 24 hours). ** $p < 0.05$ vs. AEC-Control. AC, AEC control; AT, AEC+TNF- α ; CC, CMEC control; CT, CMEC+TNF- α .

3.1.5 Oleonic acid (OA) studies

3.1.5.1 1 hour treatment studies

NO measurements (DAF-2/DA fluorescence)

The ability of OA to increase NO production was investigated in AECs and CMECs at concentrations of 10 and 40 μM for an incubation period of 1 hour. DMSO was included as vehicle controls at volumes corresponding to their respective OA concentrations.

AECs:

Treatment with both 10 and 40 μM OA for 1 hour significantly increased mean DAF-2/DA fluorescence: 10 μM OA ($132 \pm 14.4 \%$) and 40 μM ($154.2 \pm 12.1 \%$) versus 100 % Control, $p < 0.05$, $N = 9-12$ per group (Figure 3.17 A).

CMECs:

Mean DAF-2/DA fluorescence was significantly increased when CMECs were treated with 10 and 40 μM OA for 1 hour: 10 μM OA ($150.4 \pm 1.6 \%$) and 40 μM ($163.4 \pm 5.2 \%$) vs. 100 % Control, $p < 0.05$, $N = 4-7$ per group (Figure 3.17 B).

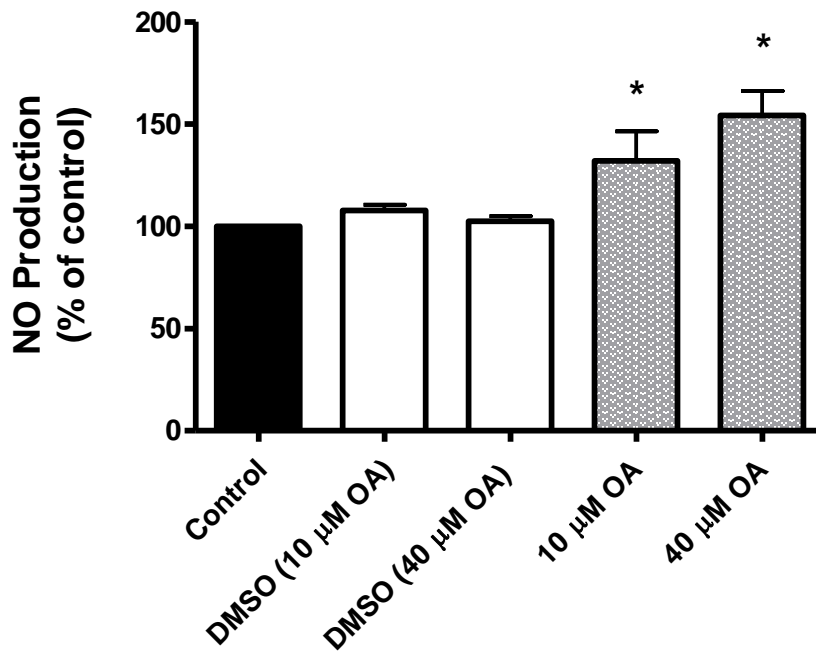


Figure 3.17 A: AECs: DAF-2/DA fluorescence data with 10 and 40 μM OA treatment for 1 hour. *p < 0.05 vs. Control; control adjusted to 100 %. (0.06 % DMSO for 10 μM OA and 0.24 % DMSO for 40 μM OA treatments).

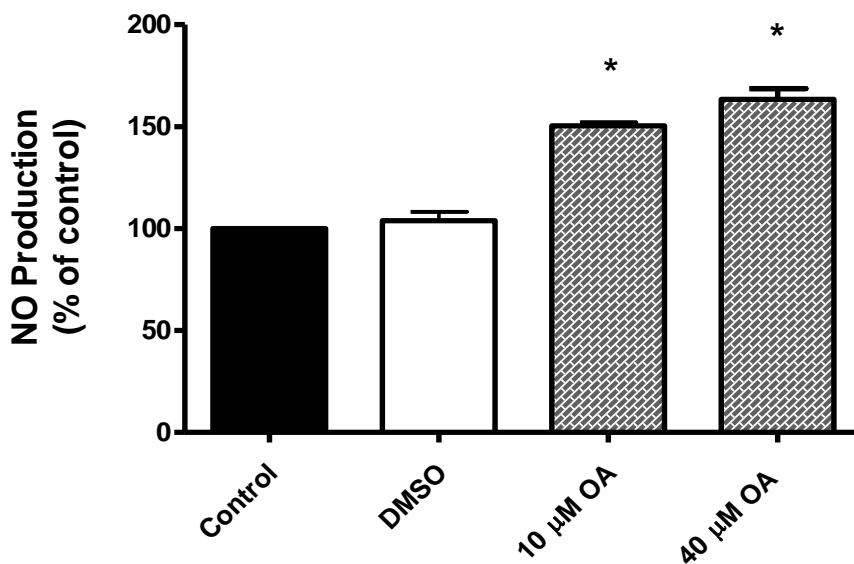


Figure 3.17 B: CMECs: DAF-2/DA fluorescence data with 10 and 40 μM OA treatment for 1 hour. *p < 0.05 vs. Control; control adjusted to 100 %. (0.06 % DMSO for 10 μM OA and 0.24 % DMSO for 40 μM OA treatments).

At this point it was decided to continue with OA treatment at a concentration of 40 μ M for all further investigations.

DCF (H₂O₂ production) fluorescence measurements with 40 μ M OA treatment for 1 hour

AECs:

Treatment with 40 μ M OA significantly decreased mean DCF fluorescence after 1 hour: 75.9 ± 2.7 % vs. 100 % Control, $p < 0.05$, $N = 5$. There were no vehicle effects observed (Figure 3.18 A).

CMECs:

After 1 hour, 40 μ M OA treatment significantly increased DCF fluorescence: 119.3 ± 6.5 % vs. 100 % Control, $p < 0.05$, $N = 6$. However, this observation was likely due to a DMSO vehicle effect: DMSO: 120 ± 10.8 % vs. 100 % Control, $p < 0.05$, $N = 3$ (Figure 3.18 B).

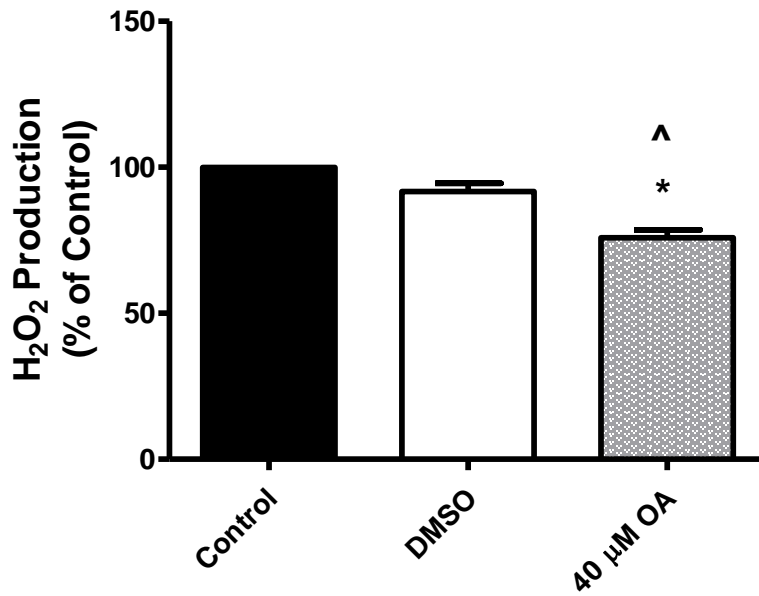


Figure 3.18 A: AECs: DCF fluorescence data with 40 μM OA treatment for 1 hour. *p < 0.05 vs. Control; control adjusted to 100 %, ^p < 0.05: vs. DMSO vehicle (0.24 % DMSO).

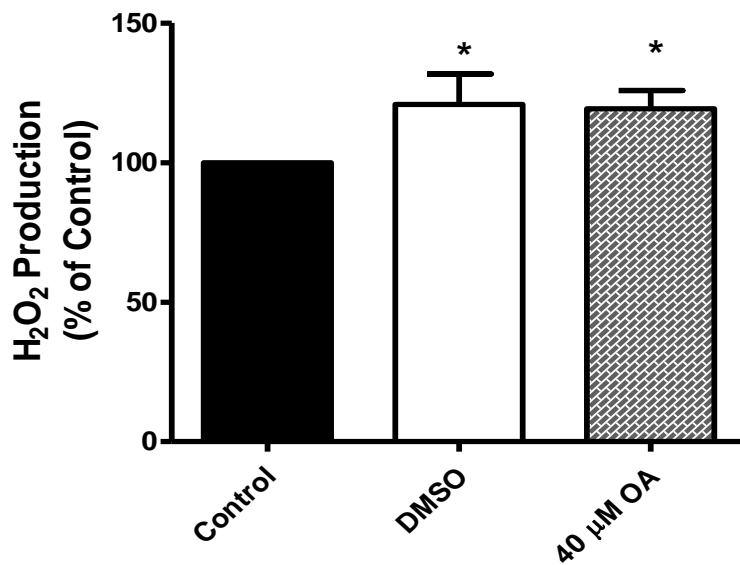


Figure 3.18 B: CMECs: DCF fluorescence data with 40 μM OA treatment for 1 hour. *p < 0.05 vs. Control; control adjusted to 100 %. 0.24 % DMSO vehicle.

Necrosis measurements with PI

AECs:

The % cellular PI uptake was reduced by ~ 50 % in AECs treated with 40 μ M OA for 1 hour compared to untreated controls: 43.33 ± 8.0 % vs. 100 % Control, $p < 0.05$, $N = 6$. DMSO as a vehicle control differed significantly with the control: 76 ± 7.4 % vs. 100 % Control, $p < 0.05$, $N = 5$. However, despite the moderate vehicle effect, OA *per se* exerted PI-lowering effects independently from the vehicle effect: 40 μ M OA (43.33 ± 8.0 %) vs. DMSO (76 ± 7.4 %), $p < 0.05$ (Figure 3.19 A).

CMECs:

Treatment of CMECs with OA 40 μ M (1 hour) significantly increased the PI uptake after 1 hour: 40 μ M OA: 132.2 ± 8.8 % vs. 100 % Control, $p > 0.05$, $N = 7$. Vehicle effects were not observed (Figure 3.19 B).

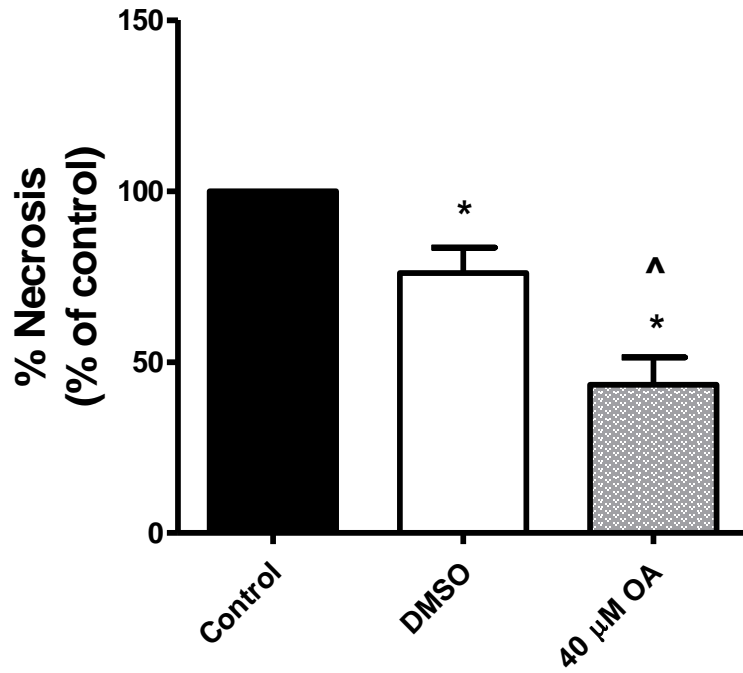


Figure 3.19 A: AECs: % propidium iodide-stained cells treated with 40 μM OA (1 hour). *p < 0.05 vs. Control; control adjusted to 100 %, ^p < 0.05 vs. DMSO (0.24 % DMSO vehicle).

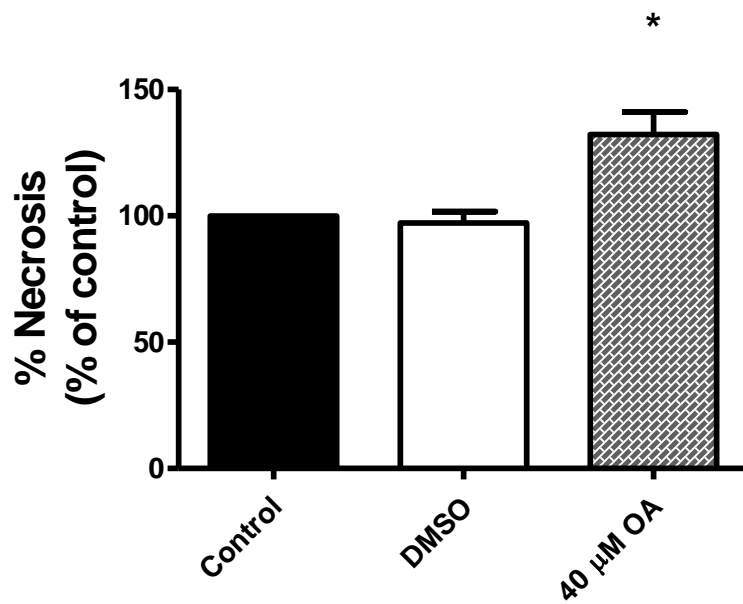


Figure 3.19 B: CMECs: % propidium iodide-stained cells treated with 40 μM OA (1 hour). *p < 0.05 vs. Control; control adjusted to 100 %. 0.24 % DMSO vehicle.

3.1.5.2 24 hour treatment studies

DAF-2/DA (NO production) fluorescence measurements with 40 μ M OA treatment for 24 hours

AECs:

There were no significant differences in the mean DAF-2/DA fluorescence following treatment with 40 μ M OA for 24 hours compared to control, untreated samples (Figure 3.20 A).

CMECs:

Treatment with 40 μ M OA for 24 hours significantly increased mean DAF-2/DA fluorescence: OA: 161.8 ± 29.6 % vs. 100 %, $p > 0.05$, $N = 7$ per group. There were no vehicle effects observed (Figure 3.20 B).

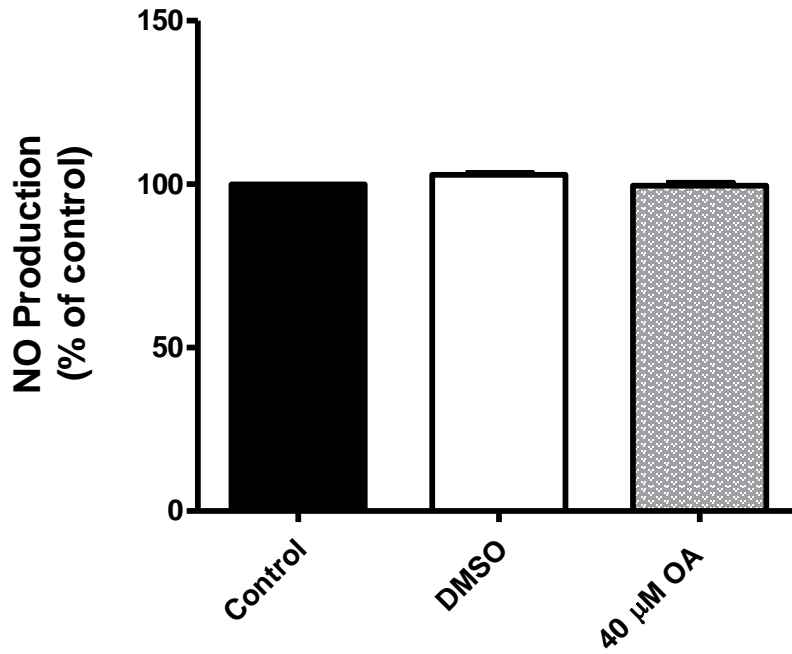


Figure 3.20 A: AECs: DAF-2/DA fluorescence data in AECs treated with 40 μM OA (24 hours). 0.24 % DMSO vehicle.

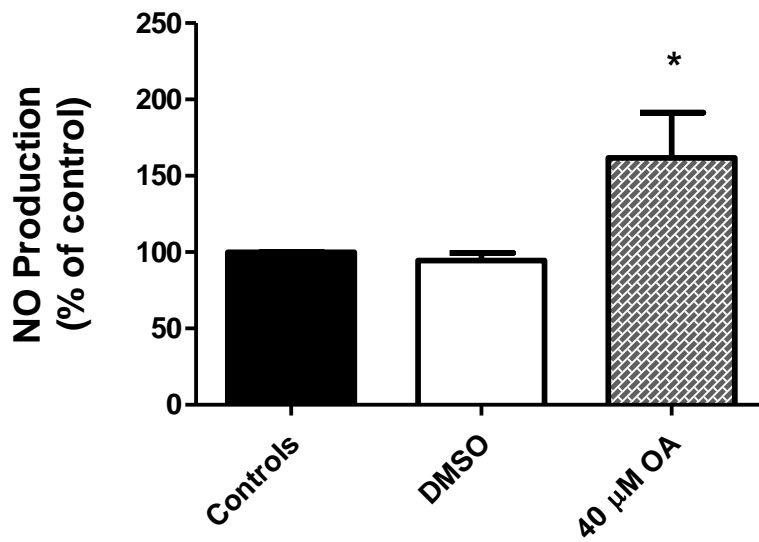


Figure 3.20 B: CMECs: DAF-2/DA fluorescence data in CMECs treated with 40 μM OA (24 hours). *p < 0.05 vs. Control; control adjusted to 100 %. 0.24 % DMSO vehicle.

DCF (H₂O₂ production) fluorescence measurements with 40 μM OA treatment for 24 hours

AECs:

Treatment with OA for 24 hours significantly decreased mean DCF fluorescence: 86.8 ± 1.3 % vs. 100 % Control, $p < 0.05$, $N = 6$. There were no vehicle effects observed (Figure 3.21 A).

CMECs:

At 24 hour treatment, OA exerted no significant effects on DCF fluorescence (Figure 3.21 B).

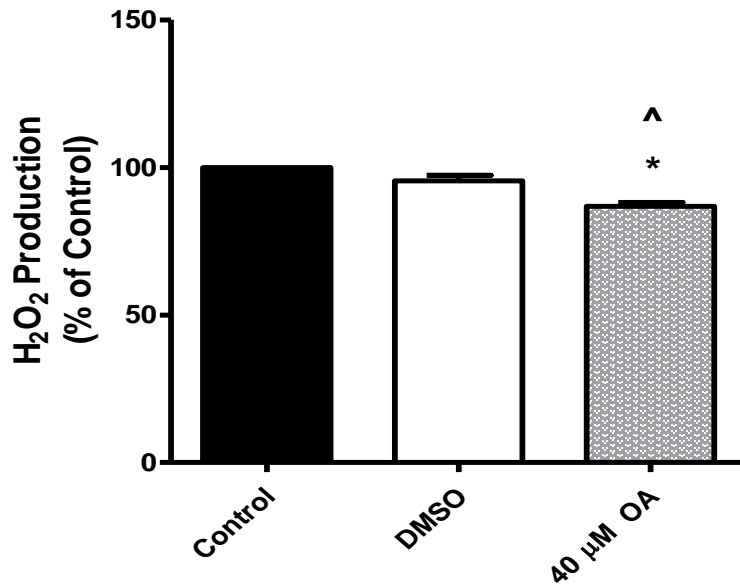


Figure 3.21 A: AECs: DCF fluorescence data in AECs treated with 40 μM OA (24 hours). *p < 0.05 vs. Control; control adjusted to 100 %, ^p < 0.05 vs. DMSO (0.24 % DMSO vehicle).

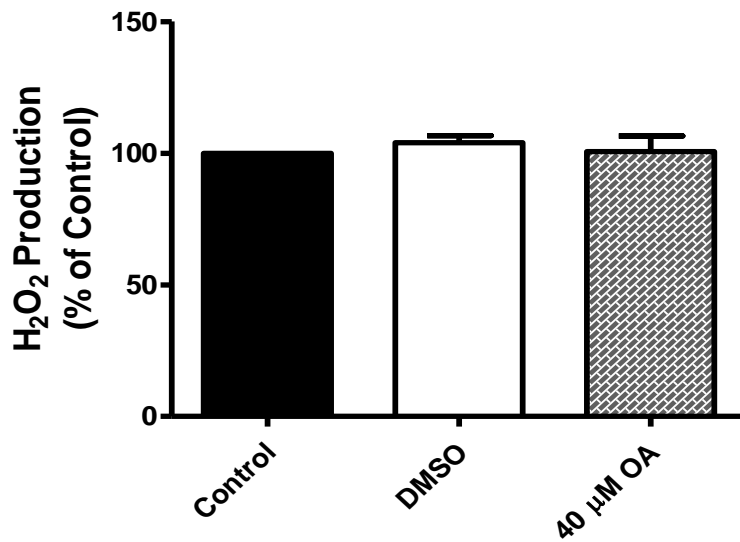


Figure 3.21 B: CMECs: DCF fluorescence data in CMECs treated with 40 μM OA (24 hours). 0.24 % DMSO vehicle.

Propidium uptake (necrosis) measurements with 40 μ M OA treatment for 24 hours

AECs:

OA significantly decreased the % propidium iodide-staining cells after 24 hours treatment: 40 μ M OA: 70.8 ± 3.9 % vs. 100 %, $p < 0.05$, $N = 6$. There were no vehicle effects observed (Figure 3.22 A).

CMECs:

There were no significant differences in the % propidium iodide-staining cells between control and OA samples after 24 hours treatment: 40 μ M OA: 87 ± 14.9 % vs. 100 % Control, $p > 0.05$, $N = 6$ (Figure 3.22 B).

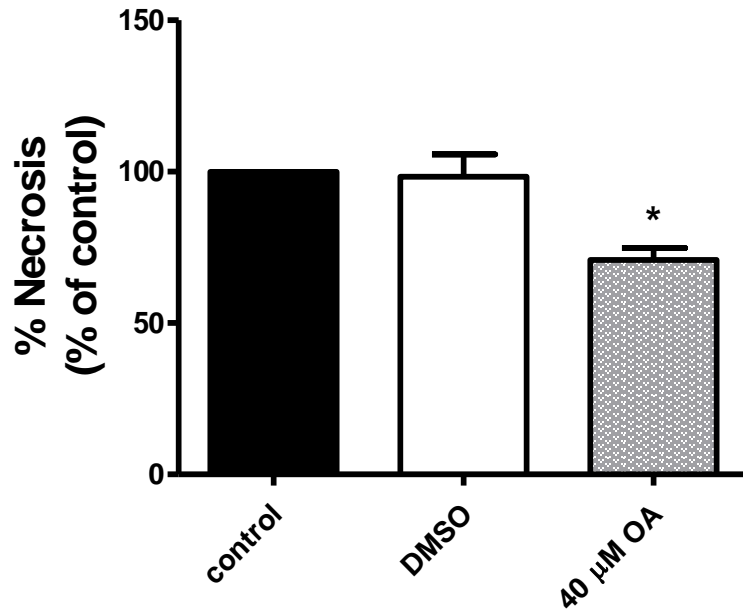


Figure 3.22 A: AECs: % propidium iodide-stained cells treated with 40 μ M OA (24 hours). * $p < 0.05$ vs. Control; control adjusted to 100 %. 0.24 % DMSO vehicle.

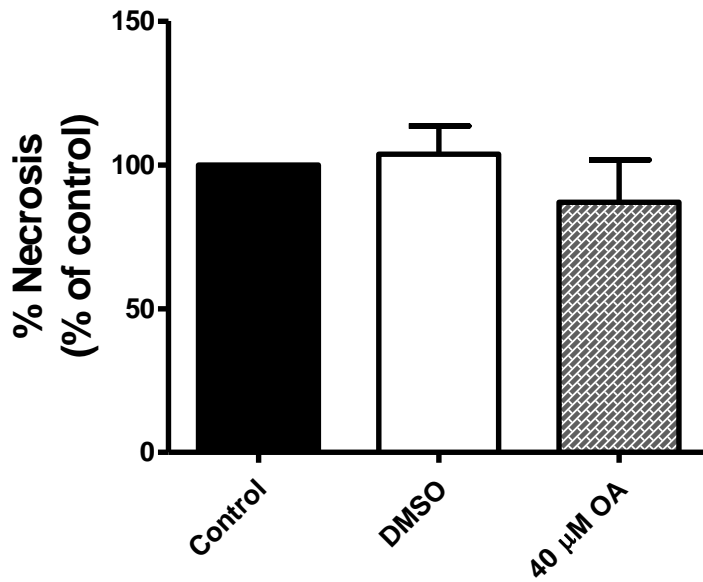


Figure 3.22 B: CMECs: % propidium iodide-stained cells treated with 40 μ M OA (24 hours). 0.24 % DMSO vehicle.

3.1.6 OA (40 μ M) pre-treatment studies.

Both AECs and CMECs were pre-treated with 40 μ M OA 1 hour prior to the administration of 20 ng / ml TNF- α for a further 24 hours.

3.1.6.1 DAF-2/DA (NO production) fluorescence measurements with OA pre-treatment

AECs:

OA treatment alone significantly, albeit modestly, increased mean DAF-2/DA fluorescence, whereas TNF- α significantly decreased DAF-2/DA fluorescence compared to control, untreated samples; there was also a significant increase in fluorescence in the OA-treated cells vs. TNF- α -treated cells: OA (106 ± 0.6 %) vs. TNF- α (85 ± 2.3 %) vs. 100 % Control, $p < 0.05$, $N = 6-12$ per group. In the OA pre-treatment samples (OA+TNF- α), the DAF-2/DA fluorescence increased by almost an identical margin as observed with OA treatment alone compared to control, untreated cells: OA + TNF- α (106.9 ± 1.5 %) vs. 100 % Control, $p < 0.05$, $N = 6$. Furthermore, the OA pre-treatment group showed significantly increased DAF-2/DA fluorescence compared to the TNF- α only group: OA + TNF- α (106.9 ± 1.5) vs. TNF- α (85 ± 2.3 %), $p < 0.05$. No DMSO vehicle effects were observed (Figure 3.23 A).

CMECs:

OA treatment alone significantly increased DAF-2/DA fluorescence, while TNF- α treatment resulted in decreased fluorescence compared to control, untreated samples; there was also a significant increase in fluorescence in the OA-treated cells vs. TNF- α -treated cells: OA (147.2 ± 17.6 %) vs. TNF- α (78.9 ± 2.9 %) vs. 100 % Control, $p < 0.05$, $N = 5-11$ per group. Although DAF-2/DA fluorescence did not differ significantly in the OA pre-treatment group compared to control, untreated samples, pre-treatment with OA did succeed in significantly increasing DAF-2/DA fluorescence compared to the TNF- α only treatment group: OA + TNF- α (128.2 ± 14.1 %) vs. 100 % Control, $p > 0.05$, $N = 7$; OA + TNF- α (128.2 ± 14.1 %) vs. TNF- α (78.9 ± 2.9 %), $p < 0.05$. No vehicle effects were observed (Figure 3.23 B).

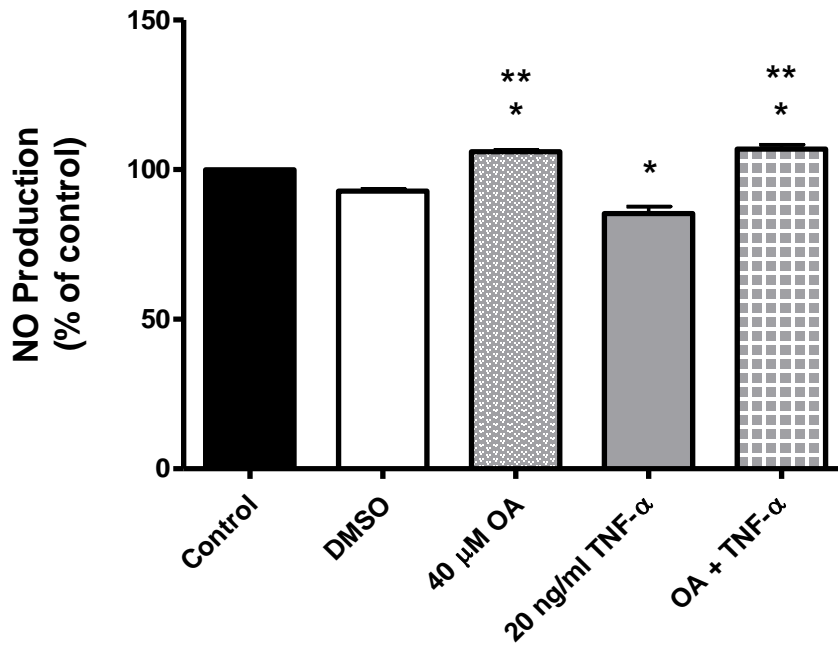


Figure 3.23 A: AECs: DAF-2/DA fluorescence data in OA, TNF- α and OA pre-treatment groups. * $p < 0.05$ vs. Control; control adjusted to 100 %, ** $p < 0.05$ vs. TNF- α .

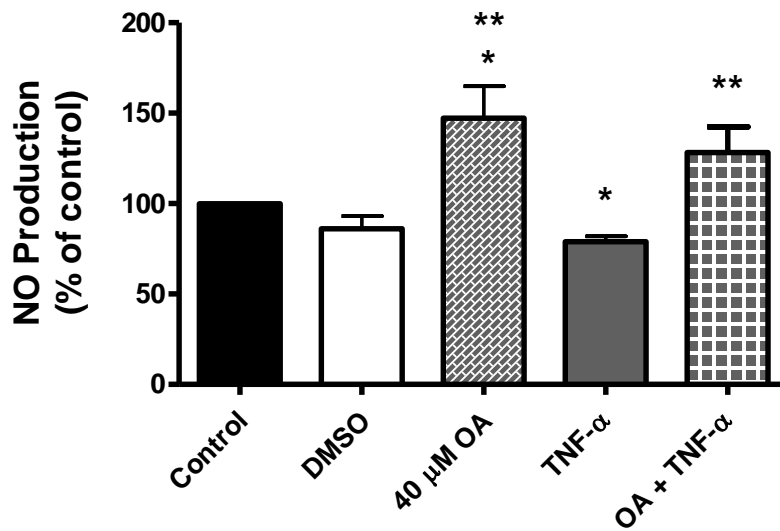


Figure 3.23 B: CMECs: DAF-2/DA fluorescence data in OA, TNF- α and OA pre-treatment groups. * $p < 0.05$ vs. Control; control adjusted to 100 %, ** $p < 0.05$ vs. TNF- α .

3.1.5.2 DCF (H₂O₂ production) fluorescence measurements with OA pre-treatment

AECs:

Mean DCF fluorescence was significantly decreased in the OA treatment group, and significantly increased in the TNF- α group compared to untreated controls; there was also a significantly lower fluorescence in the OA treatment group vs. TNF- α : OA (84.1 ± 3.4 %) vs. TNF- α (261.7 ± 21.3 %) vs. 100 % Control, $p < 0.05$, $N = 7-10$ per group. The OA pre-treatment cells showed significantly decreased DCF fluorescence compared to both TNF- α samples and control, untreated samples: OA + TNF- α (60.3 ± 2.4 %) vs. TNF- α (261.7 ± 21.3 %) vs. 100 % Control, $p < 0.05$, $N = 12$. No vehicle effects were observed (Figure 3.24 A).

CMECs:

Mean DCF fluorescence was significantly lower in OA treatment alone samples compared to TNF- α treated and control, untreated samples respectively; furthermore, DCF fluorescence was significantly increased in the TNF- α group compared to control, untreated samples: OA (66.80 ± 2.1 %) vs. TNF- α (137.1 ± 5.8 %) vs. 100 % Control, $p < 0.05$, $N = 6-7$ per group. OA pre-treatment significantly decreased DCF fluorescence compared to TNF- α treatment samples as well as control, untreated samples: OA + TNF- α (63.9 ± 3.1 %) vs. TNF- α (137.1 ± 5.8 %) vs. 100 % Control, $p < 0.05$, $N = 8$. No vehicle effects were observed (Figure 3.24 B).

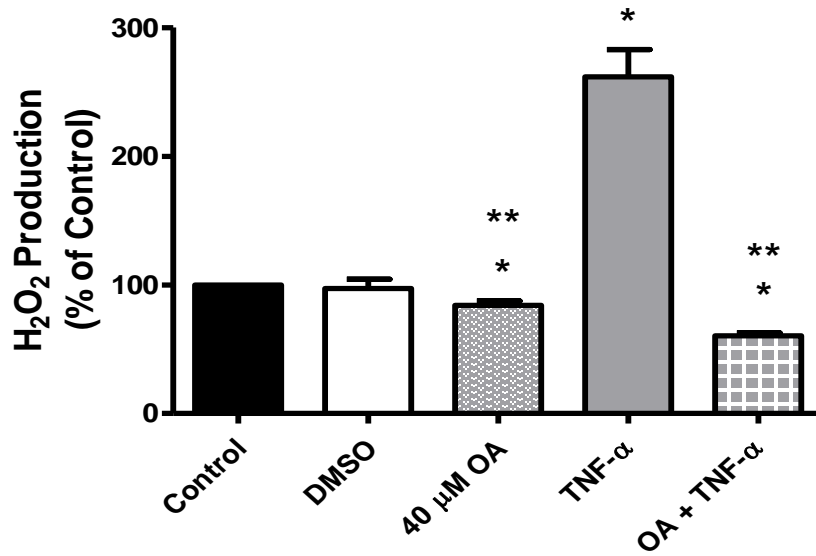


Figure 3.24 A: AECs: DCF fluorescence data in OA, TNF- α and OA pre-treatment groups. * $p < 0.05$ vs. Control; control adjusted to 100 %, ** $p < 0.05$ vs. TNF- α .

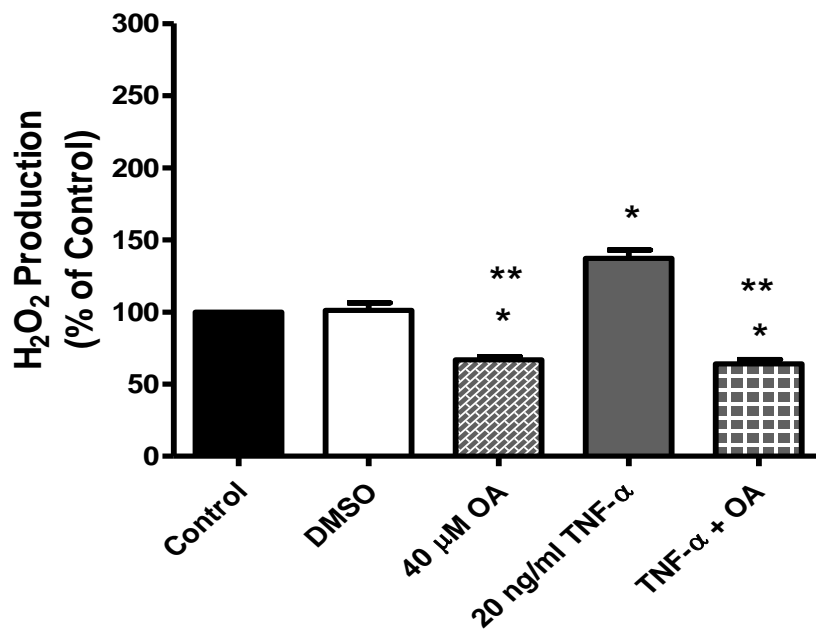


Figure 3.24 B: CMECs: DCF fluorescence data in OA, TNF- α and OA pre-treatment groups. * $p < 0.05$ vs. Control; control adjusted to 100 %, ** $p < 0.05$ vs. TNF- α .

3.1.5.3 PI uptake (necrosis) measurements with OA pre-treatment

AECs:

The % of propidium iodide-staining cells was significantly lower in the OA treatment group compared to both TNF- α and control, untreated groups, and the TNF- α group showed significantly increased propidium iodide staining compared to untreated controls: OA ($80.8 \pm 3.8\%$) vs. TNF- α ($190.5 \pm 53\%$) vs. 100% Control, $p < 0.05$, $N = 5-10$ per group. OA pre-treatment significantly decreased propidium iodide staining compared to TNF- α samples and control, untreated samples: OA + TNF- α ($66.2 \pm 3.9\%$) vs. TNF- α ($190.5 \pm 53\%$) vs. 100% Control, $p < 0.05$, $N = 9$. No DMSO vehicle effects were observed (Figure 3.25 A).

CMECs:

There were no significant differences in the propidium iodide measurements between any of the treatment groups (Figure 3.25 B).

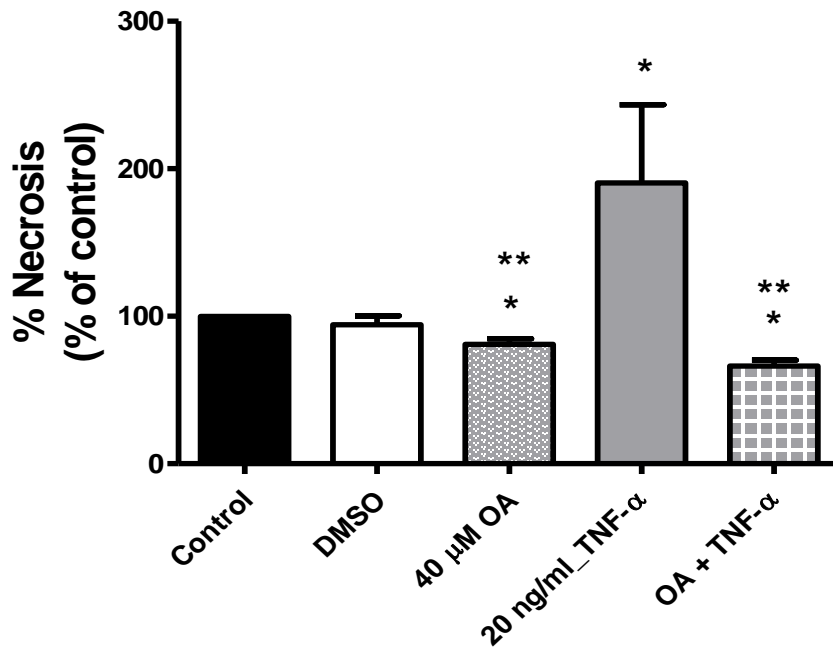


Figure 3.25 A: AECs: % propidium iodide-stained cells in OA, TNF-α and OA pre-treatment groups. *p < 0.05 vs. Control; control adjusted to 100 %, **p<0.05 vs. TNF-α. 0.24 % DMSO vehicle.

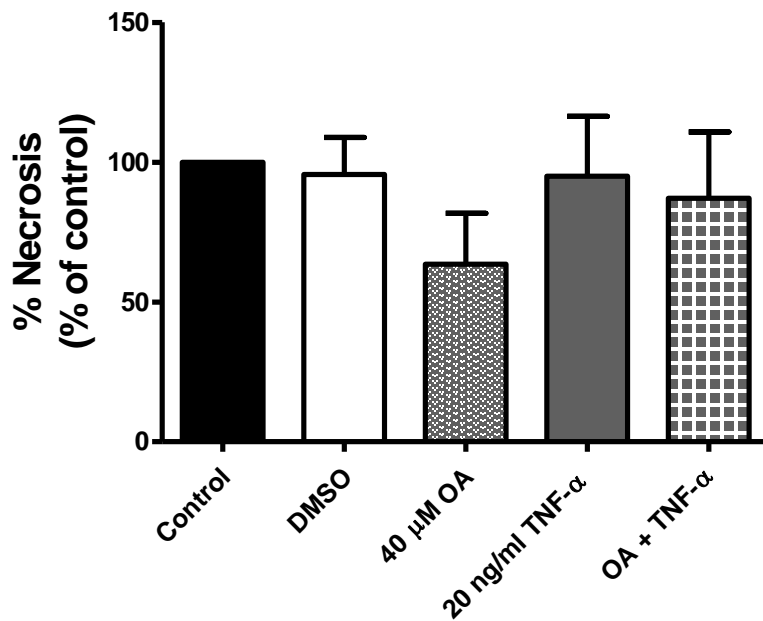


Figure 3.25 B: CMECs: % propidium iodide-stained cells in OA, TNF-α and OA pre-treatment groups. 0.24 % DMSO vehicle.

3.2 Proteomics studies

Comparing large-scale protein expression and regulation patterns in AECs and CMECs

A combined total of 2372 proteins were identified in control, untreated AECs and CMECs, of which 1695 proteins were shared, 320 were unique to AECs, and 357 unique to CMECs (Figure 3.26 A). In TNF- α -treated cells (TNF- α 20 ng / ml; 24 hours), a combined total of 2426 proteins were positively identified in AECs and CMECs, of which 1701 proteins were shared, 322 proteins were unique to AECs, and 403 unique to CMECs (Figure 3.26 B).

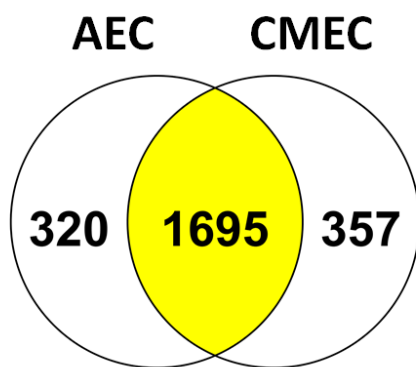


Figure 3.26 A: Venn diagram showing the total protein expression distribution in control, untreated AECs and CMECs.

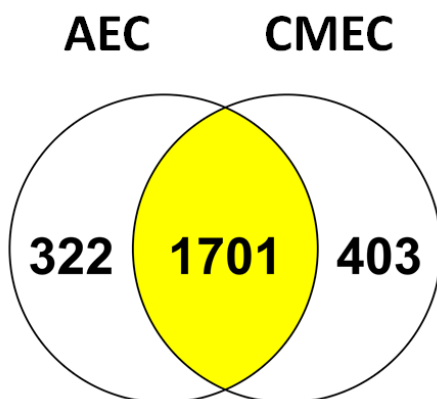


Figure 3.26 B: Venn diagram showing the total protein expression distribution in TNF- α treated AECs and CMECs.

3.2.1 Control, untreated AECs and CMECs

3.2.1.1 Comparative differential protein regulation and functional annotation analysis:

Strongly represented proteins in control, untreated AECs (compared to CMECs)

Differential protein regulation analysis showed that a total of 73 proteins (calculated by Scaffold software) and 68 proteins (calculated by Sieve software) respectively were up-regulated in control, untreated AECs vs. their CMEC counterparts (as determined by the minimum criteria of ≥ 1.5 -fold regulation and $p < 0.05$). Table 3.1 shows a list of the top up-regulated proteins in control, untreated AECs compared to CMECs. In addition to the significantly up-regulated proteins, there were 320 proteins that were only detected in AECs, of which 158 fulfilled the minimum criteria of positive identification in ≥ 2 samples. Proteins that were up-regulated in AECs, include protein Syne3 (6.8-fold up-regulated; cytoskeletal anchoring), cytosolic acyl coenzyme A thioester hydrolase (5-fold up-regulated; fatty acid metabolism), glioma pathogenesis-related protein 2 (4.8-fold up-regulated; epithelial cell migration), insulin-degrading enzyme (4.6-fold up-regulated; insulin breakdown), integrin beta (4.6-fold up-regulated; actin binding and cell adhesion molecule binding), aldehyde dehydrogenase, dimeric NADP-preferring (4.4-fold up-regulated; oxidation-reduction), fermitin-3 (3.6-fold up-regulated; haemostasis, coagulation and cell adhesion), and cytoskeleton associated protein 5 (3.6-fold up-regulated; spindle formation) (Table 3.1). A representative example of a protein abundance graph depicting the normalised total spectra of the up-regulated protein aldehyde dehydrogenase, dimeric NADP-preferring is shown in Figure 3.27 A. Figure 3.27 B is an abundance graph of the protein aldehyde dehydrogenase L1, which was only detected in control, untreated AECs.

In order to make sense of the data, a combined list of the up-regulated proteins plus those proteins that were only detected in AECs (collectively referred to as “strongly represented proteins”), was submitted to DAVID (The Database for Annotation, Visualization and Integrated Discovery) Bioinformatics Resources 6.7 on-line software for functional annotation analysis. Tables 3.2 and 3.3 show the biological processes and cellular components respectively with which the strongly represented proteins were significantly associated. Biological processes such as triglyceride mobilization, dopamine biosynthesis, microtubule polymerization/depolymerization regulation, amino acid biosynthesis, endocytosis and protein transport were highly enriched in control, untreated AECs (Table

3.2). Cellular components such as the retromer complex, endosome membrane, nuclear membrane, and vesicle membrane were highly enriched in the AECs (Table 3.3).

3.2.1.2 Comparative differential protein regulation and functional annotation analysis:

Strongly represented proteins in control, untreated CMECs (compared to AECs)

Differential protein regulation analysis showed that a total of 127 proteins (calculated by Scaffold software) and 221 proteins (calculated by Sieve software) respectively were up-regulated in control, untreated CMECs vs. their AEC counterparts (as determined by the minimum criteria of ≥ 1.5 -fold regulation and $p < 0.05$). Table 3.4 shows a list of the top up-regulated proteins in control, untreated CMECs compared to AECs. In addition to the significantly up-regulated proteins, there were 357 proteins that were only detected in CMECs, of which 162 fulfilled the minimum criteria of positive identification in ≥ 2 samples. Proteins that were significantly up-regulated in control, untreated CMECs include: protein Lamc1 (20-fold up-regulated; extracellular matrix protein), Laminin alpha 5 (12.5-fold up-regulated; extracellular matrix protein and angiogenesis), Laminin subunit beta-2 (10-fold up-regulated; extracellular matrix protein), tight junction protein-1 (10-fold up-regulated; tight junction assembly and cell-cell signalling), activated RNA polymerase II transcriptional coactivator p15 (5-fold up-regulated; transcription), AMP deaminase 3 (5-fold up-regulated; purine and energy metabolism), von Willebrand factor (5-fold up-regulated; thrombosis and platelet plug formation), and endothelial nitric oxide synthase, eNOS (1.5-fold up-regulated; nitric oxide generation) (Table 3.4). Figure 3.28 A shows a representative protein abundance graph of the protein tight junction protein-1, which was up-regulated in control, untreated CMECs. The abundance graph of the protein, BCL2-related protein A1B, which was only detected in CMECs, is shown in Figure 3.28 B.

The strongly represented proteins in control, untreated CMECs were submitted to DAVID software for functional annotation analysis. Table 3.5 shows the highly enriched biological processes with which the strongly represented proteins in CMECs associated. The top biological processes include actin filament severing, capping and depolymerization regulation, hydrogen peroxide metabolism, response to ROS, aerobic respiration, tricarboxylic acid cycle, vacuole organisation, electron transport chain and glucose

metabolic process. The highly enriched cellular components in control, untreated CMECs are shown in Table 3.6. They include the myosin 1 complex, filamentous actin, lateral plasma membrane, endoplasmic reticulum, mitochondrial outer membrane, lumen, matrix and inner membrane, lysosome, vacuole and vesicular fraction.

Table 3.1: List of up-regulated proteins in control, untreated AECs (vs. CMECs)

Identified Proteins	Fold Up AECs	P-value
Protein Syne3 (cytoskeletal anchoring)	6.8	0.0005
Cytosolic acyl coenzyme A thioester hydrolase (fatty acid metabolism)	5.0	0.002
Glioma pathogenesis-related protein 2 (epithelial cell migration)	4.8	0.041
Insulin-degrading enzyme (insulin breakdown)	4.6	0.02
Integrin beta (actin binding; cell adhesion molecule binding)	4.6	0.03
Aldehyde dehydrogenase, dimeric NADP-preferring (oxidation-reduction)	4.4	0.001
Fermitin family member 3 (hemostasis, coagulation, integrin activation, cell adhesion)	3.6	0.001
Cytoskeleton associated protein 5 (spindle formation)	3.6	0.04
CDGSH iron-sulfur domain-containing protein 1 (electron transport and oxidative phosphorylation)	3.5	0.01
Catechol O-methyltransferase (catecholamine breakdown)	3.3	0.04
Basic leucine zipper and W2 domain-containing protein 2 (cell differentiation)	3.2	0.03
Fatty acid synthase (long chain fatty acid synthesis)	3.0	0.04
Poly [ADP-ribose] polymerase 1; PARP-1 (inflammatory response; cell death pathways)	3.0	0.02
WAS protein family, member 2 (actin cytoskeleton regulation)	3.0	0.01
Copine 3 protein (membrane trafficking)	2.9	0.01
GTP-binding protein Rheb (mTOR signaling pathway)	2.8	0.03
Obg-like ATPase 1 (ATP hydrolysis)	2.8	0.005
FK506 binding protein 5 (immunoregulation; protein folding)	2.7	0.005
DNA replication licensing factor MCM6 (DNA replication)	2.6	0.002
Stathmin (microtubule disassembly)	2.6	0.006
Apoptosis regulator BAX (pro-apoptotic)	2.5	0.006
CTP synthase (ATP binding; CTP synthesis)	2.5	0.006
Cysteinyl-tRNA synthetase (gene expression; protein synthesis)	2.4	0.006
Receptor-type tyrosine-protein phosphatase beta (angiopoietin signalling; vascular remodeling and angiogenesis)	2.4	0.006
Transmembrane protein 43 (inner nuclear membrane)	2.4	0.04
NADP-dependent malic enzyme (NADPH generation for fatty acid synthesis; links glycolysis with citric acid cycle)	2.3	0.03
Mcm5 protein (DNA replication)	2.2	0.003
N-acetyl-D-glucosamine kinase (amino-sugar metabolism)	2.2	0.03
Protein Mcm2 (DNA replication)	2.2	0.004
Anoctamin (Calcium-activated chloride channel; transepithelial ion transport)	2.1	0.002
Calpain-1 catalytic subunit (degradation of extracellular matrix)	2.1	0.02

Table 3.1 (continued): List of up-regulated proteins in control, untreated AECs (vs. CMECs)

Identified Proteins	Fold Up in AECs	P-value
NAD-dependent protein deacetylase sirtuin-2 (cell cycle control; microtubule dynamics; cell differentiation; autophagy)	2.1	0.01
Nuclear autoantigenic sperm protein (DNA replication)	2.1	0.04
Nuclear pore complex protein Nup93 (nuclear pore complex assembly-disassembly)	2.1	0.04
Apolipoprotein B-100 (component of LDL and VLDL; cholesterol metabolism)	2.0	0.049
Endothelial-specific receptor tyrosine kinase (receptor for growth factors such as VEGF and angiopoietins)	2.0	0.001
Isocitrate dehydrogenase [NADP], mitochondrial	2.0	0.003
Vacuolar protein sorting-associated protein 26A (shuttling of proteins from endosomes to trans-Golgi network)	2.0	0.004

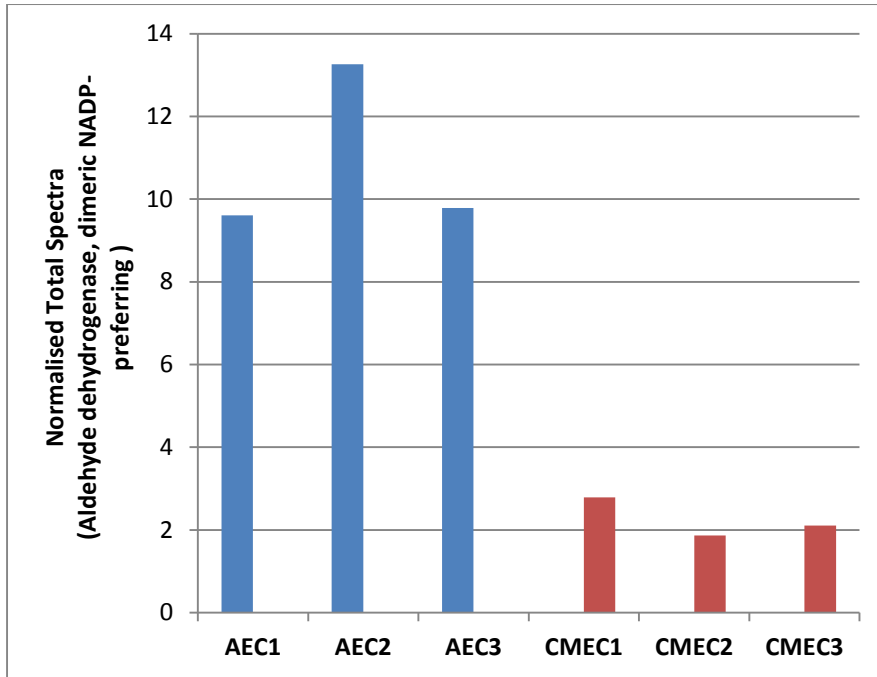


Figure 3.27 A: Graph showing the differentially regulated protein abundance (measured as normalised total spectra) of Aldehyde dehydrogenase, dimeric NADP-preferring in three control, untreated AEC samples (AEC1, AEC2, AEC3) compared to three control, untreated CMEC samples (CMEC1, CMEC2, CMEC3).

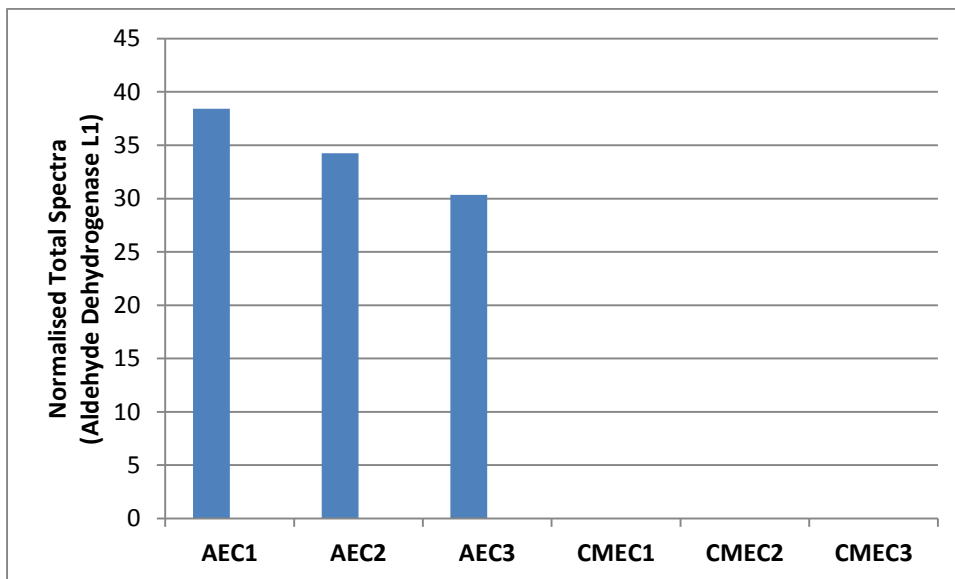


Figure 3.27 B: Graph showing the differentially regulated protein abundance (measured as normalised total spectra) of Aldehyde dehydrogenase L1 in three control, untreated AEC samples (AEC1, AEC2, AEC3) compared to three control, untreated CMEC samples (CMEC1, CMEC2, CMEC3).

Table 3.2: Biological processes associated with strongly represented proteins in control, untreated AECs (vs. CMECs)

Gene Ontology Terms: Biological Processes	Fold Enrichment	P-value
GO:0006642~triglyceride mobilization	41.7	0.046
GO:0006297~nucleotide-excision repair, DNA gap filling	32.6	0.0001
GO:0009070~serine family amino acid biosynthetic process	24.1	0.007
GO:0042417~dopamine metabolic process	14.9	0.02
GO:0031111~negative regulation of microtubule polymerization or depolymerization	14.9	0.02
GO:0008652~cellular amino acid biosynthetic process	10.6	0.001
GO:0031110~regulation of microtubule polymerization or depolymerization	10.4	0.03
GO:0034311~diol metabolic process	10.1	0.03
GO:0006584~catecholamine metabolic process	10.1	0.03
GO:0030162~regulation of proteolysis	7.9	0.01
GO:0006260~DNA replication	6.7	0.0002
GO:0016485~protein processing	6.3	0.003
GO:0043406~positive regulation of MAP kinase activity	5.1	0.04
GO:0006897~endocytosis	4.1	0.02
GO:0010324~membrane invagination	4.1	0.02
GO:0015031~protein transport	2.7	0.002
GO:0045184~establishment of protein localization	2.6	0.002
GO:0016192~vesicle-mediated transport	2.4	0.02
GO:0006928~cell motion	2.3	0.04
GO:0032268~regulation of cellular protein metabolic process	2.3	0.04
GO:0008104~protein localization	2.2	0.009
GO:0046907~intracellular transport	2.1	0.04
GO:0055114~oxidation reduction	2.0	0.03
GO:0042127~regulation of cell proliferation	2.0	0.02

Table 3.3: Cellular components associated with strongly represented proteins in control, untreated AECs (vs control, untreated CMECs)

Gene Ontology Terms: Cellular Components	Fold Enrichment	P-value
GO:0030904~retromer complex (endosomal protein sorting)	67.1	0.03
GO:0005662~DNA replication factor A complex	50.4	0.04
GO:0044440~endosomal part	10.3	0.007
GO:0010008~endosome membrane	10.3	0.007
GO:0031965~nuclear membrane	6.4	0.02
GO:0005938~cell cortex	4.6	0.009
GO:0012506~vesicle membrane	4.4	0.01
GO:0030659~cytoplasmic vesicle membrane	4.1	0.03
GO:0009986~cell surface	2.7	0.02

Table 3.4 List of up-regulated proteins in control, untreated CMECs (vs AECs)

Identified Proteins	Fold Up CMECs	P-value
Protein Lamc1 (extracellular matrix)	20.0	0.0005
Laminin, alpha 5 (extracellular matrix, angiogenesis)	12.5	0.0001
Laminin subunit beta-2 (extracellular matrix)	10.0	0.01
Tight junction protein-1(tight junction assembly, cell-cell signalling)	10.0	0.0006
Activated RNA polymerase II transcriptional coactivator p15 (transcription)	5.0	0.002
AMP deaminase 3 (purine and energy metabolism)	5.0	0.001
Rho guanine nucleotide exchange factor-7 (membrane ruffling, cell migration and attachment)	5.0	0.01
Dedicator of cytokinesis 6 (activates Cdc42 and Rac1; coagulation)	5.0	0.02
LOC683667 protein (calcium ion transport)	5.0	0.03
Procollagen, type XVIII, alpha 1 (extracellular matrix; endothelial cell morphogenesis; angiogenesis; cell adhesion)	5.0	0.002
Prostaglandin G/H synthase 1 (prostaglandin biosynthesis)	5.0	0.0001
Protein Cingulin-like 1 (cell junction assembly; RhoA and Rac1 regulation)	5.0	0.0006
von Willebrand factor (thrombosis; platelet plug formation)	5.0	0.0001
Alpha-adducin (actin cytoskeleton organisation)	3.3	0.02
Coactosin-like protein (actin binding)	3.3	0.02
Cullin-5 (proteasomal degradation of target proteins)	3.3	0.03
Endophilin-B1 (mitochondrial morphology; endosomal trafficking)	3.3	0.0004
Fermitin family homolog 2 (cell-extracellular matrix adhesion)	3.3	0.0008
Neurolysin, mitochondrial (metalloprotease; member of the renin-angiotensin pathway)	3.3	0.02
N-terminal kinase-like protein (vesicle-mediated transport)	3.3	0.047
Platelet endothelial cell adhesion molecule; PECAM-1; CD31 (cell adhesion molecular)	3.3	0.001
Protein tyrosine phosphatase non-receptor type 12 (cell growth; differentiation; adhesion; shape)	3.3	0.01
SH3 and multiple ankyrin repeat domains protein 3	3.3	0.007
SPARC (extracellular matrix)	3.3	0.0006
1-phosphatidylinositol 4,5-bisphosphate phosphodiesterase gamma-1 (receptor tyrosine kinase signalling)	2.5	0.002
Arylsulfatase B (lysosomal breakdown of large sugar molecules)	2.5	0.02
CD2-associated protein (adapter protein between membrane proteins and actin cytoskeleton)	2.5	0.003
Cleavage and polyadenylation specific factor 6, 68kDa (cleavage factor in RNA processing)	2.5	0.04
DNA-(apurinic or apyrimidinic site) lyase (DNA repair and cell redox homeostasis)	2.5	0.002
GDP-mannose 4, 6-dehydratase (fructose and mannose metabolism)	2.5	0.02
GlutaminyI-tRNA synthetase (protein biosynthesis)	2.5	0.04

Table 3.4 (continued): List of up-regulated proteins in control, untreated CMECs (vs AECs)

Identified proteins	Fold UP CMECs	P-value
Glycosyltransferase 25 domain containing 1 (lipopolysaccharide synthesis; endothelial cell adhesion)	2.5	0.008
Heat shock protein 70kDa 12B (chaperone protein; protein folding)	2.5	0.02
Inosine-5'-monophosphate dehydrogenase 2 (guanine nucleotide synthesis; cell growth)	2.5	0.01
Integrin alpha 3 variant A (cell adhesion)	2.5	0.0005
LIM and senescent cell antigen-like domains 1 isoform E (cell-cell junction; cell-matrix adhesion)	2.5	0.0001
Major vault protein (intracellular signal transduction; immune response)	2.5	0.005
Polypeptide N-acetylgalactosaminyltransferase 1 (protein glycosylation)	2.5	0.005
Probable ATP-dependent RNA helicase DDX46 (RNA splicing)	2.5	0.04
Protein Acin1 (chromatin condensation; apoptotic pathways)	2.5	0.0006
Heparan sulfate proteoglycan-2; Perlecan (vascular extracellular matrix; maintenance of endothelial barrier)	2.5	0.0001
Insulin growth factor 2 mRNA binding protein-2 (insulin growth factor-2 synthesis)	2.5	0.004
Protein RGD1309995 (endosomal transport)	2.5	0.004
Talin-2 (cell adhesion; cytoskeletal anchoring)	2.5	0.002
Rattus norvegicus utrophin (actin filament binding)	2.5	0.02
Superoxide dismutase [Mn], mitochondrial (anti-oxidant)	2.5	0.01
Gluthathione peroxidase (anti-oxidant)	2.1	0.000003
Cytochrome C subunit 6B1 (mitochondrial respiration)	2.0	0.0001
3-ketoacyl-CoA thiolase, mitochondrial (anti-apoptosis; inhibits mitochondrial damage)	2.0	0.02
Basal cell adhesion molecule (lamin alpha-5 receptor; cell adhesion)	2.0	0.005
Coronin (phagocytosis)	2.0	0.03
Keratin, type II cytoskeletal 6A (cytoskeleton; cell proliferation)	2.0	0.001
Peroxiredoxin-6 (antioxidant; reduction of hydrogen peroxide)	2.0	0.01
Unconventional myosin-Ic (intracellular movements)	2.0	0.04
Vesicle-associated membrane protein-associated protein A (vesicle trafficking)	2.0	0.0004
Endothelial cell selective adhesion molecule (cell adhesion; angiogenesis; permeability; leukocyte transmigration)	1.8	1.3×10^{-12}
Intercellular adhesion molecule (leukocyte adhesion; leukocyte transmigration)	1.8	2×10^{-12}
High density lipoprotein binding protein (Vigilin) (binds HDL; regulate cholesterol levels)	1.5	6×10^{-7}
Junctional adhesion molecule (tight junction formation; monocyte transmigration; platelet activation)	1.5	0.000002
Nitric oxide synthase (NOS3; eNOS) (Nitric oxide biosynthesis)	1.5	0.02

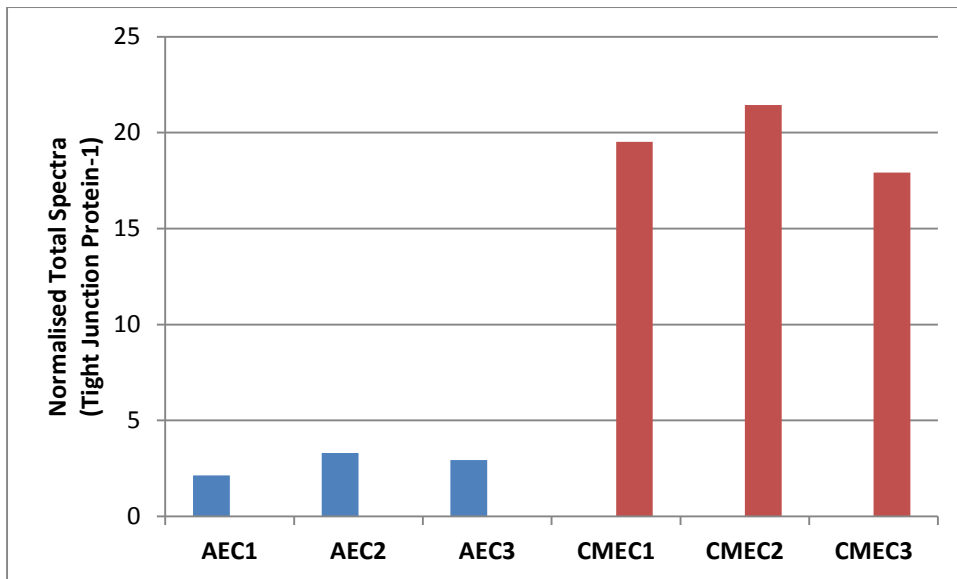


Figure 3.28 A: Graph showing the differentially regulated protein abundance (measured as normalised total spectra) of Tight junction protein-1 in three control, untreated CMEC samples (CMEC1, CMEC2, CMEC3) compared to three control, untreated AEC samples (AEC1, AEC2, AEC3).

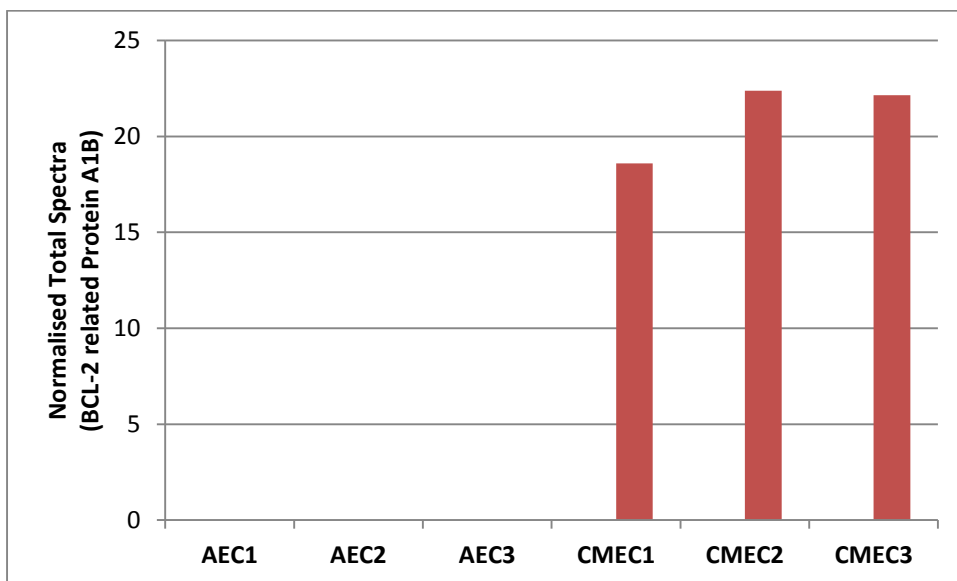


Figure 3.28 B: Graph showing the differentially regulated protein abundance (measured as normalised total spectra) of BCL-2 related protein A1B in three control, untreated CMEC samples (CMEC1, CMEC2, CMEC3) compared to three control, untreated AEC samples (AEC1, AEC2, AEC3).

Table 3.5: Biological processes associated with strongly represented proteins in control, untreated CMECs (vs control, untreated AECs)

Gene Ontology Terms: Biological Processes	Fold Enrichment	P-value
GO:0051014~actin filament severing	78.5	0.03
GO:0051693~actin filament capping	21.4	0.008
GO:0042744~hydrogen peroxide catabolic process	18.1	0.01
GO:0030834~regulation of actin filament depolymerization	15.7	0.01
GO:0042743~hydrogen peroxide metabolic process	13.1	0.003
GO:0034614~cellular response to reactive oxygen species	12.1	0.004
GO:0009060~aerobic respiration	11.6	0.005
GO:0001836~release of cytochrome c from mitochondria	11.2	0.03
GO:0008637~apoptotic mitochondrial changes	10.8	0.006
GO:0006099~tricarboxylic acid cycle	10.7	0.03
GO:0007040~lysosome organization	10.7	0.03
GO:0031333~negative regulation of protein complex assembly	10.2	0.03
GO:0046356~acetyl-CoA catabolic process	10.2	0.03
GO:0007033~vacuole organization	9.5	0.008
GO:0034599~cellular response to oxidative stress	8.9	0.009
GO:0019319~hexose biosynthetic process	8.7	0.04
GO:0045333~cellular respiration	8.6	0.0002
GO:0046496~nicotinamide nucleotide metabolic process	7.7	0.02
GO:0034637~cellular carbohydrate biosynthetic process	7.2	0.001
GO:0045454~cell redox homeostasis	6.2	0.008
GO:0022900~electron transport chain	5.5	0.01
GO:0016051~carbohydrate biosynthetic process	4.9	0.007
GO:0019882~antigen processing and presentation	4.7	0.02
GO:0007005~mitochondrion organization	4.1	0.01
GO:0005996~monosaccharide metabolic process	4.1	0.0002
GO:0006006~glucose metabolic process	4.0	0.002
GO:0008610~lipid biosynthetic process	2.5	0.03
GO:0006461~protein complex assembly	2.5	0.006
GO:0070271~protein complex biogenesis	2.5	0.006

Table 3.6: Cellular components associated with strongly represented proteins in control, untreated CMECs (vs. control, untreated AECs)

Gene Ontology Terms: Cellular Components	Fold Enrichment	P-Value
GO:0045160~myosin I complex	70.4	0.03
GO:0031941~filamentous actin	12.4	0.02
GO:0016328~lateral plasma membrane	11.7	0.03
GO:0005788~endoplasmic reticulum lumen	6.3	0.008
GO:0005741~mitochondrial outer membrane	5.1	0.006
GO:0031980~mitochondrial lumen	4.0	0.0008
GO:0005759~mitochondrial matrix	4.0	0.0008
GO:0005764~lysosome	3.9	0.002
GO:0044432~endoplasmic reticulum part	3.2	0.001
GO:0005773~vacuole	3.2	0.007
GO:0044429~mitochondrial part	3.1	0.00003
GO:0042598~vesicular fraction	3.1	0.002
GO:0005743~mitochondrial inner membrane	2.9	0.002
GO:0015629~actin cytoskeleton	2.7	0.03
GO:0005739~mitochondrion	1.9	0.0001
GO:0005829~cytosol	1.9	0.0004
GO:0005856~cytoskeleton	1.7	0.01
GO:0044430~cytoskeletal part	1.7	0.04
GO:0005886~plasma membrane	1.3	0.03

3.2.2 TNF- α treated AECs and CMECs

3.2.2.1 Differential protein regulation and functional annotation analysis: Strongly represented proteins in TNF- α treated AECs (compared to control, untreated AECs)

Differential protein regulation analysis showed that a total of 7 proteins (calculated by Scaffold software) and 23 proteins (calculated by Sieve software) respectively were up-regulated in TNF- α treated AECs vs. control, untreated AECs (as determined by the minimum criteria of ≥ 1.5 -fold regulation and $p < 0.05$). Table 3.7 shows a list of the top up-regulated proteins in TNF- α treated AECs vs. control, untreated AECs. In addition to the significantly up-regulated proteins, there were 40 proteins that were only detected in TNF- α treated AECs.

Proteins that were up-regulated in response to TNF- α include guanylate binding protein 2 (3-fold up-regulated; involved in immune response), Superoxide dismutase [Mn] mitochondrial (2.8-fold up-regulated; an antioxidant), Cystatin-B (2.8-fold up-regulated; protects against cathepsin-B induced protein degradation), sequestosome_1 (2.3-fold up-regulated; activates NF- κ B via TNF-receptor-associated factor 6), Leucine-rich repeat flightless-interacting protein 1 (2.2-fold up-regulated; involved in innate immune response and regulation of TNF- α expression), Acetyl_CoA acetyltransferase (2-fold up-regulated; involved in lipid metabolism), Ras-related protein Ral_B (1.9-fold up-regulated; cell membrane trafficking, cell proliferation and anti-apoptosis), Glutaredoxin_3 (1.7-fold; up-regulated, cell redox homeostasis), Protein NDRG1 (1.7-fold up-regulated; stress response) and caspase 3 (1.5-fold up-regulated, involved in initiation of apoptosis) (Table 3.7). Differentially regulated protein abundance of Superoxide dismutase [Mn] mitochondrial in TNF- α treated AECs compared to control, untreated AECs is shown in Figure 3.29 A. NF- κ B p49/100 was only detected in TNF- α treated AECs compared to control, untreated AECs as shown by a differentially regulated protein abundance graph in Figure 3.29 B.

Biological processes enriched in TNF- α treated AECs compared to control, untreated AECs as determined by the DAVID annotation tool are shown in Table 3.8. These were primarily associated with regulation of cell death and included release of cytochrome c from mitochondria (37-fold enriched), apoptotic mitochondrial changes (26.9-fold enriched), anti-apoptosis (8-fold enriched), and negative regulation of apoptosis (4.6-fold enriched).

Table 3.7: List of up-regulated proteins in AECs + TNF- α (vs untreated AECs)

Identified proteins	Fold Up	P-value
Guanylate binding protein 2 (immune response)	3.0	9.9×10^{-20}
Protein Rtc1 (RNA processing)	3.0	0.03
Superoxide dismutase [Mn]_ mitochondrial (anti-oxidant)	2.8	8.4×10^{-10}
Cystatin-B (inhibition of Cathepsin-B: protects proteins against cathepsins leaking out of lysosomes)	2.8	0.03
Testin (anti-cell proliferation and growth)	2.8	0.03
Multidrug resistance protein 1a (transmembrane transport)	2.4	0.005
Sequestosome_1 (activates NF- κ B via TNF-receptor-associated factor 6)	2.3	9.9×10^{-20}
Leucine-rich repeat flightless-interacting protein 1 (innate immune response; regulation of TNF expression)	2.2	0.01
MHC class I RT1.Au heavy chain (immune response)	2.1	1.2×10^{-11}
Acetyl_CoA acetyltransferase_ cytosolic (lipid metabolism)	2.0	0.000005
ATPase_H_transporting_ lysosomal 38kDa_ V0 subunit d1 (acidification of intracellular organelles necessary for protein sorting and receptor-mediated endocytosis)	1.9	0.02
Ras_related protein Ral_B (cell membrane trafficking; cell proliferation; anti-apoptosis)	1.9	8.8×10^{-8}
Protein Parp14 (immune response)	1.8	0.0002
AMP deaminase 3 (energy metabolism)	1.7	0.0001
Protein NDRG1 (Stress response)	1.7	6×10^{-11}
Glutaredoxin_3 (cell redox homeostasis)	1.7	1.8×10^{-7}
Peflin (proteolysis)	1.7	0.009
Heterogeneous nuclear ribonucleoprotein D (mRNA processing and stability)	1.6	0.007
Afadin (cell-cell junction)	1.6	0.007
Phenylalanyl_tRNA synthetase_ beta subunit (gene expression; translation)	1.6	0.01
UDP_glucose 6_dehydrogenase (extracellular matrix)	1.5	8.4×10^{-8}
Protein Pml (pro-apoptosis)	1.5	0.008
Basic transcription factor 3 (initiation of transcription)	1.5	6.3×10^{-7}
Nucleophosmin (ribosome biogenesis)	1.5	2.2×10^{-15}
Transmembrane protein 43 (nuclear envelope maintenance)	1.5	0.02
Caspase 3 (initiation of apoptosis)	1.5	2×10^{-8}

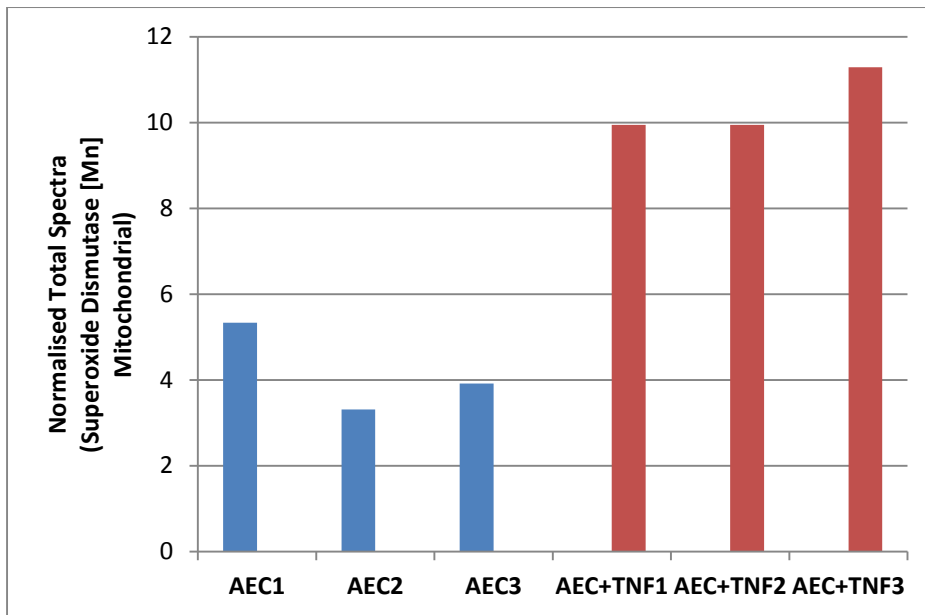


Figure 3.29 A: Graph showing the differentially regulated protein abundance (measured as normalised total spectra) of Superoxide dismutase [Mn] mitochondrial in three TNF- α treated AEC samples (AEC+TNF1, AEC+TNF2, AEC+TNF3) compared to three control, untreated AEC samples (AEC1, AEC2, AEC3).

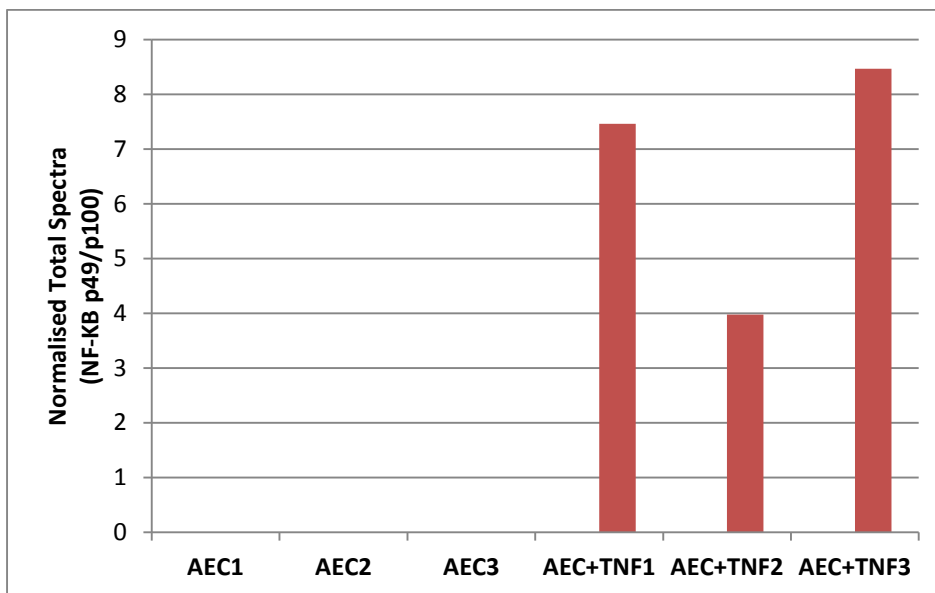


Figure 3.29 B: Graph showing the differentially regulated protein abundance (measured as normalised total spectra) of NF- κ B p49/p100 in three TNF- α treated AEC samples (AEC+TNF1, AEC+TNF2, AEC+TNF3) compared to three control, untreated AEC samples (AEC1, AEC2, AEC3).

Table 3.8: Biological processes associated with strongly represented proteins in AECs +TNF- α samples (vs control, untreated AECs)

Term	Fold Enrichment	P-value
GO:0001836~release of cytochrome c from mitochondria	37.1	0.05
GO:0008637~apoptotic mitochondrial changes	26.9	0.07
GO:0006916~anti-apoptosis	8.1	0.04
GO:0006091~generation of precursor metabolites and energy	6.6	0.02
GO:0043066~negative regulation of apoptosis	4.7	0.04
GO:0043069~negative regulation of programmed cell death	4.6	0.05
GO:0060548~negative regulation of cell death	4.6	0.05
GO:0008219~cell death	3.8	0.08
GO:0006955~immune response	3.8	0.08
GO:0042981~regulation of apoptosis	2.9	0.08
GO:0043067~regulation of programmed cell death	2.8	0.08
GO:0010941~regulation of cell death	2.8	0.08

Functional annotation analysis of Cellular Components in TNF- α -treated AECs vs control, untreated AECs did not reveal any significant results.

3.2.2.2 Differential protein regulation and functional annotation analysis: Strongly represented proteins in TNF- α treated CMECs (compared to control, untreated CMECs)

Differential protein regulation analysis showed that a total of 17 proteins (calculated by Scaffold software) and 28 proteins (calculated by Sieve software) respectively were up-regulated in TNF- α treated CMECs vs. control, untreated CMECs (as determined by the minimum criteria of ≥ 1.5 -fold regulation and $p < 0.05$). Table 3.9 shows a list of the top up-regulated proteins in TNF- α treated CMECs vs. control, untreated CMECs. In addition to the significantly up-regulated proteins, there were 61 proteins that were only detected in TNF- α treated CMECs.

In CMECs, TNF- α elicited up-regulation of proteins such as Protein Gbp5 (6-fold up-regulated; involved in inflammation and immune response), BH3 interacting domain death agonist (4.8-fold up-regulated; release of cytochrome C from mitochondria, apoptosis), intercellular adhesion molecule 1 (4-fold up-regulated, involved in cell adhesion and immune response), guanylate binding protein 2 (3.2-fold up-regulated; immune response), protein Tapbp (3-fold up-regulated; involved in regulation of leukocyte-mediated cell toxicity), plasminogen activator inhibitor (2.6-fold up-regulated; pro-clotting factor), A1b (2.2-fold up-regulated; NF-KB signalling), Protein NDRG1 (2.2-fold up-regulated; stress response), and superoxide dismutase [Mn] mitochondrial (2.2-fold up-regulated; antioxidant) (Table 3.9). A representation of the differentially regulated protein abundance of plasminogen activator inhibitor-1 in TNF- α treated CMECs compared to control, untreated CMECs is shown in Figure 3.30 A. NF-KB p49 / p100 was only detected in TNF- α treated CMECs compared to control, untreated CMECs as shown in the protein abundance graph (Figure 3.30 B).

Biological processes determined from strongly represented proteins in TNF- α treated CMECs by DAVID software annotation tool are listed in Table 3.10. Enriched biological processes in TNF- α treated CMECs (compared to control, untreated CMECs) included membrane to membrane docking (112-fold enriched), regulation of mitochondrial membrane permeability (76.6-fold enriched), release of cytochrome C from my mitochondria (40-fold enriched), apoptotic mitochondrial changes (29-fold enriched), regulation of cell-cell adhesion (26.7-fold enriched), positive regulation of nitric oxide biosynthesis (25.5-fold enriched), and leukocyte adhesion (24-fold enriched).

Table 3.9: List of up-regulated proteins in CMECs + TNF- α (vs control, untreated CMECs)

Identified proteins	Fold Up	P-value
Protein Gbp5 (inflammation; immune response)	6.0	9.99×10^{-16}
BH3 interacting domain death agonist (cytochrome C release from mitochondria; apoptosis)	4.8	0.006
Intercellular adhesion molecule 1 (immune response; cell adhesion)	4.0	3.52×10^{-8}
Glutamine--fructose-6-phosphate aminotransferase [isomerizing] 1 (carbohydrate metabolism)	3.4	0.01
Guanylate binding protein 2 (immune response)	3.2	0.0004
Protein Tapbp (regulation of leukocyte-mediated cell toxicity)	3.0	9.9×10^{-20}
Plasminogen activator inhibitor 1 (pro-clotting)	2.6	0.01
Interleukin 1 family_ member 6 (cytokine / chemokine production)	2.5	5.47×10^{-8}
BH3 interacting domain death agonist (immune response; cell adhesion)	2.5	3.46×10^{-13}
Protein Tapbp (regulation of leukocyte-mediated cell toxicity)	2.5	0.0006
Plasminogen activator inhibitor 1 (pro-clotting)	2.4	5.77×10^{-7}
A1b (NF-kB signaling)	2.2	9.9×10^{-20}
Protein NDRG1 (stress-response protein; apoptosis)	2.2	0.002
RT1.A1(F) protein (antigen presentation; immune response)	2.2	9.9×10^{-20}
Superoxide dismutase [Mn]_ mitochondrial (anti-oxidant)	2.2	9.9×10^{-20}
Cathepsin L1 (proteolysis; antigen presenting)	2	0.02
Catechol O-methyltransferase (catecholamine synthesis; response to bacterial molecules)	1.8	0.02
3-hydroxyisobutyrate dehydrogenase, mitochondrial (amino acid metabolism)	1.7	0.01
Protein Parp14 (pro-survival of injured cells)	1.7	0.0001
Plexin D1 (endothelial cell migration)	1.6	0.0001
Branched-chain-amino-acid aminotransferase, mitochondrial (amino acid metabolism)	1.5	0.01
Proteasome subunit beta type-8 (proteolysis)	1.5	0.01
Protein Serpinb9 (anti-apoptosis)	1.5	2.89×10^{-15}

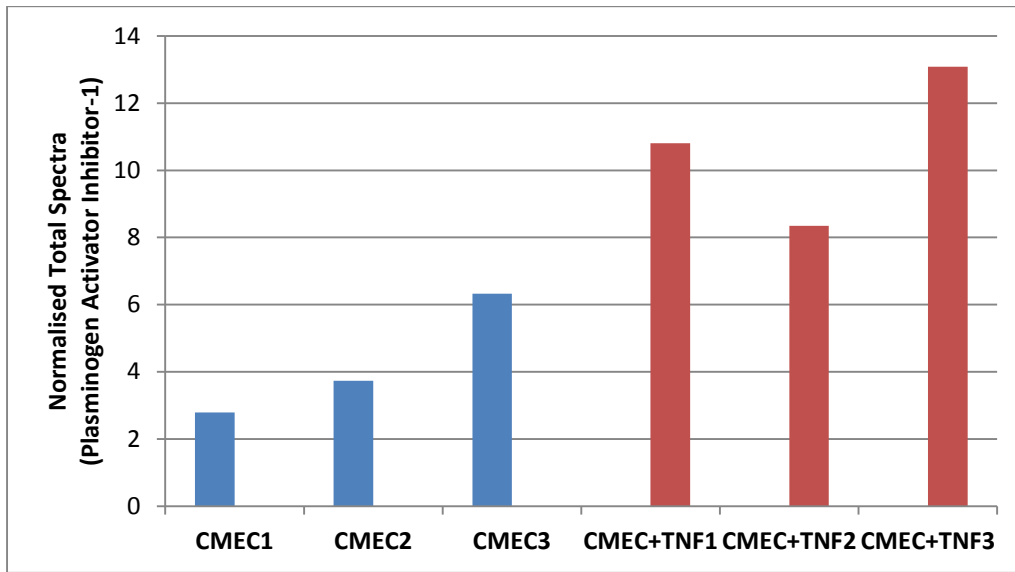


Figure 3.30 A: Graph showing the differentially regulated protein abundance (measured as normalised total spectra) of Plasminogen activator inhibitor-1 (PAI-1) in three TNF- α treated CMEC samples (CMEC+TNF1, CMEC+TNF2, CMEC+TNF3) compared to three control, untreated CMEC samples (CMEC1, CMEC2, CMEC3).

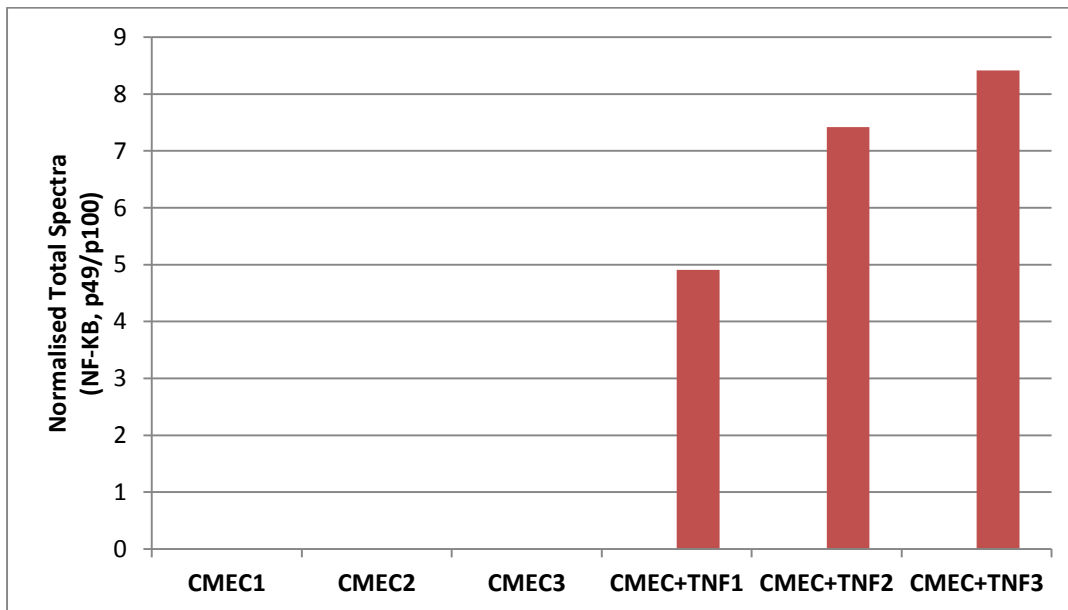


Figure 3.30 B: Graph showing the differentially regulated protein abundance (measured as normalised total spectra) of NF-KB p49/p100 in three TNF- α treated CMEC samples (CMEC+TNF1, CMEC+TNF2, CMEC+TNF3) compared to three control, untreated CMEC samples (CMEC1, CMEC2, CMEC3).

Table 3.10: Biological processes associated with strongly represented proteins in CMECs + TNF- α (vs control, untreated CMECs)

Term	Fold Enrichment	P-value
GO:0022614~membrane to membrane docking	112.4	0.02
GO:0046902~regulation of mitochondrial membrane permeability	76.6	0.0006
GO:0051881~regulation of mitochondrial membrane potential	46.8	0.04
GO:0001836~release of cytochrome c from mitochondria	40.1	0.002
GO:0008637~apoptotic mitochondrial changes	29.1	0.004
GO:0002478~antigen processing and presentation of exogenous peptide antigen	28.1	0.07
GO:0022407~regulation of cell-cell adhesion	26.8	0.07
GO:0007006~mitochondrial membrane organization	26.5	0.005
GO:0045429~positive regulation of nitric oxide biosynthetic process	25.6	0.07
GO:0007159~leukocyte adhesion	24.5	0.07
GO:0002474~antigen processing and presentation of peptide antigen via MHC class I	24.5	0.07
GO:0019884~antigen processing and presentation of exogenous antigen	22.5	0.08
GO:0048002~antigen processing and presentation of peptide antigen	21.6	0.008
GO:0022406~membrane docking	21.6	0.08
GO:0045428~regulation of nitric oxide biosynthetic process	20.8	0.08
GO:0006839~mitochondrial transport	17.9	0.01
GO:0019882~antigen processing and presentation	16.9	0.0002
GO:0050900~leukocyte migration	14.8	0.016
GO:0019221~cytokine-mediated signaling pathway	13.2	0.02
GO:0030335~positive regulation of cell migration	9.2	0.04
GO:0051272~positive regulation of cell motion	8.4	0.047
GO:0006916~anti-apoptosis	7.8	0.01
GO:0007005~mitochondrion organization	7.4	0.05
GO:0030155~regulation of cell adhesion	7.0	0.06
GO:0008283~cell proliferation	5.6	0.01
GO:0043069~negative regulation of programmed cell death	4.9	0.006
GO:0060548~negative regulation of cell death	4.9	0.006
GO:0006886~intracellular protein transport	4.9	0.02
GO:0006955~immune response	4.8	0.002
GO:0001775~cell activation	4.6	0.05
GO:0046907~intracellular transport	4.0	0.006
GO:0007155~cell adhesion	3.0	0.07

Functional annotation analysis of Cellular Components in TNF- α -treated CMECs vs control, untreated CMECs did not reveal any significant results.

3.2.2.3 Differential protein regulation and functional annotation analysis: Strongly represented proteins in TNF- α treated AECs compared to TNF- α treated CMECs

Differential protein regulation analysis showed that a total of 54 proteins (calculated by Scaffold software) and 112 proteins (calculated by Sieve software) respectively were up-regulated in TNF- α treated AECs vs. TNF- α treated CMECs (as determined by the minimum criteria of ≥ 1.5 -fold regulation and $p < 0.05$). Table 3.11 shows a list of the top up-regulated proteins in TNF- α treated AECs vs. TNF- α treated CMECs. In addition to the significantly up-regulated proteins, there were 146 proteins that were only detected in TNF- α treated CMECs.

Proteins that were up-regulated in TNF- α treated AECs compared to TNF- α treated CMECs include CD9 molecule (27.7-fold up-regulated; cell adhesion and migration), CD59 glycoprotein (19.2-fold up-regulated; immune response), D_3_phosphoglycerate dehydrogenase (10.6-fold up-regulated; oxidoreductase activity), Galectin (8.7-fold up-regulated; cell-cell interaction, cell-matrix adhesion, apoptosis), Legumain (5.9-fold up-regulated; lysosomal protein degradation, antigen presentation), Endothelin-converting enzyme 1 (5.2-fold up-regulated; endothelin-1 biosynthesis), Sequestosome_1 (3.6-fold up-regulated; activation of NF- κ B via TNF-receptor associated factor 6), Endothelial_specific_receptor_tyrosine_kinase (3.4-fold up-regulated; anti-apoptosis via PKB / Akt activation), NAD(P)H dehydrogenase [quinone] 1 (2.7-fold up-regulated; antioxidant activity), Glutathione reductase (1.9-fold up-regulated; glutathione reduction, antioxidant activity), Programmed cell death 6_interacting_protein (1.6-fold up-regulated; regulation of apoptosis and cell proliferation), Angiotensin_converting_enzyme (1.5-fold up-regulated; biosynthesis of angiotensin II), Caspase 8 (1.5-fold up-regulated, apoptosis) and Apoptosis regulator BAX (1.5-fold up-regulated; facilitates apoptosis) (Table 3.11). Graphical representation of differentially regulated protein abundance (measured as normalized total protein spectra) are shown below, where endothelin-converting enzyme 1 is up-regulated in TNF- α treated AECs compared to TNF- α treated CMECs (Figure 3.31 A), and aldehyde dehydrogenase L1 is only detected in TNF- α treated AECs compared to TNF- α treated CMECs (Figure 3.31 B).

Biological processes associated with strongly represented proteins in TNF- α treated AECs compared to TNF- α treated CMECs are shown in Table 3.12, and these include nucleotide-excision repair, DNA gap filling (36.5-fold enriched), DNA replication initiation (29.2-fold

enriched), response to reactive oxygen species (5.2-fold enriched), regulation of inflammatory response (4.8-fold enriched), regulation of cell migration (3.5-fold enriched), negative regulation of cell death (3.4-fold enriched), and regulation of cell death (2.4-fold enriched).

Cellular components that were enriched in TNF- α treated AECs compared to their CMECs counterparts include DNA replication factor C complex (39.5-fold enriched), sarcolemma (5-fold enriched), receptor complex (4.7-fold enriched), cytoplasmic vesicle membrane (4-fold enriched) and Golgi apparatus (2-fold enriched) (Table 3.13).

Table 3.11: List of up-regulated proteins in AECs + TNF- α (vs CMECs + TNF- α)

Identified proteins	Fold Up	P-value
CD9 molecule (cell adhesion and migration)	27.7	0.00001
CD59 glycoprotein (immune response)	19.2	1.9×10^{-13}
D_3_phosphoglycerate dehydrogenase (oxidoreductase activity)	10.6	9.9×10^{-20}
Galectin (cell-cell interaction, cell-matrix adhesion, apoptosis)	8.7	4.2×10^{-11}
Tyrosine-protein kinase (energy metabolism)	8.0	0.009
Embigin (cell adhesion)	7.6	1.6×10^{-14}
Biliverdin reductase A (glucose metabolism; cell growth and antioxidant)	7.5	2.3×10^{-7}
Legumain (lysosomal protein degradation; antigen presentation)	5.9	1.2×10^{-6}
Adenosine deaminase (immune response)	5.3	0.01
Endothelin-converting enzyme 1 (endothelin-1 biosynthesis)	5.2	0.003
Cytosolic 10_formyltetrahydrofolate dehydrogenase (oxidoreductase activity)	4.5	9.9×10^{-20}
Glutathione S_transferase mu 4 (glutathione binding and transferase activity)	4.3	1.3981E-05
Insulin-degrading enzyme (cleavage of polypeptides including insulin)	4.1	0.02
Importin subunit alpha (importation of proteins into the nucleus)	4.0	0.005
Integrin beta (cell adhesion)	3.9	1.9×10^{-6}
Asparagine synthetase [glutamine-hydrolyzing] (asparagine synthesis)	3.8	0.003
Protein Stom (regulation of ion channels)	3.8	1×10^{-7}
Sequestosome_1 (activates NF-KB via TRAF6)	3.6	9.9×10^{-20}
Cyclin-dependent kinase 1 (regulates cell cycle)	3.6	0.01
Fatty acid synthase (synthesis of long-chain fatty acids)	3.6	0.007
Catechol_O_methyltransferase (degradation of catecholamines)	3.6	4×10^{-8}
Fermt3 protein (cell-cell adhesion; leukocyte adhesion; plate aggregation)	3.5	0.008
Protein S100_A4 (cell cycle progression and differentiation)	3.5	0.0002
Endothelial_specific receptor tyrosine kinase (anti-apoptosis via PKB/Akt)	3.4	1×10^{-8}
DNA replication licensing factor MCM6 (DNA replication)	3.2	0.004
Protein Mcm2 (DNA replication)	3.1	0.009
Glutathione S_transferase Mu 1 (glutathione binding and transferase activity)	2.9	0.0009
Dusp3 protein (inactivation of mitogen activated protein kinases)	2.8	0.03
Protein Larp1 (cell growth and proliferation)	2.8	0.03
Protein Mcm4 (DNA replication)	2.8	0.04
Protein Cmp1 (immune response)	2.7	1×10^{-13}
NAD(P)H dehydrogenase [quinone] 1 (antioxidant activity)	2.7	9.9×10^{-20}
UDP_glucose 6_dehydrogenase (biosynthesis of extracellular matrix components)	2.7	6.9×10^{-6}
Protein Syne3 (cytoskeletal anchoring)	2.6	8×10^{-7}
Protein Lrrc32 (negative regulation of cytokine production)	2.6	1.8×10^{-9}
Anoctamin (anion transport and smooth muscle contraction)	2.6	0.03
Cb1-727 (DNA replication)	2.6	0.0004

Table 3.11 (continued): List of up-regulated proteins in AECs + TNF- α (vs CMECs + TNF- α)

Identified proteins	Fold Up	P-value
Protein Epb4112 (regulation of cell structural integrity)	2.6	0.02
Proliferating cell nuclear antigen (DNA replication)	2.4	9.9×10^{-20}
S100 calcium binding protein A10 (protein phosphorylation)	2.4	9.9×10^{-20}
Nuclear autoantigenic sperm protein (DNA replication and cell growth)	2.4	0.04
Peptidyl-prolyl cis-trans isomerase FKBP4 (Heat shock protein 90 binding)	2.4	0.02
Podocalyxin (cell adhesion and migration)	2.3	0.0007
Eukaryotic translation initiation factor 6 (ribosome binding)	2.2	1×10^{-16}
CTP synthase (DNA synthesis, immune response)	2.2	1.3×10^{-7}
Ribose_phosphate pyrophosphokinase 2 (nucleotide synthesis)	2.2	6.6×10^{-5}
FK506 binding protein (endocytosis, protein folding)	2.2	0.002
Tyrosine--tRNA ligase, cytoplasmic (interleukin-8 receptor binding)	2.2	0.001
Chloride intracellular channel protein 5 (ion absorption and secretion)	2.2	9×10^{-5}
Hypoxanthine_guanine phosphoribosyltransferase (nucleotide synthesis)	2.1	2.6×10^{-8}
Aldehyde dehydrogenase, dimeric NADP-preferring (detoxification; oxidation of toxic aldehydes)	2.1	0.03
Cysteinyl-tRNA synthetase (gene expression; protein synthesis)	2.1	0.001
Proteasome (Prosome, macropain) 26S subunit, non-ATPase, 5 (protein folding)	2.1	0.01
Ornithine aminotransferase_mitochondrial (amino acid biosynthesis)	2.1	2.5×10^{-15}
Neuronal guanine nucleotide exchange factor (activation of RhoA, Rac1 and CDC42)	2.0	0.005
Sodium_coupled neutral amino acid transporter 2 (ion and amino acid transport)	2.0	2.8×10^{-6}
Annexin (anticoagulant protein)	2.0	9.9×10^{-20}
Cysteine-rich protein 1 (zinc absorption and transport)	2.0	0.004
Phosphoserine aminotransferase (amino acid biosynthesis)	2.0	0.003
Tyrosine-protein phosphatase non-receptor type 23 (endosome sorting)	2.0	0.03
Glutamate cysteine ligase modifier subunit (glutathione synthesis)	2.0	0.0002
4F2 cell_surface antigen heavy chain (transport of L-arginine)	2.0	1.2×10^{-10}
Calpain_1 catalytic subunit (proteolysis of proteins associated with cytoskeletal remodelling)	2.0	1.1×10^{-6}
Tyrosine__tRNA ligase_cytoplasmic (interleukin-8 receptor binding)	2.0	1.4×10^{-6}
Glutathione reductase (glutathione reduction, antioxidant activity)	1.9	0.0002
Ribose_phosphate pyrophosphokinase 1 (nucleotide synthesis)	1.9	2.6×10^{-8}
Protein Thbd (endothelial cell receptor, thrombin reduction)	1.9	0.01
Copine 3 protein (membrane trafficking)	1.9	5.6×10^{-11}
Multidrug resistance protein 1a (resistance against drugs and toxins, transporter in blood-brain barrier)	1.8	1.4×10^{-14}
Protein DEK (chromatin organization)	1.8	7.8×10^{-11}
GMP synthase [glutamine_hydrolyzing] (guanine nucleotides synthase)	1.8	5.6×10^{-5}
Basic leucine zipper and W2 domain_containing protein 1 (transcription)	1.8	0.0005

Table 3.11 (continued): List of up-regulated proteins in AECs + TNF- α (vs CMECs + TNF- α)

Identified proteins	Fold Up	P-value
Isocitrate dehydrogenase [NADP]_ mitochondrial (energy metabolism)	1.8	9.9×10^{-20}
Minichromosome maintenance protein 7 (DNA replication)	1.8	7.6×10^{-6}
Acyl-CoA-binding protein (carrier of acyl-CoA esters, neuropeptide)	1.8	0.03
Phosphoribosylglycinamide formyltransferase (AMP and GMP formation)	1.8	0.03
Secretory carrier-associated membrane protein 1 (endocytosis)	1.8	0.001
Ataxin_10 (intracellular glycosylation homeostasis)	1.8	9.9×10^{-20}
Acyl_CoA thioesterase 7 (lipid homeostasis)	1.8	9.9×10^{-20}
G protein_coupled receptor_family C_group 5_member A	1.8	1.3×10^{-9}
Annexin A1 (exocytosis)	1.8	9.9×10^{-20}
Niban_like protein 1 (anti-apoptosis)	1.8	9.9×10^{-20}
Phospholipase D3 (cell death, lipid degradation)	1.7	2×10^{-14}
Programmed cell death 6_interacting protein (regulation of apoptosis and cell proliferation)	1.6	9.9×10^{-20}
Angiotensin_converting enzyme (biosynthesis of angiotensin II)	1.5	9.9×10^{-20}
Caspase 8 (apoptosis)	1.5	0.007
Apoptosis regulator BAX (facilitates apoptosis)	1.5	1.8×10^{-6}

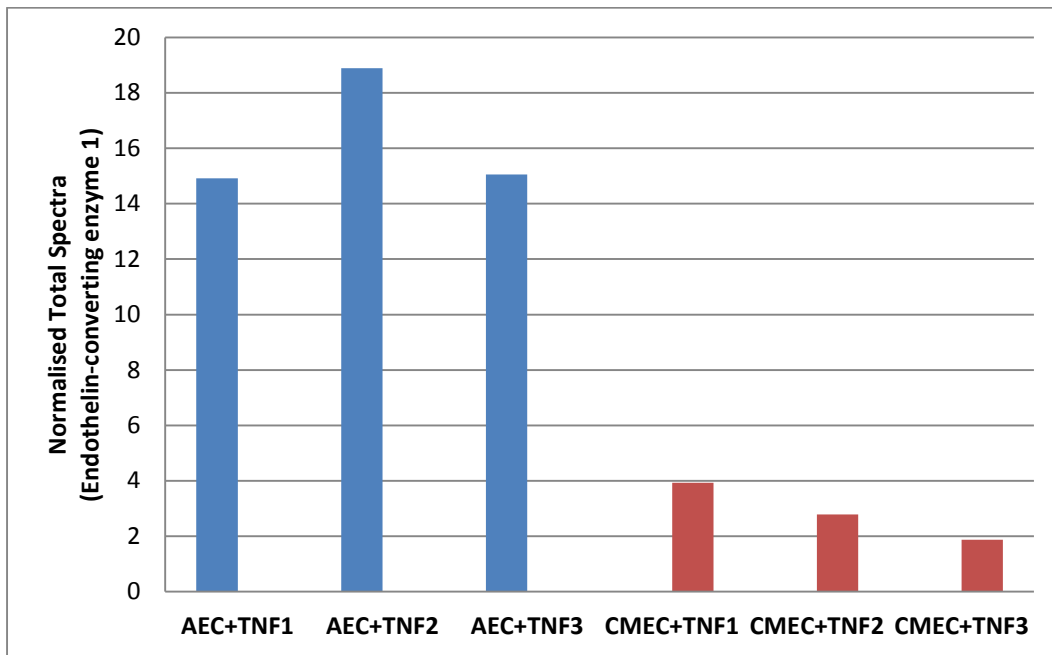


Figure 3.31 A: Graph showing the differentially regulated protein abundance (measured as normalised total spectra) of Endothelin-converting enzyme 1 in three TNF- α treated AEC samples (AEC+TNF1, AEC+TNF2, AEC+TNF3) compared to three TNF- α -treated CMEC samples (CMEC+TNF1, CMEC+TNF2, CMEC+TNF3).

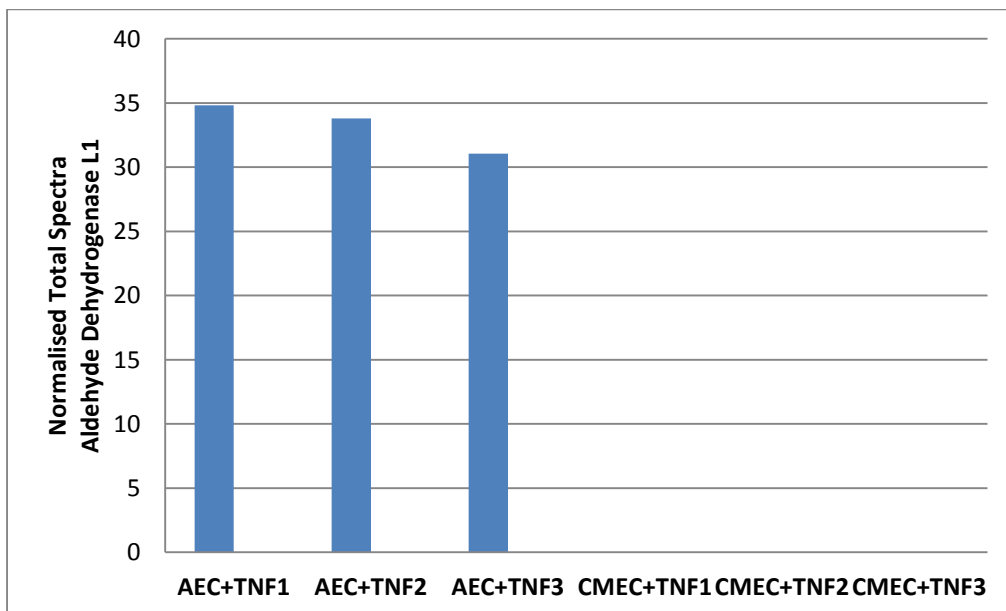


Figure 3.31 B: Graph showing the differentially regulated protein abundance (measured as normalised total spectra) of Aldehyde dehydrogenase L1 in three TNF- α treated AEC samples (AEC+TNF1, AEC+TNF2, AEC+TNF3) compared to three TNF- α -treated CMEC samples (CMEC+TNF1, CMEC+TNF2, CMEC+TNF3).

Table 3.12: Biological processes associated with strongly represented proteins in AECs + TNF- α (vs CMECs + TNF)

Term	Fold Enrichment	P-value
GO:0006297~nucleotide-excision repair, DNA gap filling	36.6	4×10^{-7}
GO:0006270~DNA replication initiation	29.3	0.004
GO:0046112~nucleobase biosynthetic process	29.3	0.004
GO:0043200~response to amino acid stimulus	12.2	0.004
GO:0000302~response to reactive oxygen species	5.3	0.01
GO:0016485~protein processing	4.9	0.02
GO:0050727~regulation of inflammatory response	4.8	0.047
GO:0046394~carboxylic acid biosynthetic process	4.6	0.004
GO:0006732~coenzyme metabolic process	4.3	0.005
GO:0006887~exocytosis	4.2	0.03
GO:0002252~immune effector process	4.0	0.03
GO:0006979~response to oxidative stress	3.7	0.01
GO:0006281~DNA repair	3.7	0.01
GO:0030334~regulation of cell migration	3.5	0.03
GO:0043066~negative regulation of apoptosis	3.5	0.00006
GO:0043069~negative regulation of programmed cell death	3.5	0.0007
GO:0060548~negative regulation of cell death	3.5	0.0007
GO:0033554~cellular response to stress	2.5	0.01
GO:0042981~regulation of apoptosis	2.4	0.001
GO:0043067~regulation of programmed cell death	2.4	0.001
GO:0010941~regulation of cell death	2.4	0.001

Table 3.13: Cellular components associated with strongly represented proteins in AECs + TNF- α (vs CMECs + TNF- α)

Term	Fold Enrichment	P-value
GO:0005663~DNA replication factor C complex	39.5	0.049
GO:0042383~sarcolemma	5.5	0.04
GO:0043235~receptor complex	4.7	0.02
GO:0045121~membrane raft	4.3	0.005
GO:0030659~cytoplasmic vesicle membrane	4.0	0.03
GO:0005635~nuclear envelope	3.6	0.02
GO:0009986~cell surface	3.2	0.002
GO:0012505~endomembrane system	2.2	0.01
GO:0005794~Golgi apparatus	2.1	0.02
GO:0005886~plasma membrane	1.4	0.02

3.2.2.4 Differential protein regulation and functional annotation analysis: Strongly represented proteins in TNF- α treated CMECs compared to TNF- α treated AECs

Differential protein regulation analysis showed that a total of 116 proteins (calculated by Scaffold software) and 150 proteins (calculated by Sieve software) respectively were up-regulated in TNF- α treated CMECs vs. TNF- α treated AECs (as determined by the minimum criteria of ≥ 1.5 -fold regulation and $p < 0.05$). Table 3.14 shows a list of the top up-regulated proteins in TNF- α treated CMECs vs. TNF- α treated AECs. In addition to the significantly up-regulated proteins, there were 166 proteins that were only detected in TNF- α treated CMECs.

Up-regulated proteins in TNF- α -treated CMECs (compared to TNF- α -treated AECs) include: Ectonucleoside triphosphate diphosphohydrolase 1 (75.2-fold enriched; inhibition of platelet aggregation), cGMP_dependent 3_5_cyclic phosphodiesterase (46.7-fold up-regulated; cAMP and cGMP activity), Protein LOC100909685 (34-fold up-regulated; motor activity), A1b (Fragment) (28.3-fold up-regulated; antigen presentation), Protein Lamc1 (20-fold up-regulated extracellular matrix), Prostaglandin G/H synthase 1 (16-fold up-regulated; prostanoids biosynthesis), Protein Pxdn (14.5-fold up-regulated; breakdown of hydrogen peroxide), Interleukin 1 family_member 6 (6.1-fold up-regulated; inflammatory cytokine), Procollagen_type XVIII_alpha 1 (6-fold up-regulated; cell adhesion, migration, apoptosis), Mitochondrial carrier homolog 2 (C. elegans) (5-fold up-regulated; mitochondrial membrane permeability and apoptosis), Rho guanine nucleotide exchange factor 2 (5-fold up-regulated; NF-KB activation, immune response), von Willebrand factor (5-fold up-regulated; pro-clotting factor), Platelet endothelial cell adhesion molecule (3.5-fold up-regulation; cell adhesion, leukocyte migration, platelet activation), Poly (ADP-ribose) polymerase family, member 3 (3.3-fold up-regulated; inflammatory gene expression and cell death), and Intercellular adhesion molecule 1 (3.1-fold up-regulated; leukocyte adhesion and migration) (Table 3.14).

Figure 3.32-A shows a graphical illustration of differentially regulated protein abundance of Platelet endothelial cell adhesion molecule in TNF- α treated CMECs compared to TNF- α treated AECs. Plexin D1 was only detected in TNF- α treated CMECs compared to TNF- α treated AECs, as shown by the differentially regulated protein abundance graph in Figure 3.32 B.

Biological processes (as determined by functional annotation analysis) that were significantly enriched in TNF- α treated CMECs compared to their AECs counterparts are listed in Table 3.15. These include actin filament severing (83.3-fold enriched), peptide antigen transport (83.3-fold enriched), protection from natural killer cell mediated cytotoxicity (55.5-fold enrichment), release of cytochrome c from mitochondria (11.9-fold enriched), apoptotic mitochondrial changes (8.6-fold enriched), and glutathione metabolic process (8.6-fold enriched). Table 3.16 shows the cellular components associated with strongly represented proteins in TNF- α treated CMECs vs. TNF- α treated AECs, which include: MHC class I peptide loading complex (58.1-fold enriched), integral to mitochondrial inner membrane (51.6-fold enriched), and endoplasmic reticulum lumen (11-fold enriched).

Table 3.14: List of up-regulated proteins in CMECs + TNF- α (vs AECs + TNF- α)

Identified proteins	Fold Up	P-value
Ectonucleoside triphosphate diphosphohydrolase 1 (inhibition of platelet aggregation)	75.2	8×10^{-14}
cGMP_dependent 3_5_cyclic phosphodiesterase (cAMP and cGMP activity)	46.7	0.00005
Protein LOC100909685 (motor activity)	34.0	0.003
A1b (Fragment) (antigen presentation)	28.3	9.9×10^{-20}
Protein Lamc1 (extracellular matrix)	20.0	0.001
Prostaglandin G/H synthase 1 (prostanoids biosynthesis)	16.0	9.9×10^{-20}
Scinderin (exocytosis)	15.1	0.015
Antigen_presenting glycoprotein CD1d (immune response)	14.9	1.5×10^{-8}
Protein Pxdn (breakdown of hydrogen peroxide)	14.5	9.9×10^{-20}
Elongation factor Tu_mitochondrial (protein synthesis)	12.5	1.9×10^{-15}
Laminin, alpha 5 (extracellular matrix)	11.1	0.0001
Plexin D1 (cell migration)	10.1	2.5×10^{-14}
Liver carboxylesterase 4 (hydrolase activity, detoxification processes)	10.0	0.0003
1_phosphatidylinositol 4_5_bisphosphate phosphodiesterase gamma_2 (transmembrane signalling)	8.8	0.003
Protein Hspg2 (extracellular matrix)	6.5	9.9×10^{-20}
Interleukin 1 family_member 6 (inflammatory cytokine)	6.1	0.01
Procollagen_type XVIII_alpha 1 (cell adhesion; migration; apoptosis)	6.0	9.9×10^{-20}
Unconventional myosin_Id (microfilament movements)	5.6	4.7×10^{-11}
Nidogen_1 (extracellular matrix binding)	5.3	0.004
Protein Alyref (gene expression)	5.3	2.1×10^{-8}
Ab2-417 (ferric ion binding)	5.0	0.001
AMP deaminase 3 (energy metabolism)	5.0	0.0003
LOC679149 protein (hydrolase activity)	5.0	0.0001
LOC683667 protein (calcium ion binding)	5.0	0.01
Mitochondrial carrier homolog 2 (C. elegans) (mitochondrial membrane permeability and apoptosis)	5.0	0.03
Neutral cholesterol ester hydrolase 1 (hydrolysis, lipid degradation)	5.0	0.009
Protein Cgnl1 (motor activity)	5.0	0.006
Protein Ptpn12 (protein dephosphorylation)	5.0	0.009
Protein Tjp1 (cell-cell junction assembly, apoptosis)	5.0	0.001
Rho guanine nucleotide exchange factor 2 (NF-KB activation)	5.0	0.005
von Willebrand factor (pro-clotting factor)	5.0	0.002
Protein phosphatase 1F (PP2C domain containing) (apoptosis)	4.1	9.9×10^{-20}
Acyl_protein thioesterase 2 (lipid hydrolysis)	3.8	0.0009
Platelet endothelial cell adhesion molecule (cell adhesion; leukocyte migration; platelet activation)	3.5	9.9×10^{-20}
Activated RNA polymerase II transcriptional coactivator p15 (transcription)	3.5	8.7×10^{-15}

Table 3.14 (continued): List of up-regulated proteins in CMECs + TNF- α (vs AECs + TNF- α)

Identified proteins	Fold Up	P-value
BH3 interacting domain death agonist (apoptosis)	3.4	4.1 x 10 ⁻¹¹
2'-5' oligoadenylate synthetase 1K (immune response; antiviral enzyme)	3.3	0.02
A-kinase anchor protein 2 (PKA binding protein)	3.3	0.005
Arhgef7 protein (Fragment) (membrane ruffling; cell attachment and migration)	3.3	0.02
Cathepsin L1 (lysosomal protein degradation)	3.3	0.03
Ddx17 protein (regulation of transcription)	3.3	0.01
Laminin subunit beta-2 (cell attachment, migration and organization)	3.3	0.004
Lipoma-preferred partner homolog (cell adhesion)	3.3	0.01
Mitochondrial carnitine/acylcarnitine carrier protein (shuttling of acylcarnitines during fatty acid oxidation)	3.3	0.03
Poly (ADP-ribose) polymerase family, member 3 (inflammatory genes expression and cell death)	3.3	0.002
SH3 and multiple ankyrin repeat domains protein 3 (dendritic spine and synapse formation)	3.3	0.03
SPARC (regulation of cell growth)	3.3	0.0003
Vasp protein (cytoskeletal remodelling)	3.3	0.03
Rho GTPase activating protein 29 (attenuates RhoA signalling)	3.2	0.0005
Coactosin like protein (actin binding protein, actin cytoskeleton regulation)	3.2	8.5 x 10 ⁻⁷
Intercellular adhesion molecule 1 (leukocyte adhesion and migration)	3.1	6 x 10 ⁻⁷
Peroxiredoxin_6 (redox regulation; reduction of hydrogen peroxide)	3.1	9.9 x 10 ⁻²⁰
Protein Tapbp (immune response)	3.1	9.9 x 10 ⁻²⁰
Guanylate binding protein 2 (immune response)	3.1	9.9 x 10 ⁻²⁰
Plasminogen activator inhibitor 1 (inhibition of fibrinolysis)	2.9	5.2 x 10 ⁻⁶
Protein LOC100912203 (redox regulation)	2.9	1.6 x 10 ⁻¹⁰
Protein Gbp5 (inflammatory response)	2.9	9.9 x 10 ⁻²⁰
Guanine nucleotide binding protein subunit gamma (Fragment) (G-protein coupled receptor signalling)	2.8	1.6 x 10 ⁻⁶
Dedicator of cytokinesis 6 (guanine nucleotide exchange factor)	2.7	0.0005
Canopy 4 homolog (Zebrafish)	2.7	0.000001
Calmodulin (calcium binding, enzymatic stimulation)	2.5	9.9 x 10 ⁻²⁰
15 kDa selenoprotein (redox regulation; regulation of protein folding)	2.5	0.03
1-phosphatidylinositol 4,5-bisphosphate phosphodiesterase gamma-1 (cell migration)	2.5	0.01
3'(2'),5'-bisphosphate nucleotidase 1 (hydrolysis of adenosine 3',5' biphosphate)	2.5	0.03
3-ketoacyl-CoA thiolase, mitochondrial (anti-apoptosis; anti-mitochondrial damage)	2.5	0.01
Arylsulfatase B (breakdown of sulfates)	2.5	0.005
C-terminal-binding protein 2 (transcription repressor)	2.5	0.03

Table 3.14 (continued): List of up-regulated proteins in CMECs + TNF- α (vs AECs + TNF- α)

Identified proteins	Fold Up	P-value
Fermitin family homolog 2 (Drosophila) (cell-extracellular matrix adhesion)	2.5	0.01
Gba protein (anti-inflammation)	2.5	0.01
GDP-mannose 4, 6-dehydratase (mannose metabolism)	2.5	0.003
Granulin (inflammatory response)	2.5	0.004
Heat shock protein 70kDa 12B (stress response)	2.5	0.009
Protein Col4a1 (anti-angiogenesis)	2.5	0.01
Protein FAM65A	2.5	0.02
Protein Smarcc2 (gene transcription)	2.5	0.008
Protein Tmtc3 (cell development)	2.5	0.03
Sideroflexin-1 (iron component transport)	2.5	0.006
UDP-glucose 4-epimerase (carbohydrate metabolism)	2.5	0.008
V-type proton ATPase subunit B, brain isoform (cell acidification)	2.5	0.003
Hsc70_interacting protein (interaction of heat shock protein 90 and 70)	2.4	1.3×10^{-11}
APEX (Fragment)	2.4	4×10^{-8}
Tricarboxylate transport protein_mitochondrial (energy metabolism)	2.4	0.00002
Astrocytic phosphoprotein PEA_15 (anti-apoptosis)	2.4	7.4×10^{-9}
LIM and senescent cell antigen_like domains 1 isoform E (cell adhesion)	2.4	0.000001
Gelsolin (actin filament assembly, anti-apoptosis)	2.1	9.9×10^{-20}
Glutathione peroxidase (anti-oxidative; reduction of hydrogen peroxide)	2.1	2.6×10^{-5}
Lactadherin (phagocytic clearance of apoptotic cells)	2.1	5.5×10^{-12}

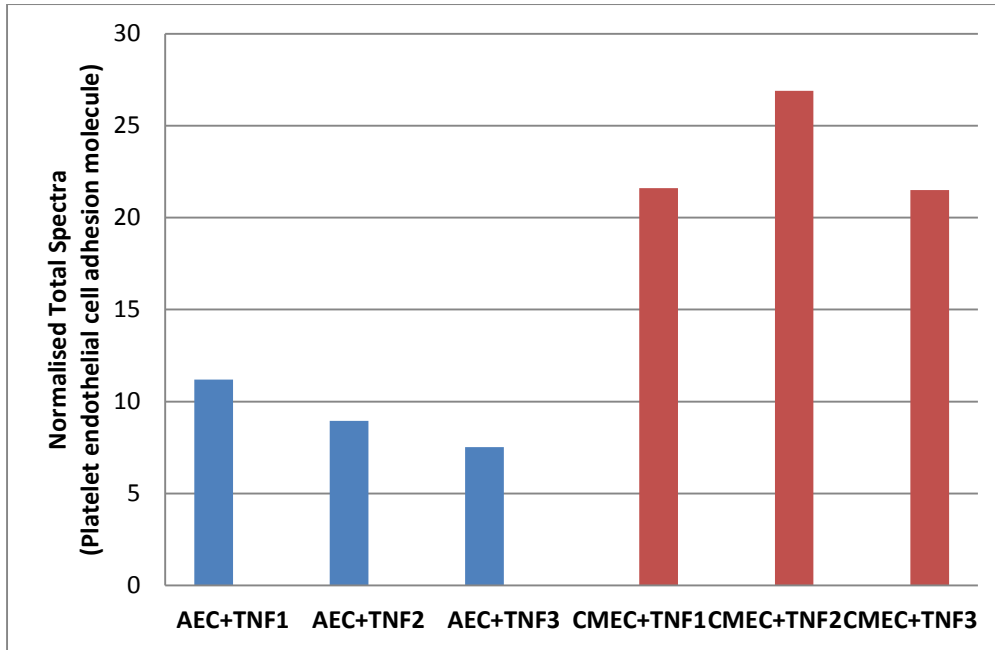


Figure 3.32 A: Graph showing the differentially regulated protein abundance (measured as normalised total spectra) of Platelet endothelial cell adhesion molecule in three TNF- α treated CMEC samples (CMEC+TNF1, CMEC+TNF2, CMEC+TNF3) compared to three TNF- α -treated AEC samples (AEC+TNF1, AEC+TNF2, AEC+TNF3).

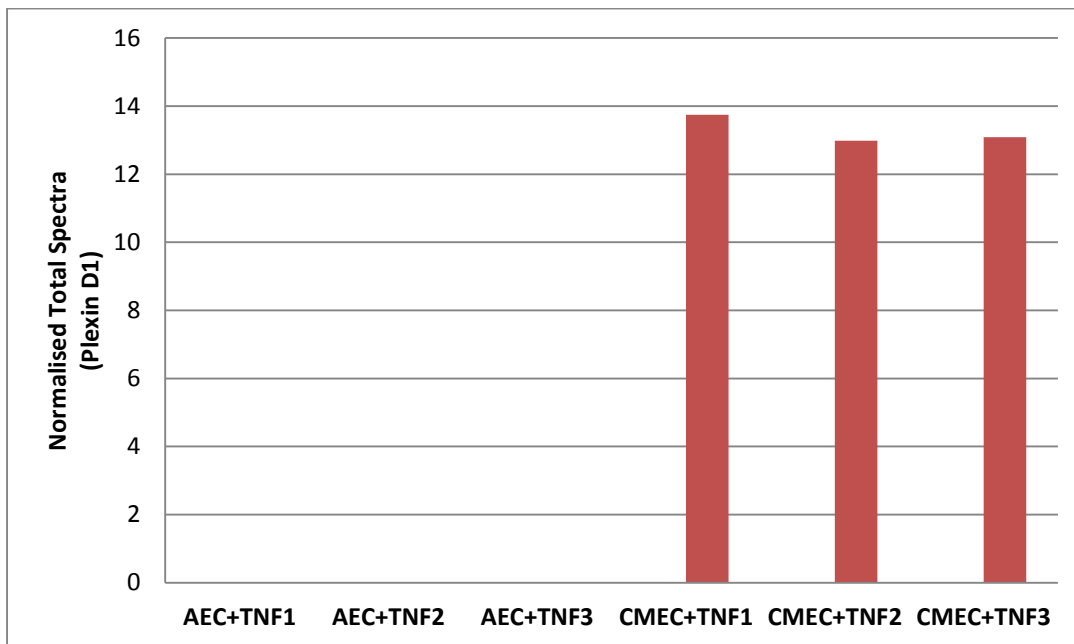


Figure 3.32 B: Graph showing the differentially regulated protein abundance (measured as normalised total spectra) of Plexin D1 in three TNF- α treated CMEC samples (CMEC+TNF1, CMEC+TNF2, CMEC+TNF3) compared to three TNF- α -treated AEC samples (AEC+TNF1, AEC+TNF2, AEC+TNF3).

Table 3.15: Biological processes associated with strongly represented proteins in CMECs + TNF- α (vs AECs + TNF- α)

Term	Fold Enrichment	P-value
GO:0051014~actin filament severing	83.4	0.02
GO:0046968~peptide antigen transport	83.4	0.02
GO:0042270~protection from natural killer cell mediated cytotoxicity	55.6	0.04
GO:0019883~antigen processing and presentation of endogenous antigen	55.6	0.04
GO:0002475~antigen processing and presentation via MHC class Ib	41.7	0.002
GO:0001916~positive regulation of T cell mediated cytotoxicity	20.8	0.008
GO:0019884~antigen processing and presentation of exogenous antigen	16.7	0.0002
GO:0001914~regulation of T cell mediated cytotoxicity	16.7	0.01
GO:0002711~positive regulation of T cell mediated immunity	12.5	0.02
GO:0001836~release of cytochrome c from mitochondria	11.9	0.02
GO:0006099~tricarboxylic acid cycle	11.4	0.03
GO:0046356~acetyl-CoA catabolic process	10.9	0.03
GO:0001912~positive regulation of leukocyte mediated cytotoxicity	10.4	0.03
GO:0019882~antigen processing and presentation	10.0	5.8×10^{-7}
GO:0006695~cholesterol biosynthetic process	10.0	0.03
GO:0022406~membrane docking	9.6	0.04
GO:0031341~regulation of cell killing	9.5	0.008
GO:0009060~aerobic respiration	9.3	0.04
GO:0008637~apoptotic mitochondrial changes	8.6	0.046
GO:0006749~glutathione metabolic process	8.6	0.046
GO:0006839~mitochondrial transport	7.1	0.02
GO:0034637~cellular carbohydrate biosynthetic process	5.1	0.04
GO:0016042~lipid catabolic process	3.7	0.02
GO:0055114~oxidation reduction	2.3	0.002

Table 3.16: Cellular components associated with strongly represented proteins in CMECs + TNF- α (vs AECs + TNF- α)

Term	Fold Enrichment	P-value
GO:0042824~MHC class I peptide loading complex	58.9	0.0009
GO:0031305~integral to mitochondrial inner membrane	51.7	0.04
GO:0005788~endoplasmic reticulum lumen	11.1	0.000006
GO:0000502~proteasome complex	5.7	0.03
GO:0044432~endoplasmic reticulum part	5.0	2.2×10^{-7}
GO:0044455~mitochondrial membrane part	4.6	0.02
GO:0005743~mitochondrial inner membrane	4.1	0.00001
GO:0031980~mitochondrial lumen	3.9	0.001
GO:0005759~mitochondrial matrix	3.9	0.001
GO:0005792~microsome	3.8	0.0001
GO:0042598~vesicular fraction	3.7	0.0002
GO:0000323~lytic vacuole	3.3	0.01
GO:0005764~lysosome	3.3	0.01
GO:0005773~vacuole	2.8	0.04
GO:0005768~endosome	2.6	0.03
GO:0005624~membrane fraction	1.9	0.009

3.3 Rat aortic ring isometric tension studies (*ex vivo* studies)

3.3.1 Biometric data

Total rat body weight

Male Wistar rats were placed on a high fat (HFD) diet or normal rat chow diet for 16 and 24 weeks respectively. At 16 weeks, HFD rats weighed significantly more compared to their time-matched lean controls: Lean (423.6 ± 13.23 g) vs. HFD (497.7 ± 9.9 g), $p < 0.05$, $N = 15$ (Figure 3.33). Similarly at 24 weeks, HFD rats exhibited significantly greater total body weights compared to time-matched lean control rats: Lean (434 ± 5.9 g) vs. HFD (503.7 ± 8.5 g), $p < 0.05$, $N = 33$ (Figure 3.34).

Intra-peritoneal fat weight

At 16 weeks, the intra-peritoneal (IP) fat weight was ~ 2-fold greater in HFD rats compared to lean control rats: Lean (11.7 ± 1.1 g) vs. HFD (22.6 ± 1.4 g), $p < 0.05$, $N = 10$ (Figure 3.35). Similar differences were observed for rats on the 24 week diet: Lean (21.4 ± 0.9 g) vs. HFD (39.7 ± 1.5), $p < 0.05$, $N = 33$ (Figure 3.36).

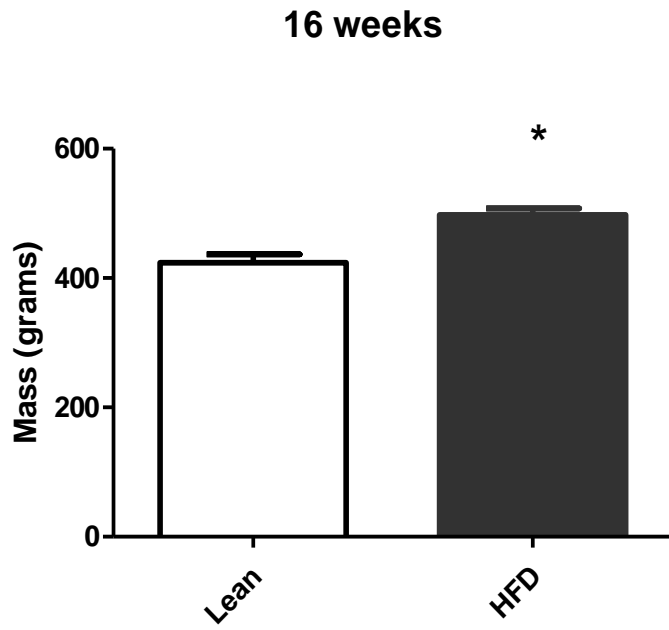


Figure 3.33: Total body weights of lean and HFD rats after 16 weeks. * $p < 0.05$ Lean vs. HFD.

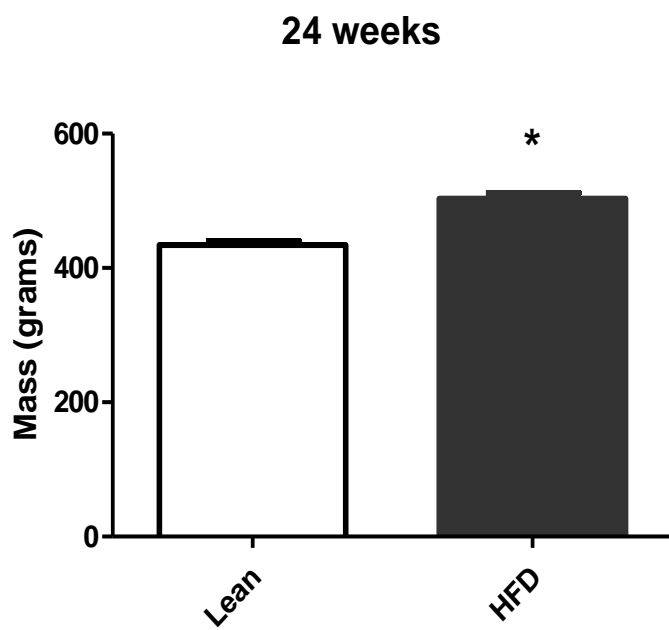


Figure 3.34: Total body weights of lean and HFD rats after 24 weeks. * $p < 0.05$ Lean vs. HFD.

16 weeks IP fat mass

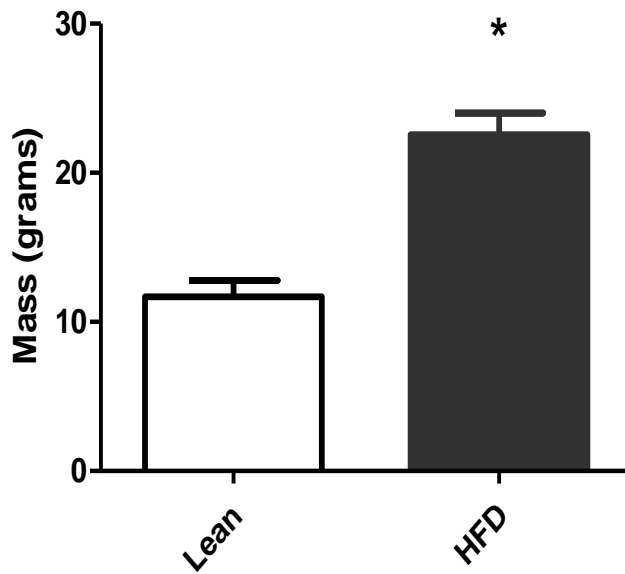


Figure 3.35: Intra-peritoneal fat mass in lean and HFD rats after 16 weeks. * $p < 0.05$ Lean vs. HFD.

24 weeks IP fat mass

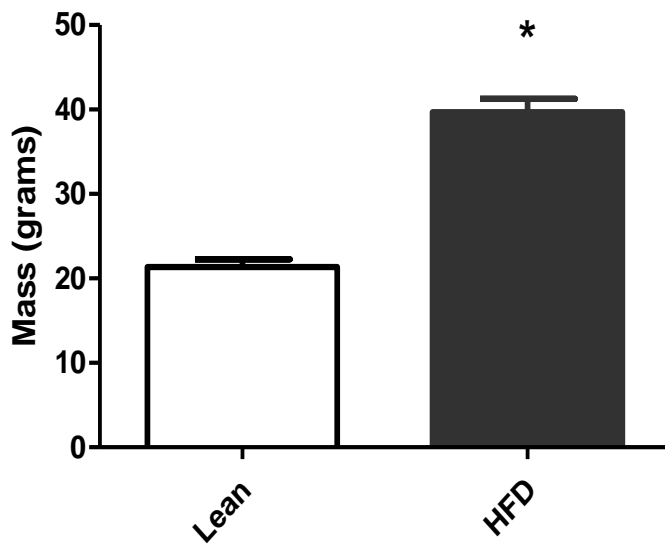


Figure 3.36: Intra-peritoneal fat mass in lean and HFD rats after 24 weeks. * $p < 0.05$ Lean vs. HFD.

3.3.2 Baseline isometric tension studies in aortic rings from Lean and HFD (16 weeks)

Aortic rings isolated from HFD rats showed pro-contractile effects in response to phenylephrine (PE) administration compared to aortic rings isolated from lean rats ($p = 0.0012$, $N = 7$) (Figure 3.37). However, there were no significant differences observed in acetylcholine (Ach)-induced relaxation in aortic rings isolated from HFD rats compared to lean rats (Figure 3.38).

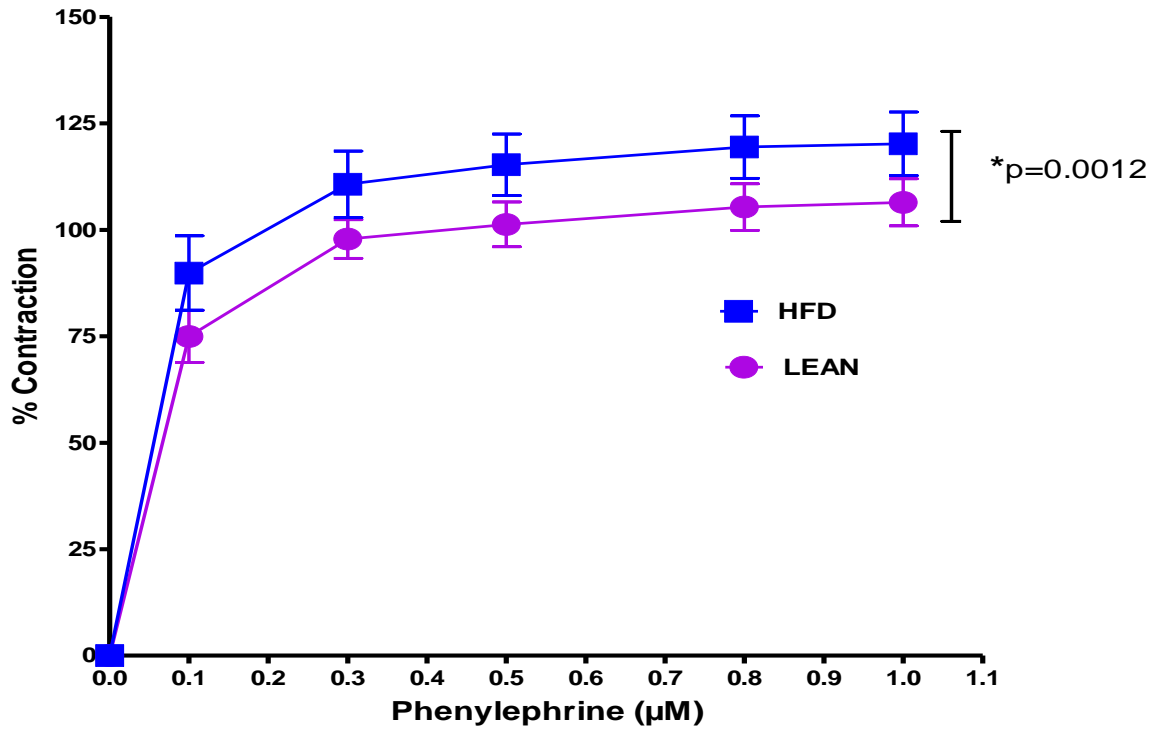


Figure 3.37: Phenylephrine-induced aortic ring contraction in lean and HFD groups (16 weeks).

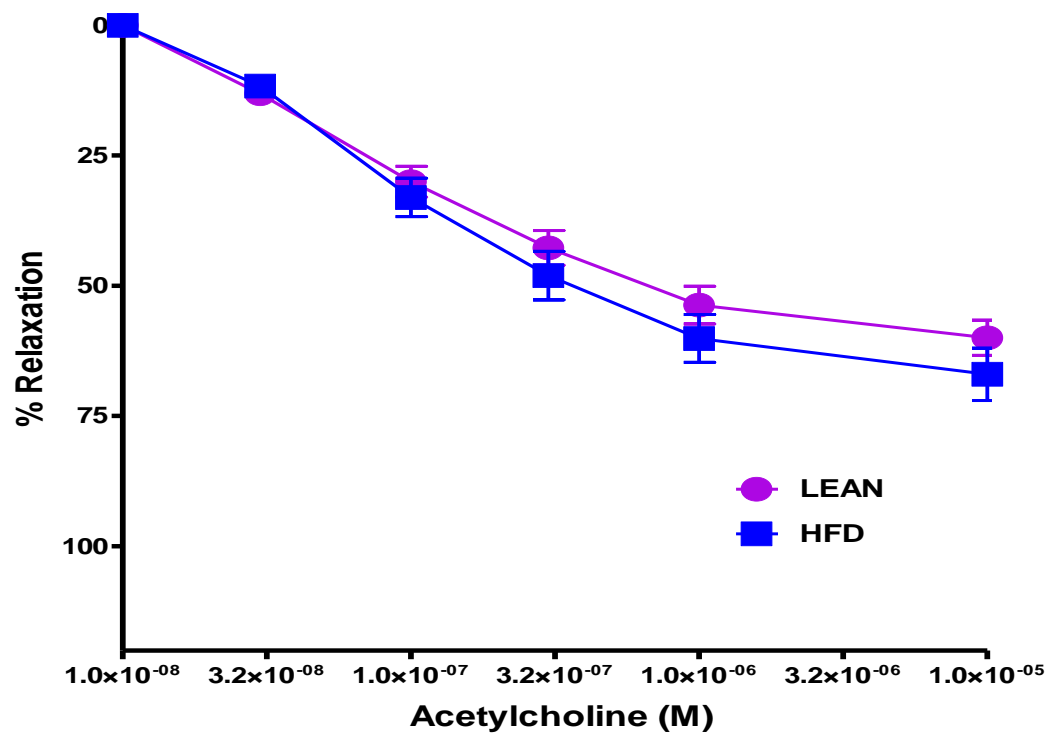


Figure 3.38: Acetylcholine-induced aortic ring relaxation in lean and HFD groups (16 weeks).

3.3.3 Effects of *ex vivo* oleanolic acid (OA) administration on aortic ring contraction and relaxation from lean and HFD rats (16 weeks)

3.3.3.1 OA administration (aortic rings from lean rats)

OA was administered into the organ bath 15 minutes prior to the standard PE-induced contraction and Ach-induced relaxation protocol. Although a pro-contractile response to PE was observed in aortic rings exposed to OA administration compared to control rings ($p = 0.02$, $N = 4-9$ per group), the rings receiving DMSO vehicle administration demonstrated a similar pro-contractile effect, which was not significantly different from the OA rings. Therefore it appears as if the response observed in the OA pre-treatment rings was due to a vehicle effect rather than the drug *per se* (Figure 3.39). The Ach-induced relaxation data showed that there were no significant differences between any of the groups ($p > 0.05$, $N = 4-9$ per group) (Figure 3.40).

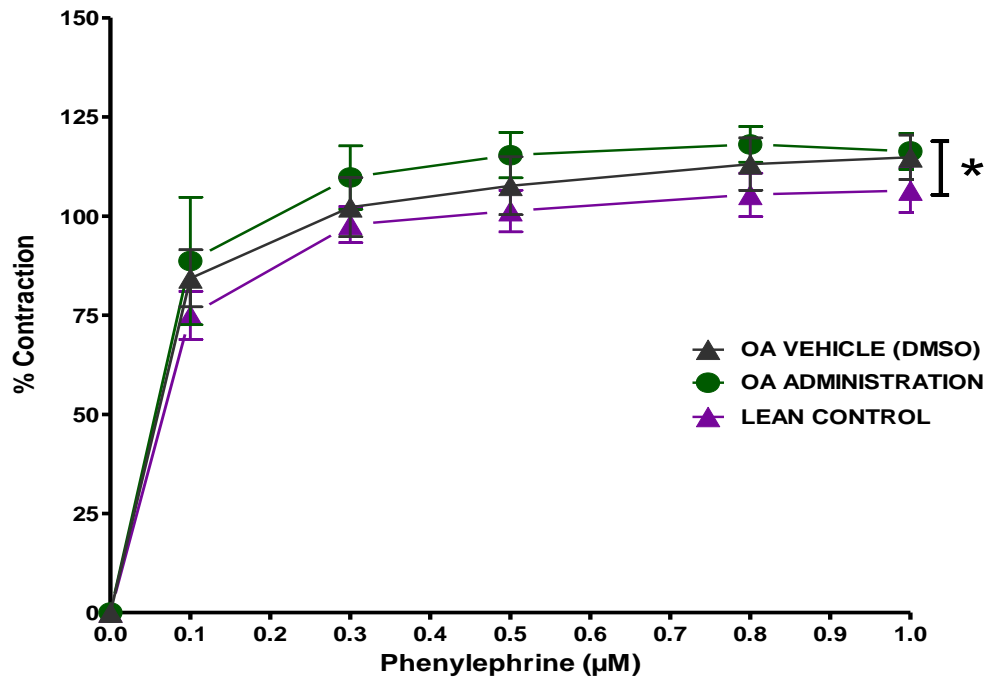


Figure 3.39: Phenylephrine-induced contraction in aortic rings from lean animals (16 weeks) exposed to OA administration. *p = 0.02: OA administration vs. lean control.

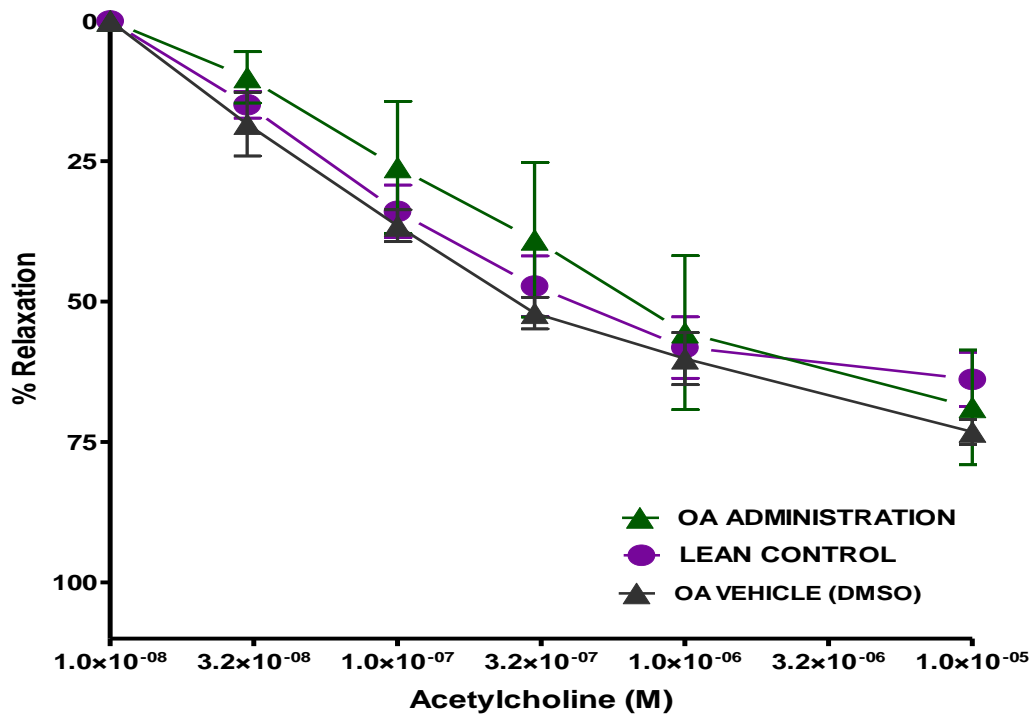


Figure 3.40: Acetylcholine-induced relaxation in aortic rings from lean animals (16 weeks) exposed to OA administration.

3.3.3.2 OA administration (aortic rings from HFD rats)

In the aortic rings of HFD rats, OA administration prior to the PE protocol induced significant anti-contraction effects compared to HFD control rings, which was not influenced by the vehicle ($p = 0.03$ $N = 4-9$ per group) (Figure 3.41). The Ach-induced relaxation data showed that there were no significant differences between any of the groups (Figure 3.42).

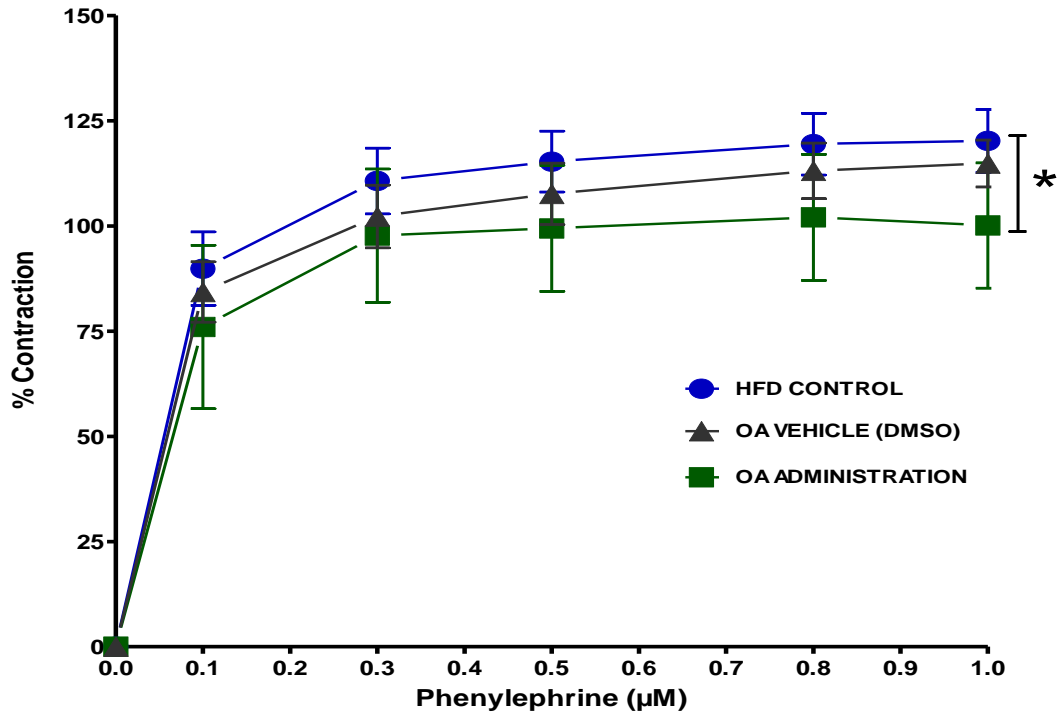


Figure 3.41: Phenylephrine-induced contraction in aortic rings from HFD animals (16 weeks) exposed to OA administration. *p = 0.03: OA administration vs. HDF control.

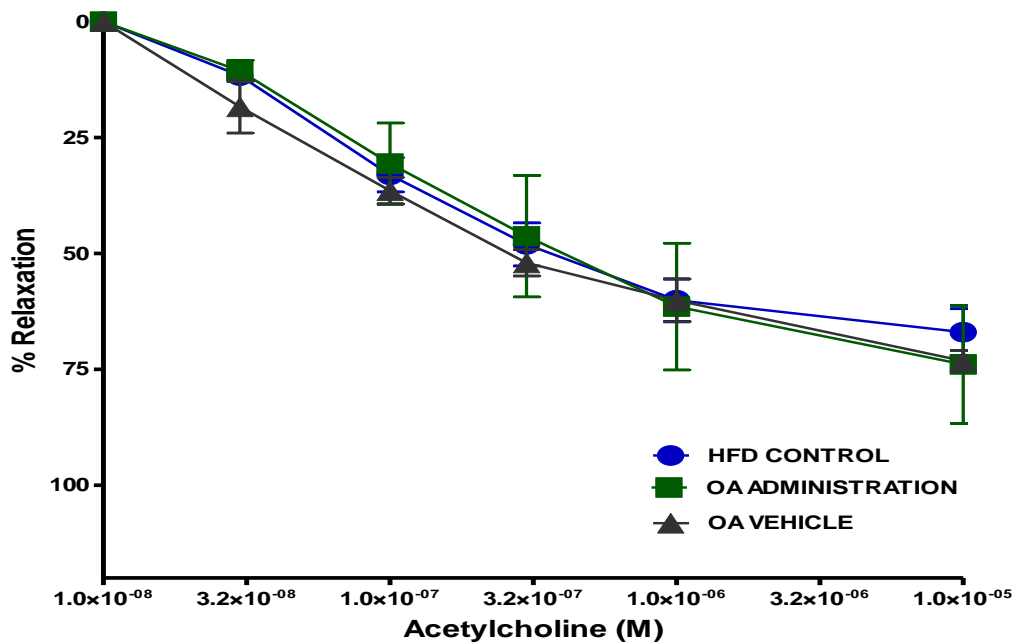


Figure 3.42: Acetylcholine-induced relaxation in aortic rings from HFD animals (16 weeks) exposed to OA administration.

3.3.4 Effects of *ex vivo* oleanolic acid (OA) administration on aortic ring contraction and relaxation from lean and HFD rats (24 weeks)

3.3.4.1 OA administration (aortic rings from lean rats)

OA administration resulted in a significantly anti-contractile response in aortic rings from lean rats compared to control rings ($p < 0.0001$ $N = 4-7$). Although the graphs may suggest that a vehicle effect was at play, statistical analysis showed that the areas under the curve of the OA pre-treatment and vehicle groups differed significantly, which indicated an additive effect exerted by OA *per se* (Figure 3.43). From the relaxation data, it is clear that OA administration exerted significant pro-relaxation responses compared to both lean control and vehicle-treated rings ($p = 0.007$ $N = 4-7$) (Figure 3.44). As a general observation, the % ACh-induced relaxation in the rings of the lean control animals was poor (<50 % relaxation at the final cumulative ACh concentration). This was most likely due age-dependent factors, as is clearly demonstrated when compared to the relaxation of control rings isolated from younger rats (± 4 weeks old) (Figure 3.44).

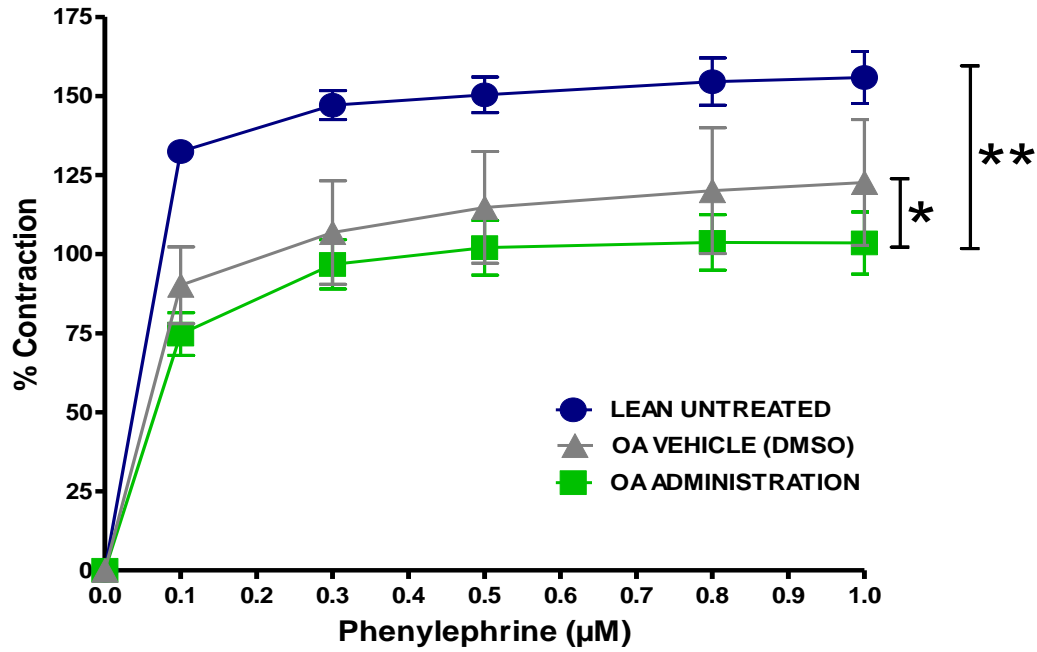


Figure 3.43: Phenylephrine-induced contraction in aortic rings from lean animals (24 weeks) exposed to OA administration. * $p = 0.05$: OA administration vs. vehicle (DMSO), ** $p < 0.0001$: OA administration vs. lean control.

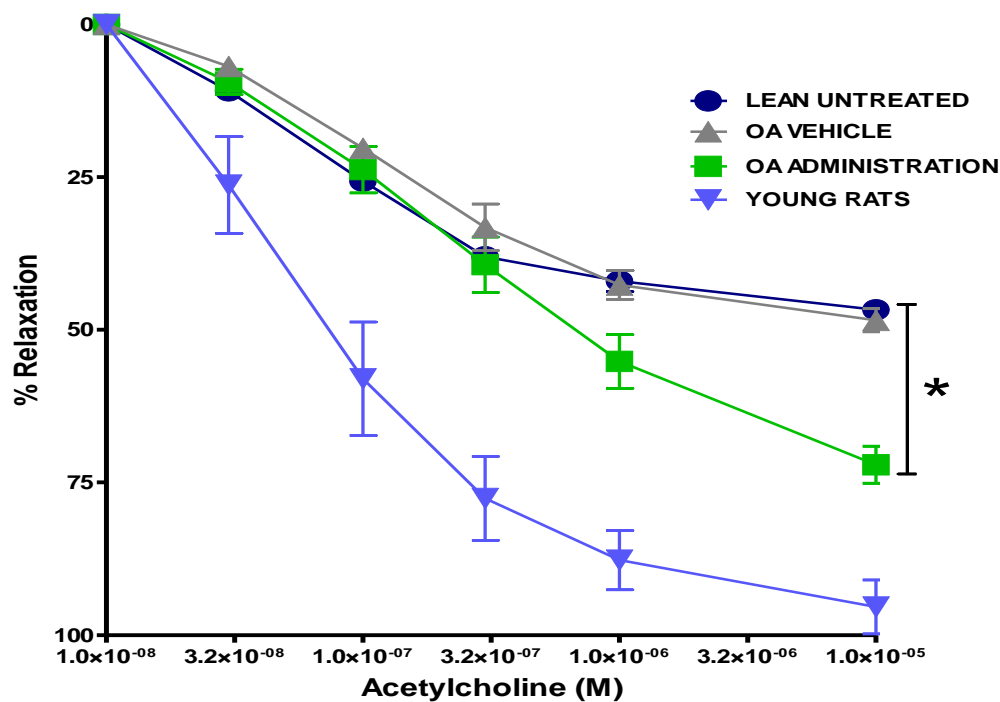


Figure 3.44: Acetylcholine-induced relaxation in aortic rings from lean animals (24 weeks) exposed to OA administration. * $p = 0.007$: OA administration vs. lean control vs. OA vehicle (DMSO).

3.3.4.2 OA administration (aortic rings from HFD rats)

Although OA administration resulted in pro-contractile effects in aortic rings isolated from HFD rats (24 weeks), this response was due to a vehicle effect exerted by the DMSO vehicle (Figure 3.45). Ach-induced relaxation was significantly impaired in aortic rings exposed to OA administration compared to HFD control rings ($p < 0.0001$, $N = 4-8$ per group) (Figure 3.46).

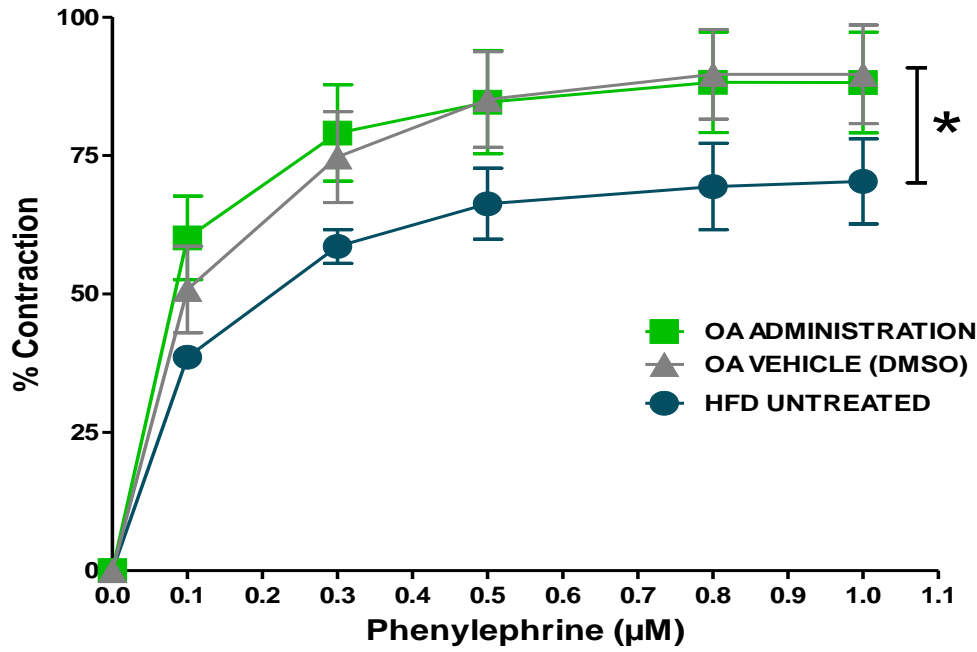


Figure 3.45: Phenylephrine-induced contraction in aortic rings from HFD animals (24 weeks) exposed to OA administration. * p = 0.003: OA administration and OA vehicle (DMSO) vs. HFD control rings.

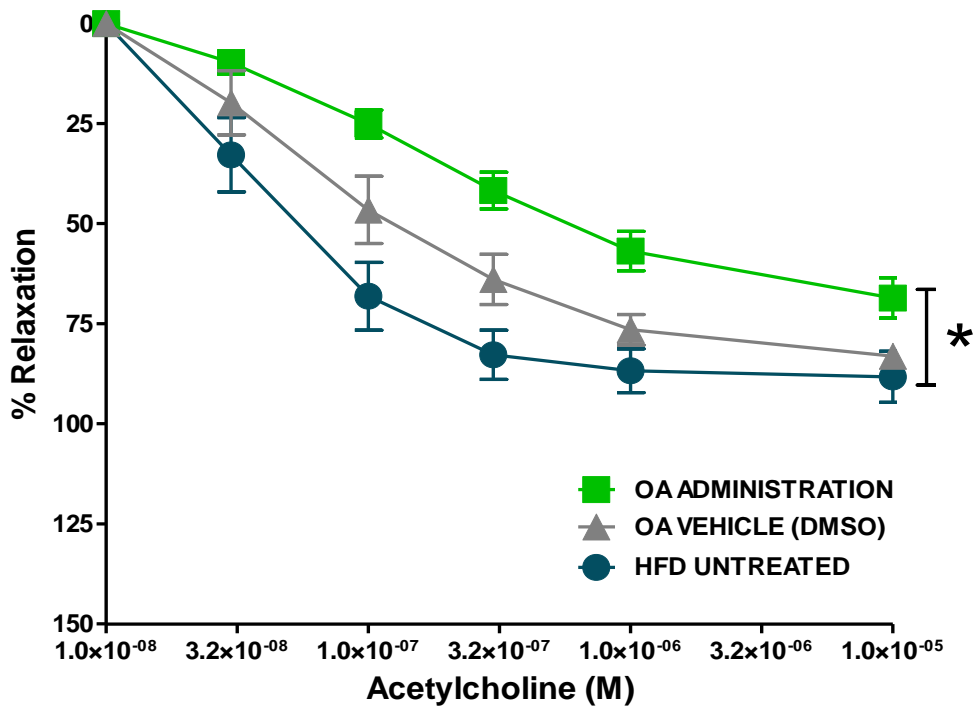


Figure 3.46: Acetylcholine-induced relaxation in aortic rings from HFD animals (24 weeks) exposed to OA administration. *p < 0.0001: OA administration vs. HFD control rings.

3.3.5 Effects of direct OA administration on rat aortic rings (24 weeks)

To assess the direct effects OA on aortic ring relaxation, the routine Ach administration protocol was replaced with three aliquots of OA administered into the organ bath in a cumulative fashion (10, 10 and 20 μM ; final concentration: 40 μM) following pre-contraction with phenylephrine. The results showed that direct OA administration had no relaxing effects on lean or HFD rats (Figure 3.47).

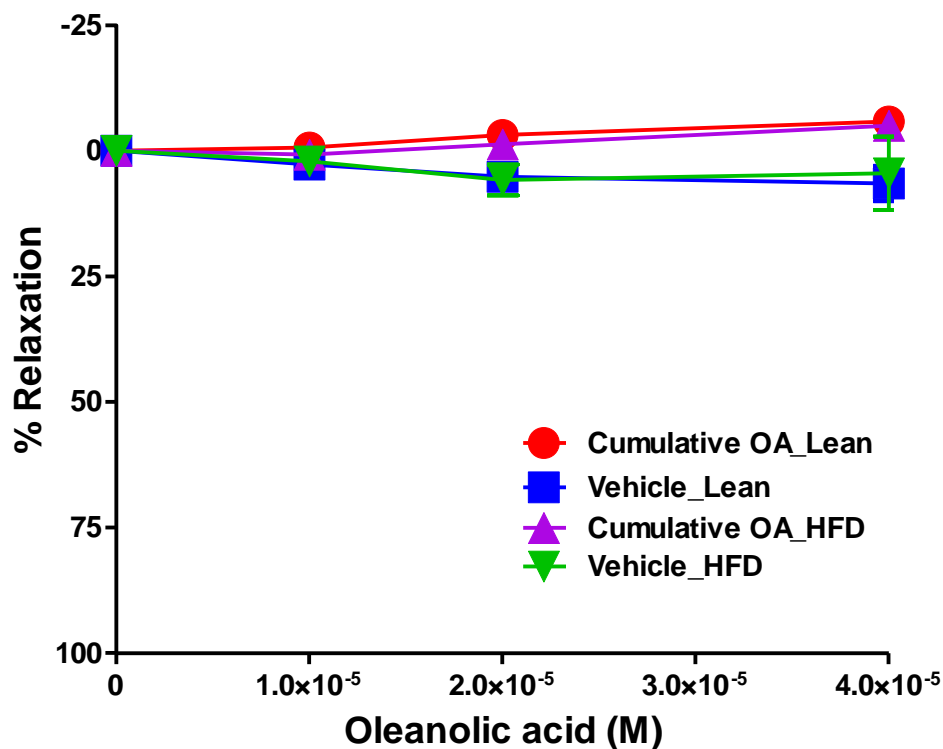


Figure 3.47: Direct, cumulative administration of OA after phenylephrine pre-contraction to assess possible pro-relaxation effects in aortic rings from lean and HFD rats.

Chapter 4

Summary and Discussion of Data

4.1 Cell culture studies (*in vitro* models)

4.1.1 Summary of findings

4.1.1.1 Baseline findings

Endothelial heterogeneity was investigated by comparing NO and ROS production in control, untreated AECs and CMECs at baseline conditions. The summarised findings are as follows:

- Baseline NO levels did not differ between AECs and CMECs (Figure 3.2),
- Baseline ONOO⁻ levels were higher in CMECs compared to AECs (Figure 3.3 A),
- Baseline H₂O₂ levels were higher in AECs compared to CMECs (Figure 3.3 B).

4.1.1.2 Endothelial injury induction findings

In this study, TNF- α , an inflammatory cytokine and a major mediator of endothelial activation, was used to simulate a state of endothelial injury in our *in vitro* cell culture models. Concentration-response curves were conducted by incubating both AECs and CMECs with 0.5, 5 and 20 ng/ml TNF- α for 24 and 48 hours. Decreased intracellular NO production, and increased ONOO⁻, H₂O₂ production and cellular necrosis were regarded as the primary markers of endothelial injury. The responses of AECs and CMECs to TNF- α were compared using the primary end points or makers of endothelial injury mentioned above. The summarised findings are as follows:

NO production

AECs: All TNF- α concentrations (0.5, 5, 20 ng/ml TNF- α) significantly decreased NO production after 24 and 48 hours (Figures 3.4 A & B).

CMECs: Only 5 and 20 ng/ml TNF- α significantly decreased NO production after 24 hours (Figure 3.4 C). However, after 48 hours, all concentrations of TNF- α significantly decreased NO production (Figure 3.4 D).

AECs vs. CMECs: NO production was significantly lower in 20 ng/ml TNF- α treated AECs compared to CMECs at similar TNF- α concentration after 48 hours (Figure 3.5 B).

ONOO⁻ production

AECs: All TNF- α concentrations significantly decreased ONOO⁻ after 24 and 48 hours (Figures 3.6 A & B).

CMECs: Similarly, all TNF- α concentrations significantly decreased ONOO⁻ after 24 and 48 hours (Figures 3.6 C & D).

AECs vs. CMECs: CMECs responded with lower ONOO⁻ production compared to AECs at all TNF- α concentrations after both 24 and 48 hours incubation periods (Figures 3.7 A & B).

H₂O₂ production

AECs: After 24 hours, all TNF- α concentrations significantly increased H₂O₂ production; however, after 48 hours, treatment with 5 and 20 ng/ml TNF- α significantly decreased H₂O₂ production (Figures 3.8 A & B).

CMECs: Only 5 and 20 ng/ml TNF- α treated cells exhibited a significantly increased H₂O₂ production after 24 hours (Figure 3.8 C). There were no significant differences in H₂O₂ production at any of the TNF- α concentrations after 48 hours (Figure 3.8 D).

AECs vs. CMECs: H₂O₂ production was significantly enhanced in AECs compared to CMECs at all TNF- α concentrations after 24 hours (Figure 3.9 A). However, after 48 hours, H₂O₂ production was significantly lower in 20 ng/ml TNF- α treated AECs compared to CMECs (Figure 3.9 B).

Necrosis

AECs: 5 and 20 ng/ml TNF- α significantly increased necrosis after 24 hours (Figure 3.10 A). However, after 48 hours, TNF- α had no significant pro-necrosis effects at any of the concentrations (Figure 3.10 B).

CMECs: Necrosis was increased at all TNF- α concentrations after 24 hours (Figure 3.10 C). After 48 hours, 0.5 and 5 ng/ml TNF- α significantly decreased necrosis, whereas 20 ng/ml TNF- α significantly increased necrosis (Figure 3.10 D).

AECs vs. CMECs: AECs exhibited lower levels of necrosis compared to CMECs at 20 ng/ml TNF- α after 48 hours (Figure 3.11 B).

Based on the findings above, 20 ng/ml TNF- α concentration and the 24 hour incubation period were chosen as the model of the endothelial injury in both AECs and CMECs and for further investigations.

4.1.1.3 Western blot analyses of signalling proteins

The summarised Western blot data are as follows:

Phospho / total ratios of eNOS were significantly decreased in control, untreated CMECs compared to control, untreated AECs, and in TNF- α treated CMECs compared to their TNF- α treated AEC counterparts (Figure 3.12 C).

Total PKB expression was significantly decreased in (Figure 3.13 A):

- TNF- α treated AECs compared to control, untreated AECs,
- Control, untreated CMECs compared to control, untreated AECs,
- TNF- α treated AECs compared to TNF- α treated CMECs.

Phosphorylated PKB was significantly decreased in (Figure 3.13 B):

- Control, untreated CMECs compared to control, untreated AECs,
- TNF- α treated AECs compared to TNF- α treated CMECs.

Phospho / total ratios of PKB were significantly increased in control, untreated CMECs compared to control, untreated AECs (Figure 3.13 C).

HSP 90 expression was significantly decreased in (Figure 3.14):

- TNF- α treated AECs compared to control, untreated AECs,
- Control, untreated CMECs compared to control, untreated AECs.

I κ B alpha expression was significantly increased in control, untreated CMECs compared to control, untreated AECs, and significantly decreased in CMECs TNF- α treated compared CMECs untreated control (Figure 3.15).

Nitrotyrosine expression was significantly increased in control, untreated CMECs compared to control, untreated AECs (Figure 3.16).

4.1.1.4 Oleanolic acid studies

The summarised findings with oleanolic acid are as follows:

1 hour baseline studies

Concentration response curves showed that both 10 and 40 μM OA concentrations (1 hour treatment) had NO producing properties in AECs and CMECs (Figure 3.17 A & B). However, 40 μM OA was chosen for further studies:

AECs: 40 μM OA significantly decreased H_2O_2 production (Figure 3.18 A) and necrosis (Figure 3.19 A) and after 1 hour.

CMECs: An increase in H_2O_2 production observed with 40 μM OA after 1 hour was likely the result of a DMSO vehicle effect (Figure 3.18 B). Necrosis was significantly increased after 1 hour treatment with 40 μM OA (Figure 3.19 B).

24 hours baseline studies

AECs:

- OA significantly decreased H_2O_2 production (Figure 3.21 A),
- OA significantly decreased necrosis (Figure 3.22 A).

CMECs:

- OA significantly increased NO production after 24 hours (Figure 3.20 B),
- OA had no significant effect on baseline H_2O_2 production (Figure 3.21 B) and necrosis (Figure 3.22 B) after 24 hours.

Oleanolic acid pre-treatment studies

AECs:

- TNF- α -treated cells showed significantly reduced NO levels vs. control, untreated cells, which was reversed when pre-treated with OA (Figure 3.23 A),
- TNF- α -treated cells showed significantly increased H₂O₂ production vs. control, untreated cells, which was abolished when pre-treated with OA (Figure 3.24 A),
- TNF- α -treated cells showed a significant pro-necrosis response vs. control, untreated cells, which was abolished when pre-treated with OA (Figure 3.25 A)

CMECs:

- TNF- α -treated cells showed significantly reduced NO levels vs. control, untreated cells, which was reversed when pre-treated with OA (Figure 3.23 B),
- TNF- α -treated cells showed significantly increased H₂O₂ production vs. control, untreated cells, which was abolished when pre-treated with OA (Figure 3.24 B),
- There were no changes observed in necrosis measurements in any of the groups (Figure 3.25 B).

4.1.2 Discussion of cell culture (*in vitro* models) data

The first part of this study focused primarily on comparing AECs and myocardial capillary derived CMECs under physiological conditions or when exposed to a harmful, pro-inflammatory stimulus, for which a model of endothelial cell injury was established in both cell lines. AECs are situated in close association with the VSMCs and the endothelial derived factors released by this cell layer are primarily dedicated at regulating vascular homeostasis, whereas CMECs are in close association with cardiomyocytes and primarily regulate cardiomyocyte function and homeostasis (Strijdom & Lochner 2009, Brutsaert 2003, Shah & MacCarthy 2000). It is known that the extracellular environment and epigenetics are important factors in determining endothelial heterogeneity (Aird 2006b). In view of the differences in their location and function, AECs and CMECs would be expected to exhibit heterogeneous responses to harmful stimuli. Endothelial injury and dysfunction have previously been studied in AECs and CMECs separately (Venugopal *et al* 2002, Okruhlicova

et al 2005). However, CMECs seems to be poorly investigated, especially with regards to their response to various harmful stimuli such as the pro-inflammatory cytokine TNF- α . In AECs, Venugopal *et al* (2002) demonstrated decreased eNOS expression and bioactivity accompanied by increased adhesion molecules VCAM 1 and ICAM 1 in response to inflammatory marker CRP (5 – 50 μ g/ml over 6, 12 and 24 hours). On the other hand, CMECs derived from streptozotocin-induced diabetic rats and a model of hypertensive rats exhibited decreased NOS activity and ultrastructural remodelling (Okruhlicova *et al* 2005). Whether endothelial heterogeneity is relevant with regards to AECs and CMECs during pathological conditions remains to be explored. Furthermore, there are a lack of studies that have investigated and compared endothelial cells from different sites addressing the eNOS-NO biosynthetic pathway, ROS production and viability in response to harmful stimuli. Whether endothelial cell heterogeneity is relevant in *in vitro* settings, when cells have been removed from their inherent environment is a subject that needs further attention. Deng *et al* (2006) demonstrated differences in gene expression in coronary AECs and saphenous vein endothelial cells in response to ox-LDL in *in vitro* settings, with coronary AECs expressing genes associated with atherogenesis while saphenous vein endothelial cells expressed anti-atherogenesis (protective) genes upon ox-LDL exposure. This suggests that some level of heterogeneity is maintained when endothelial cells are removed from their respective inherent environments. Whether this is applicable to the eNOS-NO biosynthetic pathway, ROS production and cell viability remains to be explored.

4.1.2.1 Baseline findings

NO production and the NO biosynthetic pathway

In baseline conditions, endothelial heterogeneity did not appear to exist with regards to NO production between control, untreated AECs and CMECs as measured by flow cytometric analyses of DAF-2/DA fluorescence (Figure 3.2). As eNOS is the chief constitutively expressed enzymatic source of NO in endothelial cells, we went a step further to measure and compare total and phosphorylated (Ser 1177) eNOS protein in both control, untreated AECs and CMECs by western blot analysis. Total and phosphorylated eNOS did not exhibit significant differences under baseline conditions between AECs and CMECs, though total

CMEC eNOS expression was ~ 1.4-fold greater vs. AECs (Figure 3.12 A). In the present study, proteomics analysis showed a significantly higher (~ 1.5-fold) expression of eNOS in CMECs versus AECs under control, untreated conditions (Table 3.4), suggesting that heterogeneous baseline eNOS expression patterns may exist between AECs and CMECs. The baseline relative eNOS activation (expressed as phosphorylated / total eNOS ratios) was however, significantly lower in CMECs compared to AECs, suggesting that some degree of heterogeneity also exists between CMECs and AECs in this regard. Andries *et al* (1998) demonstrated higher eNOS expression in endocardial and coronary arterial endothelium compared to CMECs and coronary vein endothelium in rat hearts. Heterogeneous distribution of the eNOS enzyme was further shown in swine, where eNOS expression was higher in conduit arteries compared to veins (Simmons *et al* 2012). Another study compared cultured rat mesenteric arteriolar and venular endothelial cells, and reported higher baseline NO synthetic capacity in venular compared to arteriolar endothelial cells as measured by high eNOS protein levels and activity (Wagner *et al* 2001). From these studies and our own findings, it is evident that endothelial cell regional specificity is relevant when determining eNOS expression and activity.

eNOS activation and inactivation are dependent on posttranslational events such as interaction with the protein caveolin-1 (Ferron *et al* 1998, Frank *et al* 2003). Interaction of eNOS with caveolin-1 is a regulatory mechanism that keeps eNOS in an inactive state, hence leading to diminished NO production until calmodulin binds to eNOS in response to a rise in intracellular calcium levels (Frank *et al* 2003). Immunofluorescence studies revealed enhanced caveolin-1 staining in CMECs compared to endocardial and arterial endothelium (Andries *et al* 1998). This might explain the low eNOS activity observed in CMECs compared to AECs in the current study.

PKB / Akt is an important upstream facilitator of eNOS phosphorylation, hence resulting in NO production (Dimmeler *et al* 1999). We further compared baseline total and phosphorylated PKB / Akt protein as measured by western blot analysis. Total PKB / Akt was heterogeneously expressed between AECs and CMECs, with CMECs exhibiting a lower baseline expression compared to AECs (Figure 3.13 A). In addition to stimulating eNOS phosphorylation, PKB / Akt is also important for survival of endothelial cells, including protection against apoptosis (Fujio & Walsh 1999). Given the location of AECs, where they

are more exposed to different factors from the circulating blood and mechanical forces such as shear stress, higher expression of PKB / Akt may be essential for cell survival and its phosphorylation may be triggered by a given stimuli at a given time. Furthermore, PKB / Akt phosphorylates eNOS at site Ser 1177 during conditions of shear stress, which in turn produces NO to regulate vasomotor activity (Luo *et al* 2000). It is therefore expected that PKB / Akt would be highly expressed in AECs compared to CMECs since they are located in the vasomotor regulating blood vessels. While eNOS activation was lower in CMECs compared to AECs, phosphorylated PKB / Akt (Ser 473) and relative PKB / Akt activation (phosphorylated / total PKB-Akt ratios) were significantly higher in CMECs compared to AECs at baseline conditions (Figure 3.13 B & C). It's difficult to elucidate why PKB / Akt activity was high while eNOS activity was low in CMEC compared to AECs. Perhaps activated PKB / Akt also possess other regulatory properties other than activating eNOS in CMECs. In human CMECs, PKB / Akt phosphorylation was associated with restoration of ROS-induced barrier dysfunction, a response which was blocked by API-2-induced PKB / Akt inhibition and not L-NAME-induced eNOS inhibition (Dossumbekova *et al* 2008). An intact CMEC barrier would be critical in regulating myocardial function and activity in *in vivo* settings.

The molecular chaperone, HSP 90, has been shown to interact with eNOS to stimulate activity and hence production of NO (Takahashi & Mendelsohn 2003b). Furthermore, HSP90 may act in co-operation with PKB / Akt forming a HSP 90-eNOS-PKB / Akt complex leading to enhanced eNOS activity (Takahashi & Mendelsohn 2003a). Interestingly, heterogeneity was also evident with regards to the baseline expression of HSP 90, which was significantly lower in CMECs compared to AECs at baseline conditions (Figure 3.14). Interaction of HSP 90 with eNOS is often stimulated by factors such as shear stress to elicit vasodilation (García-Cardena *et al* 1998). Therefore high HSP 90 expression might not be necessary in CMECs as they are located in an areas of low shear stress and non-dilating blood vessels compared to AECs. Furthermore, HSP 90 is also involved in protein folding and stress response (García-Cardena *et al* 1998). Other HSP isoforms were perhaps more expressed in CMECs compared to AECs for the purpose of protein folding and stress response. For example, our proteomics data revealed up-regulation of HSP 70 (2.5-fold up-regulated) in CMECs compared to AECs (Table 3.4). A study in endothelial cells derived from conduit arteries and veins of swine demonstrated a heterogeneous expression of HSP 90, with the arteries having a higher

expression compared to veins (Simmons *et al* 2012). This provides further evidence of endothelial heterogeneity with regards to HSP 90 expression, in endothelial cells from different vascular beds.

ROS production

Baseline intracellular ONOO⁻ and H₂O₂ levels were measured and compared in AECs and CMECs. ONOO⁻ is a powerful oxidant formed from the reaction of NO and O₂⁻ and has been implicated in eNOS uncoupling and nitration of proteins including eNOS (Fostermann & Munzel 2006). Though ONOO⁻ is often associated with cardiovascular injury, it can exert beneficial effects at low levels, such as relaxation of coronary arteries, inhibition of platelet aggregation and reduction of leukocyte - endothelial cell adherence (Lefer *et al* 1997). In the current study, AECs and CMECs exhibited heterogeneous baseline intracellular ONOO⁻ levels, with CMECs demonstrating higher baseline ONOO⁻ levels compared to AECs (Figure 3.3 A). Given the critical location of CMECs, baseline ONOO⁻ released from CMECs may play a homeostatic role in preserving myocardial function in *in vivo* settings. For example, low levels of ONOO⁻ have been reported to enhance cardiomyocyte contraction and relaxation through PKA-mediated phosphorylation of phospholamban (Kohr *et al* 2010). Our baseline ONOO⁻ findings were further validated by the western blot measurement of baseline nitrotyrosine expression, which was significantly higher in CMECs compared to AECs. Nitrotyrosine is a marker of ONOO⁻-induced protein nitration, and this thus confirmed the heterogeneous ONOO⁻ production in AECs and CMECs.

H₂O₂ is generated from the reaction between SOD and O₂⁻; however, it can also be directly generated by some ROS producing enzymes such as glucose oxidase and xanthine oxidase (Breton-Romero & Lamas 2014). Endothelial heterogeneity was evident with regards to baseline H₂O₂ production between AECs and CMECs in the present study. AECs exhibited enhanced baseline H₂O₂ production compared to CMECs (Figure 3.3 B). Since low levels of H₂O₂ possess physiological roles such as regulating endothelial cell proliferation (Stones & Collins 2002), it is tempting to speculate that higher baseline levels of H₂O₂ in AECs compared to CMECs may serve a regulatory role specific for AECs location. However, our proteomics data revealed significant up-regulation of anti-oxidants associated with H₂O₂

clearance including glutathione peroxidase (2.1-fold up-regulated) and peroxiredoxin-6 (2-fold up-regulated) in CMECs compared AECs at baseline conditions (Table 3.4). Hence this may be accountable for lower baseline H₂O₂ levels in CMECs, and the heterogeneity might lie in that these proteins are up-regulated in CMECs and not AECs resulting in differences in H₂O₂ baseline levels.

4.1.2.2 Endothelial injury induction

NO production

Inflammation is one of the major underlying mechanisms that links cardiovascular risk factors and disease conditions with endothelial injury or dysfunction (Meldrum 1998). The pro-inflammatory cytokine TNF- α is a chief mediator of inflammation (Medrum 1998) and its injurious effects including apoptosis, diminished eNOS expression and activity, diminished NO production and ROS generation on the macrovascular-derived endothelium has previously been well documented (Polte *et al* 1997, Anderson *et al* 2004, Goodwin *et al* 2007, Corda *et al* 2001). In this section the effects of TNF- α on the NO biosynthetic pathway, ROS production and necrosis in AECs and CMECs are discussed. Furthermore, unlike most studies in the literature that measure downstream breakdown products of NO metabolism such as nitrites and nitrates, direct measurements of intracellular levels of NO by means of DAF-2/DA fluorescence was done in the current study. In our hands, treatment of AECs with low (0.5 ng/ml), medium (5 ng/ml) and high (20 ng/ml) concentrations of TNF- α significantly decreased NO production after 24 and 48 hours (Figure 3.4 A & B). Anderson *et al* (2004) demonstrated a decrease in eNOS gene promoter activity with a TNF- α concentration of as low as 100 pg/ml in bovine AECs, however this study did not measure NO production. On the other hand, Goodwin *et al* (2007) reported a decrease in NO production with 10 ng/ml TNF- α in bovine AECs, measured as nitrite levels in the tissue culture medium.

In the CMECs, NO production was reduced at medium and high TNF- α concentrations (5 and 20 ng/ml) after 24 hours and at all concentration after 48 hours (Figure 3.4 C & D). As far as we are aware, the current study is the first to investigate the role of TNF- α in CMECs, as a thorough literature review did not identify any previously published papers that have

investigated the response of CMECs to TNF- α especially with regards to NO production. When studying endothelial function or dysfunction, most *in vitro*-based studies often employ endothelial cells derived from large vessels such as the HUVECs or aortic endothelial cells as they are easier to harvest, thus overlooking the possibility that their data might be, at least in part, specific to the particular endothelial cell type that cannot be extrapolated to all endothelial cells (endothelial heterogeneity) (Aird 2007b). It is evident from the literature that there is a lack of studies investigating NO production in endothelial cells derived from microvascular beds. An exception is a study by Bove *et al* (2001) that investigated the effects of 50 ng/ml TNF- α on cultured bovine pulmonary microvessel endothelial cells; however, they reported no significant effects on NO production after 24 hours treatment. Another study showed the development of a compromised rat lung microvascular endothelial cell barrier in response to 10 ng/ml TNF- α for 1 hour as demonstrated by enhanced endothelial permeability. However, NO production was not measured in this study (Sawant *et al* 2013).

The responses of AECs and CMECs to TNF- α treatment were directly compared in a time- and concentration-matched manner in order to assess whether *in vitro* heterogeneity exists between these two endothelial cell types with regards to NO production. The results showed that generally, both cell types responded with similar NO decreasing trends, with the exception of the TNF- α 20 ng/ml, 48 hours concentration and time point at which a measure of heterogeneity was present (NO production was significantly lower in AECs compared to CMECs) (Figure 3.5 B). This is suggestive that at high concentrations over longer periods, TNF- α may exert pronounced loss of NO in AECs compared to CMECs. In contrast to our findings, a study reported increased iNOS-induced NO production (measured as nitrite levels), which was more enhanced in rat AECs compared to rat lung microvascular endothelial cells in response to a combination of TNF- α (60 000 U/ml) + lipopolysaccharide (500 ng/ml), and TNF- α (60 000 U/ml + interferon-gamma (1 000 U/ml) (Geiger *et al* 1997), thus demonstrating heterogeneity in response to TNF- α between macrovascular and microvascular derived endothelial cells .

Taken together, the above data are suggestive of the development of a generally reduced NO-producing capacity in both cell types after exposure to a range of TNF- α concentrations and treatment times. Endothelial dysfunction is often defined as a state of reduced NO bio-availability, and based on this definition, there is a strong possibility that both the AECs and

CMECs have switched to a dysfunctional state induced by the pro-inflammatory stimulus (Liao 2013).

NO biosynthetic pathway

We next sought to determine whether the TNF- α -induced reduction of NO was due to diminished eNOS expression or activity. The effects of TNF- α on eNOS expression and phosphorylation (site Ser 1177) in both AECs and CMECs were further investigated by western blot analysis. TNF- α has previously been shown to reduce eNOS expression (Lai *et al* 2003, Valerio *et al* 2006). Anderson *et al* (2004) demonstrated a reduction in eNOS protein level and gene promoter activity following 24 hours treatment with 100 and 1000 pg/ml TNF- α in bovine AECs. TNF- α at 3 ng/ml (over 24 hours) in HUVECs was also shown to decrease eNOS mRNA (Yoshizumi *et al* 1993), while 10 ng/ml TNF- α treatment after 12 and 24 hours decreased eNOS expression in bovine AECs (Gonzalez-Fernandez *et al* 2001). In the present study, TNF- α had no significant effect on eNOS expression and phosphorylation or relative eNOS activation in either AECs or CMECs compared to their respective controls (Figure 3.12 A - C). This is rather surprising as TNF- α elicited significant reductions in NO production in both cell lines. As eNOS is the chief enzymatic source of NO in endothelial cells, it would be expected that TNF- α would at least diminish eNOS activity, as was determined by the analysis of eNOS phosphorylation site Ser 1177 in our endothelial cell models. It should, however, be kept in mind that eNOS activity is influenced by multiple phosphorylation sites including Ser 615 and Ser 633 (Kolluru *et al* 2010). It is possible that eNOS activity might have been regulated at different phosphorylation sites other than Ser 1177 in TNF- α treated AECs and CMECs compared to their respective controls.

While some authors reported on reduced eNOS expression, others have shown that TNF- α may possess stimulatory effects on eNOS phosphorylation. In human dermal microvascular endothelial cells, 20 ng/ml TNF- α (at 1, 3, and 6 hours) significantly increased eNOS phosphorylation at site Ser 1177, a response which was diminished by wortmanin inhibition of PKB/Akt (Kawanaka *et al* 2002). This was further supported by the findings of De Palma *et al* (2006), where 50 ng/ml TNF- α (for 6 hours) significantly increased PKB / Akt-mediated activation of eNOS (phosphorylation site was not specified). The pathway involved included activation of neutral-sphingomyelinase-2 leading to activation of sphingosine-kinase 1 and

sphingosine-1-phosphate which ultimately activates PKB / Akt, leading to eNOS phosphorylation (De Palma *et al* 2006). From the above study, it appears that TNF- α may stimulate eNOS phosphorylation via other pathways.

A heterogeneous response was observed between TNF- α treated AECs and CMECs, with TNF treated CMECs exhibiting lower relative eNOS activation (expressed as phosphorylated / total eNOS ratios) compared to TNF- α treated AECs (Figure 3.12 C). However, this response may not be attributable to TNF- α , as a similar response was observed at baseline (control, untreated) conditions (section 4.3.2). The observations made by Andries *et al* (1998) with immunofluorescence studies where CMECs showed high caveolin-1 staining may also explain the lower eNOS activity in TNF- α treated CMECs. Furthermore, Wang *et al* (2008) demonstrated via immunofluorescence and western blot analysis, that 0.5 ng/ml TNF- α (over 4 hours) significantly enhanced caveolin-1 density in endothelial cells derived from porcine pulmonary arteries. Hence, TNF- α may exacerbate the lower eNOS activity in CMECs compared to AECs.

The effects of TNF- α on PKB / Akt expression and phosphorylation (site Ser 473) were further investigated by western blot analysis. While TNF- α elicited no effect on PKB / Akt expression in CMECs compared to their respective controls, there was a significant reduction in PKB / Akt expression in AECs compared to their respective controls in the present study (Figure 3.13 A). Since PKB / Akt is upstream of eNOS, the reduction in PKB / Akt expression in response to TNF- α in AECs may represent an early phase initiation of endothelial injury. However, PKB / Akt phosphorylation (site Ser 473) or relative activation (expressed of phospho / total PKB / Akt ratios) was not affected by TNF- α in both AECs and CMECs (Figure 3.13 B & C). While TNF- α would be expected to decrease PKB / Akt phosphorylation in endothelial cells, other studies have reported that TNF- α significantly increases phosphorylation as demonstrated by De Palma *et al* 2006 (50 ng/ml TNF- α for 6 hours), Murao *et al* 2000 (10 ng /ml TNF- α for 2 hours, Palmieri *et al* 2014 (10 ng/ml TNF- α for 1 hour) in HUVECs. PKB / Akt activation may be important for endothelial cell survival in response to TNF- α .

TNF- α elicited heterogeneous PKB / Akt expression and phosphorylation in AECs and CMECs. PKB / Akt expression and phosphorylation were significantly reduced in TNF- α treated AECs

compared to TNF- α treated CMECs (Figure 3. 13 A – C). Hence the PKB / Akt pathway appears to be compromised in AECs compared to CMECs in response to TNF- α . This may represent a step in the initiation of endothelial injury in AECs compared to CMECs.

As HSP 90 is another protein involved in modulating eNOS activity, we investigated the effects of TNF- α on HSP 90 expression in both AECs and CMECs. TNF- α treated AECs exhibited lower HSP 90 expression compared to its respective control, while TNF- α treated CMECs showed no significant response in HSP 90 expression compared to their respective control (Figure 3.14). The reduction of HSP 90 expression in TNF- α treated AECs may have been an initial step in the disruption of the NO biosynthetic pathway. However, the HSP 90-PKB / Akt-eNOS complex does not portray a convincing model of a compromised NO biosynthetic pathway, since PKB / Akt and eNOS activity were not affected by TNF- α in AECs. The same could be said for CMECs as HSP 90 expression, PKB Akt and eNOS activity were not affected by TNF- α . Hence our protein signalling data do not coincide with reduced NO levels observed following TNF-treatment in both cell lines. However, taking into consideration the reduced HSP 90 and total PKB expression in AECs in response to TNF- α , this pathway could have signalled an initiating step in rendering the AECs dysfunctional, while it proved to be resistant in CMECs. The reduced NO bioavailability in both AECs and CMECs probably represents the initial step of endothelial activation before the signalling pathway is compromised. With regards to direct comparison, HSP 90 expression did not differ in TNF- α treated AECs compared to their CMECs counterparts. Hence, TNF- α did not elicit a heterogeneous expression of this particular protein.

ROS production

TNF- α has previously been linked to the increased generation of mitochondrial and NADPH oxidase-mediated ROS, thus leading to oxidative stress and endothelial injury (Chen *et al* 2008). In the current study, the intracellular ROS levels in AECs and CMECs exposed to TNF- α -treatment were investigated by measuring ONOO⁻ and H₂O₂. Many studies measure ONOO⁻ indirectly, through western blot analysis of nitrotyrosine expression. Though we also applied this method, we first measured intracellular levels of ONOO⁻ by flow cytometric analysis of DHR-123 fluorescence. Interestingly, in our hands ONOO⁻ levels were significantly

decreased at all TNF- α concentrations following both 24 and 48 hours incubation periods, in both AECs and CMECs. These findings are unexpected and contradict what has been previously reported in the literature. In a study by Neumann *et al* (2006), 100 ng/ml TNF- α increased ONOO⁻ production (as determined by immunofluorescence and western blot analysis of nitrotyrosine expression) after 30 minutes of treatment in pulmonary microvessel endothelial cells, however, this effect was reversed after 4 hours. It has to be noted that the TNF- α concentration used in the study by Neumann (100 ng/ml) is very high and supra-physiological. Despite this shortcoming, one could speculate that the incubation periods in our study were too long, and that a burst in ONOO⁻ production might have occurred at an earlier time-point. Another study also reported an increase in ONOO⁻ production following 40 ng/ml TNF- α over a period of 24 hours, as measured by enhanced nitrotyrosine expression in human umbilical vein endothelial cells (Xia *et al* 2010). However, this was accompanied by increased iNOS-induced NO, and O₂⁻ production (Xia *et al* 2010). Our nitrotyrosine data did not reveal any significant differences in both TNF- α treated AECs and CMECs compared to their respective controls (Figure 3.16). iNOS expression is known to be induced by inflammatory cytokines such as TNF- α , leading to production of large amounts of NO, which via the reaction with O₂⁻ leads to ONOO⁻ formation (Yamaoka *et al* 2002, Lancel *et al* 2004, Xia *et al* 2010). Given the reduced NO levels observed with TNF- α treatment in the current study, it was decided not to measure iNOS expression. In addition, separate studies in our laboratory failed to show iNOS expression in CMECs upon TNF- α stimulation [C Westcott; PhD dissertation; University of Stellenbosch 2014]. It can also be speculated that in response to the TNF- α stimuli, the cells were able to up-regulate protective enzymes such as SOD, to rapidly quench O₂⁻ hence preventing formation of ONOO⁻. In support of this postulation, the proteomics data showed significant up-regulation of SOD in both TNF- α -treated AECs (2.8 fold; Table 3.7; Figure 3.29) and CMECs (2.2-fold; Table 3.9).

An interesting trend was noticed when comparing TNF- α concentration and time-matched ONOO⁻ levels between the two cell types. Although both cell types responded to TNF- α treatment with reduced ONOO⁻ levels versus control, untreated values, the relative degree of decrease in the CMECs was consistently more pronounced compared to the AECs (Figure 3.7 A & B). These responses are even more intriguing given that the baseline ONOO⁻ levels

were significantly higher in the CMECs than in AECs (Figure 3.3 A). The biological significance of these heterogeneous responses is unclear, and difficult to explain given the data to our disposal. Furthermore, our nitrotyrosine data did not coincide with the observed ONOO⁻ findings, as there were no significant differences in nitrotyrosine expression in TNF- α treated AECs compared to TNF- α treated CMECs (Figure 3.16).

The role of TNF- α in H₂O₂ production was also investigated in both AECs and CMECs. In AECs, 24 hours TNF- α treatment significantly increased intracellular H₂O₂ production by ~3-fold at all concentrations, however, this trend was abolished and even reversed after 48 hours (Figures 3.8 A & B). In agreement with our 24 hour data, treatment of bovine AECs with 0 – 100 U/ml TNF- α resulted in a dose-dependent increase in H₂O₂ production after 30 minutes (Leopold *et al* 2003), whereas another study showed that 2 ng/ml TNF- α significantly increased H₂O₂ production after 1 hour in human AECs (Chen *et al* 2002). Both these studies applied microplate fluorometer analysis of DCF fluorescence to measure H₂O₂ levels. An increase in H₂O₂ production has also been demonstrated in HUVECs treated with 40 ng/ml TNF- α for 24 hours (Xia *et al* 2010) or 1 and 10 ng/ml TNF- α for 1 hour (Corda *et al* 2001). After the 48 hour period our cells might have recovered from the TNF- α -mediated ROS production, possibly by up-regulating the ROS defence enzymes such as catalase which is responsible for decomposing H₂O₂ to water and oxygen; this, however does not necessarily negate the possible harmful effects exerted earlier by the profound increases in H₂O₂ observed at 24 hours. In the CMECs, TNF- α significantly increased H₂O₂ production at medium (5 ng/ml) and high (20 ng/ml) concentrations at 24 hours; however, the relative increases were not as profound as observed in the AECs (Figure 3.8 C). Similar to the AECs, the increased H₂O₂ production disappeared after 48 hours treatment (Figure 3.8 D). In a study by Li *et al* (2005), 100 U/ml TNF- α resulted in an increase in DCF-stained coronary microvascular endothelial cells 30 minutes.

The direct, concentration and time matched comparative data between AECs and CMECs demonstrated significant heterogeneity with regards to TNF- α -induced H₂O₂ production as shown by consistently higher levels in the AECs compared to CMECs at 24 hours treatment (Figure 3.9). Conversely, in the 48 hour treatment groups, the heterogeneous responses disappeared, with the exception of the 20 ng/ml TNF- α groups, which showed higher levels in the CMECs versus AECs. In a study that also compared macrovascular and microvascular

endothelial cell responses, Wang *et al.* (2002) investigated the effects of a TNF- α (20 ng/ml, for 24 hours) + neutrophil challenge on pulmonary artery endothelial cells and pulmonary microvascular endothelial cells. In contrast to our 24 hour findings, they demonstrated increased DCF fluorescence in the pulmonary microvascular endothelial cells compared to macrovascular pulmonary artery endothelial cells, which exhibited no significant effects. A heterogeneous response was also demonstrated in another study on HUVECs and human microvascular endothelial cells, with the former showing significant increases in H₂O₂ production, and the latter exhibiting no significant effects following exposure to high glucose treatment (Patel *et al* 2013). From the data of these studies, as well as our own data (particularly the 24 hour TNF- α treatment groups), there is evidence to suggest that considerable heterogeneity exists between endothelial cells from larger blood vessels (such as the aorta, pulmonary artery and human umbilical vein) and endothelial cells from microvascular beds (such as CMECs and the pulmonary microvasculature) with regards to H₂O₂ production in response to a harmful stimulus.

Cell necrosis

TNF- α has been shown to induce both apoptotic and necrotic cell death via TNFR1 (Lin *et al* 2004). Involvement of ROS has been implicated in TNF- α induced cell necrosis (Ardestani *et al* 2013), and Lin *et al* (2004) demonstrated the abolishment of TNF- α induced necrosis by a ROS scavenger, butylated hydroxyanisole, in mouse embryonic fibroblasts. Binding of TNF- α to TNFR1 leads to the recruitment of TNFR1 associated death domain (TRADD). In a necrotic death pathway, it has been suggested that TNFR-associated factor 2 (TRAF2) and receptor-interacting protein (RIP) are further recruited, forming a complex which leads to accumulation of ROS and cell necrosis (Figure 4.1) (Lin *et al* 2004). In the current study, AECs exhibited a high percentage of necrotic cells following 5 and 20 ng/ml TNF- α treatment for 24 hours, whereas 48 hours treatment showed no significant effect (Figure 3.10 A – B). Similarly in CMECs, all TNF- α concentrations significantly increased necrosis after 24 hours (Figure 3.10 C). Interestingly, 5 ng/ml TNF- α significantly decreased necrosis, whereas 20 ng/ml TNF- α significantly increased necrosis after 48 hours in CMECs (Figure 3.10 D). TNF- α did not elicit a heterogeneous response with regards to necrosis after 24 hours treatment

between AECs and CMECs. However, following 48 hours with 20 ng/ml TNF- α , CMECs exhibited a higher necrosis percentage compared to their AECs counterparts. Hence in CMECs, high concentrations of TNF- α for a longer treatment period compromised cell viability. Variable findings on TNF- α and endothelial cell viability have been reported in the literature. According to Wang *et al* (1996), 5-50 ng/ml TNF- α did not induce necrosis following incubation periods of 6-24 hours in HUVECs. In pulmonary microvessel endothelial cells, 50 ng/ml TNF- α had no effect on cell viability after 24 hours as determined by the trypan blue exclusion assay (Bove *et al* 2001). Conversely, in pulmonary artery endothelial cells, 50 ng/ml TNF- α significantly reduced cell viability after 48 hours, as measured by crystal violet staining (Polte *et al* 1997). In line with the findings of the current study, Corda *et al* (2001) demonstrated a significant increase in necrosis following 1 hour exposure of HUVECs to 10 ng/ml TNF- α , which was accompanied by increased H₂O₂ levels.

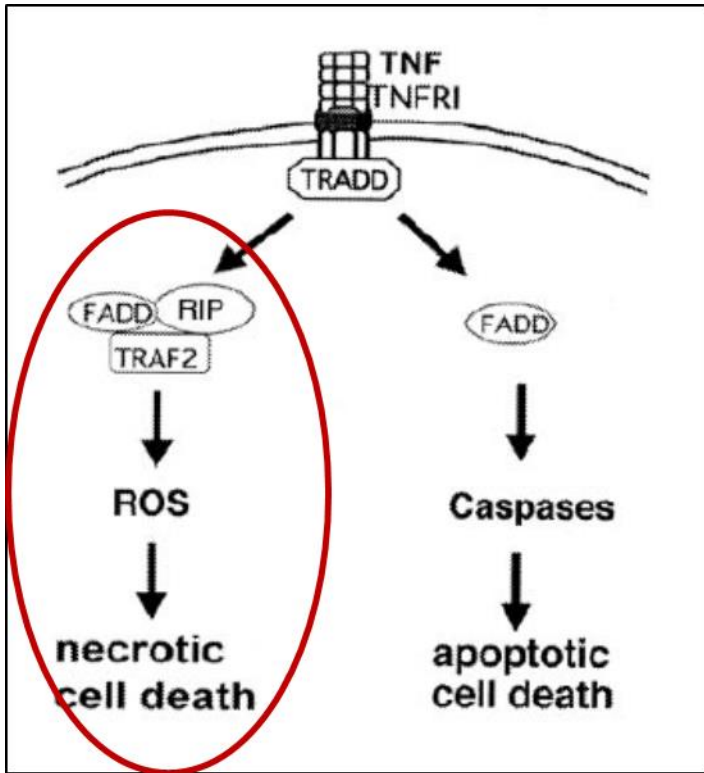


Figure 4.1: Proposed mechanism of TNF- α induced cell necrosis (Lin *et al* 2004).

The TNF- α signalling pathway

NF- κ B forms an integral part of the TNF- α inflammatory signalling pathway. I κ B-alpha interacts with NF- κ B keeping it inactive during physiological conditions, and hence, it is an important post-translational modulator of NF- κ B activity. Diminished expression of I κ B has previously been used as a marker of enhanced NF- κ B activity (Zhou *et al* 2003). TNF- α has previously been shown to induce NF- κ B activity and monocyte adhesion in human AECs, a pathway indicative of endothelial activation (Csiszar *et al* 2006). In the current study, I κ B-alpha expression was significantly down-regulated in TNF- α treated CMECs compared to control, untreated CMECs (Figure 3.15). This is indicative of enhanced NF- κ B activity and hence an inflammatory response in CMECs following stimulation with TNF α . This was further supported by our proteomics data where NF- κ B was only detected in TNF- α treated CMECs compared to their respective control (Figure 3.30 B). Though our western blot data did not yield any significant differences, I κ B-alpha exhibited a decreasing trend in TNF- α treated AECs compared to control, untreated AECs. This was also confirmed by our proteomics data, where NF- κ B was only detected in TNF- α treated AECs compared to their respective control (Figure 3.29 B). This is suggestive of an inflammatory response in both AECs and CMECs in response to TNF- α .

Heterogeneity was evident when comparing baseline I κ B-alpha expression in control, untreated CMECs vs. AECs, where CMECs exhibited higher baseline expression of I κ B-alpha (Figure 3.15). This finding could be suggestive of lower baseline NF- κ B activity and inflammation in CMECs. Low NF- κ B activity could translate into lower expression of baseline inflammatory proteins and resistance to endothelial activation in CMECs compared to AECs.

4.1.2.3 Oleonic acid studies

A growing body of literature has focused on the putative beneficial properties of certain plant extracts on the vascular system, many of which, are postulated to act through modulation of endothelial function (Schmitt & Dirsch 2009). OA is one such plant extract that has been shown to possess endothelio-protective properties. OA has been shown to induce endothelium-dependent relaxation in mesenteric arteries, stimulate eNOS phosphorylation at Ser 1177 in human umbilical vein endothelial cells (Rodriguez-Rodriguez *et al* 2008), and stimulate PGI₂ release in coronary smooth muscle cells (Martinez-Gonzalez *et al* 2008). We set out to investigate the effects of OA in AECs and CMECs and to additionally evaluate whether the putative protective effects will further reveal heterogeneity between the two endothelial cell types. Short term (1 hour) treatment with OA resulted in enhanced NO production in both AECs and CMECs compared to the respective control, untreated samples (Figure 3.17 A & B). At 24 hours OA treatment, only the CMECs responded with increased NO production (Figure 3.20 B). In AECs, OA further reduced baseline necrosis and H₂O₂ production after 1 and 24 hours treatments (Figures 3.18 A, 3.19 A, 3.21 A, 3.22 A). OA has previously been shown to decrease baseline H₂O₂ levels and apoptosis in H9c2 cells (Cardiomyoblasts) (Mapanga *et al* 2012). However, this was not the case in CMECs, as 1 hour OA treatment significantly increased necrosis (Figure 3.19 B) and no significant differences in either necrosis or H₂O₂ were observed following 24 hours treatments. Supraphysiological levels of NO may potentially be cytotoxic. In high amounts, NO is available for a reaction with O₂⁻ leading to the formation of potent cytotoxic oxidant, nitrotyrosine (Gobbel *et al* 1997). For example, high levels of NO have been shown to induce both apoptosis and necrosis in rat cardiomyocytes (Uchiyama *et al* 2002). As endothelial cells exhibit variable responses to stimuli, the enhanced NO above control levels following 1 hour OA treatment might have been harmful in CMECs as evidenced by the enhanced necrosis. This might also have been a short lived response, as OA elicited no harm after 24 hours in CMECs.

In light of the NO stimulatory properties of OA, and in some cases the anti-necrotic and antioxidant effects observed in our cells, we further investigated the putative anti-endothelial injury properties of OA pre-treatment in endothelial cells exposed to 24 hours of TNF- α treatment. Pre-treatment with OA, not only significantly reversed the TNF- α -induced

reduction in NO production, but also abolished the TNF- α -induced H₂O₂ production and necrosis in AECs (Figures 3.23 A, 3.24 A, 3.25 A). Similar trends were observed in the CMECs with regards to NO and H₂O₂ production (Figures 3.23 B, 3.24 B); however no significant effects were observed with necrosis. Overall, the data suggest that OA exerted anti-endothelial injury properties in both AECs and CMECs. In agreement with our data, OA reduced hyperglycaemia-induced oxidative stress and apoptosis in H9c2 cells (Mapanga *et al* 2012). In HUVECs, OA blunted lipopolysaccharide-induced expression of adhesion molecules, leukocyte adhesion, NF-KB activation and production of TNF- α , and further restored endothelial barrier function (Lee *et al* 2013). This is suggestive that OA may exert its anti-inflammatory properties via diminishing NF-KB activity in endothelial cells. According to Rodriguez-Rodriguez *et al* (2008), OA significantly increased eNOS phosphorylation at Ser 1177 and PKB / Akt phosphorylation at Ser 473 in human umbilical vein endothelial cells. Hence PKB / Akt-eNOS pathway may be the chief mechanism of inducing NO production in endothelial cells. In myocardial ischaemia-reperfusion, cardioprotective mechanisms of OA were associated with increased mitochondrial antioxidants such as glutathione and alpha-tocopherol (Du & Ko 2006). In hypertensive rats, OA normalized protein levels of the antioxidants, glutathione peroxidase and SOD (Somova *et al* 2003). Hence the mechanisms underlying OA-induced oxidative stress reduction in the current study may be through up-regulation of cellular antioxidant proteins. Antioxidant mechanisms of OA remain under-investigated in endothelial cells, in fact, mechanisms underlying endothelio-protective properties of OA are poorly investigated.

4.2 Proteomics

4.2.1 Endothelial cell proteomics

Proteomics provides a tool for broad spectrum analysis and characterisation of protein expression and regulation in cells under physiological conditions or in response to certain stimuli (Anderson & Anderson 1998). Since proteomic analyses provide an opportunity for exploration of a large number of proteins, it may potentially lead to discovery of novel signalling pathways and biomarkers in response to a variety of stimuli or pathological conditions (Vivanco *et al* 2007). Hence, endothelial cell proteomics may be of great value in endothelial physiology and may yield vital information in relation to endothelial function or dysfunction and hence prevention of cardiovascular disease. Furthermore, in the subject of endothelial heterogeneity, proteomics may represent an invaluable tool for characterization of differential protein expression and regulation in endothelial cells from distinct vascular beds. Nonetheless, a wide gap exists in the literature with regards to studies focusing on vascular endothelial proteomics (Richardson *et al* 2010), particularly in the context of differential protein expression and regulation in endothelial cells from distinct vascular beds. The analysis of HUVECs is over-represented in the field of vascular proteomics (Bruneel *et al* 2003, Richardson *et al* 2010), due to its availability and relatively wide supply; however this trend is in conflict with the reality of endothelial heterogeneity. Furthermore, studies that have applied endothelial cell proteomics in response to stimuli such as TNF- α are limited. In the present study, proteomic analyses were performed in two endothelial cell lines isolated from distinct vascular sites, namely AECs and CMECs, to characterise the differences in protein expression and regulation between these two cell lines. We further investigated changes in protein expression and regulation in response to TNF- α in both cell lines.

4.2.2 Large scale protein expression and regulation in control, untreated AECs and CMECs

A total of 2372 proteins were identified in both untreated AECs and CMECs, 1695 of which were shared by both cell lines. 320 proteins were exclusively identified in AECs whereas 357 were exclusive to CMECs (Figure 3.26 A). As far as we are aware, these proteomic data

represent the most comprehensive documentation of its kind in AECs and CMECs to date. For the purposes of this study, “strongly represented proteins” refers to proteins that are detected only in a given cell type PLUS proteins that are significantly up-regulated in a given cell type relative to the other cell type.

4.2.2.1 Strongly represented proteins in untreated control AECs compared to CMECs

In this section, **strongly represented proteins in AECs, and their functional annotation analysis** will be discussed as shown in Tables 3.1 and 3.2.

In previous-proteomics based studies, microarray analysis and real-time PCR revealed 299 genes that were up-regulated in endocardial endothelium and 201 genes that were up-regulated in AECs (Hendrickx *et al* 2004). Genes upregulated in endocardial endothelium included those encoding for ion exchange channels, inositol-1,4,5-triphosphate receptor, transforming growth factor β 2, oxidized low density lipoprotein receptor 1 and apolipoprotein E all which may possess a regulatory role in cardiac function (Hendrickx *et al* 2004). Conversely, genes up-regulated in AECs encoded angiogenic protein Decorin, gap junction protein connexin 26, VCAM-1 and vasopressin V1a receptor (Hendrickx *et al* 2004). In HUVECs, proteomic analysis led to the identification of 53 endothelial proteins (Bruneel *et al* 2003). These proteins included cytoskeletal proteins, proteins involved in apoptosis and cell senescence regulation, coagulation proteins, proteins concerned with antigen presentation, as well as enzymatic proteins (Bruneel *et al* 2003).

In the present study, cytoskeletal proteins such as protein syne3, cytoskeleton associated protein 5, and WAS protein family (member 2), were highly up-regulated in AECs. The cytoskeleton is involved in maintenance of cell shape and polarity and it is important in transduction of shear stress-induced signals (Resnick *et al* 2003, Morgan *et al* 2011). In endothelial cells, the cytoskeleton is also important in maintenance of barrier functions and further serves as a scaffold for organisation of membrane proteins inside the cell (Ziegler *et al* 2012). Protein syne3 (6.8-fold up-regulated) anchors the cell nucleus to the cytoskeleton and has previously been shown to be highly expressed in human AECs (Morgan *et al* 2011). In human AECs, protein syne3 is involved in regulation of cell morphology. For example,

silencing protein syne3 resulted in a shift from the characteristic endothelial cell cuboidal shape to an elongated shape (Morgan *et al* 2011). Interestingly, the switch in endothelial cell morphology from cuboidal to elongation is often a response of mechanical stimuli such as unidirectional shear stress (Potter *et al* 2011). Furthermore, silencing protein syne3 abrogated flow-induced cell migration in human AECs (Morgan *et al* 2011). Hence protein syne3 may play a homeostatic role during mechanical stress.

Proteins associated with fatty acid metabolism were also upregulated in AECs. These included cytosolic acyl coenzyme A thioester hydrolase, and fatty acid synthase. Furthermore, according to the functional annotation analysis, the most highly enriched biological process in AECs was triglyceride mobilization (41-fold enriched). Cytosolic acyl coenzyme A thioester hydrolases (5-fold up-regulated) is responsible for the hydrolysis of acyl coenzyme A to the free fatty acid and coenzyme A, and is hence involved in the regulation of intracellular levels of acyl coenzyme A, free fatty acids and coenzyme A (Hunt *et al* 2005). Fatty acid synthase catalyses the synthesis of long chain fatty acid and it is known to promote cell proliferation and angiogenesis in endothelial cells (Browne *et al* 2006, Seguin *et al* 2012). In addition to proteins associated with fatty acid metabolism, Apolipoprotein B-100, a component of VLDL and LDL was also upregulated in AECs. Apolipoprotein B-100 is involved in cholesterol assembly and mobilization, and its overexpression has previously been linked with atherosclerosis (Ouguerram *et al* 2004, Olofsson & Boren 2005). Since AECs line the conduit aorta, they might be adapted to metabolize fatty acids and lipids from the circulating blood, a function that could be construed as less essential in the endothelial cells of the cardiac microvascular circulation.

Insulin-degrading enzyme was also up-regulated in AECs compared to CMECs (Table 3.1). In addition to its insulin and glucagon breakdown role, insulin-degrading enzyme has previously been shown to be abundantly expressed in brain endothelial cells, where it is responsible for the degradation of amyloid beta peptides (Lynch *et al* 2006). Insulin receptors have been identified in vascular endothelial cells, and binding of insulin has been shown to regulate vascular tone through the PKB / Akt-eNOS pathway and ET-1 (Vicent *et al* 2003). Hence, in AECs the role of insulin-degrading enzyme may be to regulate insulin levels. The up-regulation of insulin-degrading enzyme would indeed be more essential in AECs compared to CMECs as they are situated in a vascular tone regulating blood vessel.

Catechol O-methyltransferase is an enzyme responsible for degradation of the catecholamines such as dopamine, epinephrine, and norepinephrine (Gogos *et al* 1998). This enzyme was up-regulated in AECs compared to CMECs (Table 3.1). Unlike CMECs, AECs line the smooth muscle containing aorta which possess vasoactive properties such as vasodilating and vasoconstricting (Strijdom & Lochner 2009). Catecholamines such as norepinephrine possess vasoconstrictory effects (Hirano *et al* 2007), and hence catechol O-methyltransferase in AECs may serve to regulate cellular levels of such catecholamines. In fact, lack of catechol O-methyltransferase in rats has been associated with hypertension (Hirano *et al* 2007, Hernandez *et al* 2013).

Poly [ADP-ribose] polymerase 1 (PARP-1), an enzyme which is activated in response to DNA damage, and responsible for DNA repair (Pacher & Szabo 2007) was up-regulated in AECs compared to CMECs. PARP-1 activation has been linked with conditions that induce DNA damage such as oxidative and nitrosative stress (Mathews & Berk 2008, Szabo *et al* 2004). However, enhanced activity of PARP-1 may lead to cell energy depletion and consequently endothelial cell death (Szabo *et al* 2004, Pacher & Szabo 2007, Mathews & Berk 2008). Hence, PARP-1 has been implicated in conditions such as ED and cardiovascular diseases (Szabo *et al* 2004, Pacher & Szabo 2007, Mathews & Berk 2008). In addition to DNA damage, PARP-1 seems to be stimulated by stressful conditions including low shear stress-induced inflammation (Qin *et al* 2013). Considering the location of AECs, where they are exposed to different factors from the circulation (some which may elicit injury to cells) and mechanical forces exerted by the circulating blood, PARP-1 may be essential in AECs for stress response and DNA damage repair.

A pro-apoptotic protein, BAX, was up-regulated in AECs compared to CMECs (Table 3.1). BAX is a member of the BCL-2 family, and is usually activated in response to cell stress including ROS and cytokines (Aoki *et al* 2001, Molostvov *et al* 2002). Upon its activation, BAX translocates from the cytosol to mitochondria where it induces the release of cytochrome C, hence leading to apoptosis (Finucane *et al* 1999). Physiologically, apoptosis plays a homeostatic role in the programmed cell death of damaged cells (Finucane *et al* 1999). Given the location of the AECs and exposure to different stimuli including mechanical forces, BAX may play a homeostatic role of regulating death of damaged cells.

Aldehyde dehydrogenase primarily plays a role in detoxification of toxic compounds such as aldehydes, which have been associated with oxidative stress and lipid peroxidation (Ohsawa *et al* 2003). This protein was up-regulated (4.4-fold) in AECs compared to CMECs (Table 3.1, Figure 3.27 A). There is lack of literature on the effects of aldehyde dehydrogenase in endothelial cells. However, in human umbilical vein endothelial cells, aldehyde dehydrogenase activity was associated with a reduction in ROS accumulation, endothelial barrier dysfunction and endothelial dysfunction (Solito *et al* 2013). Owing to their location, up-regulation of this aldehyde dehydrogenase in AECs may perhaps participate in the detoxification of aldehydes derived from the circulation, hence preventing ROS accumulation and lipid peroxidation.

4.2.2.2 Strongly represented proteins in untreated control CMECs compared to AECs

In this section, **strongly represented proteins in CMECs, and their functional annotation analysis** will be discussed as shown in Tables 3.4 and 3.5.

A number of extracellular matrix proteins were up-regulated in CMECs including protein lamc1 (20-fold), laminin alpha 5 (12.5-fold), laminin subunit beta-2 (10-fold), procollagen, type XVIII, alpha 1, heparan sulfate proteoglycan-2, SPARC, and fermitin family homolog 2 (Table 3.4). This suggests that CMECs may be more involved with angiogenesis than their AEC counterparts. The extracellular matrix not only confers structure and organization of endothelial cells in the blood vessels, but it is important in endothelial cell migration, survival and proliferation (Davies & Senger 2005). Angiogenesis plays an important role in formation of new blood vessels, and CMECs have been shown to play a major role in cardiac angiogenesis (Li *et al* 2015). Furthermore, proteins involved in cell proliferation, growth, adhesion and migration were also up-regulated. These included protein tyrosine phosphatase non-receptor type 12, talin-2, basal cell adhesion molecule, endothelial cell selective adhesion molecule, integrin alpha 3 variant A, platelet endothelial cell adhesion molecule (PECAM-1; CD31), and Rho guanine nucleotide exchange factor-7. The importance of PECAM-1 in angiogenesis has previously been illustrated, where blocking PECAM-1 resulted in cessation of tube formation by angiogenic rat capillary endothelial cells (DeLisser *et al* 1997) and human umbilical vein endothelial cells (Cao *et al* 2002). Likewise, tube

formation and cell migration was diminished in endothelial cells derived from endothelial selective adhesion molecule knockout mice (Ishida *et al* 2003).

Proteins associated with intercellular junctions such as tight junction protein-1 (Figure 3.28 A), protein cingulin-like 1, LIM and senescent cell antigen-like domains 1 isoform E, and junctional adhesion molecule were also up-regulated in CMECs. Endothelial junctions play a major role in regulation of endothelial cell permeability, leukocyte extravasation, and angiogenesis (Dejana *et al* 1995, Wallez & Huber 2008). Tight junctions are responsible for the close cell-to-cell association forming a protective and functional barrier (Dejana *et al* 1995). This suggests that CMECs may play an important role in the maintenance of barrier function. In CMECs a functional barrier would be critical in regulating passage of substances to the underlying cardiomyocytes. Unlike AECs, CMECs are strategically arranged to be in paracrine communication with cardiomyocytes, and hence substances released from CMECs are able to influence cardiomyocyte growth and function, and vice versa (Strijdom *et al* 2009). The intercellular junctions may act as sieve for substances that diffuse from CMECs to cardiomyocytes. Furthermore, PECAM-1 is expressed at endothelial cell junctions and in addition to angiogenesis it is also involved in preservation of the endothelial barrier and regulation of leukocyte transmigration during inflammatory conditions (Cao *et al* 2002, Privratsky *et al* 2010).

Compared to AECs, the pro-thrombotic protein, Von Willebrand factor, enzyme prostaglandin G/H synthase and nitric oxide synthase (NOS3 /eNOS) were significantly up-regulated in CMECs (Table 3.4). Although the western blot data did not show any statistical significance, total eNOS expression was ~1.4-fold higher in CMECs compared to AECs (Figure 3.12 A). The fact that eNOS was up-regulated in CMECs compared to AECs was quite an interesting and potentially a novel finding. Fish *et al* (2005) stated that eNOS is highly expressed in medium to large sized arterial blood vessels for vasomotor and vascular homeostasis regulation purposes. In the present study, we show that the expression of eNOS is more abundant in the microvascular (CMECs) compared to macrovascular endothelial cells (AECs), hence refuting this notion. Prostaglandin G/H synthase is responsible for biosynthesis of prostaglandin, the precursor of PGI₂ and TXA₂. In CMECs, eNOS-derived NO and other endothelial derived factors such as PGI₂ diffuses into the underlying cardiomyocytes (*in vivo* settings) in a paracrine manner where it modulates

cardiomyocyte growth and function in addition to maintaining the endothelial surface integrity (Strijdom *et al* 2009, Shah & MacCarthy 2000). As it has previously been shown, eNOS expression and NO production are higher in CMECs compared to cardiomyocytes (Strijdom *et al* 2006).

CMECs exhibited up-regulation of antioxidant proteins such as superoxide dismutase [Mn] (mitochondrial) (MnSOD), glutathione peroxidase, and peroxiredoxin-6 (Table 3.4). MnSOD is responsible for clearance of O_2^- through dismutation into H_2O_2 and water, whereas glutathione peroxidase and peroxiredoxin-6 are responsible for the reduction of H_2O_2 , hence protecting cells from oxidative damage. Glutathione peroxidase and peroxiredoxin-6 could explain why CMECs exhibited lower levels of H_2O_2 compared AECs under baseline conditions as measured by flow cytometric analysis of DCF fluorescence (Figure 3.3 B). This was also reflected by the enriched biological processes, where H_2O_2 catabolic process was 18.1-fold enriched in CMECs (Table 3.5). H_2O_2 has previously been associated with cardiomyocyte death and myocardial dysfunction (Meldrum *et al* 1998). The degradation of H_2O_2 by CMECs, as reflected by the up-regulated proteins and the enriched biological processes associated with anti-oxidant activity, may be essential for protection of the underlying cardiomyocytes against cell death and consequent myocardial injury. Furthermore, proteins involved in the regulation of apoptosis such as BCL-2 related protein A1B, protein Acin1 and 3-ketoacyl-CoA thiolase (mitochondrial) were up-regulated in CMECs (Table 3.4). Interestingly, BCL-2 is an apoptosis repressor protein which antagonizes the pro-apoptotic effects of BAX (which was up-regulated in AECs). In fact, BCL-2 related protein A1B was only detected in CMECs and not AECs. BCL-2 related protein A1B is activated by NF- κ B and its expression has been associated with decreased apoptosis (Zong *et al* 1999). Apoptotic activity of CMECs would most likely negatively affect the underlying cardiomyocytes, as CMEC-derived factors such as NO and ET1, are dedicated at regulating underlying cardiomyocyte function and activity. Therefore, it is speculated that the up-regulation of the anti-apoptotic proteins observed in the CMECS could serve to preserve underlying cardiomyocyte function and existence.

4.2.3 Large scale protein expression and regulation in TNF- α treated AECs and CMECs

TNF- α (20 ng/ml, over 24 hours) resulted in 2426 proteins being up-regulated in both AECs and CMECs. Of these proteins, 1701 proteins were shared by both AECs and CMECs, while 322 were unique to AECs and 403 unique to CMECs.

4.2.3.1 Strongly represented proteins in TNF- α treated AECs (compared to control, untreated AECs)

In this section, **strongly represented proteins in TNF- α -treated AECs and their functional annotation analysis** will be discussed as shown in Tables 3.7 and 3.8.

Differential protein regulation analysis revealed 30 proteins that were up-regulated in AECs in response to TNF- α compared to control, untreated AECs. Furthermore, 40 proteins were detected in TNF- α treated AECs only compared to control, untreated AECs. In a previous proteomics-based study on HUVECs, treatment with TNF- α resulted in differential regulation of 21 proteins, with 9 proteins up-regulated, 11 down-regulated and 1 expressed only with TNF- α treatment (Ma *et al* 2006). The up-regulated proteins included a stress response protein, MAP kinase kinase kinase protein (MEKKS), whereas eNOS was amongst the down-regulated proteins (Ma *et al* 2006).

In AECs, TNF- α elicited up-regulation of proteins associated with the immune response and inflammation including guanylate binding protein 2, leucine-rich repeat flightless-interacting protein 1, MHC class I RT1.Au heavy chain, and protein Parp14. Guanylate binding protein 2 (3-fold up-regulated) belongs to a group of GTPases which possess anti-viral activities and its expression is often elicited by the cytokines such as interferon gamma, TNF- α and interleukin-1 β (IL-1 β) in endothelial cells (Tripal *et al* 2007, Yamamoto *et al* 2012). The role of guanylate binding protein 2 in endothelial cells has not been well described; however, other isoforms such as guanylate binding protein 1 has been shown to inhibit endothelial cell proliferation and expression of matrix metalloproteinase (Verstal & Jeyaratnam 2011).

NF- κ B p49/p100, a transcription factor which plays a major role in TNF- α signalling, was only detected in TNF- α treated AECs compared to control, untreated AECs (Figure 3.29 B). This is indicative of the activation of pro-inflammatory signalling processes by TNF- α in the AECs. NF- κ B regulates downstream transcription of inflammatory genes encoding for cytokines, and proteins involved in proliferation, differentiation, the immune response and regulation of apoptosis in response to stimuli such as TNF- α (Kempe *et al* 2005). Binding of TNF- α to TNFR1 leads to trimerization of the receptors and subsequent release of the silencer of death domain (SODD) from the intracellular domain of TNFR1 (Jiang *et al* 1999). This is followed by recruitment of TRADD to the exposed intracellular domain of TNFR1 which in turn recruit TNFR associated factor 2 (TRAF2), and RIP (Hsu *et al* 1995) (Figure 4.2). Successive downstream signalling pathways lead to phosphorylation and subsequent degradation of the inhibitory I κ B-alpha by the I κ B kinase (IKK complex), hence leading to the release of the active NF- κ B into the nucleus for gene transcription (Hsu *et al* 1996) (Figure 4.2). Though not significant, western blot data showed a modest \sim 16% reduction in I κ B-alpha expression in TNF- α treated AECs compared to control, untreated AECs (Figure 3.15).

Recruitment of fas-associated death domain (FADD) to the TNFR1-TRADD complex leads to cell death through cleavage of caspase 8 followed by cleavage caspase 3 which in turn initiates apoptotic cell death (Hsu *et al* 1996, Lin & Lin 2008) (Figure 4.2). Caspase 3 was 1.5-fold up-regulated in the TNF- α treated AECs compared to their control untreated AEC counterparts (Table 3.7). This is suggestive of the activation of the TNF- α -mediated apoptotic cell death pathway in the AECs. Our data is consistent with the literature. TNF- α at a concentration of 10 ng/ml over 24 hours was shown to increase apoptosis and caspase 3 activity in bovine glomerular endothelial cells (Messmer *et al* 1999). In human coronary artery endothelial cells, TNF- α (40 ng/ml) was also shown to induce apoptosis and caspase 3 activity (Chen *et al* 2004).

The induction of NF- κ B activity in TNF- α -treated AECs was further validated by the up-regulation (2.3-fold) of sequestosome 1 (Table 3.7). Sequestosome 1 modulates NF- κ B activity via TNFR associated factor 6 (TRAF6) following TNF- α or IL-1 stimulation (Zotti *et al* 2014). The underlying mechanism include ubiquitination of the regulatory subunit of the IKK complex, NEMO, leading to phosphorylation of the I κ B-alpha and subsequent activation of NF- κ B (Zotti *et al* 2014). In addition to NF- κ B activation, sequestosome 1 is also involved in

induction of autophagy, a homeostatic process which involves the auto-degradation of damaged cell organelles and proteins (Zhou *et al* 2013). Reduction of autophagy has been implicated in endothelial senescence, enhanced ROS production, inflammation, atherogenesis and vascular aging (Xiong *et al* 2014, Chen *et al* 2013, Salminen *et al* 2012).

MnSOD was up-regulated (2.8-fold) in response to TNF- α in AECs compared to control, untreated AECs (Table 3.7) (Figure 3.29 A). This is in support of our flow cytometry data, where 0.5, 5 and 20 ng/ml TNF- α (24 hours) resulted in increased H₂O₂ levels as measured by flow cytometric analysis of DCF fluorescence (Figure 3.8 A). Indeed, TNF- α has previously been shown to increase MnSOD expression as a protective mechanism against oxidative stress (Warner *et al* 1991, Wong & Goeddel 1988, Nakata *et al* 1993). Furthermore, removal of O₂⁻ through the dismutation process may also play a protective role against inflammation, as oxidative stress is known to be pro-inflammatory (Li & Zhou 2011).

In addition to MnSOD, other protective proteins such as cystatin B was up-regulated (2.8-fold) following TNF- α treatment in AECs (Table 3.7). Cystatin B is an inhibitor of lysosomal cathepsin B, a cysteine protease involved in protein degradation (Mort & Buttle 1997). In HUVECs, TNF- α was shown to activate cathepsin B, which in turn initiates caspase-independent cell death (cathepsin-dependent cell death) (Madge *et al* 2003). The cathepsin-dependent cell death involves loss of mitochondrial membrane potential and release of cytochrome c from the mitochondria (Li & Pober 2005). Interestingly, amongst the biological processes associated with strongly represented proteins in TNF- α treated AECs, release of cytochrome C was highly enriched (37.1-fold), suggesting high apoptotic activity in TNF- α treated AECs (Table 3.8). Therefore, the expression of cystatin B was presumably an attempt by the cells to alleviate cathepsin B-dependent cell death.

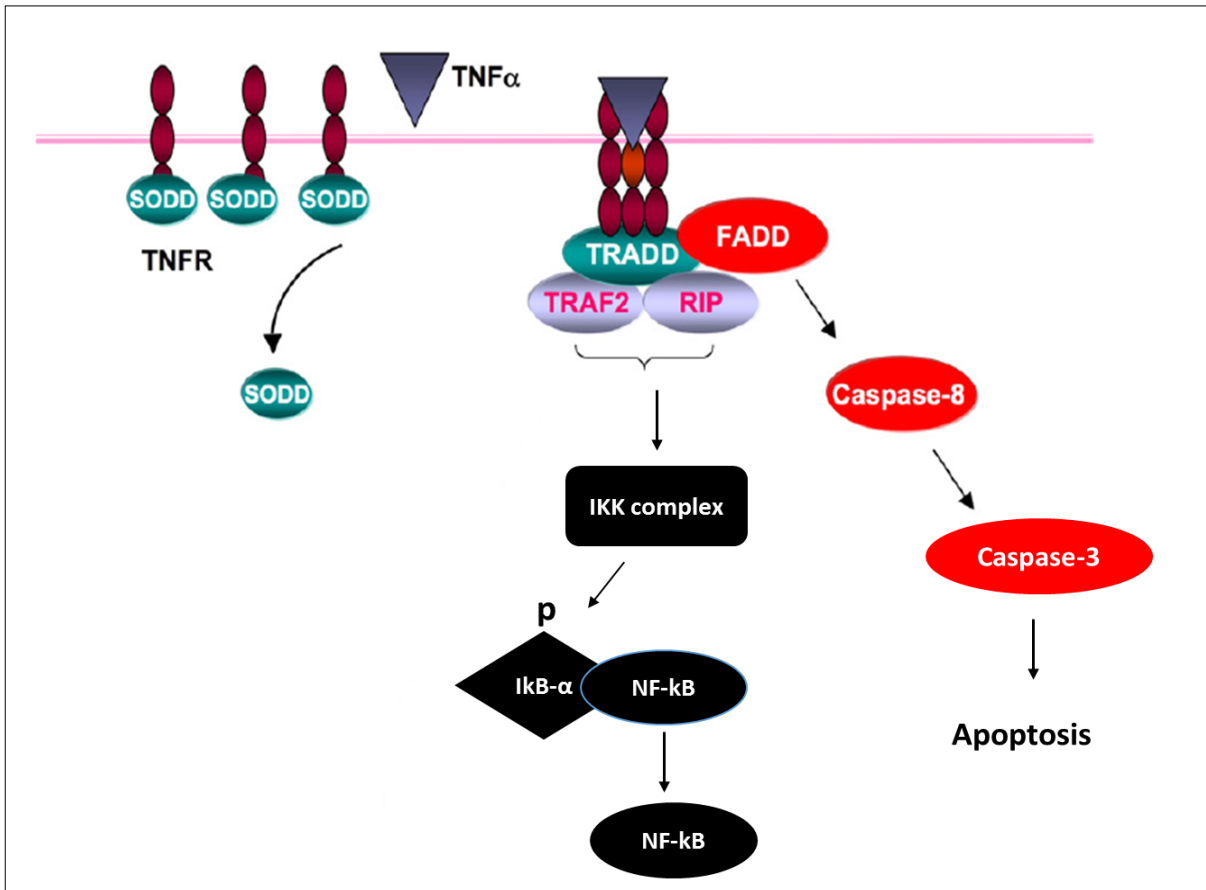


Figure 4.2: The TNF- α signalling pathway (Modified from Li & Lin 2008).

4.2.3.2 Strongly represented proteins in TNF- α treated CMECs (compared to control, untreated CMECs)

In this section, **strongly represented proteins in TNF- α -treated CMECs and their functional annotation analysis** will be discussed as shown in Tables 3.7 and 3.8.

Differential protein regulation analysis revealed a total of 45 proteins that were up-regulated in response to TNF- α in CMECs; furthermore, a total of 61 proteins were only detected in TNF- α treated CMECs compared to control, untreated CMECs. Proteins associated with the immune response and inflammation were up-regulated in TNF- α treated CMECs compared to control, untreated CMECs. This response was also observed in TNF- α treated AECs (see section 4.2.3.2), however, the up-regulated proteins in the AECs were different except for one immune response protein (guanylate binding protein 2) that was up-regulated in both TNF- α treated AECs and CMECs. This is indicative that some level of heterogeneity in protein expression in response to TNF- α exists between these two cell lines. Immune response proteins up-regulated in TNF- α treated CMECs included protein Gbp5 (6-fold) (guanylate binding protein 5), intercellular adhesion molecule 1 (ICAM-1) (4-fold), protein Tapbp and guanylate binding protein 2 (3.2-fold) (Table 3.9).

Enhanced expression of ICAM-1 is induced by pro-inflammatory cytokines including TNF- α , and it plays a role in leukocyte transmigration (Lawson & Wolf 2009). TNF- α -induced expression of ICAM-1 has previously been shown in most endothelial cell lines including HUVECs, human lung microvascular endothelial cells, human AECs and rat CMECs (Burke-Gaffney & Helewell 1996, Chen *et al* 2001, Li *et al* 2010). ICAM-1 is one of the inflammatory genes that are transcriptionally regulated by NF- κ B in response to TNF- α (Paxton *et al* 1997, Min *et al* 2005). Similar to the TNF- α treated AECs, NF- κ B was also uniquely expressed in TNF- α treated CMECs (with no expression detected in control, untreated CMECs). Moreover, our western blot data showed a significant reduction in I κ B- α expression in TNF- α CMECs compared to control, untreated CMECs (Figure 3.15). This is suggestive of a TNF- α -mediated activation of NF- κ B and hence a pro-inflammatory response in CMECs. Furthermore, another pro-inflammatory cytokine, Interleukin 1 family member 6 (Interleukin 36- α ; IL-36 α) was 2.5-fold up-regulated in TNF- α treated CMECs compared to control, untreated CMECs. There appears to be a lack of studies investigating the effects of IL-36 α in endothelial cells, but it has previously been shown to be involved in production of cytokines

and chemokines including IL-1 β , IL-6, IL-12, and TNF- α in bone marrow dendritic cells (Vigne *et al* 2011). Moreover, IL-36 α has been shown to induce NF-KB activity in mouse macrophage and neutrophil infiltration in mouse lungs (Ramadas *et al* 2012). These results thus implicate IL-36 α in the involvement of an inflammatory response.

A pro-apoptotic protein, BH3 interacting domain death agonist (Bid) was ~4.8-fold up-regulated in TNF- α treated CMECs compared to control, untreated CMECs (Table 3.9). Bid is cleaved by cathepsins or caspase 8, after which it translocates to the mitochondria, inducing mitochondrial membrane permeability and release of cytochrome C (Billien *et al* 2009). This was reflected by the enriched biological processes in our TNF- α treated CMECs, which included regulation of mitochondrial membrane permeability (76.6-fold enriched), regulation of mitochondrial membrane potential (46.8-fold enriched), release of cytochrome C from mitochondria (40.1-fold enriched), and apoptotic mitochondrial changes (29.1-fold enriched) (Table 3.10). Hence TNF- α appears to have induced some apoptotic activity in CMECs. This response appears to have been more profound in TNF- α treated CMECs compared to TNF- α treated AECs, hence heterogeneity was evident in this regard.

TNF- α elicited a 2.6-fold up-regulation of plasminogen activator inhibitor 1 in CMECs (Table 3.9, Figure 3.30 A). Plasminogen activator inhibitor 1 is a pro-clotting factor with a homeostatic role of preventing excess bleeding during injury (Mehta & Shapiro 2008). However, plasminogen activator inhibitor 1 may lead to thrombolytic resistance, accumulation of blood clots and consequent occlusion of the vessel, leading to myocardial ischaemia (Handt *et al* 1996). Previous studies have linked the expression of plasminogen activator inhibitor 1 with TNF- α in endothelial cells (Swiatkowska *et al* 2005, Soeda *et al* 1998, Handt *et al* 1996). Clinically, elevated plasminogen activator inhibitor 1 has been used as a marker of endothelial dysfunction (Meigs *et al* 2006, Belo *et al* 2002). Hence, the up-regulation of plasminogen activator alpha 1 in TNF- α treated CMECs compared to their respective control could be an indicator of the cells switching into a dysfunctional state.

Like cathepsin B, cathepsin L1 is a cysteine protease involved in breakdown of proteins. Cathepsin L1 was 2-fold up-regulated in TNF- α treated CMECs compared to control, untreated CMECs. Cathepsin L1 plays a role in antigen presentation, but has also been implicated in the process of atherogenesis through the remodelling of vascular extracellular

matrix (Zhang F *et al* 2009, Kitamoto *et al* 2007). Furthermore, cleavage of collagen XVIII by cathepsin L1 generates endostatin, a protein that inhibits angiogenesis (Zhang F *et al* 2009). According Zhang F *et al* (2009), endostatin diminished endothelium dependent vasodilation in bovine coronary arteries. However, in the heart, cathepsin L appears to play a more protective role. For example, it has been shown to be involved in cardiac repair and remodelling following myocardial infarction (Sun *et al* 2011). Hearts from cathepsin L1 deficient mice exhibited dilated cardiomyopathy (Stypmann *et al* 2002). Hence, up-regulation of this protein in CMECs may be a protective instinct, for myocardial repair in response to insult.

Similarly to AECs, MnSOD was also up-regulated (2.2-fold) in TNF- α treated CMECs compared to control, untreated CMECs. This also supports our DCF fluorescence data, where 5 and 20 ng/ml TNF- α over 24 hours increased H₂O₂ production in CMECs, suggestive of the dismutation of O₂⁻ into H₂O₂ and water by SOD (Figure 3.8 C).

Finally, a state of endothelial activation appeared to be induced in the CMECs in response to TNF- α as evidenced by the up-regulation of inflammatory mediators such ICAM-1 and IL-36 α , and NF- κ B activation. Furthermore, biological processes that were enriched included antigen processing and presentation (16.9-fold enriched), leukocyte migration (14.8-fold enriched), the cytokine-mediated signalling pathway (13.2-fold enriched) and cell activation (4.6-fold enriched) (Table 3.10). In addition to this, NO production was significantly decreased following 24 hours of TNF- α treatment (Figure 3.4 C), whereas ROS (H₂O₂) production (Figure 3.8 C) and necrosis (Figure 3.10 C) were increased. This is a clear indication of TNF- α -induced endothelial injury.

In the next two sections, we directly compared the TNF-treated AEC and CMEC proteomic data with the objective to gain a more focussed insight into possible heterogeneous responses between the two cell types as a result of TNF- α treatment.

4.2.3.3 Differential protein regulation and functional annotation analysis: Strongly represented proteins in TNF- α treated AECs compared to TNF- α treated CMECs.

Proteins associated with cell adhesion and migration were up-regulated in TNF- α treated AECs compared to TNF- α treated CMECs. These included CD9 molecule, galectin, fermt3 protein and podocalyxin (Table 3.11). In a previous study in TNF- α treated HUVECs (20 ng/ml TNF- α for 20 hours), CD9 molecule (27.7-fold up-regulated) was shown to partner with other transmembrane proteins including CD81, CD151, ICAM-1 and VCAM-1 forming microdomains that mediate leukocyte intercellular adhesion and migration (Barreiro *et al* 2005, 2008). In our cells however, ICAM-1 was only up-regulated in TNF- α treated CMECs and not AECs. Although both cell types showed a pro-inflammatory response, there was considerable heterogeneity in terms of the proteins involved. Galectin (8.7-fold up-regulated in TNF- α -treated AECs vs their CMEC counterparts) plays a role in cell proliferation, cell adhesion and migration, immune response and apoptosis of endothelial cell bound T cells (Hsieh *et al* 2008, Perillo *et al* 1995). Apoptosis of endothelial cell bound T cells might be a mechanism through which galectin regulates endothelial cell-leukocyte adhesion. Fermt3 protein plays a role in activation of integrin beta which facilitates leukocyte adhesion to endothelial cells (Moser *et al* 2009). Integrin beta is a cell adhesion molecule which was 3.9-fold up-regulated in TNF- α AECs compared to CMECs. Up-regulation of these proteins is indicative of inflammation and hence TNF- α -induced endothelial activation in AECs. Though this response was also observed in CMECs, the proteins mediating endothelial activation appears to differ between AECs and CMECs.

Biliverdin reductase A was 7.5-fold up-regulated in TNF- α treated AECs compared to their CMECs counterparts (Table 3.11). Biliverdin reductase A converts biliverdin to bilirubin which has been shown to possess antioxidant activity, hence conferring protection from ROS (Baranano *et al* 2002). In HUVECs, silencing biliverdin reductase led to enhanced lipopolysaccharide induced- oxidative stress (Jansen *et al* 2010). Hence, biliverdin reductase A could contribute to the antioxidant pathways of the cells to alleviate the oxidative effects of TNF- α in AECs. Other protective proteins up-regulated in TNF- α treated AECs compared

to TNF- α treated CMECs included glutathione S-transferase Mu 4, glutathione S-transferase Mu 1, NAD(P)H dehydrogenase [quinone] 1, aldehyde dehydrogenase (dimeric NADP-preferring), and glutathione reductase (Table 3.11). Glutathione S-transferase Mu 4, and glutathione S-transferase Mu 1 conjugate with glutathione and are involved in detoxification processes. NAD(P)H dehydrogenase [quinone] 1 plays a role in detoxification of xenobiotics and scavenging of O_2^- , hence acting as an antioxidant (Siegel *et al* 2004). Glutathione reductase is responsible for the reduction of glutathione, which plays a major role in the defence against oxidative stress (Harlan *et al* 1984). Hence, it appears that AECs were able to up-regulate anti-oxidant enzymes in response to TNF- α to a greater extent compared to their CMEC counterparts. This may possibly account for decreased $ONOO^-$ levels in TNF- α treated AECs (at all TNF- α concentrations) as measured by flow cytometric analysis of DHR-123 fluorescence (Figure 3.7 A), however, this response was also observed in CMECs. As mentioned in the above sections, only H_2O_2 production was increased by TNF- α , but this can be attributable to the dismutation of O_2^- by MnSOD.

Endothelin-converting enzyme 1, an enzyme responsible for ET-1 biosynthesis was up-regulated in TNF- α treated AECs compared to their AECs counterparts (Table 3.11, Figure 3.31 A). Since AECs line the smooth muscle containing blood vessel, ET-1 released from AECs would serve a vasoconstrictory role and hence play a role in vasomotor function under physiological conditions. However, ET-1 production is enhanced during pathophysiological conditions such as endothelial dysfunction, hence contributing to initiation of cardiovascular diseases (Molet *et al* 2000). In HUVECs, a mixture of TNF- α (20 ng/ml), IL-1 β (20 U/ml) and interferon gamma (100 U/ml) and chemokines resulted in enhanced mRNA expression of both endothelin-converting enzyme and ET-1 (Molet *et al* 2000). Angiotensin II converting enzyme, responsible for the biosynthesis of angiotensin II was also up-regulated in TNF- α treated AECs compared to their CMECs counterparts. Like ET1, angiotensin II is a potent vasoconstrictor which in the case of AECs, is most likely involved in vasomotor regulation during physiological conditions. However, during pathophysiological conditions, angiotensin II contributes to initiation of cardiovascular diseases, owing to hyperconstriction of the blood vessels. In contrast to our findings, TNF- α (0.1-10 ng/ml) for 24 hours resulted in a dose dependent decrease of ACE mRNA expression in human umbilical vein endothelial cells (Saijonmaa *et al* 2001). These differences could be attributable to cell line differences or

TNF- α concentration differences. Co-culture of human AECs with monocytes led to a decrease in ACE activity, a response which was believed to be attributable to the monocyte-induced stimulation of TNF- α and IL-1, as antibodies against TNF- α and IL-1 reversed this response (Papapetropoulos *et al* 1996). As inflammatory cytokines have stimulatory effects on iNOS, NO produced from iNOS may affect ACE activity (Ackermann *et al* 1998). This might explain the observations from the above mentioned study. However, iNOS expression or NO production was not measured in this study. In our hands, TNF- α (0.5, 5 and 20 ng/ml over 24 hours) significantly decreased NO production in AECs (Figure 3.4 A). The up-regulation of endothelin-converting enzyme and ACE, and the reduced NO levels in AECs could represent a switch towards a dysfunctional state. One of the key characteristics of endothelial dysfunction is the shift in balance, where vasoconstrictory factors such as ET-1 outweigh vasodilatory factors such as NO. The up-regulation of these vasoconstrictory proteins is suggestive that AECs were progressing from the activated state and adopting a dysfunctional phenotype, while CMECs appear to have maintained an activated state as shown by the up-regulation of inflammatory proteins such as ICAM-1 and IL-36 α .

4.2.3.4 Differential protein regulation and functional annotation analysis: Strongly represented proteins in TNF- α treated CMECs compared to TNF- α treated AECs.

Ectonucleoside triphosphate diphosphohydrolase 1 (CD39) was highly up-regulated (75.2-fold) in TNF- α treated CMECs compared to TNF- α treated AECs (Table 3.14). CD39 inhibits platelet aggregation and is expressed in platelets, endothelial cells and leukocytes (Koziak *et al* 1999). Mice transfected with the CD39 gene has been shown to be resistant to occlusive thrombus formation in response to ferric chloride-induced carotid artery injury compared to their controls (Huttinger *et al* 2012). Furthermore, mice lacking CD39 (CD39 $-/-$ mice) demonstrated increased cerebral infarct volume compared to their genotypic CD39 $+/+$ controls (Marcus *et al* 2001). CD39 hydrolyses ATP and ADP released from activated platelets to AMP which is further converted to adenosine (Marcus *et al* 2001, Colgan *et al* 2006). Adenosine possesses anti-inflammatory, anti-thrombotic and cardioprotective properties (Colgan *et al* 2006). Since CMECs line myocardial capillaries, up-regulation of CD39 in response to injury would serve a critical role in preventing capillary occlusion in *in vivo* settings and consequent myocardial infarction. Up-regulating CD39 might have also

been a counter-acting mechanism for pro-clotting factors, von Willebrand factor (5-fold up-regulated) and plasminogen activator inhibitor (2.9-fold up-regulated), which were also up-regulated in TNF- α treated CMECs compared to their AECs counterpart.

cGMP_dependent 3_5_cyclic phosphodiesterase (PDE2A), a gene coding for PDE2 was up-regulated (46.7-fold) in TNF- α treated CMECs compared to TNF- α treated AECs (Table 3.14). PDE2 is involved in the termination of cAMP and cGMP activity both of which has been shown to play a role in the regulation of endothelial permeability (Draijer *et al* 1995). In HUVECs, TNF- α (10 ng/ml, 18 hours incubation time) significantly increased PDE2 activity which resulted in increased endothelial permeability (Seybold *et al* 2005). Similarly, Surapisitchat *et al* (2007) showed an increase in PDE2 expression and enhanced permeability in HUVECs following 24 hours of 10 ng/ml TNF- α treatment. Inflammatory cytokines including TNF- α have previously been associated with an altered endothelial cell barrier. The up-regulation of PDE2A could be an indication of increased endothelial permeability in TNF- α treated CMECs compared to TNF- α treated AECs. Generally capillaries (except in the blood brain barrier) exhibit high permeability for solute exchange as compared to the arteries (Aird 2007a). Inflammation-induced permeability and leukocyte trafficking is said to primarily occur in the postcapillary venules, but can also take place in other vessels including capillaries, veins and arterioles (Aird 2007a). Leukocyte transmigration is mediated by proteins such as ICAM-1, VCAM-1, E-selectin and PECAM-1 (Aird 2007a), and hence the up-regulation of ICAM-1 (3.1-fold up-regulated) and PECAM-1 (3.5-fold up-regulated) (Table 3.14) in TNF- α treated CMECs compared to TNF- α treated AECs could be another indication of inflammation-induced permeability.

Although H₂O₂ production was increased in both AECs and CMECs in response to TNF- α after 24 hours as shown by our flow cytometry data, proteins specifically associated with the degradation of H₂O₂ were up-regulated in TNF- α treated CMECs compared to TNF- α AECs. These included Protein Pxdn (14.5-fold up-regulated), Peroxiredoxin, and Glutathione peroxidase (Table 3.14). This could have been an attempt by the CMECs to reduce TNF- α -induced H₂O₂ production. This might explain why H₂O₂ production was lower in TNF- α treated CMECs compared to TNF- α AECs treated after 24 hours at all concentrations, as shown by DCF fluorescence data (Figure 3.9 A).

4.3 Rat isometric tension studies (ex vivo studies)

4.3.1 Summary of findings

4.3.1.1 Biometric data

Male Wistar rats receiving the high fat diet for either 16 or 24 weeks exhibited greater total body mass and intraperitoneal fat mass compared to their age and time-matched lean controls (Figures 3.33 – 3.36).

4.3.1.2 Isometric tension studies in aortic rings from lean and HFD rats (16 week diet)

Aortic rings derived from HFD rats exhibited a pro-contractile response to PE compared to rings isolated from lean rats (Figure 3.37).

4.3.1.3 Effects of *ex vivo* oleanolic acid (OA) administration on aortic ring contraction and relaxation from lean and HFD rats (16 week diet).

In aortic rings isolated from lean rats, administration of OA elicited a pro-contractile response to PE, however, this was likely due to a vehicle effect (Figure 3.39).

In aortic rings isolated from HFD rats, administration of OA resulted in an anti-contractile response to PE (Figure 3.41).

4.3.1.4 Effects of *ex vivo* oleanolic acid (OA) administration on aortic ring contraction and relaxation from lean and HFD rats (24 week diet)

OA elicited an anti-contractile response in aortic rings isolated from lean rats (Figure 3.43). Furthermore OA exerted pro-relaxing effects in response to Ach in aortic rings from lean rats (Figure 3.44).

The pro-contractile effects observed in aortic rings from HFD rats were due to a vehicle effect (Figure 3.45). OA pre-administration impaired Ach-induced relaxation in aortic rings from 24 weeks HFD rats (Figure 3.46).

4.3.1.5 Effects of direct OA administration on aortic rings (24 week diet)

Direct administration of OA following cumulative contraction with PE, had no relaxing effects on aortic rings from lean and HFD rats (Figure 3.47).

4.3.2 Discussion of data

Obesity poses a great medical challenge as it often occurs hand in hand with cardiovascular diseases and metabolic disorders such as insulin resistance (Campia *et al* 2012). Obesity is often associated with reduced endothelial NO bioavailability owing to enhanced endogenous production of NOS inhibitor ADMA, oxidative stress and eNOS uncoupling (Toda & Okamura 2013). Furthermore, conditions such as insulin resistance leads to an imbalance in endogenous production of NO and ET-1, with the scale tipping in favour of ET-1 production, hence leading to hyper-contraction of blood vessels (Potenza *et al* 2005). In this set of experiments, isometric tension studies were performed to study the vascular function in *ex vivo* settings of thoracic aortas derived from a model of high fat diet fed obese rats and age-matched lean control rats. In addition to enhanced total body and intraperitoneal fat mass, our model of HFD rats has previously been shown to exhibit high fasting blood glucose, triglyceride and insulin levels (Salie *et al* 2014).

4.3.2.1 Isometric tension studies in aortic rings from lean and HFD rats (16 week diet)

Subsequent to a 16 week feeding period, aortic rings isolated from HFD rats exhibited an enhanced contractile response to PE compared to rings from their lean counterparts (Figure 3.37). This is in agreement with the findings by Boustany-Kari *et al* (2007), where mesenteric arteries from rats fed a moderately high fat diet for 11 weeks, demonstrated an enhanced contractile response to PE, potassium chloride and serotonin. This is not surprising as

obesity is often associated with hypertension owing to amongst other factors, activation of the renin-angiotensin system (Kotsis *et al* 2010). Furthermore, Ach-induced relaxation was reported to be blunted in mesenteric arteries isolated from diet induced obese rats (Naderali *et al* 2001) and thoracic aortas from obese / diabetic mice (Seto *et al* 2010). Endothelial dysfunction is a common feature in obesity and is characterised by impaired vasodilation (Perticone *et al* 2001). In our hands, however, the pro-contractile response observed was not matched by reduced Ach-induced relaxation, which was found to be similar in aortic rings from HFD and lean rats (Figure 3.38). We suspect that the age of the rats may also have played a role, as the Ach-induced vasorelaxation in aortic rings from both lean and HFD rats was modest. It has previously been shown that progressive age is associated with a decline in endothelial function (Celemajer *et al* 1994). For example, contraction has been shown to be enhanced in aortic rings isolated from 15 weeks old rats compared to 7 and 11 weeks old rats, whereas relaxation was enhanced in aortic rings from 7 weeks old rats compared to 11 and 15 weeks old rats (Rohra *et al* 2006). This trend was also observed in our own investigations showing that relaxation was greater in aortic rings isolated from young rats (\pm 4 weeks old) compared to older rats (Figure 3.44).

In summary, in our hands, the HFD of 16 weeks induced modest signs of aortic endothelial dysfunction as shown by the pro-contractile response observed in these rings. Possible mechanisms include the modulation of vasoactive mediators released by dysfunctional perivascular adipose tissue that affect endothelial function such as reduced adiponectin (resulting in reduced anti-contractile effects), and increased reactive oxygen species (induction of pro-contractility) [for review see: Szasz *et al* 2010].

4.3.2.2 Effects of *ex vivo* oleanolic acid (OA) pre-administration on aortic ring contraction and relaxation from lean and HFD rats (16 and 24 week diet).

In view of the short-term NO stimulatory properties of OA in both AECs and CMECs (Figure 3.17 A & B), we further studied the vascular reactivity effects of OA on aortic rings derived from 16 and 24 weeks lean and HFD rats. Very few studies have investigated the role of OA in vascular reactivity or function in aortic rings. Furthermore, there appears to be lack of studies that investigated the effects of OA on vascular reactivity or function in aortic rings

derived from diet-induced obese rats. In a previous study, aortic rings isolated from rats fed a diet supplemented with OA for 12 weeks were shown to demonstrate a reduced contractile response to PE and an enhanced Ach-induced vasorelaxation (Rodriguez-Rodriguez *et al* 2007). Furthermore, OA has previously been shown to possess anti-hypertensive properties via modulation of NO production and antioxidant activity (Samova *et al* 2003, Bachhav *et al* 2011).

In our 16 week diet group, *ex vivo* pre-administration of OA prior PE-induced contraction and Ach-induced relaxation in aortic rings from lean rats, resulted in an enhanced contractile response to PE (Figure 3.39). However, this response was likely due to a vehicle effect. Furthermore, OA pre-administration had no significant effect on Ach-induced relaxation compared to the untreated aortic rings from lean rats (Figure 3.40). Hence, it appears that pre-administration of OA prior PE-induced contraction and Ach-induced relaxation had no significant effect on rings from 16 week lean rats. This was not the case in the aortic rings isolated from the lean older rats (24 week diet group), where pre-administration of OA elicited an anti-contractile response to PE and a pro-relaxing response to Ach (Figure 3.43 & 3.44). It is interesting that pre-administration of OA improved vascular function in the rings isolated from older lean rats as compared to those isolated from the lean 16 week diet group. The link between OA and vascular function in advanced age is not clear in the literature. However, since OA has been shown to improve conditions such as hypertension, oxidative stress and inflammation (all which are associated with advanced age) (Samova *et al* 2003, Bachhav *et al* 2011, Lee *et al* 2013), it is possible that OA is able to modulate vascular function in advanced age. This may possibly explain our observations in the rings isolated from the lean 24 week diet group.

In aortic rings isolated from HFD rats (16 week diet group), pre-administration of OA elicited an anti-contractile response to PE compared to untreated rings isolated HFD rats (Figure 3.41). As HFD has been previously associated with impaired vascular function (Boustany-Kari *et al* 2007), it is possible that pre-administration of OA acutely improved endothelial function in aortic rings from HFD rats. However, when compared to age-matched lean control aortic rings, there was no difference in Ach-induced relaxation (Figure 3.42). In the older 24 week HFD group, the pro-contractile response observed following OA pre-administration appeared to have been influenced by the vehicle in aortic rings isolated from

HFD rats (Figure 3.45). Interestingly, OA pre-administration significantly blunted Ach-induced relaxation in HFD-isolated aortic rings (24 week diet group) (Figures 3.46). It is not clear why OA elicited this response in the aortic rings from older HFD-induced obese rats. Whether OA is ineffective or harmful when faced with both advanced age and obesity is unclear. Further investigations are necessary on the effects of OA and vascular function in obesity and / or advanced age. In previous studies, OA was either given to the rats as part of the diet or it was used as a direct vasorelaxant in place of Ach in aortic rings (Rodriguez-Rodriguez *et al* 2007, Rodriguez-Rodriguez *et al* 2004 & 2008). To our knowledge, we are the first to test a pre-administration treatment model of OA. Interestingly, the pre-administration model yielded variable results in both 16 and 24 week diet groups, with OA exhibiting beneficial effects only in 16 week HFD rats and in 24 week diet lean rats only.

4.3.2.3 Effects of direct OA administration on aortic rings (24 week diet)

The direct vasorelaxing effects of OA were investigated by administration of OA in a cumulative manner in PE-contracted aortic rings isolated from lean and HFD rats receiving the high fat diet for 24 weeks. OA did not elicit a relaxing response in aortic rings isolated from either lean or HFD rats (Figure 3.47). These findings contradict previous findings in the literature as OA has been shown to directly induce vasorelaxation in PE or noradrenaline contracted rat aorta and mesenteric arteries (Rodriguez-Rodriguez *et al* 2004 & 2008). OA-induced vasorelaxation was abolished upon the removal of the endothelium or addition of NO inhibitors such as ADMA and L-NAME (Rodriguez-Rodriguez *et al* 2004 & 2008). This thus positions NO as a central mediator of OA-induced vasorelaxation. The age of the male Wistar rats used in the above mentioned previous studies were in the range of 10-12 and 12-16 weeks respectively. The age of the rats in our 24 weeks diet rats could have potentially affected the responsiveness of the aortas to direct OA administration.

4.4 Integration of findings

4.4.1 Baseline endothelial heterogeneity in AECs and CMECs

The baseline flow cytometry data demonstrated that NO production did not differ between AECs and CMECs, hence endothelial heterogeneity was not observed in this regard. The heterogeneous protein expression and phosphorylation patterns of the NO biosynthetic pathway are summarised in Table 4.1. Although western blot analysis demonstrated a non-significant ~ 1.4-fold higher total eNOS expression in CMECs, proteomics did show a significant eNOS up-regulation in CMECs compared to AECs. These findings are suggestive of a heterogeneous expression of eNOS in AECs and CMECs. This was an interesting finding as eNOS is usually thought to be expressed at lower quantities in cardiac microvascular endothelial cells, compared to larger-sized coronary vessels where eNOS is required for vasomotor regulating purposes.

In addition to higher eNOS protein levels, prostaglandin G/H synthase also showed a higher expression in CMECs compared to AECs. Prostaglandin G/H synthase synthesises prostaglandin, a precursor of vasodilatory PGI₂ and vasoconstrictory TXA₂. Since CMECs line non-vasomotor regulating capillary vessels, it can be presumed that the PGI₂ and TXA₂ expressed in CMECs would be dedicated at regulating endothelial function and underlying cardiomyocyte function and activity. For example PGI₂ and TXA₂ play opposing, yet homeostatic roles in regulating platelet aggregation in endothelial cells (Nemr *et al* 2003). Furthermore, CMEC-derived PGI₂ play a role in regulating cardiac contractile performance (Brutsaert 2003). On the other hand, AECs demonstrated up-regulation of proteins that are associated with regulating vasomotor function including insulin degrading enzyme and catechol O-methyltransferase. Higher expression of PKB / Akt and HSP 90 in AECs compared with CMECs (Table 4.1), may be a vasomotor function adaptive trait, as these proteins are involved in eNOS activation in conditions of shear stress (Luo *et al* 2000). Taken together, this is indicative that endothelial heterogeneity with regards to baseline endothelial function exists between these two cell lines, and that each cell line is adapted to function in their own respective internal environments. This further indicates that, in our hands, some measure of endothelial heterogeneity was observed in the *in vitro* setting, despite removal from their *in vivo* environments.

Table 4.1: Heterogeneous protein expression and phosphorylation patterns under baseline conditions

Protein expression / phosphorylation	AECs	CMECs
Total eNOS	low	Non-significant, but 1.4-fold higher expression, 1.5-fold significant up-regulation via proteomics
p eNOS (ser 1177)	similar	similar
Relative eNOS activation	high	low
Total PKB / Akt	high	low
p PKB / Akt (Ser 473)	low	high
Relative PKB / Akt activation	low	high
HSP 90	high	low

Endothelial heterogeneity was also observed with regards to baseline ROS production between AECs and CMECs. These findings were further supported by up-regulation of antioxidant proteins which were more pronounced in CMECs compared to AECs. Baseline ONOO⁻ levels were lower in AECs, while H₂O₂ levels were lower in CMECs. The lower H₂O₂ levels in CMECs compared to AECs could be accounted for by the up-regulation of H₂O₂ degrading proteins which included glutathione peroxidase and peroxiredoxin-6. These findings suggest that CMECs showed a higher H₂O₂ degrading capacity compared to AECs, an adaptive trait that might serve to protect the underlying cardiomyocytes from oxidative stress and consequent cell death. Furthermore, an up-regulation of MnSOD was observed in CMECs compared to AECs. Hence, CMECs appear to be equipped with a more pronounced defence system against oxidative stress compared to AECs.

4.4.2 Heterogeneity in AEC and CMEC model of endothelial injury

An *in vitro* model of endothelial injury in both AECs and CMECs was successfully achieved with TNF- α as evidenced by:

- Decreased NO production
- Increased H₂O₂ production
- Increased necrosis
- Up-regulation of inflammatory proteins
- Up-regulation of apoptotic proteins

The increase in H₂O₂ levels in both TNF- α treated AECs and CMECs was validated by the up-regulation of MnSOD as demonstrated by the proteomics data (Figure 4.3). This suggests that the TNF- α -stimulated O₂⁻ was rapidly dismutated into H₂O₂ and water. Moreover, the up-regulation of MnSOD and reduction in NO production were in agreement with the reduced ONOO⁻ levels observed in both TNF- α treated AECs and CMECs (Figure 4.3).

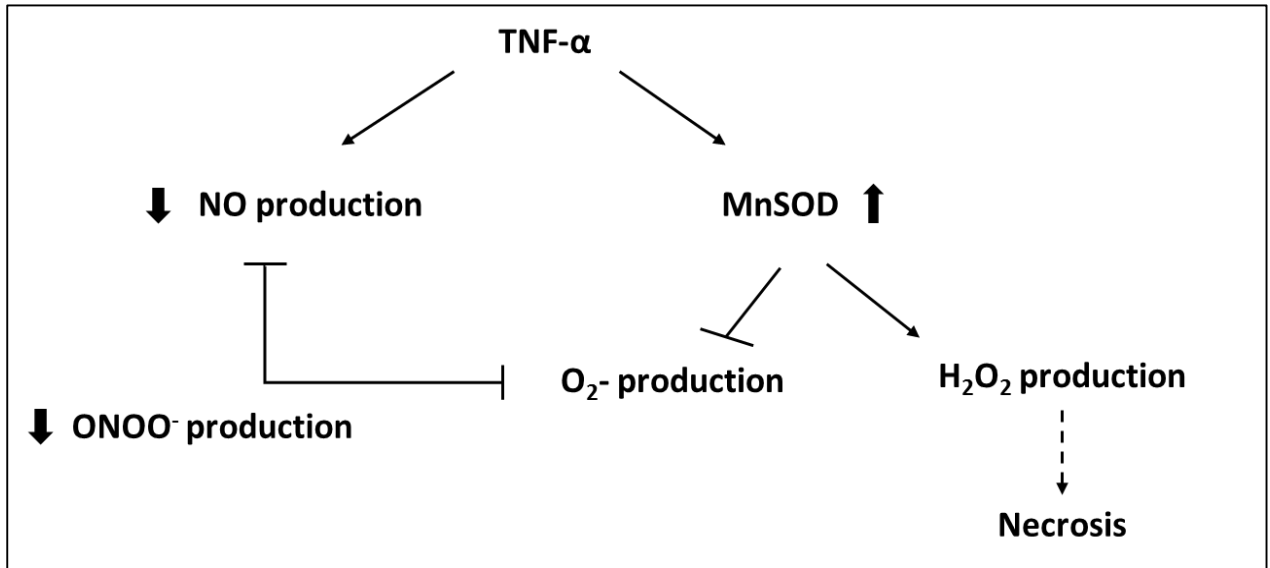


Figure 4.3: Summary of the effects of TNF- α on NO production, ROS production and necrosis in AECs and CMECs.

4.4.2.1 TNF- α signalling in AECs (compared to control, untreated AECs)

TNF- α elicited expression of NF- κ B in AECs as was shown by the proteomics data. The western blot data supported the proteomics findings by revealing a modest $\sim 16\%$ reduction in I κ B-alpha expression in TNF- α treated AECs compared to their untreated counterparts. A reduction in I κ B-alpha is a marker of enhanced NF- κ B activity, and hence both these findings were strongly suggestive of an inflammatory response elicited by TNF-alpha in the AECs (Zhou *et al* 2003). In the AECs, NF- κ B activity appeared to be regulated through TRAF6 (Figure 4.4), as was demonstrated by the up-regulation of sequestosome 1 which is known to facilitate I κ B-alpha phosphorylation and modulation of NF- κ B activity via TRAF6 (Wooten *et al* 2005, Zotti *et al* 2014). Activation of NF- κ B leads to regulation of inflammatory genes, which in the AECs included genes encoding for guanylate binding protein 2 and protein parg 14, both of which were up-regulated (Figure 4.4). TNF- α appeared to have switched on pro-apoptosis pathways in the AECs as was shown by the up-regulation of caspase 3 (Figure 4.4). In a model of mouse embryonic fibroblasts, Lin *et al* (2004) reported that TNF- α led to ROS accumulation which in turn resulted in necrosis. We propose that, in our hands, binding of TNF- α to TNF- α receptors led to ROS accumulation (O_2^-), which consequently led to up-regulation of MnSOD. Dismutation of O_2^- led to increased intracellular H_2O_2 levels, which could have overwhelmed the cells, hence triggering necrotic cell death (Figure 4.4).

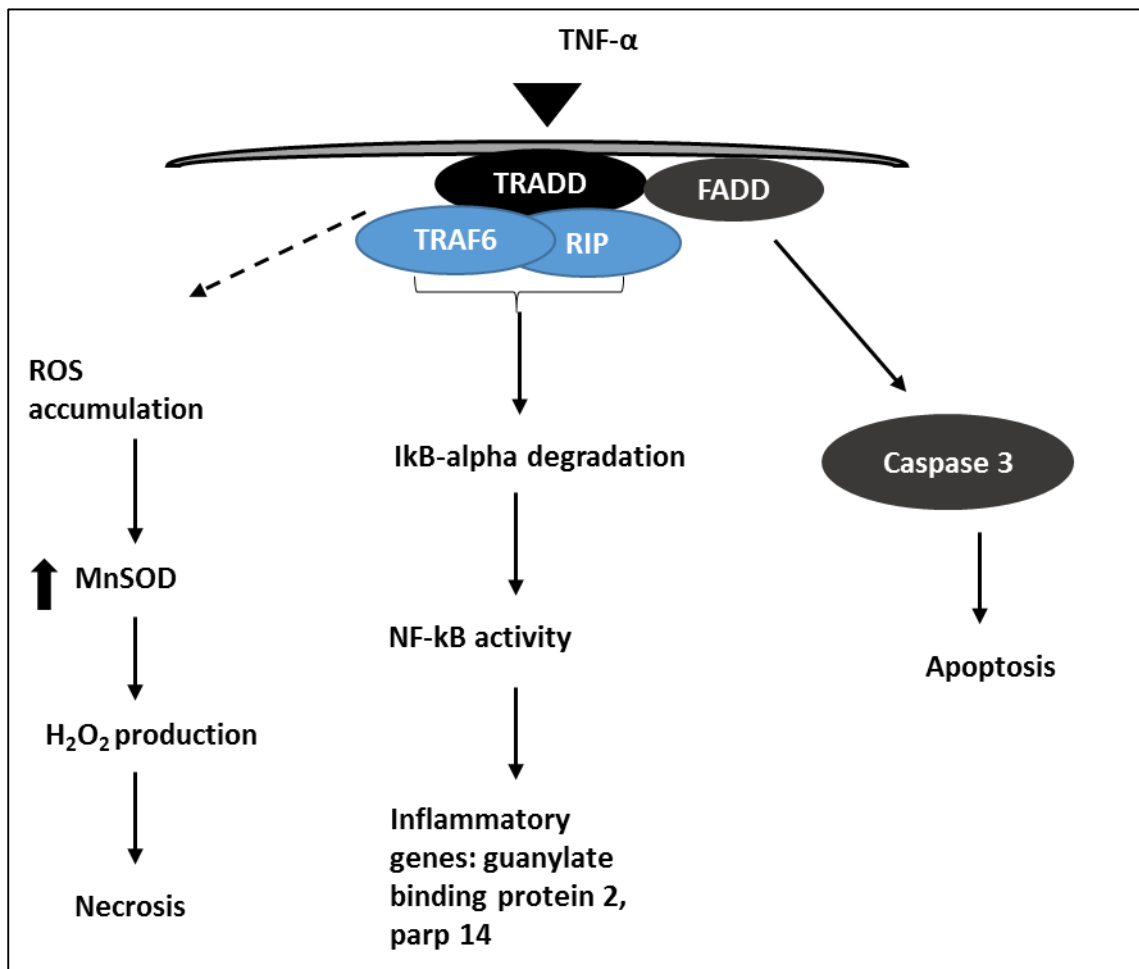


Figure 4.4: Proposed TNF- α signalling in the AECs based on the integration of flow cytometry, western blot and proteomic data.

4.4.2.2 TNF- α signalling in CMECs (compared to control, untreated CMECs)

Similarly to AECs, TNF- α elicited the up-regulated expression of NF-KB in CMECs. NF-KB activity was confirmed by decreased expression of I κ B-alpha as determined through western blotting. In CMECs, TNF- α elicited up-regulation of inflammatory genes ICAM-1 and IL-36, in addition to guanylate binding protein 2 which was also up-regulated in TNF- α treated AECs compared to their respective controls (Figure 4.5). The CMECs also responded to TNF- α treatment in terms of apoptosis; however, in contrast to AECs, the protein mediating apoptosis in CMECs seemed to have been Bid rather than caspase-3 (Figure 4.5). Bid may be cleaved by caspase 8, after which it translocates to the mitochondria, leading to enhanced mitochondrial membrane permeability and release of cytochrome C (Billien *et al* 2009). The necrotic cell death pathway appears to have been similar in both CMECs and AECs (Figure 4.5).

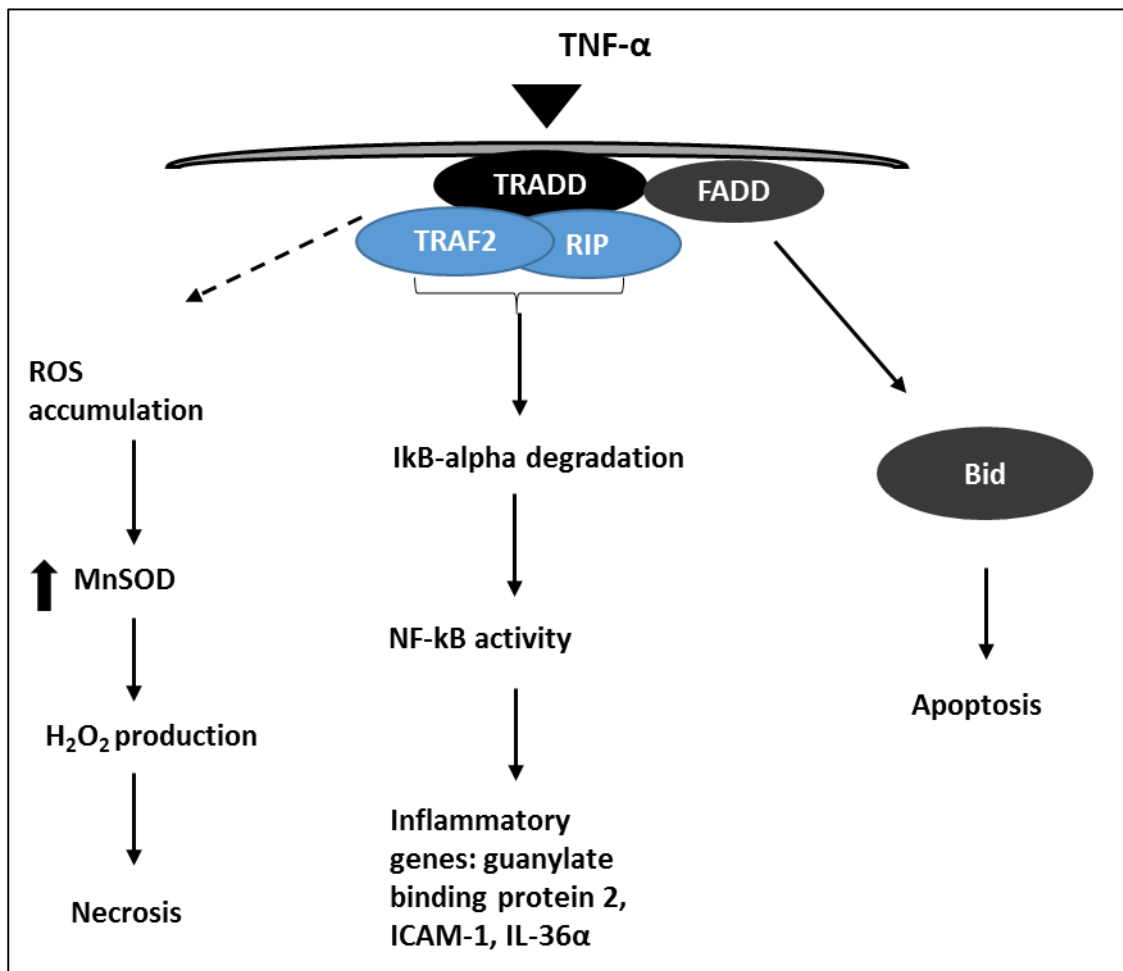


Figure 4.5: Proposed TNF-α signalling in the CMECs based on the integration of flow cytometry, western blot and proteomic data.

4.4.2.3 NO production and eNOS signalling in TNF- α treated AECs vs. TNF- α treated CMECs.

TNF- α only elicited a heterogeneous response in NO production between AECs and CMECs at the higher concentration of 20 ng/ml TNF- α after 48 hours, where NO production was lower in AECs compared to CMECs. These findings suggest that, when exposed to a high TNF- α concentration for longer periods, AECs were more susceptible to the injurious effects of TNF- α than CMECs using reduced NO production as the marker of effect.

Relative eNOS activation was significantly lower in TNF- α treated CMECs compared to their AEC counterparts, however, this response was also observed in baseline untreated conditions. Hence TNF- α might not have played an additive role in this heterogeneous response. AECs responded to TNF- α with a lower PKB / Akt expression and phosphorylation compared to CMECs. Endothelial heterogeneity was not observed with regards to HSP 90 expression in TNF- α treated AECs and CMECs. Although the combined HSP 90-PKB / Akt-eNOS pathway findings were not sufficiently convincing to conclude that the AECs were more prone to endothelial dysfunction, the compromised PKB / Akt pathway suggests that the AECs may have been more susceptible to the injurious effects of TNF- α with regards to this important upstream activator of eNOS compared to CMECs.

Proteomics revealed a differential up-regulation of endothelin converting enzyme and angiotensin II converting enzyme in TNF- α treated AECs compared to their CMEC counterparts. These proteins are responsible for the synthesis of the vasoconstrictive peptides ET-1 and angiotensin II respectively. As previously described, endothelial dysfunction is associated with an imbalance in the endothelial release of vasoconstrictors such as ET-1 and angiotensin II at the expense of vasodilators such as NO (Esper *et al* 2006, Strijdom & Lochner 2009). The overall reduction in NO production and up-regulation of endothelin converting and angiotensin II converting enzymes may suggest that the AECs were switching from an activated state to a dysfunctional state in response to TNF- α compared to CMECs (Figure 4.6).

While the AECs seemingly demonstrated progression to a dysfunctional state, CMECs appeared to have maintained an activated state. This was evidenced by up-regulation of proteins associated inflammation-induced permeability and leukocyte transmigration such

as PDE2A, ICAM-1, IL-36 α and PECAM-1 in TNF- α treated CMECs, which was not observed in their AEC counterparts. Endothelial dysfunction is a precursor of atherosclerosis, a condition that principally affects large blood vessels including the aorta and coronary arteries (Deng *et al* 2006). The progression of the AECs towards a dysfunctional state may be an indicator of their propensity to developing atherosclerosis, as these cells are situated in the large conduit aorta.

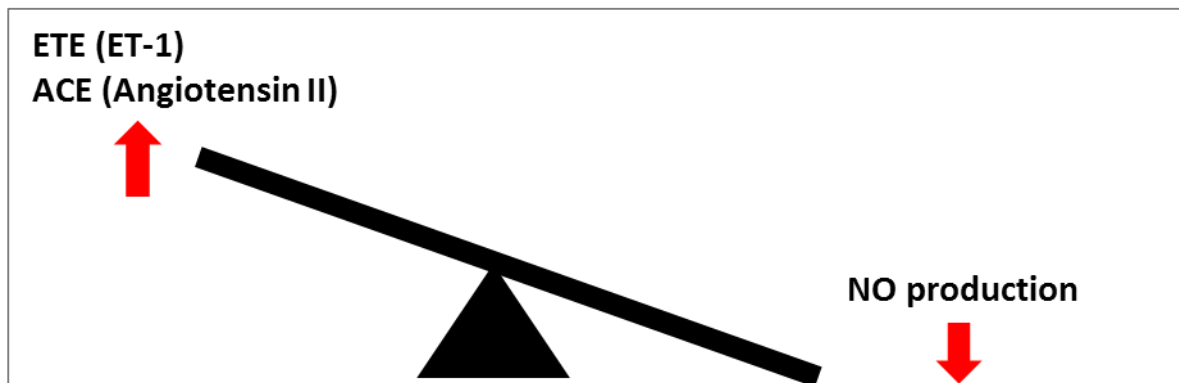


Figure 4.6: The loss of balance in vasoconstrictor and vasodilator factor synthesis in TNF- α treated AECs compared to TNF- α CMECs. ETE = endothelin converting enzyme, ACE = angiotensin II converting enzyme.

4.4.2.4 ROS production in TNF- α treated AECs vs. TNF- α treated CMECs

TNF- α elicited a heterogeneous response with regards to ROS production and the up-regulation of anti-oxidant proteins between AECs and CMECs. Intracellular ONOO⁻ and H₂O₂ production were lower in TNF- α treated CMECs compared TNF- α treated AECs. However, the ONOO⁻ levels did not coincide with nitrotyrosine expression, as there were no significant differences in nitrotyrosine expression between AECs and CMECs following TNF- α treatment. The lower H₂O₂ levels in TNF- α treated CMECs compared to their AEC counterparts were attributable to the up-regulation of proteins associated with H₂O₂ degradation including, protein pxdn, peroxiredoxin, and glutathione peroxidase. The anti-oxidant proteins up-regulated in TNF- α treated AECs compared to TNF- α treated CMECs are mostly associated with detoxification processes and scavenging of O₂⁻, and these included biliverdin reductase A, NAD(P)H dehydrogenase [quinone] 1, aldehyde dehydrogenase (dimeric NADP-preferring). The higher levels of ONOO⁻ and H₂O₂ in TNF- α treated AECs may be suggestive of a higher O₂⁻ production compared to TNF- α treated CMECs, and the up-regulation of anti-oxidant proteins was most likely a way of counteracting ROS production. See Table 4.2 for anti-oxidant proteins in TNF- α treated AECs compared to TNF- α treated CMECs.

Table 4.2: Heterogeneous anti-oxidant protein up-regulation in response to TNF- α

TNF-α treated AECs	TNF-α treated CMECs
Biliverdin reductase A	Protein pxdn
Glutathione S_transferase Mu 4	Peroxiredoxin
Glutathione S_transferase Mu 1	Glutathione peroxidase
NAD(P)H dehydrogenase [quinone] 1	
Aldehyde dehydrogenase (dimeric NADP-preferring)	
Glutathione reductase	

4.4.2.5 Cell viability in TNF- α treated AECs vs. TNF- α treated CMECs

Endothelial heterogeneity with regards to necrosis between AECs and CMECs was only observed with 20 ng/ml TNF- α after 48 hours, with CMECs showing increased necrosis compared to the AECs. This suggests that at a high concentration over a longer period, TNF- α may be more cytotoxic to CMECs compared to AECs. The role of TNF- α in apoptosis is well known (Deshpande *et al* 2000, Rastogi *et al* 2012). TNF- α elicited an up-regulation of pro-apoptotic proteins in both AECs and CMECs, however there appeared to be heterogeneity in terms of the proteins expressed. In TNF- α treated AECs, the up-regulated apoptotic proteins included caspase 8 and BAX, while Bid and PARP3 were up-regulated in TNF- α treated CMECs compared to their AEC counterparts.

4.4.2.6 TNF- α signalling in AECs vs. CMECs

Proteomics revealed expression of NF- κ B in both TNF- α treated AECs and CMECs, which is indicative of an inflammatory response. NF- κ B activity was comparable between TNF- α treated AECs and TNF- α treated CMECs, as was validated by the I κ B-alpha expression, which was similar between these two cell lines in response to TNF- α . However, in the AECs, I κ B-alpha degradation and hence NF- κ B activity seemed to be modulated via TRAF6, as was demonstrated by a differential up-regulation of sequestosome 1 in TNF- α treated AECs compared to TNF- α treated CMECs. Endothelial heterogeneity was also observed with regards to the up-regulated inflammatory proteins in AECs and CMECs in response to TNF- α , suggesting that endothelial activation was mediated by different proteins in the two cell lines (Figure 4.7 & 4.8).

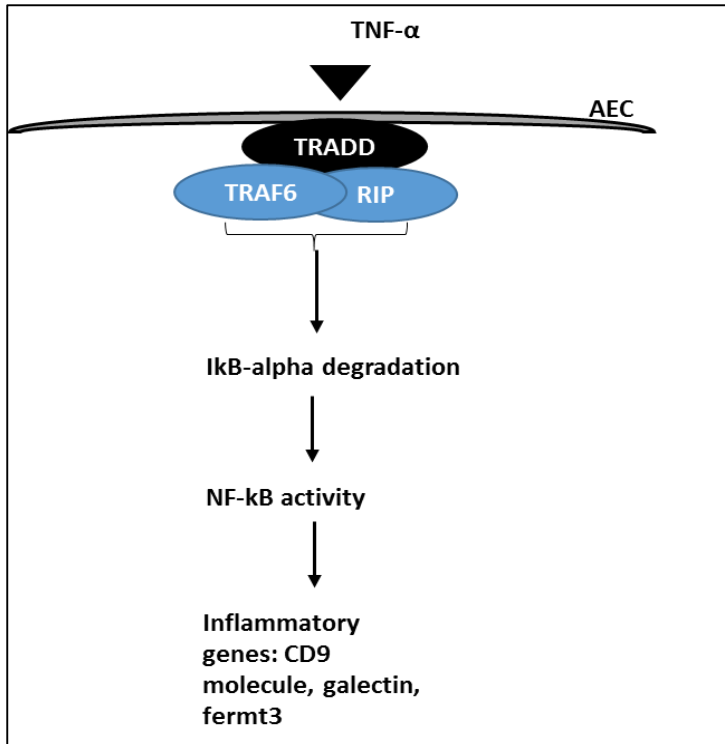


Figure 4.7: TNF-α signalling in AECs compared to CMECs.

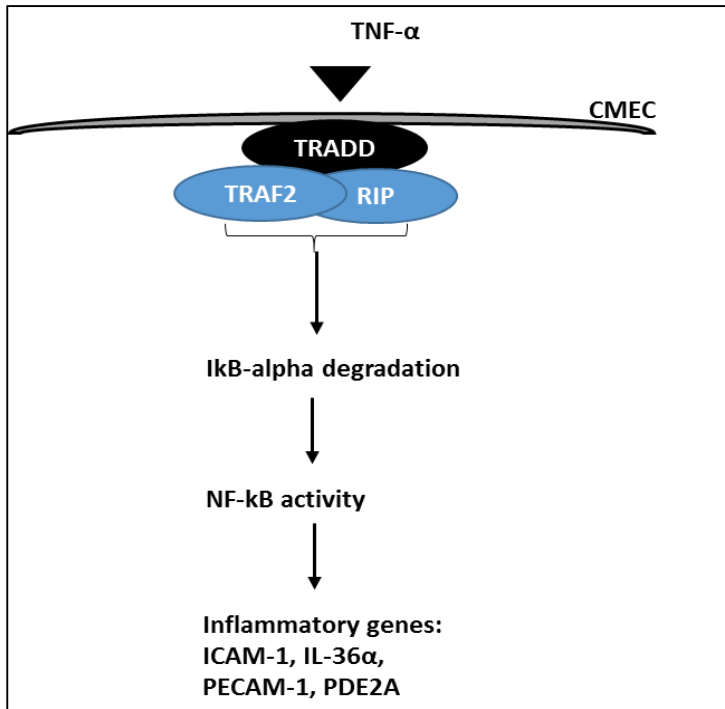


Figure 4.8: TNF-α signalling in CMECs compared to AECs.

4.4.2.7 Modulation of endothelial injury by OA

The fact that endothelial injury and dysfunction are reversible conditions is of major significance in the prevention of cardiovascular diseases, especially in clinical settings. Plant extracts such as OA have gained attention due to their putative beneficial properties on vascular function. The endothelio-protective properties of OA has previously been documented (Rodriguez-Rodriguez *et al* 2004, Martinez-Gonzalez *et al* 2008), and hence we investigated its role in reversing endothelial injury the AECs and CMECs. Reduced NO bioavailability is considered to be the hallmark of endothelial injury or dysfunction. In this study, TNF- α resulted in decreased NO production in both AECs and CMECs. In our hands, 1 hour pre-treatment with OA significantly reversed TNF- α -induced injury, by restoring NO production. Previous studies have shown that OA can stimulate PKB / Akt and eNOS activity, which may explain its NO modulating properties. Though TNF- α did appear to convincingly affect the eNOS-NO biosynthetic pathway, it is possible that OA pre-treatment might have enhanced this pathway leading to restoration of NO production. It should also be kept in mind that TNF- α might have abolished NO production via other eNOS phosphorylation sites that were not investigated in this study, and that OA could have modulated eNOS activity through one of these phosphorylation sites.

We further showed that pre-treatment with OA significantly decreased TNF- α -induced H₂O₂ production in both AECs and CMECs, a finding which suggests that OA may possess anti-oxidant properties or stimulatory properties on endogenous anti-oxidant systems. It was previously reported that OA may possess stimulatory properties on SOD and glutathione peroxidase anti-oxidant systems (Samova *et al* 2003). This could explain the reduction of H₂O₂ production in the current study. The fact that OA was able to abolish H₂O₂ production may also explain the diminished necrosis with OA pre-treatment in AECs. Unfortunately, in these set of experiments, CMECs did not show any response with regards to necrosis induction by TNF- α or OA pre-treatment.

From these findings, it appears that the injurious effects of TNF- α can be reversed by OA. Unfortunately, western blots or proteomics studies were not performed in OA studies, hence the mechanism of action of OA in AECs and CMECs in the current study is unknown. Lee *et al* (2013), showed that OA may exert anti-inflammatory properties through

decreasing NF- κ B activity. This mechanism may contribute the reversal of TNF- α -induced injury by OA as was observed in the current study.

4.4.3. Aortic ring experiments

An *ex vivo* model of endothelial injury was included in this study by investigating the vascular function of thoracic aortas derived from HFD induced obese rats compared to age-matched lean control rats. The *ex vivo* model of endothelial injury was achieved as evidenced by an enhanced contractile response to PE in aortic rings from HFD rats compared to lean rats. However, Ach-induced relaxation did not differ between aortic rings from HFD rats and lean rats. This is suggestive that NO production was maintained in aortic rings from HFD rats, although a pro-contractile response to PE was observed. Endothelial dysfunction may be characterised by the state at which vasoconstrictive factors such as ET-1 and angiotensin II are enhanced at the expense of vasodilatory factors such as NO (Esper *et al* 2006). The pro-contractile response observed in aortic rings from HFD rats could represent an initial step towards a dysfunctional state. Furthermore, obesity is associated with perivascular adipose tissue-derived release of pro-contractile factors such as ROS and inflammatory cytokines (including TNF- α) at the expense of anti-contractile factors such as adiponectin (Szasz *et al* 2013). This might have contributed to the pro-contractile response observed in rings from HFD rats.

In a similar fashion to our cultured cell experiments, the putative protective role of OA was also investigated in the aortic ring model. Aortic rings from lean and HFD rats were subjected to pre-administration of OA 15 minutes prior to PE-induced contraction and Ach-induced relaxation. This led to anti-contractile response to PE in aortic rings from 16 week HFD rats. As discussed above pro-contractile factors released from perivascular tissue in obesity include ROS. Given the fact that OA was able to modulate ROS production in our *in vitro* models (AECs and CMECs), the anti-contractile response observed in the *ex vivo* model might be attributable to the ability of OA to lower ROS. Pre-administration of OA further resulted in an anti-contractile and pro-relaxing response to PE and Ach respectively in aortic rings from older 24 week diet lean rats. And hence the putative endothelio-protective properties observed in the *in vitro* model could be translated to the *ex vivo* models.

Direct administration OA instead of Ach, failed to elicit relaxation in aortic rings isolated from 24 week lean and HFD rats. This was in contradiction to previous findings in the literature (Rodriguez-Rodriguez *et al* 2004, 2008), however, in our view, the older age of the rats in the current study might have potentially affected the responses of the aortas to the direct relaxing effects of OA.

Chapter 5

Conclusions

This study was divided in two main aims:

- The principal aim of this study was to investigate and compare the function of aortic endothelial cells and cardiac microvascular endothelial cells at baseline conditions and in response to a pathophysiological stimulus usually associated with cardiovascular risk factors.
- The second aim of this study was to measure the endothelium-dependent vasomotor responses of aortic rings derived from obese and lean, age-matched control rats to a phenylephrine and acetylcholine challenge.

Endothelial heterogeneity is often overlooked when investigating endothelial function, activation and dysfunction, as it is usually assumed that all endothelial cells are the same and will yield similar responses to pathophysiological stimuli. AECs and CMECs were chosen in this study, as they are located in two distinct microenvironments of the vascular system. These two cell lines are exposed to different factors and serve distinct specialized roles in their respective environments. Endothelial heterogeneity has not previously been investigated in AECs and CMECs, especially with regards to NO production, the NO biosynthetic signalling pathway, and ROS production at baseline or in response to TNF- α , one of the body's primary pro-inflammatory cytokines. Furthermore, very little is known with regards to the response of CMECs to TNF- α -induced endothelial injury. Hence, the work of this PhD was expected to generate novel findings with regards to baseline endothelial heterogeneity between AECs and CMECs, and their heterogeneous responses to TNF- α -induced endothelial injury. Furthermore, proteomics studies were applied for comprehensive analysis of protein expression and regulation in AECs and CMECs at baseline conditions and in response to TNF- α . This was expected to add to the novelty of this study, as the comparative proteomic analysis between AECs and CMECs had not been previously performed at baseline and in response to TNF- α . The inflammatory cytokine TNF- α was chosen as the pathological stimulus to induce endothelial injury, as its role in endothelial activation and dysfunction is well known. We further investigated the responses of AECs and

CMECs to the putative endothelio-protective properties of the triterpenoid OA at baseline and TNF- α treated conditions.

The challenge that obesity poses on endothelial function has become apparent, and hence an *ex vivo* model which allowed us to study the vascular function in aortic rings from lean and HFD rats was also included. It was further investigated whether the endothelio-protective properties of OA observed in AECs and CMECs (the *in vitro* model), would also be observed in the *ex vivo* model. Little is known about the effects of OA in vascular function and obesity. Hence, the findings in this section were expected to add novel insights to the existing literature on the putative beneficial effects of OA in endothelial function.

Several techniques previously developed in our laboratory and from previous studies were undertaken in order to achieve the aims of the current study:

- Flow cytometry technique: measuring NO production, ROS production and necrosis,
- Western blot analysis: measuring protein expression and phosphorylation,
- Proteomics: broad spectrum analysis of protein expression and regulation,
- Isometric tension organ bath studies: *ex vivo* measurement of vascular function in aortas from lean and HFD rats.

Baseline studies: Although baseline NO production was similar between AECs and CMECs, endothelial heterogeneity was observed with regards to the protein expression and phosphorylation patterns of the NO biosynthetic pathway (eNOS, PKB / Akt and HSP 90). Interestingly, eNOS expression was found to be higher in CMECs (as discussed in chapters 4.1 & 4.2) compared to AECs, while relative activated eNOS levels were higher in AECs. The fact that eNOS protein was higher in the CMECs compared to AECs is, as far as we are aware, a novel finding as eNOS expression is generally considered to be relatively low in the microcirculation of the heart. The fact that PKB / Akt and HSP 90 expression was higher in AECs compared CMECs was not a surprise as these proteins are essential for eNOS activation in large vessels during conditions of shear stress. However, it was interesting to note that activated PKB / Akt levels were higher in the CMECs, whilst activated eNOS levels were lower compared to AECs. It was therefore concluded that activated PKB / Akt may possess regulatory properties such as cell survival and hence barrier integrity in CMECs.

Overall these findings are novel and demonstrate endothelial heterogeneity with regards to the baseline NO biosynthetic signalling pathway between AECs and CMECs.

Baseline ROS production was heterogeneous between AECs and CMECs as was demonstrated by the higher ONOO⁻ levels and nitrotyrosine expression in CMECs compared to AECs. H₂O₂ levels were higher in AECs compared to CMECs. However, the up-regulation of H₂O₂ catabolic enzymes (glutathione peroxidase and peroxiredoxin-6) as demonstrated by proteomics could be responsible for the lower levels of H₂O₂ in CMECs. Hence, we demonstrate for the first time that endothelial heterogeneity exist with regards to ONOO⁻ and H₂O₂ production between AECs and CMECs, and that CMECs possess higher H₂O₂ catabolic capacity than AECs.

Endothelial injury: Concentration response curves were conducted with 0.5, 5 and 20 ng/ml TNF- α over 24 and 48 hours periods, however the 20 ng/ml TNF- α concentration and 24 hour time point was chosen as the optimal experimental protocol for endothelial injury induction. An *in vitro* model of endothelial injury was successfully achieved in both AECs and CMECs as was evidenced by:

- Decreased NO production
- Increased H₂O₂ production
- Increased necrosis
- Up-regulation of apoptotic proteins
- Activation of the inflammatory pathway

The NO biosynthetic signalling (HSP 90-PKB / Akt-eNOS) pathway did not correspond with the reduced NO levels in both AECs and CMECs, however the reduction in PKB / Akt and HSP 90 expression in AECs was possibly suggestive of the initiation of a dysfunctional NO biosynthetic pathway in AECs. The NO biosynthetic pathway in CMECs appeared to be resistant to the injurious effects of TNF- α . This was not in agreement with previous findings as discussed in chapter 4.1, section 4.1.2.2. With regards to endothelial heterogeneity, it was demonstrated that the PKB / Akt pathway was compromised in TNF- α treated AECs compared to their CMEC counterparts. Taking into consideration that 20 ng/ml over 48 hours led to lower NO production in AECs compared to CMECs, we conclude that AECs were

more susceptible to TNF- α induced endothelial injury with regards to the NO biosynthesis pathway.

Our data suggested that the increased H₂O₂ levels in response to TNF- α were possibly due to dismutation of O₂⁻ as was demonstrated by the up-regulation MnSOD in both TNF- treated AECs and CMECs. We concluded that the high levels of H₂O₂ could be a plausible explanation for the enhanced necrosis in both AECs and CMECs. The role of TNF- α in apoptosis is well known, and hence up-regulation of apoptotic proteins, caspase 3 in AECs and Bid in CMECs, was not a surprise. However this finding was novel with regards to the heterogeneous expression of apoptotic proteins in AECs and CMECs.

The up-regulation of NF- κ B and decreased expression of I κ B-alpha was indicative of the activation of intracellular pro-inflammatory signalling pathways and hence an inflammatory response in both TNF- α treated AECs and CMECs. It was shown that NF- κ B activity in AECs was likely to be regulated through TRAF6, and not TRAF2, thus demonstrating heterogeneity in this regard. The up-regulation of inflammatory proteins in response to TNF- α was an indicator of endothelial activation in both AECs and CMECs. We demonstrated for the first time that endothelial activation is heterogeneously mediated through up-regulation of different inflammatory proteins in response to TNF- α in AECs and CMECs. These included CD9 molecule, galectin and fermt3 protein in TNF- α treated AECs, and ICAM-1, IL-36 α , PDE2A, PECAM-1 in TNF- α treated CMECs.

We conclude that AECs demonstrated progression to a dysfunctional state as was evidenced by up-regulation of endothelin converting enzyme and angiotensin II converting enzyme, while CMECs probably remained in an activated state. These findings are novel as we demonstrate for the first time a heterogeneous response of AECs and CMECs to TNF- α -induced endothelial injury. Human umbilical vein endothelial cells are often the cells of choice when studying endothelial function and dysfunction. Here we show that endothelial cells do not necessarily respond in the same manner to pathophysiological stimuli. Although end-points such as reduced NO bioavailability may be a general marker of endothelial injury or dysfunction in most endothelial cell lines, protein expression and regulation in response to pathophysiological stimuli may differ from cell line to cell line as was demonstrated by our proteomics data. Furthermore, the expression and phosphorylation patterns of certain

proteins may also differ as was demonstrated through western blot in the current study. Hence endothelial heterogeneity is relevant when studying endothelial injury and the signalling mechanisms involved. It should however be kept in mind that in *in vivo* conditions, these cells are constantly exposed to different factors according to their respective environments, which might influence their response to pathophysiological stimuli. For example release of factors such as adiponectin from the perivascular adipose tissue would influence the response of AECs to injury in *in vivo* conditions. Factors released from underlying VSMCs and cardiomyocytes may also influence the responses of AECs and CMECs to endothelial injury respectively. Hence, our *in vitro* findings may not completely reflect the responses of AECs and CMECs *in vivo* situations.

Modulation of endothelial injury by OA: Given the fact endothelial injury and dysfunction are reversible conditions, and that OA has previously been shown to possess endothelio-protective properties, it was expected that pre-treatment with OA prior treatment with TNF- α , would reverse the injurious effects of TNF- α . Although further investigations are necessary, we were excited to observe that OA pre-treatment was indeed successful in reversing the injurious effects of TNF- α through restoration of NO production and reducing H₂O₂ production in both AECs and CMECs, as well as necrosis in AECs. Further studies investigating the OA signalling mechanisms in both AECs and CMECs are necessary.

Proteomics: Baseline proteomic analysis revealed the identification of 2372 proteins in AECs and CMECs, while a total of 2426 were revealed in both TNF- α treated AECs and CMECs. This represented the most comprehensive documentation of its kind in AECs and CMECs to date, and hence a novel contribution to existing vascular proteomic databases. Proteomics data revealed heterogeneous protein expression and regulation patterns between AECs and CMECs at baseline conditions and in response to TNF- α . Most of the proteins up-regulated in AECs and CMECs at baseline conditions demonstrated that each of these cell lines are adapted to function in their respective internal environments. This finding was novel, as we show that some level of endothelial heterogeneity exists between AECs and CMECs when cultured in *in vitro* settings. Changes in protein expression and regulation in response to TNF- α were also demonstrated. The proteins up-regulated in response to TNF- α included inflammatory proteins, apoptotic proteins, and anti-oxidant proteins. These proteins were

heterogeneously expressed, indicating endothelial heterogeneity with regards to signalling mechanisms involved in TNF- α -induced injury in AECs and CMECs.

Isometric tension studies (*ex vivo* studies): The pro-contractile responses demonstrated in aortic rings from 16 week HFD compared to lean rats, could be indicative of the release of pro-contractile factors from dysfunctional perivascular adipose tissue or the initial stages of endothelial function impairment. Our OA pre-administration model demonstrated enhanced vascular function in aortic rings from 16 week HFD rats and 24 week diet lean rats. It is not clear why pre-administration of OA elicited a pro-contractile response in aortic rings from 24 week HFD rats, however, it is possible that the factors released by a dysfunction perivascular adipose tissue and the advanced age of rats overwhelmed the beneficial properties of OA. Direct administration of OA failed to elicit relaxation in aortic rings from 24 week diet rats. This was in contrast to previous findings, and hence we conclude the age of the rats might have played role. Overall, OA appears to exert some beneficial properties in vascular function as was shown in our pre-treatment models. However, further studies are necessary to elucidate the signalling mechanisms involved.

In summary the work of this PhD provided comprehensive novel insights with regards to:

- Baseline endothelial heterogeneity in AECs and CMECs.
- Heterogeneous responses of AECs and CMECs to TNF- α .
- Signalling mechanisms involved in TNF- α induced endothelial injury in both AECs and CMECs.
- Heterogeneous TNF- α signalling in AECs and CMECs.
- Reversibility of TNF- α -induced endothelial injury through the bioactive triterpenoid OA.

Finally, in view of the above findings and conclusions, we successfully proved our hypothesis, which stated that AECs and CMECs will exhibit heterogeneity under baseline conditions or in response to insult. Furthermore, we hypothesized that OA will lead to increased NO production in both AECs and CMECs. This was indeed the response that was observed. Unfortunately the mechanisms of action of OA were not investigated.

As was demonstrated by the enhanced contractile response in aortic rings from HFD rats, obesity led to a compromised vascular function in HFD rats, which could have been an early sign of a dysfunctional endothelium as per our hypothesis. This response was significantly reversed by the pre-administration of OA. Hence, we were able to prove our hypotheses in this regard.

Limitations of the current study:

The following additions to the investigations of the current study would have added greater value to the current findings, however due to cost and time constraints these experiments were not applied:

- Western blotting of more proteins involved in the NO biosynthetic pathway such as caveolin-1, and investigating other phosphorylation sites involved in eNOS activation.
- Extensive western blotting to support the finding of the proteomics data.
- Application of western blotting and proteomics in OA studies, to elucidate the signalling mechanisms involved in AECs and CMECs at baseline conditions or with TNF- α treatments.
- Use of younger rat models to study the *ex vivo* vascular reactivity of aortas from lean and HFD rats.
- Use of younger rat models to study effects of OA on vascular reactivity of aortas from lean and HFD.
- Application of western blotting and proteomics in the aortas to investigate the signalling mechanisms involved.
- Consideration of the possibility that the heterogeneity observed in the *in vitro* models are not necessarily a reflection of the *in vivo* setting; however, the fact that heterogeneity was demonstrated, which could be explained in terms of the *in vivo* location and function of CMECs and AECs respectively, does add credibility to the findings of this study.

Outputs emanating directly or indirectly from the current study

Research articles:

1. **Mudau M**, Genis A, Lochner A, Strijdom H. Endothelial dysfunction: the early predictor of atherosclerosis. *Cardiovasc J Afr* 2012;23:222-231.
2. Genis A, Smit S, Westcott C, **Mthethwa M**, Strijdom H. Attenuation of eNOS-NO biosynthesis, up-regulation of antioxidant proteins and differential protein regulation in TNF-alpha-treated cardiac endothelial cells: Early signs of endothelial dysfunction. In: *Endothelial Dysfunction: Risk Factors, Role in Cardiovascular Diseases and Therapeutic Approaches* (Nova Scientific Publishers, Hauppauge, NY, USA) 2014.

Conference contributions:

1. **Mudau M**, Strijdom H. The pathophysiological response of aortic endothelial cells and cardiac microvascular endothelial cells to proinflammatory TNF-alpha: Does endothelial heterogeneity play a role? Physiology Society of Southern Africa Annual Conference: Stellenbosch, September 2012.
2. Graham R, **Mudau M**, Westcott C, Strijdom H. Investigating the pro-injury properties of ADMA and TNF- α , and endothelioprotective effects of oleonic acid and fenofibrate in cardiac microvascular endothelial cells (CMECs). Physiology Society of Southern Africa Congress, Stellenbosch, September 2012.
3. Genis A, Smit S, Westcott C, **Mudau M**, Strijdom H. A complete profile of the cardiac microvascular endothelial cell proteome, following a 24 hour TNF- α treatment. Physiology Society of Southern Africa Annual Congress, Stellenbosch, September 2012.
4. **Mudau M**, Strijdom H. The heterogeneous response of aortic endothelial cells and cardiac endothelial cells to proinflammatory TNF-alpha. Annual Academic Day: Tygerberg 2012.
5. Genis A, Smit S, Westcott C, **Mudau M**, Strijdom H. Cardiac microvascular endothelial cells treated for 24 hours with TNF-alpha, what does the total protein profile of this cell type reveal? Annual Research Day, Faculty of Medicine and Health Sciences, Stellenbosch University, August 2012.
6. Strijdom H, Smit S, Westcott C, **Mudau M**, Genis A. Proteomic characterization of cardiac endothelial cell responses to TNF-alpha, hypoxia and asymmetric dimethylarginine (ADMA) stimulation. *SA Heart* 2012; 9(3): 194.
7. Strijdom H, Genis A, **Mudau M**, Westcott C, Lochner A. Effects of low-dose TNF- α administration on oxidative/nitrosative stress, the Akt/eNOS/NO pathway and viability in cardiac endothelial cells. *Atherosclerosis Supplements* 2011; 12(1): 68.

8. Strijdom H, Westcott C, **Mudau M**, Van Rensburg S, Genis A. Microvascular endothelial cell responses to inflammatory stimulation. SA Heart 2011; 8(4): 257.
9. **M Mudau**, Genis A, Westcott C, Strijdom J. The responses of aortic endothelial cells and cardiac microvascular endothelial cells to tumor necrosis factor alpha: Does endothelial heterogeneity matter? IUPS Congress, UK Birmingham 2013.
10. C. Westcott, A. Genis, **M. Mthethwa**, H. Strijdom. Short term fenofibrate treatment increases nitric oxide production in cardiac endothelial cells through a nitric oxide synthase-independent mechanism. Frontiers in CardioVascular Biology, Barcelona, Spain, July 2014.

Honours students co-supervised:

Roxanne Graham: graduated 2012

References

- Ackermann A, Fernández-Alfonso M S, Sánchez de Rojas R, *et al.* Modulation of angiotensin-converting enzyme by nitric oxide. *Br J Pharmacol* 1998; 124: 291-298.
- Adatia I, Barrow SE, Stratton VM, *et al.* Thromboxane A₂ and prostacyclin biosynthesis in children and adolescents with pulmonary vascular disease. *Circulation* 1993; 88: 2117-2122.
- Ahmad M, Zhang Y, Papharalambus C, Alexander RW. Role of isoprenylcysteine carboxyl methyltransferase in tumor necrosis factor- α stimulation of expression of vascular cell adhesion molecule-1 in endothelial cells. *Arterioscler Thromb Vasc Biol* 2002; 22: 759-764.
- Aird WC. Endothelial cell heterogeneity. *Cold Spring Harb Perspect Med* 2012; 2: a006429.
- Aird WC. Mechanisms of endothelial cell heterogeneity in health and disease. *Circ Res* 2006; 98: 159-162.
- Aird WC. Phenotypic heterogeneity of the endothelium:I. Structure, function and mechanisms. *Circ Res* 2007; 100:158-173. (a)
- Aird WC. Phenotypic heterogeneity of the endothelium: II. Representative vascular beds. *Circ Res* 2007; 100: 174-190. (b)
- Ait-Oufella H, Maury E, Lehoux S, *et al.* The endothelium: physiological functions and role in microcirculatory failure during severe sepsis. *Intensive Care Med* 2010, 36: 1288-1298.
- Anderson HDI, Rahmutula D, Gardener DG. Tumor necrosis factor- α inhibits endothelial nitric-oxide synthase gene promoter activity in bovine aortic endothelial cells. *J Biol Chem* 2004; 279: 963-969.
- Anderson NL and Anderson NG. Proteome and proteomics: new technologies, new concepts, and new words. *Electrophoresis* 1998; 19: 1853-1861.
- Andrew PJ, Mayer B. Enzymatic function of nitric oxide synthases. *Cardiovasc Res* 1999; 43: 521-531.
- Andries LJ, Brutsaert DL, Sys SU. Nonuniformity of endothelial constitutive nitric oxide synthase distribution in cardiac endothelium. *Circ Res* 1998; 82: 195-203.
- Aoki M, Nata T, Morishita R, *et al.* Endothelial apoptosis induced by oxidative stress through activation of NF- κ B: Antiapoptotic effect of antioxidant agents on endothelial cells. *Hypertension* 2001; 38: 48-55.
- Ardestani S, Deskins D, Young PP. Membrane TNF-alpha-activated programmed necrosis is mediated by ceramide-induced reactive oxygen species. *J Mol Signal* 2013; 8: 12.

Azumi H, Inoue N, Takeshita S, *et al.* Expression of NADH / NADPH oxidase p22phox in human coronary arteries. *Circulation* 1999; 100: 1494-1498.

Bach FH, Hancock WW, Ferran C. Protective genes expressed in endothelial cells: a regulatory response to injury. *Immunol Today* 1997; 18: 483-486.

Bachhav SS, Patil SD, Bhutada MS, Surana SJ. Oleanolic acid prevents glucocorticoid-induced hypertension in rats. *Phytother Res* 2011; 10: 1435-1439.

Balakumar P, Kaur T, Singh. Potential targets sites to modulate vascular endothelial dysfunction: Current perspective and future directions. *Toxicology* 2008; 245: 49-64.

Balligand J.-L. Heat shock protein 90 in endothelial nitric oxide synthase signalling: following the lead(er)? *Circ Res* 2002; 90: 838-841.

Baranano DE, Rao M, Ferris CD, Snyder SH. Biliverdin reductase: A major physiologic cytoprotectant. *PNAS* 2002; 99 16093-16098.

Barnes PJ, Karin M. Nuclear factor-kB: A pivotal transcriptional factor in chronic inflammatory disease. *N Engl J Med* 1997; 336: 1066-1071.

Barreiro O, Yanez-Mo M, Sala-Valdes M, *et al.* Endothelial tetraspanin microdomains regulate leukocyte firm adhesion during extravasation. *Blood* 2005; 105: 2852-2861.

Barreiro O, Zamai M, Yanez-Mo M, *et al.* Endothelial adhesion receptors are recruited to adherent leukocytes by inclusion in preformed tetraspanin nanoplateforms. *J Cell Biol* 2008; 183: 527-542.

Barton M, Haudenschild CC, d'Uscio LV, *et al.* Endothelin ETA receptor blockade restores NO-mediated endothelial function and inhibits atherosclerosis in apolipoprotein E-deficient mice. *Proc Natl Acad Sci* 1998; 95: 14367–14372.

Bayraktutan U, Draper N, Lang D, Shah AM. Expression of functional neutrophil-type NADPH oxidase in cultured rat coronary microvascular endothelial cells. *Cardiovasc Res* 1998; 38: 256–262.

Beckman JA, Creager MA. The nonlipid effects of statins on endothelial function. *Trends Cardiovasc Med* 2006; 16: 156-162.

Beckman JS. Oxidative damage and tyrosine nitration from peroxynitrite. *Chem Res Toxicol* 1996; 9: 836-844.

Belo L, Santos-Silva A, Rumley A, *et al.* Elevated tissue plasminogen activator as a potential marker of endothelial dysfunction in pre-eclampsia: correlation with proteinuria. *J Int Gynaecol Obstet* 2002; 109: 1250-1255.

Bennett MR. Apoptosis of vascular smooth muscle cells in vascular remodelling and atherosclerotic plaque rupture. *Cardiovasc Res* 1999; 41: 361-368.

Benowitz NL. Cigarette smoking and cardiovascular disease: pathophysiology and implications for treatment. *Prog Cardiovasc Dis* 2003; 46: 91-111.

Berkowitz DE, White R, Li D, Minhas KM, *et al.* Arginase reciprocally regulates nitric oxide synthase activity and contributes to endothelial dysfunction in aging blood vessels. *Circulation* 2003; 108: 2000-2006.

Berliner JA, Navab M, Fogelman AM, *et al.* Atherosclerosis: Basics and mechanism. *Circulation* 1995; 91: 2488-2496.

Billien LP, Shamas-Din A, Andrew DW. Bid: a bax-like BH3 protein. *Oncogene* 2009; 27: S93-S104.

Blair A, Shaul PW, Yuhanna IS, Conrad PA, Smart EJ. Oxidized low density lipoprotein displaces endothelial nitric-oxide synthase (eNOS) from plasmalemmal caveolae and impairs eNOS activation. *J Biol Chem* 1999; 274: 32512-9.

Blann AD. Endothelial cell activation, injury, damage and dysfunction: separate entities or mutual terms? *Blood Coagul Fibrinolysis* 2000; 11: 623-630.

Böger RH, Bode-Böger S, Szuba A, *et al.* Asymmetric dimethylarginine (ADMA): a novel risk factor for endothelial dysfunction, its role in hypercholesterolemia. *Circulation* 1998; 98: 1842-1847.

Böger RH, Böger-Bode SM, Tsao PS, *et al.* An endogenous inhibitor of nitric oxide synthase regulates endothelial adhesiveness for monocytes. *J Am Coll Cardiol* 2000; 36: 2287-2295.

Bohm F, Pernow J. The importance of endothelin-1 for vascular dysfunction in cardiovascular disease. *Cardiovasc Res* 2007; 76: 8-18.

Booth G, Stalker TJ, Lefer AM. Mechanisms of amelioration of glucose-induced endothelial dysfunction following inhibition of protein kinase C in vivo. *Diabetes* 2002; 51: 1556-1564.

Boulanger CM, Tanner FC, Bea M-L, *et al.* Oxidized low density lipoprotein induce mRNA expression and release of endothelin from human and porcine endothelium. *Circ Res* 1992; 70: 1191-1197.

Boutstany-Kari CM, Gong M, Akers WS, *et al.* Enhanced vascular contractility and diminished coronary artery flow in rats made hypertensive from diet-induced obesity. *Int J Obes* 2007; 31: 1652-1659.

Bove K, Neumann P, Gertzberg N, *et al.* Role of eNOS-derived NO in mediating TNF-induced endothelial barrier dysfunction. *Am J Physiol Lung Cell Mol Physiol* 2001; 280: L914-L922.

Bradford, M. A Rapid and Sensitive Method for the Quantitation of Microgram Quantities of Protein Utilizing the Principle of Protein-Dye Binding. *Anal Biochem* 1976; 72: 248-254.

Bradshaw D, Nannan N, Laubscher R, *et al* South African National Burden of Disease Study 2000: Estimates of Provincial Mortality. Western Cape Province: MRC 2000. Available: <http://www.mrc.ac.za/bod/westerncape>.

Brandes RP, Fleming I, Busse R. Endothelial aging. *Cardiovasc Res* 2005; 66: 286-294.

Brasier AR. The nuclear factor- κ B-interleukin-6 signalling pathway mediating vascular inflammation. *Cardiovasc Res* 2010; 86: 211-218.

Breton-Romero R, Lamas S. Hydrogen peroxide signaling in vascular endothelial cells. *Redox Biology* 2014; 2: 529-534.

Brooks A, Lelkes PI, Rubanyi GM. Gene expression profiling of human aortic endothelial cells exposed to disturbed flow and steady laminar flow. *Physiol Genomics* 2002; 9: 27-41.

Browne CD, Hindmarsh EJ, Smith JW. Inhibition of endothelial cell proliferation and angiogenesis by orlistat, a fatty acid synthase inhibitor. *FASEB J* 2006; 20: 2027-2035.

Bruckdorfer R. The basics about nitric oxide. *Mol Aspect Med* 2005; 26: 3-31.

Bruneel A, Labas V, Mailloux A, *et al*. Proteomic study of human umbilical vein endothelial cells in culture. *Proteomics* 2003; 3: 714-723.

Brutsaert DL, Franssen P, Andries LJ, *et al*. Cardiac endothelium and myocardial function. *Cardiovasc Res* 1998; 38: 281-290.

Brutsaert DL. Cardiac endothelial-myocardial signalling: its role in cardiac growth, contractile performance, and rhythmicity. *Physiol Rev* 2003; 83: 59-115.

Bulua AC, Simon A, Maddipati R, *et al*. Mitochondrial reactive oxygen species promote production of proinflammatory cytokines and are elevated in TNFR1-associated periodic syndromes (TRAPS). *J Exp Med* 2011; 208: 519-533.

Burke A, Fitzgerald GA. Oxidative stress and smoking-induced vascular injury. *Prog Cardiovasc Dis* 2003; 46: 79-90.

Burke-Gaffney A, Hellewell PG. Tumour necrosis factor- α -induced ICAM-1 expression in human vascular endothelial and lung epithelial cells: modulation by tyrosine kinase inhibitors. *Br J Pharmacol*. 1996; 119: 1149-1158.

Caballero AE. Endothelial Dysfunction in Obesity and Insulin Resistance: A Road to Diabetes and Heart Disease. *Obesity Research* 2003; 11: 1278-1289.

Cai H, Harrison DG. Endothelial dysfunction in cardiovascular disease: the role of oxidant stress. *Circ Res* 2000; 87: 840-844.

Campia U, Tesouro M, Cardillo C. Human obesity and endothelium-dependent responsiveness. *Br J Pharmacol* 2012; 165: 561-573.

Cao G, O'Brien CD, Zhou Z, *et al.* Involvement of human PECAM-1 in angiogenesis and in vitro endothelial migration. *Am J Physiol Cell Physiol* 2002; 282: C1181-C1190.

Carraro S, Giordano G, Piacentini G, *et al.* Asymmetric dimethylarginine in exhaled breath condensate and serum of children with asthma. *Chest*. 2013; 144: 405-410.

Celemajer DS, Sorensen KE, Spiegelhalter DJ, *et al.* Aging is associated with endothelial dysfunction in healthy men years before the age-related decline in women. *J Am Coll Cardiol* 1994; 24: 471-476.

Chen J, Mehta JL, Haider N, *et al.* Role of caspases in Ox-LDL-induced apoptotic cascade in human coronary artery endothelial cells. *Circ Res* 2004; 94: 370-376.

Chen ML, Yi L, Jin X, *et al.* Resveratrol attenuates vascular endothelial inflammation by inducing autophagy through the cAMP signaling pathway. *Autophagy* 2013; 9: 2033-2045.

Chen X, Andresen BT, Hill M, *et al.* Role of reactive oxygen species in tumor necrosis factor- α induced endothelial dysfunction. *Curr Hypertens Rev* 2008; 4: 245-255.

Chen Y-H, Lin S-J, Chen J-W, *et al.* Magnolol attenuates VCAM-1 expression *in vitro* in TNF- α -treated human aortic endothelial cells and *in vivo* in the aorta of cholesterol-fed rabbits. *British Journal of Pharmacology* 2002; 135: 37-47.

Chen YH, Lin SJ, Ku HH, *et al.* Salvianolic acid B attenuates VCAM-1 and ICAM-1 expression in TNF- α -treated human aortic endothelial cells. *J Cell Biochem* 2001; 82: 512-521.

Cheng Y, Austin SC, Rocca B, *et al.* Role of prostacyclin in the cardiovascular response to thromboxane A₂. *Science* 2002; 296: 593-541.

Coats P, Johnston F, MacDonald J, *et al.* Endothelium-derived hyperpolarizing factor. Identification and mechanisms of action in human subcutaneous resistance arteries. *Circulation* 2001; 103: 1702-1708.

Cohen RA, Vanhoutte PM. Endothelium dependent hyperpolarization. Beyond nitric oxide and cyclic GMP. *Circulation* 1995; 92: 3337-3349.

Colgan SP, Eltzhig HK, Eckle T, Thompson LF. Physiological roles for ecto-5'-nucleotidase (CD73). *Purinergic Signal* 2006; 2: 351-360.

Cominacini L, Rigoni A, Pasini AF, *et al.* The binding of oxidized low density lipoprotein (ox-LDL) to ox-LDL receptor-1 reduces the intracellular concentration of nitric oxide in

endothelial cells through an increased production of superoxide. *J Biol Chem* 2001; 276: 13750-13755.

Cooke JP, Andon NA, Girerd XJ, *et al.* Arginine restores cholinergic relaxation of hypercholesterolemic rabbit thoracic aorta. *Circulation* 1999; 83: 1057-1067.

Cooke JP. Asymmetrical dimethylarginine: The Uber marker? *Circulation* 2004; 109: 1813-1818.

Corda S, Laplace C, Vicaut E, Duranteau J. Rapid reactive oxygen species production by mitochondria in endothelial cells exposed to tumor necrosis factor- α is mediated by ceramide. *Am J Respir Cell Mol Biol* 2001; 24: 762-768.

Cowan CL, Cohen RA. Two mechanisms mediate relaxation by bradykinin of pig coronary artery: NO-dependent and -independent responses. *Am J Physiol* 1991; 261: H830-835.

Csiszar A, Smith K, Labinsky N, *et al.* Resveratrol attenuates TNF- α -induced activation of coronary arterial endothelial cells: role of NF- κ B inhibition. *Am J Physiol Heart Circ Physiol*. 2006; 291: H1694-H1699.

Daff S. NO synthase: structure and mechanisms. *Nitric Oxide* 2010; 23: 1-11.

Davies GE, Senger DR. Endothelial extracellular matrix: Biosynthesis, remodeling, and functions during vascular morphogenesis and neovessel stabilization. *Circ Res*. 2005; 97: 1093-1107.

Davies PF. Endothelial mechanisms of flow mediated atheroprotection and susceptibility. *Circ Res* 2007; 101: 10-12.

Davignon J, Ganz P. Role of endothelial dysfunction in atherosclerosis. *Circulation* 2004; 109: 27-32.

De Caterina R, Libby P, Peng H-B, *et al.* Nitric oxide decreases cytokine-induced endothelial activation. Nitric oxide selectively reduces endothelial expression of adhesion molecules and proinflammatory cytokines. *J Clin Invest* 1995; 96: 60-68.

De Palma C, Meacci E, Perrotta C, *et al.* Endothelial nitric oxide synthase activation by tumor necrosis factor alpha through neutral sphingomyelinase 2, sphingosine kinase 1, and sphingosine 1 phosphate receptors: a novel pathway relevant to the pathophysiology of endothelium. *Arterioscler Thromb Vasc Biol* 2006; 26: 99-105.

Deanfield JE, Halcox JP, Rabelink TJ. Endothelial function and dysfunction: Testing and clinical relevance. *Circulation* 2007; 115: 1285–1295.

Deaton C, Froelicher ES, Wu LH, *et al.* The global burden of cardiovascular disease. *Eur J Cardiovasc Nurs* 2011; 10: S5-13.

Dejana E, Corada M, Lampugnani MG. Endothelial cell-to-cell junctions. *FASEB J* 1995; 9: 910-918.

Dejana E. Endothelial cell-cell junctions: Happy together. *Mol Cell Biol* 2004; 5: 261-270.

Dela Paz NG, D'Amore P. Arterial versus venous endothelial cells. *Cell Tissues Res* 2009; 335: 5-16.

DeLisser HM, Christofidou-Solomidou M, Strieter RM, *et al.* Involvement of endothelial PECAM-1 / CD31 in angiogenesis. *Am J Pathol* 1997; 151: 671-677.

Deng D.X-F, Tsalenko A, Vailaya A, *et al.* Differences in vascular bed disease susceptibility reflect differences in gene expression response to a high fat diet. *Circ Res* 2006; 98: 200-208.

Deshpande SS, Angkeow P, Huang J, Ozaki M, Irani K. Rac 1 inhibits TNF- α -induced endothelial cell apoptosis: dual regulation by reactive oxygen species. *FASEB J* 2000; 14: 1705-1714.

Dikalov AE, Gongora MC, Harrison DG, *et al.* Upregulation of NOX1 in vascular smooth muscle leads to impaired endothelium-dependent relaxation via eNOS uncoupling. *Am J Physiol Heart Circ Physiol* 2010; 299: H673-H679.

Dimmeler S, Fleming I, Fisslthaler B, *et al.* Activation of nitric oxide synthase in endothelial cells by Akt-dependent phosphorylation. *Nature* 1999; 399: 601-605.

Donato AJ, Gano LB, Eskurza I, *et al.* Vascular endothelial dysfunction with aging: endothelin-1 and endothelial nitric oxide synthase. *Am J Physiol Heart Circ Physiol* 2009; 297: H425-H432.

Dossumbekova A, Berdyshev EV, Gorshkova I, *et al.* Akt activates NOS3 and separately restores barrier integrity in H₂O₂-stressed human cardiac microvascular endothelium. *Am J Physiol Heart Circ Physiol* 2008; 295: H2417-H2426.

Draijer R, Atsma DE, van der Laarse A, van Hinsbergh VW. cGMP and nitric oxide modulate thrombin-induced endothelial permeability. Regulation via different pathways in human aortic and umbilical vein endothelial cells. *Circ Res* 1995; 76: 199-208.

Draude G, Hrboticky N, Lorenz RL. The expression of the lectin-like oxidized low-density lipoprotein receptor (LOX-1) on human vascular smooth muscle cells and monocytes and its down-regulation by lovastatin. *Biochem Pharm* 1999; 57: 383-386.

Drummond GR, Cai H, Davis ME, *et al.* Transcriptional and posttranscriptional regulation of endothelial nitric oxide synthase expression by hydrogen peroxide. *Circ Res* 2000; 86: 347-354.

Dryden NH, Sperone A, Martin-Almedina S, *et al.* The transcription factor Erg control endothelial cell quiescence by repressing activity of nuclear factor (NF)-KB p65. *J Biol Chem* 2012; 15: 12331-42.

Du Y, Ko KM. Oleonic acid protects against myocardial ischaemia-reperfusion injury by enhancing mitochondrial antioxidant mechanism mediated by glutathione and apha-tocopherol in rats. *Planta Med* 2006; 72: 222-227.

Dudzinski D, Michel T. Life history of eNOS: partners and pathways. *Cardiovasc Res* 2007; 75: 247-260.

Edwards G, Dora KA, Gardener MJ, *et al.* k^+ is an endothelium-derived hyperpolarizing factor in rat arteries. *Nature* 1998; 396: 269-272.

Eliseyeva MR. Endothelium: A road from mystery to discovery. *International Journal of Biomedicine* 2013; 3 (1): 9-11.

Esen AM, Barutcu I, Acar M, *et al.* Effects of smoking on endothelial function and wall thickness of brachial artery. *Circ J* 2004; 68: 1123-1126.

Esper RJ, Nordaby RA, Vilarino JO, *et al.* Endothelial dysfunction: A comprehensive appraisal. *Cardiovasc Diabetol* 2006; 5:4.

Fenster BE, Tsao PS, Rockson SG. Endothelial dysfunction: clinical strategies for treating oxidant stress. *Am Heart J* 2003; 146: 218-226.

Feron O, Dessy C, Moniotte S, *et al.* Hypercholesterolemia decreases nitric oxide production by promoting the interaction of caveolin and nitric oxide synthase. *J Clin Invest* 1999; 103: 897-905.

Feron O, Saldana F, Michel JB, Michel T. The endothelial nitric-oxide synthase-caveolin regulatory cycle. *J Biol Chem* 1998; 273: 3125-3128.

Finucane DM, Bossy-Wetzel E, Waterhouse NJ, Cotteri TG, Green DR. Bax-induced caspase activation and apoptosis via cytochrome C release from mitochondria is inhibitable by Bcl-xL. *J Biol Chem* 1999; 274: 2225-2233.

Fish JE, Matouk CC, Rachlis A, *et al.* The expression of endothelial nitric oxide synthase is controlled by a cell specific histone code. *J Biol Chem* 2005; 280: 24824-24838.

Fisslthaler B, Dimmeler S, Hermann C, *et al.* Phosphorylation and activation of the endothelial nitric oxide synthase by fluid shear stress. *Acta Physiol Scand* 2000; 168: 81-88.

Fleming I, Busse R. Molecular mechanisms involved in the regulation of the endothelial nitric oxide synthase. *Am J Physiol Regul Intergr Comp Physiol* 2003; 284: R1-R2.

Fleming I. Molecular mechanisms underlying the activation of eNOS. *Pflugers Arch – Eur J Physiol* 2010; 459: 793-806.

Florey L. The endothelial cell. *BMJ* 1977; 5512: 487-490.

Forstermann U, Munzel T. Endothelial nitric oxide synthase in vascular disease: from marvel to menace. *Circulation* 2006; 113: 1708-1714.

Fostermann U, Boissel J-P, Kleinert H. Expressional control of the 'constitutive' isoforms of nitric oxide synthase (NOS I and NOS III). *FASEB J* 1998; 12: 773-790.

Fostermann U, Sessa WC. Nitric oxide synthases: regulation and function. *European heart Journal* 2011. doi: 10.1093/eurheartj/ehr304.

Frank PG, Woodman SE, Park DS, Lisanti MP. Caveolin, Caveolae, and endothelial cell function. *Arterioscler Thromb Vasc Biol* 2003; 23: 1161-1168.

Fujio Y, Walsh K. Akt mediates cytoprotection of endothelial cells by vascular endothelial growth factor in an anchorage-dependent manner. *J Biol Chem* 1999; 274: 16349-16354.

Fukui T, Ishizaka N, Rajagopalan S, *et al.* p22phox mRNA expression and NADPH oxidase activity are increased in aortas from hypertensive rats. *Circ Res.* 1997; 80: 45–51.

Furchgott RF, Zawadzki JV. The obligatory role of endothelial cells in the relaxation of arterial smooth muscle by acetylcholine. *Nature.* 1980; 288: 373-376.

Galan M, kassan M, kadowitz PJ, *et al.* Mechanism of endoplasmic reticulum stress-induced vascular endothelial dysfunction. *Biochimica et Biophysica Acta* 2014; 1843: 1063-1075.

Galley HF, Webster NR. Physiology of the endothelium. *Br J Anaesth* 2004; 93: 105-113.

Gao X, Belmadani S, Picchi A, *et al.* Tumor necrosis factor- α induces endothelial dysfunction in *Lepr^{db}* mice. *Circulation* 2007; 115: 245-254.

García-Cardena G, Fan R, Shah V, *et al.* Dynamic activation of endothelial nitric oxide synthase by Hsp90. *Nature* 1998; 392: 821-824.

Geiger M, Stone A, Mason SN, *et al.* Differential nitric oxide production by microvascular and macrovascular endothelial cells. *Am J Physiol* 1997; 273: L275-L281.

Geraldes P, King GL. Activation of protein kinase C isoforms and its impact on diabetic complications. *Circ Res* 2010; 106: 1319-1331.

Gillham JC, Myers JE, Baker PN, Taggart MJ. TNF- α alters nitric oxide- and endothelium-derived hyperpolarizing factor- mediated vasodilatation in human omental arteries. *Hypertens Pregnancy* 2008; 27: 29-38.

Girard J-P, Springer TA. High endothelial venules (HEVs): specialized endothelium for lymphocyte migration. *Immunology Today* 1995; 16 (9): 449-457.

Gkaliagkousi E, Ritter J, Ferro A. Platelet-derived nitric oxide signaling and regulation. *Circ Res* 2007; 101: 654-662.

Gobbel GT, Chan TY-Y, Chan PK. Nitric oxide- and superoxide-mediated toxicity in cerebral endothelial cells. *JPET* 1997; 282: 1600-1607.

Goedecke JH, Jennings CL, Lambert EV. Obesity in South Africa. In editors: Steyn K, Fourie J, Temple N. *Chronic diseases of lifestyle in South Africa 1995-2005*. MRC 2006.

Gogos JA, Morgan M, Luine V, *et al.* Catechol-O-methyltransferase-deficient mice exhibit sexually dimorphic changes in catecholamine levels and behaviour *Proc Natl Acad Sci USA* 1998; 95: 9991-9996.

Goldin A, Beckman JA, Schmidt AM, Creager MA. Advanced glycation end products: Sparking the development of diabetic vascular injury. *Circulation* 2006; 114: 597-605.

González-Fernández F, Jiménez A, López-Blaya A, *et al.* Cerivastatin prevents tumor necrosis factor- α -induced downregulation of endothelial nitric oxide synthase: role of endothelial cytosolic proteins. *Atherosclerosis* 2001; 155: 61-70.

Goodwin BL, Pendleton LC, Levy MM, *et al.* Tumor necrosis factor- α reduces argininosuccinate synthase expression and nitric oxide production in aortic endothelial cells. *Am J Physiol Heart Circ Physiol* 2007; 293: H1115-H1121.

Gorlach A, Brandes RP, Nguyen K, *et al.* A pg91phox containing NADPH oxidase selectively expressed in endothelial cells is a major source of oxygen radical generation in the arterial wall. *Circ Res* 2000; 87: 26-32.

Greenblatt EP, Loeb AL, Longnecker, DE. Marked regional heterogeneity in the magnitude of EDRF/NO mediated vascular tone in awake rats. *J. Cardiovasc. Pharmacol* 1993; 21: 235-240.

Griendling KK, Sorescu D, Ushio-Fukai M. NADPH oxidase: role in cardiovascular biology and disease. *Circ Res* 2000; 86: 494-501.

Grindlieng KK, Minieri CA, Ollenshaw JD, Alexander RW. Angiotensin II stimulates NADH and NADPH oxidase activity in cultured vascular smooth muscle cells. *Circ Res* 1994; 74: 1141-1148.

Grundey SM, Benjamin IJ, Burke GL, *et al.* Diabetes and cardiovascular disease: A statement for healthcare professionals from the American Heart Association. *Circulation* 1999; 100: 1134-1146.

Gu L, Okada Y, Clinton S, *et al.* Absence of monocyte chemoattractant protein-1 reduces atherosclerosis in low-density lipoprotein-deficient mice. *Mol Cell* 1998; 2: 275-281.

Guthikonda S, Woods K, Sinkey CA, *et al.* Role of xanthine oxidase in conduit artery endothelial dysfunction in cigarettes smokers. *Am J Cardiol* 2004; 93: 664-668.

Guzik TJ, Mussa S, Gastaldi D, *et al.* Mechanisms of increased vascular superoxide production in human diabetes mellitus, role of NAD(P)H oxidase and endothelial nitric oxide synthase. *Circulation* 2002; 105: 1656-1662.

Guzik TJ, West NEJ, Black E. Vascular superoxide production by NADPH oxidase: association with endothelial dysfunction and cardiovascular risk factors. *Circ Res* 2000; 86: e85-e90.

Hadi HAR, Carr CS, Suwaidi JAL. Endothelial dysfunction: Cardiovascular risk factors, therapy and outcomes. *Vascular Health and Risk Management* 2005; 1: 183-198.

Handt S, Jerome WG, Tietze L, Hantgan RR. Plasminogen activator inhibitor secretion by endothelial cells increases fibrinolytic resistance of an *in vitro* fibrin clot: evidence for a key role of endothelial cells in thrombolytic resistance. *Blood* 1996; 87: 4204-4213.

Harlan JM, Levine JD, Callahan KS, *et al.* Glutathione redox cycle protects cultured endothelial cells against lysis by extracellularly generated hydrogen peroxide. *J Clin Invest* 1984; 73: 706-713.

Harrison D, Grienling KK, Landmesser U, *et al.* Role of oxidative stress in atherosclerosis. *Am J Cardiol* 2003; 91: 7A-11A.

Harrison DG. (2012) Oxidative Stress and Vascular Inflammation, in *Inflammatory Diseases of Blood Vessels, Second Edition* (eds G. S. Hoffman, C. M. Weyand, C. A. Langford and J. J. Goronzy), Wiley-Blackwell, Oxford, UK. doi: 10.1002/9781118355244.ch9

Heitzer T, Yla-Herttuala S, Luoma J, *et al.* Cigarette smoking potentiates endothelial dysfunction of forearm resistance vessels in patients with hypercholesterolemia. *Circulation* 1996; 93: 1346-1356.

Hendrickx J, Goggen K, Weinberg EO, *et al.* Molecular diversity of cardiac endothelial cells *in vitro* and *in vivo*. *Physiol Genomics* 2004; 19: 198-206.

Hernandez M, Hernandez I, Rodriguez F, *et al.* Endothelial dysfunction in gestational hypertension induced by catechol-O-methyltransferase inhibition. *Exp Physiol* 2013; 98: 856-866.

Herrera MD, Mingorance C, Rodríguez- Rodríguez R, *et al.* Endothelial dysfunction and aging: an update. *Ageing Res Rev* 2010; 9: 142-152.

Hirano Y, Tsunoda M, Shimosawa T, *et al.* Suppression of catechol-O-methyltransferase activity through blunting of alpha2-adrenoceptor can explain hypertension in Dahl salt-sensitive rats. *Hypertens Res* 2007; 30: 269-278.

Holvoet P, Mertens A, Verhamme P, *et al.* Circulating oxidized LDL is a useful marker for identifying patients with coronary artery disease. *Arterioscler Thromb Vasc Biol* 2001; 21: 844-848.

Hotamisligil GS, Arner P, Caro JF, *et al.* Increased adipose tissue expression of tumor necrosis factor-alpha in human obesity and insulin resistance. *J Clin Invest* 1995; 95: 2409-2415.

Hsieh PCH, Davis ME, Lisowski LK, Lee RT. Endothelial-cardiomyocyte interactions in cardiac development and repair. *Annu Rev Physiol* 2006; 68: 51-66.

Hsieh SH, Yng NW, Wu MH, *et al.* Galectin-1, a novel ligand of neuropilin-1, activates VEGFR-2 signaling and modulates the migration of vascular endothelial cells. *Oncogene* 2008; 27: 3746-3753.

Hsu H, Shu HB, Pan MG, Goeddel DV. TRADD-TRAF2 and TRADD-FADD interactions define two distinct TNF receptor 1 signal transduction pathways. *Cell* 1996; 84: 299-308.

Hsu H, Xiong J, Goeddel DV. The TNF receptor 1-associated protein TRADD signals cell death and NF-kappa B activation. *Cell* 1995; 81: 495-504.

Hsueh WA, Lyon CJ, Quinones MJ. Insulin resistance and the endothelium. *Am J Med* 2004; 117: 109-117.

Huang DW, Sherman BT, Lempicki RA. Systematic and integrative analysis of large gene lists using DAVID Bioinformatics Resources. *Nature Protoc* 2009, 4: 44-57.

Huang PL. Endothelial nitric oxide synthase and endothelial dysfunction. *Curr Hypertens Rep* 2003; 5: 473-480.

Hubert HB, Feinleib M, McNamara PM, Castelli WP: Obesity as an independent risk factor for cardiovascular disease: a 26-year follow-up of participants in the Framingham Heart Study. *Circulation* 1983; 67:968-977.

Huisamen B, George C, Dietrich d, Genade S. Cardioprotective and anti-hypertensive effects of *Prosopis glandulosa* in rat models of pre-diabetes. *Cardiovasc J Afr* 2013; 24: 10-16.

Hunt BJ, Jurd KM. Endothelial cell activation: a central pathophysiological process. *BMJ* 1998; 316: 1328-1329.

Hunt MC, Yamada J, Maltais LJ, *et al.* A revised nomenclature for mammalian acyl-CoA thioesterases/hydrolases. *J. Lipid Res* 2005; 46: 2029-2032.

Hutchingson PJA, Palmer RMJ, Moncada S. Comparative pharmacology of EDRF and nitric oxide on vascular strips. *Eur J Pharmacol* 1987; 141: 445-451.

Huttinger ZM, Milks MW, Nickoli MS, *et al.* Ectonucleotide Triphosphate Diphosphohydrolase-1 (CD39) Mediates Resistance to Occlusive Arterial Thrombus Formation after Vascular Injury in Mice. *Am J Pathol* 2012; 181: 322-333.

Ignarro LJ, Buga GM, Wood KS, Byrns RE, Chaudhuri G. Endothelium-derived relaxing factor produced and released from artery and vein is nitric oxide. *Proc Natl Acad Sci USA* 1987; 84:9265-9269.

Ishida T, Kundu RK, Yang E, *et al.* Targeted disruption of endothelial cell-selective adhesion molecule inhibits angiogenic processes in vitro and in vivo. *J Biol Chem* 2003; 278: 34598-34604.

Ito A, Tsao PS, Adimoolam S, *et al.* Novel mechanisms for endothelial dysfunction: dysregulation of dimethylarginine dimethylaminohydrolase. *Circulation* 1999; 99: 3092-3095.

Jansen T, Hortmann M, Oelze M, *et al.* Conversion of biliverdin to bilirubin by biliverdin reductase contributes to endothelial cell protection by heme oxygenase-1-evidence for direct and indirect antioxidant actions of bilirubin. *J Mol Cell Cardiol* 2010; 49: 186-195.

Jiang Y, Woronicz JD, Liu W, Goeddel DV. Prevention of constitutive TNF receptor 1 signaling by silencer of death domains. *Science* 1999; 283: 543-6.

Jones SA, O'Donnell VB, Wood JD, *et al.* Expression of phagocyte NADPH oxidase components in human endothelial cells. *Am J Physiol* 1996; 271: H1626-H1634.

Kalra VK, Ying Y, Deemer K, *et al.* Mechanism of cigarette smoke condensate induced adhesion of human monocytes to cultured endothelial cells. *J Cell Physiol* 1994; 160: 154-162.

Kassan M, Choi S-K, Galan M, *et al.* Enhanced NF- κ B activity impairs vascular function through PARP-1-, SP-1-, and COX-2-dependent mechanisms in type 2 diabetes. *Diabetes* 2013; 62: 2078-2087.

Kataoka H, Kume N, Miyamoto S. Oxidized LDL modulates Bax/Bcl-2 through the lectin-like Ox-LDL receptor-1 in vascular smooth muscle cells. *Arterioscler Thromb Vasc Biol* 2001; 21: 955-60.

Katusic ZS. Mechanisms of endothelial dysfunction induced by aging: role of arginase I. *Circ Res* 2007; 101: 640-641.

Kawanaka H, Jones MK, Szabo IL, *et al.* Activation of eNOS in rat portal hypertensive gastric mucosa is mediated by TNF-alpha via the PI3-kinase-Akt signaling pathway. *Hepatology* 2002; 35: 393-402.

Kempe S, Kestler H, Lasar A, Wirth T. NF- κ B controls the global pro-inflammatory response in endothelial cells: evidence for the regulation of a pro-atherogenic program. *Nucleic Acids Res* 2005; 33: 5308-5519.

Kessler P, Popp R, Busse R, Schini-Kerth VB. Proinflammatory mediators chronically downregulate the formation of the endothelium-derived hyperpolarizing factor in arteries via a nitric oxide/cyclic GMP-dependent mechanism. *Circulation* 1999; 99: 1878-1884.

Khan BV, Harrison DG, Olbrych MT, *et al.* Nitric oxide regulates vascular cell adhesion molecule 1 geneexpression and redox-sensitive transcriptional events in human vascular endothelial cells. *Proc. Natl. Acad. Sci. USA* 1996; 93: 9114-9119.

Kim I, Xu W, Reed JC. Cell death and endoplasmic reticulum stress: disease relevance and therapeutic opportunities. *Nat Rev Drug Discov* 2008; 7: 1013-1030.

Kim J, Montagnani M, Koh KK, Quon MJ. Reciprocal relationships between insulin resistance and endothelial dysfunction: Molecular and pathophysiological mechanisms. *Circulation* 2006; 113: 1888-1904.

Kitamoto S, Sukhova GK, Sun J, *et al.* Cathepsin L deficiency reduces diet-induced atherosclerosis in low-density lipoprotein receptor-knockout mice. *Circulation* 2007; 115: 2065-2075.

Kluge MA, Fetterman JL, Vita JA. Mitochondria and endothelial function. *Circ Res* 2013; 112: 1171-1188.

Kobayashi T, Tahara Y, Matsumoto M, *et al.* Roles of thromboxane A₂ and prostacyclin in the development of atherosclerosis in apoE-deficient mice. *J Clin Invest* 2004; 114: 784-794.

Kohr MJ, Traynham CJ, Roof SR, *et al.* cAMP-independent activation of protein kinase A by the peroxynitrite generator SIN-1 elicits positive inotropic effects in cardiomyocytes. *J Mol Cell Cardiol* 2010; 48: 645-648.

Kolluru GK, Siamwala JH, Chatterjee S. eNOS phosphorylation in health and disease. *Biochemie* 2010; 92: 1186-1198.

Kotsis V, Stabouli S, Papakatsika S, *et al.* Mechanisms of obesity-induced hypertension. *Hypertens Res* 2010; 33: 386-393.

Koya D, King GL. Protein kinase C activation and the development of diabetic complications. *Diabetes* 1998; 47: 859-866.

Koziak K, Sevigny J, Robson SC, *et al.* Analysis of CD39/ATP diphosphohydrolase (ATPDase) expression in endothelial cells, platelets and leukocytes. *Thromb Haemost* 1999; 82: 1538-1544.

Krysko DV, Vanden Berghe T, D'Herde K, Vandenabeele P. Apoptosis and necrosis: detection, discrimination and phagocytosis. *Methods* 2008; 44: 205-221.

Kuzkaya N, Weissmann N, Harrison DG, *et al.* Interaction of peroxynitrite, tetrahydrobiopterin, ascorbic acid, and thiols. *J Biol Chem* 2003; 278: 22546–22554.

Laccore DA, Baekkevold ES, Garrido I, *et al.* Plasticity of endothelial cells: rapid dedifferentiation of freshly isolated high endothelial venule endothelial cells outside the lymphoid tissue microenvironment. *Blood* 2004; 103: 4164-4172.

Lai PFH, Mohamed F, Monge J-C, Stewart DJ. Downregulation of eNOS mRNA expression by TNF- α : identification of the functional characterization of RNA-protein interactions in 3'UTR. *Cardiovasc Res* 2003; 59: 160-168.

Lancel S, Tissier S, Mordon S, *et al.* Peroxynitrite decomposition catalysts prevent myocardial dysfunction and inflammation in endotoxemic rats. *J Am Coll Cardiol* 2004; 43: 2343-2358.

Landmesser U, Spiekermann S, Dikalov S, *et al.* Vascular oxidative stress and endothelial dysfunction in patients with chronic heart failure: Role of xanthine-oxidase and extracellular superoxide dismutase. *Circulation* 2002; 106: 3073-3078. (a)

Landmesser U, Cai H, Dikalov S, *et al.* Role of p47phox in vascular oxidative stress and hypertension caused by angiotensin II. *Hypertension* 2002; 40: 511-515.(b)

Laubichler, Aird WC, Maienschein J. The endothelium in history. In Aird WC (editor). *Endothelial biomedicine*. Cambridge University Press 2007: 5-19.

Lawson C, Wolf S. ICAM-1 signaling in endothelial cells. *Pharmacol Rep* 2009; 61: 22-32.

Lee W, Yang EJ, Ku SK, *et al.* Anti-inflammatory effects of oleanolic acid on LPS-induced inflammation *in vitro* and *in vivo*. *Inflammation* 2013; 36: 94-102.

Lefer DJ, Scalia R, Campbell B, *et al.* Peroxynitrite inhibits leukocyte-endothelial cell interactions and protects against ischemia-reperfusion injury in rats. *J Clin Invest* 1997; 99: 684-691.

Lehr H-A, Frei B, Arfors KE. Vitamin C prevents cigarette smoke-induced leucocyte aggregation and adhesion to endothelium *in vivo*. *Proc Natl Acad Sci USA* 1994; 91: 7688-7692.

Leopold JA, Zhang Y-Y, Scribner AW, *et al.* Glucose-6-phosphate dehydrogenase overexpression decreases endothelial cell oxidative stress and increase bioavailable nitric oxide. *Arterioscler Thromb Vasc Biol* 2003; 23: 411-417.

Li C, Zhou H-M. The Role of manganese superoxide dismutase in inflammation defence. *Enzyme Research* 2011, Article ID 387176, 6 pages, 2011. doi:10.4061/2011/387176.

Li D, Chen H, Romeo F, *et al.* Statins modulate oxidized low-density lipoprotein mediated adhesion molecule expression in human coronary artery endothelial cells: role of LOX-1. *J Pharm Exp Ther* 2002; 302: 601-605.

Li D, Singh RM, Liu L, *et al.* Oxidized-LDL through LOX-1 increases the expression of angiotensin converting enzyme in human coronary artery endothelial cells. *Cardiovasc Res* 2003; 57: 238-243.

Li F, Yuan Y, Guo Y, *et al.* Pulsed magnetic field accelerate proliferation and migration of cardiac microvascular endothelial cells. *Bioelectromagnetics* 2015; 36: 1-9.

Li H, Wallerath T, Münzel T, Förstermann U. Regulation of endothelial-type NO synthase expression in pathophysiology and in response to drugs. *Nitric Oxide Biol Chem* 2002; 7: 149-164.

Li JH, Pober JS. The cathepsin B death pathway contributes to TNF plus IFN- γ -mediated human endothelial injury. *J Immunol* 2005; 175: 1858-1866.

Li J-M, Fan LM, Christie MR, Shah AJ. Acute tumor necrosis factor alpha signaling and NADPH oxidase in microvascular endothelial cells: Role of p47^{phox} phosphorylation and binding to TRAF4. *Mol Cell Biol* 2005; 25: 2320-2330.

Li J-M, Shah AJ. Mechanisms of endothelial cell NADPH oxidase activation by angiotensin II. *J Biol Chem* 2003; 278: 12094-12100.

Li L, Roumeliotis N, Sawamura T, Renier G. C-reactive protein enhances LOX-1 expression in human aortic endothelial cells: relevance of LOX-1 to C-reactive protein-induced endothelial dysfunction. *Circ Res* 2004; 95: 877-883.

Li Y-Z, Liu X-H, Rong H, *et al.* Carbachol inhibits TNF- α -induced endothelial barrier dysfunction through alpha 7 nicotinic receptors. *Acta Pharmacologica Sinica* 2010; 31: 1389-1394.

Liao JK, Shin WS, Lee WY, Clark SC. Oxidised low-density lipoprotein decreases the expression of endothelial nitric oxide synthase. *J Biol Chem* 1995; 270: 319-324.

Liao JK. Linking endothelial dysfunction with endothelial cell activation. *J Clin Invest* 2013; 123: 540-541.

Libby P, Ridker PM, Maseri A. Inflammation and atherosclerosis. *Circulation* 2002; 105: 1135-1143.

Limaye V, Vadas M. The vascular endothelium: structure and function. In Fitridge R and Thompson M, editors. *Mechanisms of Vascular Disease: A Textbook for vascular Surgeons*. Cambridge University Press 2006:1-13.

Lin H, Lin X. Positive and negative signalling components involved in TNF- α induced NF- κ B activation. *Cytokine* 2008; 41: 1-8.

Lin Y, Choksi S, Shen HM, *et al.* Tumor necrosis factor-induced nonapoptotic cell death requires receptor-interacting protein-mediated cellular reactive oxygen species accumulation. *J Biol Chem*. 2004; 279: 10822-10828.

Liu J, Lu C, Li F, *et al.* PPAR- α agonist fenofibrate upregulates tetrahydrobiopterin level through increasing the expression of guanosine 5'-triphosphate cyclohydrolase-I in human umbilical vein endothelial cells. *PPAR Research* 2011; 2011: doi: 10.1155/523520.

Liu J, Sun H, Wang X, *et al.* Effects of oleanolic acid and maslinic acid on hyperlipidemia. *Drug Develop Res* 2007; 68: 261-266.

Liu J. Pharmacology of oleanolic acid. *J Ethnopharmacol* 1995; 49: 57-58.

Liu S, Premont RT, Kontos CD, *et al.* Endothelin-1 activates endothelial cell nitric-oxide synthase via heterotrimeric G-protein $\beta\gamma$ subunit signalling to protein kinase B / Akt. *J Biol Chem* 2003; 278: 49929-49935.

Luo Z, Fujio Y, Kureishi Y, *et al.* Acute modulation of endothelial Akt/PKB activity alters nitric oxide-dependent vasomotor activity in vivo. *J Clin Invest* 2000; 106: 493-499.

Lynch JA, George AM, Eisenhauer PB, *et al.* Insulin degrading enzyme is localized predominantly at the cell surface of polarized and unpolarized human cerebrovascular endothelial cell cultures. *J Neurosci Res* 2006; 83: 1262-1270.

Ma Z-C, Gao Y, Wang J, *et al.* Proteomic analysis effects of ginsenoside Rg1 on human umbilical vein endothelial cells stimulated by tumor necrosis factor. *Life Sciences* 2006; 79: 175-181.

MacNaul KL, Hutchinson NI. Differential expression of iNOS and cNOS mRNA in human vascular smooth muscle cells and endothelial cells under normal and inflammatory conditions. *Biochem Biophys Res Commun* 1993; 196: 1330-1334.

Madge LA, Li J-H, Choi J, Pober JS. Inhibition of Phosphatidylinositol 3-Kinase Sensitizes Vascular Endothelial Cells to Cytokine-initiated Cathepsin-dependent Apoptosis. *J Biol Chem* 2003; 278: 21295-21306.

Maeda S, Miyauchi T, Sakai S, *et al.* Prolonged exercise causes an increase in endothelin-1 production in the heart in rats. *Am J Physiol* 1998; 275: H2105–H2112.

Makino A, Scott BT, Dillmann WH. Mitochondrial fragmentation and superoxide anion production in coronary endothelial cells from a mouse model of type 1 diabetes. *Diabetologia* 2010; 53: 1783-1794.

Malek A, Izumo S. Physiological fluid shear stress causes downregulation of endothelin-1 mRNA in bovine aortic endothelium. *Am J Physiol* 1992; 263: C389–C396.

Malyszko J. Mechanisms of endothelial dysfunction chronic kidney disease. *Clinica Chimica Acta* 2010; 411: 1412-1420.

Mannarino E, Pirro M. Molecular biology of atherosclerosis. *Clin Cases Miner Bone Metab* 2008; 5: 57-62.

Mapanga RF, Rajamani U, Dlamini N, *et al.* Oleanolic acid: a novel cardioprotective agent that blunts hyperglycemia-induced contractile dysfunction. *PLoS ONE* 2012; 7: e47322. doi: 10.1371 / journal.pone.0047322.

Mapanga RF, Tufts MA, Shode FO, Musabayane CT. Renal effects of plant-derived oleanolic acid in streptozotocin-induced diabetic rats. *Ren Fail* 2009; 31: 481-491.

Marcus AJ, Broekman MJ, Drosopoulos JH, *et al.* Inhibition of platelet recruitment by endothelial cell CD39/ecto-ADPase: significance for occlusive vascular diseases. *Ital Heart J* 2001; 2: 824-830.

Marowitz H. LOX-1 and atherosclerosis: proof of concept in LOX-1 knockout mice. *Circ Res* 2007; 100: 1534-1536.

Martinez-Gonzalez J, Rodriguez-Rodriguez R, Gonzalez-Diez M, *et al.* Oleanolic acid induces prostacyclin release in human vascular smooth muscle cells through a cyclooxygenase-2-dependent mechanism. *J Nutr* 2008; 138: 443-448.

Mas M. A closer look at the endothelium: its role in the regulation of vasomotor tone. *Eur Urol* 2009; 8:48-57.

Mathers CD, Loncar D. Projections of global mortality and burden of disease from 2002 to 2030. *PLoS Med* 2006; 3(11): e442. doi:10.1371/journal.pmed.0030442

Mathews MT, Berk BC. PARP-1 inhibition prevents oxidative and nitrosative stress-induced endothelial cell death via transactivation of the VEGF receptor 2. *Arterioscler Thromb Vasc Biol* 2008; 28: 711-717.

Matoba T, Shimokawa H, Kubota H, *et al.* Hydrogen peroxide is an endothelium-derived hyperpolarizing factor in human mesenteric arteries. *Biochem Biophys Res Commun* 2002; 290: 909-913.

Matthews JR, Botting CH, Panico M, *et al.* Inhibition of NF-kappaB DNA binding by nitric oxide. *Nucleic Acids Res* 1996; 24: 2236–2242.

Matz RL, Schott C, Stoclet JC, *et al.* Age-related endothelial dysfunction with respect to nitric oxide, endothelium-derived hyperpolarising factor and cyclooxygenase products. *Physiol Res* 2000; 49: 11-18.

Mebazaa A, Wetzel R, Cherian M, Abraham M. Comparison between endocardial and great vessel endothelial cells: morphology, growth, and prostaglandin release. *Am J Physiol* 1995; 268: H250-H259.

Mehta JL, Chen J, Hermont PL, *et al.* Lectin-like, oxidized low-density lipoprotein receptor-1 (LOX-1): A critical player in the development of atherosclerosis and related disorders. *Cardiovasc Res* 2006; 69: 36-45.

Mehta PK, Griendling KK. Angiotensin II cell signalling: physiological and pathological effects in the cardiovascular system. *Am J Physiol Cell Physiol* 2007; 292: C82-C97.

Mehta R, Shapiro AD. Plasminogen activator inhibitor type 1 deficiency. *Haemophilia* 2008; 14: 1255-1260.

Meigs JB, O'Donnel CJ, Tofler GH, *et al.* Hemostatic Markers of Endothelial Dysfunction and Risk of Incident Type 2 Diabetes: The Framingham Offspring Study. *Diabetes* 2006; 55: 530-537.

Meldrum DR, Dinarello CA, Cleveland JC Jr, *et al.* Hydrogen peroxide induces tumor necrosis factor alpha-mediated cardiac injury by a P38 mitogen-activated protein kinase-dependent mechanism. *Surgery* 1998; 124: 291-296.

Meldrum DR. Tumor necrosis factor in the heart. *Am J Physiol* 1998; 274: R577-R595.

Messmer UK, Briner VA, Pfeilschifter J. Tumor necrosis factor-alpha and lipopolysaccharide induce apoptotic cell death in bovine glomerular endothelial cells. *Kidney Int* 1999; 55: 2322-2337.

Michiels C. Endothelial cell functions. *J Cell Physiol* 2003; 196: 430-443.

Mihm MJ, Jing L, Bauer JA. Nitrotyrosine causes selective vascular endothelial dysfunction and DNA damage. *J Cardiovasc Pharmacol* 2000; 36: 182-187.

Min JK, Kim YM, Kim SW, *et al.* TNF-related activation-induced cytokine enhances leukocyte adhesiveness: induction of ICAM-1 and VCAM-1 via TNF receptor-associated factor and

protein kinase C-dependent NF-kappaB activation in endothelial cells. *J Immunol* 2005; 175: 531-540.

Minuz P, Barrow SE, Cockcroft JR, Ritter JM. Prostacyclin and thromboxane biosynthesis in mild essential hypertension. *Hypertension* 1990; 15: 469-474.

Mittal M, Siddiqui MR, Tran K, *et al.* Reactive oxygen species in inflammation and tissue injury. *Antioxid Redox Signal* 2014; 20: 1126-1167.

Molet S, Furukawa K, Maghazechi A, *et al.* Chemokine- and cytokine-induced expression of endothelin 1 and endothelin-converting enzyme 1 in endothelial cells. *J Allergy Clin Immunol* 2000; 105: 333-338.

Molnar J, Yu S, Mzhavia N, *et al.* Diabetes induces endothelial dysfunction but does not increase neointimal formation in high-fat diet fed C57BL/6J mice. *Circ Res* 2005; 96: 1178-84.

Molostvov G, Morris A, Rose P, Basu S. Modulation of Bcl-2 family proteins in primary endothelial cells during apoptosis. *Pathophysiol Haemost Thromb* 2002; 32: 85-91.

Moncada S, Higgs EA, Vane JR. Human arterial and venous tissues generate prostacyclin (prostaglandin X), a potent inhibitor of platelet aggregation. *Lancet* 1977; 1: 18-20.

Morawietz H, Deurrschmidt N, Niemann B, *et al.* Induction of the oxLDL receptor by LOX-1 by endothelin-1 in human endothelial cells. *Biochem Biophys Res Commun* 2001; 284: 961-965.

Morawietz H. LOX-1 and atherosclerosis: Proof of concept in LOX-1-knockout mice. *Circ Res*. 2007; 100: 1534-1536.

Morgan JT, Pfeiffer ER, Thirkill TL, *et al.* Nesprin-3 regulates endothelial cell morphology, perinuclear cytoskeletal architecture, and flow-induced polarization. *Mol Biol Cell* 2011; 22: 4324-4334.

Moro MA, Russell RJ, Celtek S, *et al.* cGMP mediates the vascular and platelets actions of nitric oxide: confirmation using an inhibitor of the soluble guanylyl cyclase. *Proc Natl Acad Sci USA* 1996; 93: 1480-1485.

Mort JS, Buttle DJ. Cathepsin B. *Int J Biochem Cell Biol* 1997; 29: 715-720.

Moser M, Bauer M, Schmid S, *et al.* Kindlin-3 is required for beta2 integrin-mediated leukocyte adhesion to endothelial cells. *Nat Med* 2009; 15:300-305.

Most P, Lerchenmuller C, Rengo G, *et al.* S100A1 deficiency impairs postischemic angiogenesis via compromised proangiogenic endothelial cell function and nitric oxide synthase regulation. *Circ Res* 2013; 112: 66-78.

Mudau M, Genis A, Lochner A, Strijdom H. Endothelial dysfunction: the early predictor of atherosclerosis. *Cardiovasc J Afr* 2012; 23: 222-231.

Mukherjee D, Nissen SE, Topol EJ. Risk of cardiovascular events associated with selective COX-2 inhibitors. *JAMA* 2001; 286: 954-959.

Murakami H, Murakami R, Kambe F, *et al.* Fenofibrate activates AMPK and increases eNOS phosphorylation in HUVEC. *Biochem Biophys Res Commun* 2006; 341: 973-978.

Murao K, Ohyama T, Imachi H, *et al.* TNF-alpha stimulation of MCP-1 expression is mediated by the Akt/PKB signal transduction pathway in vascular endothelial cells. *Biochem Biophys Res Commun* 2000; 276: 791-796.

Nachman RL. Endothelium: from cellophane to orchestral maestro. *J Clin Invest.* 2012; 122(3): 796-797.

Naderali EK, Brown MJ, Pickavance LC, *et al.* Dietary obesity in the rat induces endothelial dysfunction without causing insulin resistance: a possible role for triacylglycerols. *Clin Sci* 2001; 101: 499-506.

Nakashima M, Mambouli J-V, Taylor AA, Vanhoutte PM. Endothelium-dependent hyperpolarization caused by bradykinin in human coronary arteries. *J Clin Invest* 1993; 92: 2867-2871.

Nakata T, Suzuki K, Fujii J, *et al.* Induction and release of manganese superoxide dismutase from mitochondria of human umbilical vein endothelial cells by tumor necrosis factor-alpha and interleukin-1 alpha. *Int J Cancer* 1993; 55: 646-650.

Neil K, Lewis SJ, James R, *et al.* Extensive tyrosine nitration in human myocardial inflammation: evidence for the presence of peroxynitrite. *Crit Care Med* 1997; 25: 812-819.

Nemr R, Lasserre B, Chahine R. Effects of nicotine on thromboxane/prostacyclin balance in myocardial ischemia. *Prostaglandins Leukot Essent Fatty Acids* 2003; 68: 191-195.

Neumann P, Gertzberg N, Vaughan E, *et al.* Peroxynitrite mediates TNF- α induced endothelial barrier dysfunction and nitration of actin. *Am J Physiol Lung Cell Mol Physiol* 2006; 290: L674-L684.

Nie H, Wu J-L, Zhang M, *et al.* Endothelial nitric oxide synthase-dependent tyrosine nitration of prostacyclin synthase in diabetes in vivo. *Diabetes* 2006; 55: 3133-3141.

Nishida M, Carley WW, Gerritsen ME, *et al.* Isolation and characterization of human and rat cardiac microvascular endothelial cells. *Am J Physiol Heart Circ Physiol* 1994; 33: H639-H652.

Ohashi J, Sawada A, Nakashima S, *et al.* Mechanisms for enhanced endothelium-derived hyperpolarizing factor-mediated responses in microvessels in mice. *Circ J* 2012;76: 1768-1779.

Ohbayashi A, Hiraga T, Okubo M, *et al.* Characteristics of porcine coronary artery endothelial cells in culture: comparison with aortic endothelium. *Biochem. Biophys Res Commun* 1994; 202: 504-511.

Ohsawa I, Nishimaki K, Yasuda C, Kamino K, Ohta S. Deficiency in a mitochondrial aldehyde dehydrogenase increases vulnerability to oxidative stress in PC12 cells. *J Neurochem* 2003; 84: 1110-1117.

Okruhlicova L, Tribulova N, Weismann P, *et al.* Ultrastructure and histochemistry of rat myocardial capillary endothelial cells in response to diabetes and hypertension. *Cell Res* 2005; 15: 532-538.

Oldendorf WH, Cornford ME, Brown WJ. The large apparent work capability of the blood-brain barrier: a study of the mitochondrial content of capillary endothelial cells in brain and other tissues of the rat. *Ann Neurol* 1977; 1: 409-417.

Olofsson SO, Boren J. Apolipoprotein B: A clinically important apolipoprotein which assembles atherogenic lipoproteins and promotes the development of atherosclerosis. *J Intern Med* 2005; 258: 395-410.

Onody A, Csonka C, Giricz Z, Ferdinandy P. Hyperlipidemia by a cholesterol-rich diet leads to enhanced peroxynitrite formation in rat hearts. *Cardiovasc Res* 2003; 58: 663-670.

Ouguerram K, Chetiveaux M, Zair Y, *et al.* Apolipoprotein B100 metabolism in autosomal-dominant hypercholesterolemia related mutations in PCSK9. *Arterioscler Thromb Vasc Biol* 2004; 24: 1448-1453.

Pacher P, Czabo C. Role of poly (ADP-ribose) polymerase 1 (PARP-1) in cardiovascular diseases: the therapeutic potential of PARP inhibitors.

Palmieri D, Perogo P, Palombo D. Estrogen receptor activation protects TNF- α -induced endothelial dysfunction. *Angiology* 2014; 65: 17-21.

Papapetropoulos A, Antonov A, Virmani R, *et al.* Monocyte- and cytokine-induced downregulation of angiotensin-converting enzyme in cultured human and porcine endothelial cells. *Circ Res* 1996; 79: 512-523.

Papapetropoulos A, Zhou Z, Gerassimou C, *et al.* Interaction between the 90-kDa heat shock protein and soluble guanylyl cyclase: physiological significance and mapping of the domains mediating binding. *Mol Pharmacol* 2005; 68: 1133-1141.

Park A. Hyperlipidaemia. *Medicine* 2009; 37: 497:499.

Park JY, Takahara N, Gabriele A, *et al.* Induction of endothelin-1 expression by glucose: an effect of protein kinase C activation. *Diabetes* 2000; 49: 1239-1248.

Pasceri V, Cheng JS, Willerson JT, *et al.* Modulation of C-reactive protein mediated monocyte chemoattractant protein-1 induction in human endothelial cells by anti-atherosclerosis drugs. *Circulation* 2001; 103: 2531–2534.

Passerini AG, Shi C, Francesco NM, *et al.* Regional determinants of arterial endothelial phenotype dominate the impact of gender or short-term exposure to a high fat diet. *Biochem Biophys Res Commun* 2005; 332: 142-148.

Patel H, Chen J, Das KC, Kavdia M. Hyperglycemia induces differential change in oxidative stress at gene and functional levels in HUVEC and HMVEC. *Cardiovascular Diabetology* 2013, 12: 142.

Paxton LL, Li LJ, Secor V, *et al.* Flanking sequences for the human intercellular adhesion molecule-1 NF-kappaB response element are necessary for tumor necrosis factor alpha-induced gene expression. *J Biol Chem* 1997; 272: 15928-15935.

Peng H-B, Libby P, Liao JK. Induction and stabilization of I κ B- α by nitric oxide mediates inhibition of NF κ B. *J Biol Chem* 1995; 270: 14214-14219.

Perillo NL, Pace KE, Seilhamer JJ, Baum LG. Apoptosis of T cells mediated by galectin-1. *Nature* 1995; 378: 736-739.

Perticone F, Ceravolo R, Candigliota M, *et al.* Obesity and body fat distribution induce endothelial dysfunction by oxidative stress: protective effect of vitamin C. *Diabetes* 2001; 50: 159-165.

Pfeifer A, Klatt P, Massberg S, *et al.* Defective smooth muscle regulation in cGMP kinase I-deficient mice. *EMBO J* 1998; 17: 3045-3051.

Picchi A, Gao X, Belmadani S, *et al.* Tumor necrosis factor- α induces endothelial dysfunction in the prediabetic metabolic syndrome. *Circ Res* 2006; 99: 69-77.

Pignatelli B, Li CO, Boffetta P, *et al.* Nitrated and oxidized plasma proteins in smokers and lung cancer patients. *Cancer Res* 2001; 61: 778-784.

Piper HM, Spahr R, Mertens S, Krutzfeldt A, Watanabe H. Microvascular endothelial cells from heart. In: Piper HM (editor). *Cell culture techniques in heart vessel and research*. Springer-Verlag 1990: 158-173.

Pirillo A, Norata GD, Catapano AL. LOX-1, OxLDL, and atherosclerosis. *Mediators Inflamm* 2013; 2013: 152786. doi: 10.1155/2013/152786.

Pleger ST, Harris DM, Shan C, *et al.* Endothelial S100A1 modulates vascular function via nitric oxide. *Circ Res* 2008; 102: 786–794.

Poiller J, Goosens A. Oleanolic acid. *Phytochemistry* 2012; 77: 10-15.

Pollock DM, Keith TL, Highsmith RF. Endothelin receptors and calcium signalling. *FASEB J* 1995; 9: 1196-1204.

Polte T, Oberle S, Schroder H. Nitric oxide protects endothelial cells from tumor necrosis factor- α -mediated cytotoxicity: possible involvement of cyclic GMP. *FEBS Letters* 1997; 409: 46-48.

Potenza MA, Marasciulo FL, Chieppa DM, *et al.* Insulin resistance in spontaneously hypertensive rats is associated with endothelial dysfunction characterized by imbalance between NO and ET-1 production. *Am J Physiol Heart Circ Physiol* 2005; 289: H813–H822.

Potter CM, Lundberg MH, Harrington LS, *et al.* Role of shear stress in endothelial cell morphology and expression of cyclooxygenase isoforms. *Arterioscler Thromb Vasc Biol* 2011; 31: 384-391.

Pries AR, Secomb TW, Gaehtgens P. Endothelial surface layer. *Eur J Physiol* 2000; 440: 653-666.

Privratsky JR, Tourdot BE, Newman DK, Newman PJ. The anti-inflammatory actions of platelet endothelial cell adhesion molecule-1 do not involve regulation of endothelial cell NF- κ B. *J Immunol* 2010; 184: 3157-3163.

Qin WD, Wei SJ, Wang XP, *et al.* Poly (ADP-ribose) polymerase 1 inhibition protects against low shear stress induced inflammation. *Biochim Biophys Acta* 2013; 1833: 59-68.

Quehenberger P, Bierhaus A, Fasching P, *et al.* Endothelin 1 transcription is controlled by nuclear factor- κ B in AGE stimulated cultured endothelial cells. *Diabetes* 2000; 49: 1561-1570.

Raij L, DeMaster EG, Jaimes EA. Cigarette smoke-induced endothelium dysfunction: role of superoxide anion. *J Hypertens* 2001; 19: 891-897.

Rakugi H, Tabuchi Y, Nakamaru M, *et al.* Evidence for endothelin-1 release from resistance vessels of rats in response to hypoxia. *Biochem Biophys Res Commun* 1990; 169: 973–977.

Ramadas RA, Ewart SL, Iwakura Y, *et al.* IL-36 α exerts pro-inflammatory effects in the lungs of mice. *PLoS One*. 2012; 7(9):e45784. doi: 10.1371/journal.pone.0045784.

Raman CS, Li H, Martasek P, *et al.* Crystal structure of constitutive endothelial nitric oxide synthase: a paradigm for pterin function involving a novel metal center. *Cell* 1998; 95: 939-950.

Rastaldo R, Pagliaro P, Capello S, Penna C, Mancardi D, Westerhof N, Losano G. Nitric oxide and cardiac function. *Life Sciences* 2007; 81: 779-793.

Rastogi S, Rizwani W, Joshi B, *et al.* TNF- α response of vascular endothelial and vascular smooth muscle cells involve differential utilization of ASK1 kinase and p73. *Cell Death and Differentiation* 2012; 19: 274-283.

Reiter CD, Teng R-J, Beckman JS. Superoxide reacts with nitric oxide to nitrate tyrosine at physiological pH via peroxynitrite. *J Biol Chem* 2000; 275: 32460-32466.

Reitsma S, Slaaf DW, Vink H, *et al.* The endothelial glycocalyx: composition, functions and visualization. *Eur J Physiol* 2007; 454: 345-359.

Resnick N, Yahav H, Shay-Salit A, *et al.* Fluid shear stress and the vascular endothelium: for better and for worse. *Prog Biophys Mol Biol* 2003; 81: 177-199.

Reuter TY. Diet-induced models for obesity and type 2 diabetes. *Drug Discov Today Dis Models* 2007; 4: 3-8.

Richardson MR, Lai X, Witzmann FA, Yoder MC. Venous and arterial endothelial proteomics: mining for markers and mechanisms of endothelial diversity. *Expert Rev Proteomics*. 2010; 7:823-831.

Rochette L, Lorin J, Zeller M, *et al.* Nitric oxide synthase inhibition and oxidative stress in cardiovascular diseases: possible therapeutic targets? *Pharmacology & Therapeutics* 2013; 140: 239-257.

Rodriguez-Rodriguez R, Herrera MD, De Sotomayor MA, *et al.* Pomace olive oil improves endothelial function in spontaneously hypertensive rats by increasing endothelial nitric oxide synthase expression. *Am J Hypertens* 2007; 20: 728-734.

Rodriguez-Rodriguez R, Herrera MD, Perona JS, *et al.* Potential vasorelaxant effects of oleanolic acid and erythrodiol, two triterpenoids contained in 'orujo' olive oil, on rat aorta. *Br J Nutr* 2004; 92: 635-642.

Rodriguez-Rodriguez R, Stankevicius E, Herrera MD, *et al.* Oleanolic acid induces relaxation and calcium-independent release of endothelium-derived nitric oxide. *Br J Pharmacol* 2008; 155: 535-546.

Rohra DK, Zubairi HS, Ohizumi Y. Endothelial dysfunction underlying the increased contractility in aorta from older rats. *Pak J Physiol* 2006; 2: 8-11.

Ross R. Atherosclerosis: an inflammatory disease. *N Engl J Med* 1999; 340: 115-126.

Rubanyi GM, Vanhoutte PM. Superoxide anions and hyperoxia inactivate endothelium-derived relaxing factor. *Am J Physiol* 1986; 250: H822-H827.

Ryoo S, Lemmon CA, Soucy KG, *et al.* Oxidized low density lipoprotein-dependent endothelial arginase II activation contributes to impaired nitric oxide signalling. *Circ Res* 2006; 99: 951-960.

Saijonmaa O, Nyman T, Fyhrquist F. Downregulation of angiotensin-converting enzyme by tumor necrosis factor-alpha and interleukin-1beta in cultured human endothelial cells. *J Vasc Res* 2001; 38: 370-378.

Sakurai H, Suzuki S, Kawasaki N, *et al.* Tumor necrosis factor- α -induced IKK phosphorylation of NF- κ B p65 on serine 536 is mediated through the TRAF2, TRAF5 and TAK1 signaling pathway. *J Biol Chem* 2003; 278: 36916-36923.

Salie R, Huisamen B, Lochner A. High carbohydrate and high fat diets protect the heart against ischaemia/reperfusion injury. *Cardiovasc Diabetol* 2014; 13: 109

Salminen A, Kaarniranta K, Kauppinen A. Inflammaging: disturbed interplay between autophagy and inflammasomes. *Aging* 2012; 4: 166-175.

Sawamura T, Kume N, Aoyama T, *et al.* An endothelial receptor for oxidized low-density lipoprotein. *Nature* 1997; 386: 73-77.

Sawant DA, Tharakan B, Wilson RL, *et al.* Regulation of tumor necrosis factor- α -induced microvascular endothelial cell hyperpermeability by recombinant B-cell lymphoma-extra large. *J Surg Res* 2013; 184: 628-637.

Schmieder RE, Hilgers KF, Schlaich MP, Schmidt BMW. Renin-angiotensin system and cardiovascular risk. *Lancet* 2007; 369: 1208-1219.

Schmitt CA, Dirsch VM. Modulation of endothelial nitric oxide by plant-derived products. *Nitric oxide* 2009; 21: 77-91.

Schneider JG, Tilly N, Hierl T, *et al.* Elevated plasma endothelin-1 levels in diabetes mellitus. *Am J Hypertens* 2002; 15: 967-972.

Schütze S, Machleidt T, Krönke M. The role of diacylglycerol and ceramide in tumor necrosis factor and interleukin-1 signal transduction. *J Leukoc Biol* 1994; 56: 533-541.

Schwartz BG, Kloner RA. Cardiovascular implications of erectile dysfunction. *Circulation* 2011; 123: e609-e611.

Seals DR, Jablonski KL, Donato JA. Aging and vascular endothelial functions in humans. *Clin Sci (Lond)* 2011; 120: 357-375.

Seguin F, Carvalho MA, Bastos DC, *et al.* The fatty acid synthase inhibitor orlistat reduces experimental metastases and angiogenesis in B16-F10 melanomas. *Br J Cancer* 2012; 107: 977-987.

Sen A, Most P, Peppel K. Induction of micro RNA-138 by proinflammatory cytokines causes endothelial cell dysfunction. *FEBS Letters* 2014; 588: 906-914.

Senthil S, Sridevi M, Pugalendi KV. Cardioprotective effect of oleanolic acid on isoproterenol-induced myocardial ischemia in rats. *Toxicol Pathol* 2007; 35: 418-423.

Seto SW, Lam TY, Or PM, *et al.* Folic acid consumption reduces resistin level and restores blunted acetylcholine-induced aortic relaxation in obese / diabetic mice. *J Nutr Biochem* 2010; 21: 872-880.

Seybold J, Thomas D, Witzernath M, *et al.* Tumor necrosis factor- α -dependent expression of phosphodiesterase 2: role in endothelial hyperpermeability. *Blood* 2005; 105: 3569-3576.

Shah AM, MacCarthy PA. Paracrine and autocrine effects of nitric oxide on myocardial function. *Pharmacol Ther* 2000; 86: 49-86.

Shenouda SM, Widlansky ME, Chen K, *et al.* Altered mitochondrial dynamics contributes to endothelial dysfunction in diabetes mellitus. *Circulation* 2011; 124: 444-453.

Shimokawa H, Yasuda S. Myocardial ischemia: Current concepts and future perspectives. *Journal of Cardiology* 2008; 52: 67-78.

Shimokawa H, Yasutake H, Fujii K, *et al.* The importance of the hyperpolarizing mechanism increases as the vessel size decreases in endothelium-dependent relaxations in rat mesenteric circulation. *J Cardiovasc Pharmacol* 1996; 28: 703-711.

Shishehbor MH, Avile RJ, Brennan M-L, *et al.* Association of nitrotyrosine levels with cardiovascular disease and modulation by statin therapy. *JAMA* 2003; 289: 1679-1680.

Siegel D, Gustafson DL, Dehn DL, *et al.* NAD(P)H: Quinine oxidoreductase 1: role as a superoxide scavenger. *Mol Pharmacol* 2004; 65: 1238-1247.

Simionescu M, Gafencu A, Antohe F. Transcytosis of plasma macromolecules in endothelial cells: A cell biological survey. *Microsc Res Tech* 2002; 57: 269-288.

Simmons GH, Padilla J, Laughli MH. Heterogeneity of endothelial cell phenotype within and amongst conduit vessels of the swine vasculature. *Exp Physiol* 2012; 97: 1074-1082.

Smolenski A. Novel roles of cAMP / cGMP-dependent signalling in platelets. *J Thromb Haemost* 2012; 10: 167-176.

Soderling SH, Beavo JA. Regulation of cAMP and cGMP signaling: new phosphodiesterases and new functions. *Curr Opin Cell Biol* 2000; 12: 174-179.

Soeda S, Tsunoda T, Kurokawa Y, Shimeno H. Tumor necrosis factor- α -induced release of plasminogen activator inhibitor-1 from human umbilical vein endothelial cells: involvement of intracellular ceramide signaling event. *Biochimica et Biophysica Acta* 1998; 1448: 37-45.

Solito R, Corti F, Chen CH, *et al.* Mitochondrial aldehyde dehydrogenase-2 activation prevents β -amyloid-induced endothelial cell dysfunction and restores angiogenesis. *J Cell Sci* 2013; 126: 1952-1961.

Somova LO, Nadar A, Rammanan P, Shode FO. Cardiovascular, antihyperlipidemic and antioxidant effects of oleanolic acid and ursolic acid in experimental hypertension. *Phytomedicine* 2003; 10: 115-121.

Spiecker M, Darius H, Kaboth K, Hübner F, Liao JK. Differential regulation of endothelial cell adhesion molecule expression by nitric oxide donors and antioxidants. *J Leukoc Biol* 1998; 63: 732-739.

Sprague RS, Bowles EA, Hanson MS, *et al.* Prostacyclin analogs stimulate receptor-mediated cAMP synthesis and ATP release from rabbit and human erythrocytes. *Microcirculation* 2008; 15: 461-471.

Stankevicius E, Kevelaitis E, Vainorius E, *et al.* Role of nitric oxide and other endothelium-derived factors. *Medicina* 2003; 39: 333-341.

Steyn K. The Heart and Stroke foundation South Africa. Heart disease in South Africa: Media data document. MRC 2007. Available: <http://www.mrc.ac.za/chronic/heartandstroke>.

Stone JR, Collins T. The role of hydrogen peroxide in endothelial proliferative responses. *Endothelium* 2002; 9: 231-238.

Strijdom H, Jacobs S, Hattingh S, Page C, Lochner A. Nitric oxide is higher in rat cardiac microvessel endothelial cells than ventricular cardiomyocytes in baseline and hypoxic conditions: a comparative study. *FASEB J* 2006; 20: 314-316.

Strijdom H, Chamane N, Lochner A. Nitric oxide in the cardiovascular system: a simple molecule with complex actions. *Cardiovasc J Afr* 2009; 20: 303-310.

Strijdom H, Lochner A. Cardiac endothelium: More than just a barrier! *SA Heart* 2009; 6: 174-185.

Stuehr D, Pou S, Rosen GM. Oxygen reduction by nitric oxide synthases. *J Biol Chem* 2001; 276: 14533-14536.

Stypmann J, Gläser K, Roth W, *et al.* Dilated cardiomyopathy in mice deficient for the lysosomal cysteine peptidase cathepsin L. *Proc Natl Acad Sci U S A* 2002; 99: 6234-6239.

Sud N, Black SM. Endothelin-1 impairs nitric oxide signalling in endothelial cells through a PKC δ -dependent activation of STAT3 and decrease eNOS expression. *DNA Cell Biol* 2009; 28: 543-553.

Sun M, Chen M, Liu Y, *et al.* Cathepsin-L contributes to cardiac repair and remodelling post-infarction. *Cardiovasc Res* 2011; 89: 374-383.

Surapisitchat J, Jeon KI, Yan C, Beavo JA. Differential regulation of endothelial cell permeability by cGMP via phosphodiesterases 2 and 3. *Circ Res* 2007; 101: 811-818.

Swiatkowska M, Szemraj J, Cierniewski CS. Induction of PAI-1 expression by tumor necrosis factor alpha in endothelial cells is mediated by its responsive element located in the 4G/5G site. *FEBS J* 2005; 272:5821-5831.

Szabo C, Pacher P, Zsengeller, *et al.* Angiotensin II-mediated endothelial dysfunction: role of poly (ADP-ribose) polymerase activation. *Mol Med* 2004; 10: 1-6.

Szasz T, Bomfim GF, Webb RC. The influence of perivascular adipose tissue on vascular homeostasis. *Vascular Health and Risk Management* 2013; 9: 105-116.

Takahashi S, Mendelsohn ME. Calmodulin-dependent and -independent activation of endothelial nitric-oxide synthase by heat shock protein 90. *J Biol Chem* 2003; 278: 9339-9344 (a).

Takahashi S, Mendelsohn ME. Synergistic activation of endothelial nitric-oxide synthase (eNOS) by HSP90 and Akt. *J Biol Chem* 2003; 278: 30821-30827 (b).

Teodoro T, Zhang L, Alexander T, *et al.* Oleonic acid enhances insulin secretion in pancreatic β -cells. *FEBS Lett* 2008; 582: 1375-1380.

Thorin E, Shatos MA, Shreeve SM, *et al.* Human vascular endothelium heterogeneity: A comparative study of cerebral and peripheral cultured vascular endothelial cells. *Stroke* 1997; 28: 375-381.

Thorin E, Shreeve SM. Heterogeneity of vascular endothelial cells in normal and disease states. *Pharmacol Ther* 1998; 78 (3): 155-166.

Toda N, Okamura T. Obesity impairs vasodilatation and blood flow increases mediated by endothelial nitric oxide: an overview. *J Clin Pharmacol* 2013; 53: 1228-1239.

Togashi H, Sakuma I, Yoshioka M, *et al.* A central nervous system action of nitric oxide in blood pressure regulation. *J Pharmacol Exp Ther* 1992; 262: 343-347.

Tripal P, Bauer M, Naschberger E, *et al.* Unique features of different members of the human guanylate-binding protein family. *J Interferon Cytokine Res* 2007; 27: 44-52.

Uchiyama T, Otani H, Okada T, *et al.* Nitric oxide induces caspase-dependent apoptosis and necrosis in neonatal rat cardiomyocytes. *J Mol Cell Cardiol* 2002; 34: 1049-1061.

Usharani P, Fatima N, Muralidhar N. Effects of Phyllanthus emblica extract on endothelial dysfunction and biomarkers of oxidative stress in patients with type 2 diabetes mellitus: a randomized, double-blind, controlled study. *Diabetes, Metabolic Syndrome and Obesity: Targets and Therapy* 2013; 6: 275-284.

Valerio A, Cardile A, Cozzi V, *et al.* TNF- α downregulates eNOS expression and mitochondrial biogenesis in fat and muscle of obese rodents. *J clin Invest* 2006; 116: 2791-2798.

Van Der Loo B, Labugger R, Skepper JN, *et al.* Enhanced peroxynitrite formation is associated with vascular aging. *J Exp Med* 2000; 192: 1731-1743.

VanTeefflen JW, Brands J, Stroes ES, *et al.* Endothelial glycocalyx: Sweet shield of blood vessels. *Trends Cardiovasc Med* 2007;17: 101-105.

Venugopal SK, Devaraj S, Yuhuanna I, *et al.* Demonstration that C-reactive protein decreases eNOS expression and bioactivity in human aortic endothelial cells. *Circulation* 2002; 106: 1439-1441.

Versari D, Daghini E, Viridis A, *et al.* Endothelial dysfunction as a target for prevention of cardiovascular disease. *Diabetes Care* 2009; 32: S314-S321.

Verstal DJ, Jeyaratnam JA. The Guanylate-Binding Proteins: emerging Insights into the Biochemical Properties and Functions of This Family of Large Interferon-Induced Guanosine Triphosphatase. *J Interferon Cytokine Res* 2011; 31: 89-97.

Viatour P, Merville MP, Bours V, Chariot A. Phosphorylation of NF-kappaB and IkappaB proteins: implications in cancer and inflammation. *Trends Biochem Sci* 2005; 30: 43-52.

Vicent D, Ilany J, Kondo T, *et al.* The role of endothelial insulin signaling in the regulation of vascular tone and insulin resistance. *J Clin Invest* 2003; 111: 1373-1380.

Vigne S, Palmer G, Lamacchia C, *et al.* IL-36R ligands are potent regulators of dendritic and T cells. *Blood* 2011; 118: 5813-5823.

Viridis A, Schiffrin EL. Vascular inflammation: a role in vascular disease in hypertension? *Curr Opin Nephrol Hypertens* 2003; 12: 181-187.

Vivanco F, Mas S, Darde VM, *et al.* Vascular proteomics. *Proteomics Clin Appl* 2007; 1: 1102-1122.

Wagner L, Hoey JG, Erdely A, *et al.* The nitric oxide pathway is amplified in venular vs arteriolar cultured rat mesenteric endothelial cells. *Microvascular Research* 2001; 62: 401-409.

Wajant H, Pfizenmaier K, Scheurich P. Tumor necrosis factor signaling. *Cell Death Differ* 2003; 10: 45-65.

Walker AE, Kaplon RE, Lucking SM, *et al.* Fenofibrate improves vascular endothelial function by reducing oxidative stress while increasing endothelial nitric oxide synthase in healthy normolipidemic older adults. *Hypertension* 2012; 60: 1517-1523.

Wallez Y, Huber P. Endothelial adherens and tight junctions in vascular homeostasis, inflammation and homeostasis. *Biochimica et Biophysica Acta* 2008; 1778: 794-809.

Wang JH, Redmond HP, Watson RWG, *et al.* Mechanisms involved in the induction of human endothelial cell necrosis. *Cell Immunol* 1996; 168: 91-99.

Wang HU, Chen ZF, Anderson DJ. Molecular distinction and angiogenic interaction between embryonic arteries and veins revealed by ephrin-B2 and its receptor Eph-B4. *Cell* 1998; 93: 741-753.

Wang L, Lim E-J, Toborek M, *et al.* The role of fatty acids and caveolin-1 in tumor necrosis factor α -induced endothelial cell activation. *Metabolism Clinical and Experimental* 2008; 57: 1328-1339.

Wang Q, Pfeiffer GR, Stevens T, Doerschuk CM. Lung microvascular and arterial endothelial cells differ in their responses to intercellular adhesion molecule-1 ligation. *American Journal of Respiratory and Critical Care Medicine* 2002; 166: 872-877.

Warner BB, Burhans MS, Clark JC, Wispé JR. Tumor necrosis factor- α increases Mn-SOD expression: protection against oxidant injury. *Am J Physiol* 1991; 260: L296-L301.

Weber C, Erl W, Weber K, *et al.* Increased adhesiveness of isolated monocytes to endothelium is prevented by vitamin C intake in smokers. *Circulation* 1996; 93: 1448-1492.

Weil BR, Westby CM, Guildler GP, *et al.* Enhanced endothelin-1 system activity with overweight and obesity. *Am J Physiol Heart Circ Physiol* 2011; 301: H689-H695.

Wesson De, Simoni J, Green DF. Reduced extracellular pH increases endothelin-1 secretion by human renal microvascular endothelial cells. *J Clin Invest* 1998; 101: 578-583.

White AR, Ryoo S, Li D, *et al.* Knockdown of arginase I restores NO signaling in the vasculature of old rats. *Hypertension* 2006; 47: 245-251.

Wong GH, Goeddel DV. Induction of manganese superoxide dismutase by tumor necrosis factor: possible protective mechanism. *Science* 1988; 242: 941-944.

Wooten MW, Geetha T, Seibenhener ML, *et al.* The p62 Scaffold Regulates Nerve Growth Factor-induced NF- κ B Activation by Influencing TRAF6 Polyubiquitination. *J Biol Chem* 2005; 280: 35625-35629.

Xia Z, Luo T, Liu H, *et al.* L-Arginine enhances nitrate stress and exacerbates tumor necrosis factor- α toxicity to human endothelial cells in culture: Prevention by propofol. *J Cardiovasc Pharmacol* 2010; 55: 358–367.

Xiong Y, Yeparri G, Forbitech M, *et al.* ARG2 impairs endothelial autophagy through regulation MTOR and PRKAA / AMPK signalling in advanced atherosclerosis. *Autophagy* 2014; 10: 2223-2238.

Xu B, Chibber R, Ruggerio D, *et al.* Impairment of vascular endothelial nitric oxide synthase activity by advanced glycation end products. *FASEB J* 2003; 17: 1289-1291.

Xu Y-F, Wan X-L, Xu Y, *et al.* Reported oral administration of oleanolic acid produces cholestatic liver injury in mice. *Molecules* 2013; 18: 3060-3071.

Yagamuchi Y, Haginaka J, Morimoto S, *et al.* Facilitated nitration and oxidation of LDL in cigarette smokers. *Eur J Invest* 2005; 35: 186-193.

Yamamoto M, Okuyama M, Ma JS, *et al.* A cluster of interferon- γ -inducible p65 GTPases plays a critical role in host defence against *Toxoplasma gondii*. *Immunity* 2012; 37: 302-313.

Yamaoka J, Kabashima K, Kawanishi M, *et al.* Cytotoxicity of IFN- γ and TNF- α for vascular endothelial cells is mediated by nitric oxide. *Biochem Biophys Res Commun* 2002; 291: 780-786.

Yan J, Tie G, Messina LM. Tetrahydrobiopterin, L-Arginine and vitamin C act synergistically to decrease oxidative stress, increase nitric oxide and improve blood flow after induction of hindlimb ischemia in the rat. *Mol Med* 2012; 18: 676-684.

Yang LL, Gros R, Kabir MG, *et al.* Conditional cardiac overexpression of endothelin-1 induces inflammation and dilated cardiomyopathy in mice. *Circulation* 2004; 109: 255–261.

Yang R-L, Shi Y-H, Hao G, *et al.* Increasing oxidative stress in human: Relation between malondialdehyde and atherogenic index. *J Clin Biochem Nutr* 2008; 43: 154-158.

Yang Y-M, Huang A, Kaley G, Sun D. eNOS uncoupling and endothelial dysfunction in aged vessels. *Am J Physiol* 2009; 297: H1829-H1836.

Yokoyama M. Oxidant stress and atherosclerosis. *Curr Opin Pharmacol* 2004; 4: 110–115.

Yoshizumi M, Perrella MA, Burnett Jr JC, Lee ME. Tumor necrosis factor downregulates an endothelial nitric oxide synthase mRNA by shortening its half-life. *Circ Res* 1993; 73: 205-209.

Youle FJ, Van Der Blik AM. Mitochondrial fission, fusion, and stress. *Science* 2012; 337: 1062-1065.

Zhang C, Xu X, Potter BJ, *et al.* TNF- α contributes to ED in ischemia / reperfusion injury. *Arterioscler Thromb Vasc Biol* 2006; 26: 475-480.

Zhang F, Zhang Y, Li PL. Dependence of cathepsin L-induced coronary endothelial dysfunction upon activation of NAD(P)H oxidase. *Microvasc Res.* 2009; 78: 45-50.

Zhang H, Park Y, Wu J, *et al.* Role of TNF- α in vascular dysfunction. *Clin Sci* 2009; 116: 219-230.

Zhang J, DeFelice AF, Hanig JP, Colastky T. Biomarkers of endothelial cell activation serve as potential surrogate markers for drug-induced vascular injury. *Toxicol Pathol* 2010; 38: 856-871.

Zhou L, Wang H-F, Ren H-G, *et al.* Bcl-2 dependent upregulation of autophagy by sequestosome 1 / p62 in vitro. *Acta Pharmacologica Sinica* 2013; 34: 651-656.

Zhou M, Gu L, Zhu N, *et al.* Transfection of a dominant-negative mutant NF- κ B inhibitor (I κ Bm) represses p53-dependent apoptosis in acute lymphoblastic leukemia cells: interaction of I κ Bm and p53. *Oncogene* 2003; 22: 8173-8144.

Ziegler ME, Souda P, Jin Y-P, *et al.* Characterization of the endothelial cell cytoskeleton following HLA Class I ligation. *PLoS ONE* 2012; 7: e29472. doi:10.1371/journal.pone.0029472.

Zivkovic V, Djuric D, Turjacanin- Pantelic D, *et al.* The effects of cyclooxygenase and nitric oxide synthase inhibition on cardiodynamic parameters and coronary flow in isolated rat hearts. *Exp Clin Cardiol* 2013; 18: e102-e110.

Zong W-X, Edelstein LC, Chen C, *et al.* The prosurvival Bcl-2 homolog Bfl-1/A1 is a direct transcriptional target of NF- κ B that blocks TNF- α -induced apoptosis. *Genes Dev* 1999; 13: 382-387.

Zotti T, Scudiero I, Settembre P, *et al.* TRAF-6-mediated ubiquitination of Nemo requires P62/ Sequestosome. *Molecular Immunology* 2014; 58: 27-31.

Zou M-H, Shi C, Cohen RA. Oxidation of the zinc-thiolate complex and uncoupling of endothelial nitric oxide synthase by peroxynitrite. *J Clin Invest* 2002; 109: 817-826.